ProQuest Number: 10290313

ProQuest 10290313

ENHANCEMENTS TO REVERSE ENGINEERING:

SURFACE MODELLING AND SEGMENTATION OF CMM DATA

BY
RAYMAN A. BARDELL

A thesis submitted in partial fulfilment of the requirements of The Nottingham Trent University for the degree of Doctor of Philosophy

September 2000

Abstract

Reverse Engineering (RE) is a relatively new field, which aims to reproduce a physical prototype accurately. This involves the main stages of data collection, modelling and machining. One approach to data collection utilises the Co-ordinate Measuring Machine (CMM), using a touch-trigger probe. This contact measurement method is employed in this work, resulting in three-dimensional (3D) surface data of a physical part. Surface modelling follows data collection as the next stage of RE, where a best-fit model is generated, interpolating these data points.

An automatic surface generation methodology is developed in this work, utilising the ACIS® Computer Aided Geometric Design (CAGD) development tool. This results in C^1 continuous Gregory/Charrot patches, which are merged to form a global B-spline surface model. Classic free-form modelling techniques have associated limitations, affecting accuracy. This work aims to reduce these errors, improving the accuracy of the RE process. The initial study has identified two types of global surface in physical prototypes, known as free-form continuous surfaces, and composite discontinuous surfaces. These require different modelling strategies to minimise modelling errors.

There has been limited research in the area of surface model analysis, applied to automatically generated surfaces. This present work focuses on a novel method for analysing the accuracy of a generated surface model, highlighting regions of the surface that deviate from the CMM data. With free-form objects, deviations can be used to define the smoothness of the CMM data. With composite objects, these deviations occur at areas of extreme curvature change. The development of a data-set partitioning tool investigates a unique method of predicting surface model accuracy, where a model is generated from a fraction of the available data-set.

The accurate modelling of composite surfaces derived from CMM data has received little attention to date. In this work, surface models of this type are interrogated, using a novel curvature-based surface decomposition method, allowing individual smooth local sub-surfaces to be modelled. This utilises a seed region growing methodology, which clusters points of the same surface type as a sub-surface, allowing assessment of the sub-surface in terms of cosmetic quality. This provides a method of determining and segmenting specific surface types from the global surface, reducing inaccuracies caused by the modelling of adjacent surfaces of differing types.

The main areas of novel research presented in this thesis lie in the areas of accuracy analysis, introducing deviation analysis, and surface type recognition, developing a novel seed region growing methodology, applied to CMM data.

Contents

Chapter 1. Introduction

Chapter 2. Reverse Engineering Methodologies

Chapter 3. Data Collection, Modelling and Machining

Chapter 4. Enhancements to the Reverse Engineering Process

Chapter 5. Experimental Results of Novel Work

Chapter 6. Conclusions and Future Developments

Acknowledgements

List of Abbreviations

3D	Three-dimensional
ANN	Artificial Neural Network
APT	Automatically Programmed Tools
B-rep	Boundary representation
CAD	Computer Aided Design
CAE	Computer Aided Engineering
CAGD	Computer Aided Geometric Design
CAM	Computer Aided Manufacture
CC	Cutter Contact
CII	Computer Integrated Inspection
CIM	Computer Integrated Manufacturing
CL	Cutter Location
CMES	Co-ordinate Measuring
CMM	Co-ordinate Measuring Machine
CNC	Computer Numerically Controlled
CSG	Constructive Solid Geometry
DA	Deviation Analysis
DMIS	Dimensional Measuring Interface Standard
DSP	Data-set partitioning
GUI	Graphical User Interface
H	Mean curvature
IGES	Initial Graphics Exchange Specification
K	Gaussian curvature
k_1	Primary curvature
k_2	Secondary curvature
MARG	Manufacturing Automation Research Group
NC	Numerical Control
NMA	New Model Analysis
NURBS	Non-Uniform Rational B-Splines
PC	Personal Computer
RE	Reverse Engineering
RES	Reverse Engineered Surface
SE	Simultaneous Engineering

SPC   Statistical Process Control

STEP   STandard for the Exchange of Product Data

VRML   Virtual Reality Modelling Language

Chapter 1.

Introduction

1.1   Introduction

Computer Aided Design (CAD) has progressed dramatically over recent years, however many design applications still involve the construction of a prototype model at the concept stage. This is often the case, as a true 'feeling' of a three-dimensional (3D) part cannot be ascertained easily from a 2D computer screen. Prototype models are usually made from clay or wood, by stylists [MA, 1998], and do not involve the use of mathematical methods to determine shape [BEZIER, 1990]. The functionality of the part may put mathematical constraints on the design, but aesthetic properties are easier to design by hand.

To translate this physical prototype into a CAD environment it must be digitised, obtaining 3D surface data. For parts with complicated geometry, this part-digitisation is achieved manually [KREJCI, 1995]. This 3D data is used to generate an open surface model, from which draft drawings can be made, viewing the part from various directions. This works towards improving the flow of information between relevant parties, where a CAD file can be used to demonstrate a potential design. This is logistically easier than passing a physical prototype between departments of an organisation. This can also involve design specifications sent between customer and supplier in electronic format, via the Internet. The generation of a surface model from digitised data is essential for the manufacture of unique replacement parts where CAD was not used in the original design. A reproduction part, a mould or a pressing tool may be required, which can be manufactured, improving the quality of fit and verifying the geometry [MASON, 1990]. In these cases, the generated surface model can be used to

create part-programs to accurately reproduce the physical prototype, forming the Computer Numerically Controlled (CNC) machining stage of Computer Aided Manufacture (CAM).

The above process is an aspect of Computer Aided Engineering (CAE), known as Reverse Engineering (RE). This is a relatively new term which, as the name suggests, is the inverse of conventional 'design-to-build' engineering. In many cases, RE can be used to generate 3D shapes much faster than creating a new CAD model [PENG, 1998]. A main concern of RE is obtaining an accurate mathematical definition of the surface in question, utilising Computer Aided Geometric Design (CAGD) techniques. This is necessary for optimum surface model accuracy, correlating the generated surface with the collected 3D data points. This is particularly the case with smooth sculptured surfaces, also known as free-form surfaces.

Common engineering practices involve 2½ D prismatic surfaces, where 2D contours on various levels are stacked [DUNCAN, 1989]. However, many engineering applications require the manufacture of sculptured surfaces, both for aesthetic and aerodynamic reasons [YAU, 1997], [KIM, 1988]. These are also defined as natural surfaces [DUNCAN, 1989]. These free-form surfaces are ideally suited to automatic methods of generating continuous surface models, traditionally used in the RE process. However, more complex composite surfaces do not have such a straightforward solution. In this work, a composite surface is defined as a global surface containing discontinuous regions where different local surfaces intersect. This often includes a mixture of sculptured and geometric surface types. These discontinuous regions cause modelling errors, when applying automatic free-form modelling techniques.

The aim of this thesis is to discuss novel work implemented, aimed at improving the current RE technology, based on automatically generating a free-form surface model from Co-ordinate Measuring Machine (CMM) point data, with minimum user-interaction. In particular, this work concentrates on the analysis of free-form and composite surfaces, and novel methods of improving the modelling of composite surfaces. Very few published works discuss the RE of composite surfaces [CHEN, 1997].

This chapter starts by introducing the various aspects of conventional RE, before summarising novel enhancements to the RE process. This work is concerned with improving the conventional RE process, introducing a number of refinement methods.

1.2   Conventional Reverse Engineering

RE can be defined as:

> *'The systematic evaluation of a product with the purpose of replication. This involves either direct copies or adding improvements to existing design'* [ARONSON, 1996].

Conventional RE is made up of three stages, outlined in figure 1.1, and discussed briefly below.
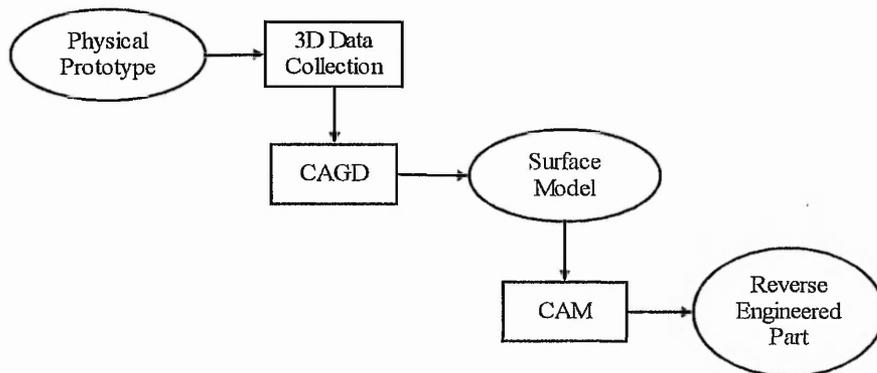
Figure 1.1. Conventional RE process.

1.2.1   Data Collection

The digitisation of a physical prototype is necessary for the first stage of RE. There are a number of techniques for the collection of data from physical objects, discussed further in chapter 2. This work utilises the CMM, where a touch trigger probe collects data over a pre-defined area of the surface at a pre-defined density. There are accuracy issues with contact data collection, which are discussed in chapter 3. Data collection results in 3D Cartesian co-ordinate surface data, utilised in a surface fitting stage.

1.2.2   Surface Fitting

3D point data is utilised in a surface fitting module, where a best-fit surface is generated from these points. Where the physical prototype is a sculptured free-form surface, there is generally a close correlation between data points and the surface model. Automatic modelling methods are reliable, when based on data collected in a continuous manner, despite associated errors [MENQ, 1996]. However, the surface fitting of data points collected from composite surfaces can cause inaccuracies, where the correlation between the fitted surface and the data points can vary, depending on the extent of the surface discontinuities. These deviations are unavoidable using automatic free-form modelling methodologies. The development of a surface generation methodology, utilising the ACIS® geometric modeller, is discussed in chapter 3. Data collection and surface modelling, when taken together, can be described as Part-to-CAD RE, concluding with a generated surface model. However, the complete RE process includes the manufacture of a reproduction part.

1.2.3   Reproduction Part Machining

The concluding stage of conventional RE is the machining stage, which utilises the best-fit surface derived from the CMM data. CNC machine paths are deduced from surface information, generating part-programs, accurately reproducing the original prototype. However, errors may be introduced where the part to be machined contains discontinuities, discussed in chapter 3.

1.3   Novel Reverse Engineering Refinement Methods

An evaluation of the current RE technology is discussed fully in chapter 2. In conventional RE, limited information is available on the accuracy and efficiency of the overall process [LEE, 1990]. There is also a lack of adequate methodologies when dealing with composite surface models. Therefore, in addition to the three main processes of data collection, modelling and machining, a number of improvements to the conventional RE process have been made in this thesis, leading to greater process control, discussed in chapter 4. A novel accuracy analysis module is developed,

presented in section 4.2, allowing verification of a generated model. The accurate modelling of composite surfaces forms a necessary step towards improving the RE process for a wider range of complex surfaces, forming the major novel work discussed in chapter 4.

1.3.1 Accuracy Analysis

It is desired in Part-to-CAD RE for the generated surface model to be assessed and validated. This involves highlighting any deviations of the surface from the collected CMM data, allowing action to be taken to improve the surface model accuracy, where necessary. This accuracy is highly dependent on the patch size and surface parameterisation used to generate a global surface, discussed fully in chapters 3 and 4. Confidently analysing the amount of CMM data necessary to generate acceptable surface models is also investigated, as a novel data-partitioning tool. This stage of deviation analysis aims to optimise the amount of CMM data needed at the model generation stage.

The assessment of surfaces is necessary, analysing both aesthetic and functional properties [SMITH, 1994]. This usually takes the form of a physical inspection of the reverse engineered reproduction part. However, an assessment of the CAD model can save time and money in the RE process. This work is specific to composite surface models, discussed further in chapter 4. Conclusions from this assessment stage lead to novel work aimed at improving the accuracy of composite surface models, involving curvature-based surface segmentation.

1.3.2 Surface Segmentation

Part-to-CAD RE generally results in a globally continuous free-form model, constructed from CMM data points. However, in cases where the original prototype contains a number of distinct surfaces, errors occur at the surface-surface intersections. These are discontinuous regions which cannot be modelled accurately using continuous free-form techniques. As a novel enhancement to the RE process, the automatically generated free-form surface can be decomposed, eliminating the source of potential error. Accurately modelling a physical prototype made up of composite surfaces has received

limited attention. Deducing further knowledge of the surface can improve modelling, involving local curvature analysis. This novel work is discussed in chapter 4.

1.4   Thesis Structure

- Chapter 2, entitled 'Reverse Engineering Methodologies', comprises of a critique of the past and current technologies relating to this area. The background and history of data collection is discussed, as are the fundamental methodologies for CAGD. Methods of surface model decomposition are discussed, and the main issues of machining are introduced.

- Chapter 3, entitled 'Data Collection, Modelling and Machining', discusses work done, forming aspects of conventional Reverse Engineering. This examines strategies and methods of data collection and inspection. Work developed here for generic data collection is discussed, utilising the CMM, resulting in Cartesian co-ordinate data. Data collection errors are also discussed. The modelling methodology developed in this work, using the ACIS® geometric modeller is discussed. Methods of improving free-form surface model accuracy are examined, as are potential modelling errors. The reproduction part machining stage is also discussed.

- Chapter 4, entitled 'Enhancements to the Reverse Engineering Process', discusses methods of improving RE. This includes novel methods of accuracy analysis, forming a deviation analysis stage. Composite surface model segmentation is discussed, based on surface curvature, which utilises a seed region growing methodology.

- Chapter 5 shows experimental results from the novel work discussed in chapter 4.

- Chapter 6 concludes the thesis, summarising and discussing the work carried out and how it benefits the current RE process. Future developments, which may further improve this process, are also discussed.

Chapter 2.

Reverse Engineering Methodologies

2.1   Introduction

Reverse Engineering (RE) is vital to industry, working towards accurate and repeatable methods of reproducing a physical part. This is an effective tool in Simultaneous Engineering (SE), as it shortens the design-to-manufacture lead-time [BIDANDA, 1994]. RE is also useful to the medical industry, in the manufacture of implants and prosthetics [MA, 1998]. This chapter provides a survey of the current RE technology, and its evolution.

RE can be divided into the four main modules of:

- Data collection
- Surface modelling
- Model segmentation
- Part machining

This chapter gives an overview of the fundamental aspects of these areas, taken as individual modules, and also as integrated components of RE. The areas where methodologies are lacking are highlighted, demonstrating the novel contributions this present work makes to RE technology.

2.2   Methods of Obtaining Data from Physical Objects

Historically, the need for accurate metrology has been evident with architecture and astronomy, but more recently with the necessary precision of mechanical moving parts. As mechanisms have become more intricate, there is a growing need for the mechanical parts to be manufactured accurately. The onset of mass production, with the

manufacture of identical complex parts in large volumes, has created this need for repeatable precision. In the early to middle 1900s, the assembly lines of automobiles called for the standardisation of part dimensions within certain tolerances. This was mainly due to the improvement of machining, and techniques in gauging accuracy.

Original methods of measurement involved the use of fixed gauges to check tolerances, which were replaced with instrument gauges. To begin with, visual reed gauges were used in the inspection process, involving optical magnification. Pneumatic gauging followed, which allowed for high-speed measurement, based on velocity of airflow [BOSCH, 1995a]. For many quality assurance applications these traditional gauges are still used today, for mechanical parts with functional dimensions [YAU, 1990]. Dimensional information is necessary for a number of quantitative reasons. Parts may be components of a larger assembly, thus they must have an associated fit tolerance. This calls for repeatable accuracy at the manufacturing stage. Inspection of this is essential, to control this process.

Smooth surfaces, rather than geometrical shapes, are often desired, particularly in the case of physical prototype models for the aeronautical and automotive industries [CATANIA, 1992]. Here, the designer's judgment is often relied upon, creating a physical prototype without a mathematical model. The smoothness of this physical surface is difficult to ascertain, as this smoothness 'property' could be dependent on the function of the part, or for aesthetic reasons [SMITH, 1994]. This makes the assessment of surface form difficult. Methods of determining the 'goodness' of a surface result in an assessment of cosmetic quality [BALENDRAN, 1993]. Manual methods are often based on visual analysis, such as reflectance properties. Surface analysis using reflection lines involves the analysis of the surface's curvature by visual methods [FARIN, 1990]. Skilled personnel can assess surfaces accurately using a soft glove, using sensory touch information to feel surface deviations. These deviations include peaks or valleys [BALENDRAN, 1989]. Where a fit between two parts is needed, fine powder (often blue) can be used on adjacent parts, and the closeness of fit can be determined by the amount of powder removed and remaining. Master gauge comparison measures the degree of deviation of the inspected surface from that of a reverse profile master, often requiring a microscope [IP, 1992].

Automatic methods of contact surface inspection, such as the Coordinate Measuring Machine (CMM), lead to the analysis of the collected data from the surface in question. Here, the object is digitised, defining a mathematical surface to the collected points. This gives quantitative properties to an original object partly designed by qualitative properties. Due to widespread use, the CMM is the most popular RE tool, where they have become integral parts of many companies [BIDANDA, 1994]. CMMs can evaluate form, orientation and profile according to geometric dimensioning and tolerances [GRANT, 1995]. However, there are cases where an automated gauging system is preferred to the CMM. The CMM was never intended to replace all instruments at all tolerances [HOCKEN, 1995], as it cannot check all types of geometric tolerance [ELMARAGHY, 1987].

2.2.1   CMM Contact Measurement

The CMM records data at the centre of a small spherical probe, typically 2mm in diameter, which touches the object. This is known as a touch-trigger probe, commonly used for CMM data collection. More detail on the CMM components can be found in chapter 3. The CMM can collect data in a scanning mode, where the touch-trigger probe collects data by pecking the object in parallel scan lines. Analogue scanning probes differ from touch-trigger probes, as they take points while the stylus continuously touches the part being inspected, based mainly on inductive displacement transducers [NI, 1995]. Contact probes can form a sensor-based non-intrusive process to check dimensional accuracy and deviations from geometric tolerances during CNC machining operation [ZHOU, 1992].

During data collection, a finite number of quantitative points are collected from the object. This process takes a number of steps [YAU, 1990]:

- Specification
- Planning
- Verification
- Execution
- Comparative Analysis

Adequate planning is important, due to potential long inspection times. Also this decreases the likelihood of collisions and machine resetting. The main advantage of the CMM is the ability to collect data automatically, however where very complex shapes are digitised, data collection can be achieved manually [KREJCI, 1995].

As well as the CMM, other manual contact methods include electromagnetic digitising, where a magnetic field is above the part, and a hand-held stylus traces the surface, detecting the position and orientation of the stylus. However, only non-metallic objects can be measured. Sonic digitising uses sound waves to calculate position, where a hand-held stylus traces the object and emits an ultrasonic impulse. Time recordings, relative to mounted microphone sensors, calculate the coordinates [BIDANDA, 1994]. In the case of automatic CMM data collection, programming is usually required. Methods of CMM part-programming include self-teach, off-line programming, and CAD programming.

In an on-line mode, programming involves manual data collection in a 'self teach' mode [KREJCI, 1995]. Each manual measurement and probe move is recorded and saved in a program file, which can then be used to automatically inspect similar parts [NI, 1995]. This can be enhanced to represent visually each data point on a Personal Computer (PC), in real-time, allowing verification.

Generally, programs are written off-line, but may contain prompts for the user to move the CMM probe in real-time, defining start and end positions for scan lines. Data is traditionally gathered off-line, which often involves large amounts of data-capture in the hope of minimising modelling errors [SEILER, 1994]. CMMs are generally programmed and controlled in a native language, such as the CMES (Co-ordinate Measuring) CMM language [LK, 1992]. CMES, and other native languages, are being replaced by the Dimensional Measuring Interface Standard (DMIS) [DMIS, 1995], which allows bi-directional communication between computer systems and inspection equipment [KREJCI, 1995]. This is based on a neutral format, which is 'feature-based' rather than using scan lines, allowing functionality to play a part at the CAD stage [SIVAYOGANATHAN, 1994].

With parts that differ slightly, programming can incorporate a 'family' structure to define features of a part. Particular features can then be included or excluded, depending on the part being automatically inspected [CASE, 1994]. This forms a CAD-directed inspection process, requiring a CAD file of the part to be inspected. Features are selected and a part-program can be generated, saving development time [SIVAYOGANATHAN, 1994]. These part families are useful for Computer Aided Classification, allowing the planning of expert inspection tasks [ELMARAGHY, 1987].

Measuring instruments are often assumed to have no significant errors, however, errors become apparent when a particular measurement is repeated, or compared with other measurement devices. Measurements obtained from the CMM follow a stable normal distribution, where repeatability errors can be reduced or eliminated by averaging repeated results [LAWRENCE, 1993]. Work has been done to improve the CMM accuracy and speed [KATEBI, 1994], but in all cases the increased accuracy reduces speed, vastly increasing the inspection time. CMM errors are usually determined based on rigid body kinematics assumptions and linear temperature effects. Work has been carried out on relating location errors to the volumetric measuring accuracy, including non-rigid body effects and thermally induced effects [TEEUWSEN, 1989]. The effect of temperature variation on the part dimensions and machine performance is the biggest problem with high levels of accuracy. Methods of on-line compensation are under way [BOSCH, 1995b]. Due to the difficulties in determining the required point density to ensure accurate modelling, interactive data collection at identified regions can take place [SEILER, 1991].

The CMM is traditionally associated with contact measurement, however complex physical parts can cause problems at the data collection stage. Sensible part orientation and an adequate scan line density can reduce these potential errors, resulting in an optimum data-set. A major limitation occurs when inspecting a part containing acute angles, which are impossible to measure using contact methods. New methods of CMM data collection, integrating contact and non-contact probes are continuously being developed, to improve accuracy [BUTLER, 1994]. The integration of contact and non-contact data collection will gain the benefits offered by both methods of inspection. The integration of range finding sensors and the CMM is possible, however, whilst this is

cheaper than a machine vision system, it has larger errors than the touch-trigger probe CMM [CHE, 1992]. The inability of the CMM to measure flexible surfaces can be overcome by combining the CMM and a laser, forming CAD-based inspection [CHENG, 1995]. However, contact data collection has a higher degree of accuracy than non-contact measurement. A touch trigger CMM has an accuracy of 1 μm. This compares with 10 μm for a laser probe, and 100 μm for a scanning probe [SMITH, 1994].

2.2.2   Non-Contact Data Collection Methods

Where soft materials and surfaces that may distort are present, it is undesirable or impractical to use a contact measuring device. In these cases, non-contact optical probes, such as the laser probe can be used, which are mainly based on the principle of triangulation [KEAT, 1994], [ZHUANG, 1995]. However, triangulation methods always suffer from shadowing problems due to separation between source and detectors [BESL, 1985], [CHENG, 1995].

Optical methods are much faster at inspecting, not involving the slow approach to the surface, as needed with contact measuring. A disadvantage of this speed improvement is a reduction in accuracy, thus non-contact CMM probes are rarely used at present [BOSCH, 1995a]. Non-contact sensors are sensitive to the environment and fragile in nature, thus often a more robust touch-trigger probe is used [ZHOU, 1992]. Optical methods are also expensive, with a major limitation being that only dark surfaces can be measured in stable conditions with constant illumination. Often, optical methods result in cloud data which must be thinned before input to a CAD system [CHEN, 1997]. Digitised sensor data refers to the input matrix of numerical values which can represent intensity, range or any other scalar parameter [BESL, 1985]. Range data is usually produced in the form of a rectangular array of numbers, referred to as a 'depth map' or 'range image', where the numbers quantify the distances from the sensor focal plane to the object surface [BESL, 1988]. Spot or line range finding involves projected and reflected light detected by cameras, where a projection of a point is viewed at an oblique angle, and the offset from a defined datum is measured [KEAT, 1994]. Digitised

intensity images are arrays of numbers that indicate the brightness at points on a regularly spaced grid and have no explicit information on depth [BESL, 1985]. Range image formation is conceptually a simpler process than intensity image formation, which can be active or passive.

Active methods project energy onto a scene to measure range, in the form of specialised light or sound. The accuracy of laser range finders depend on the return signal power, which in turn depends on the transmitted power, distance to object and objects' surface reflectance. Image processing isolates the bright pixels and depth, determined by triangulation [BESL, 1985].

Passive methods do not project energy, involving ambient light [BESL, 1985]. Stereo scanning, using two images from two viewpoints allows a depth map to be obtained [BIDANDA, 1994]. Moiré topography involves the illumination of a surface with patterns of light, resulting in fringe patterns which are used to retrieve contour information. This method can deduce depths of a surface from photographs [DUNCAN, 1989]. Pattern projection methods use laser line or grid projections, allowing many more points to be measured in a similar way to flying spot scan methods. This involves the interference of two beams of light, known as an interferometric technique, aiming for invariant surface recognition, based on scan line optical data [KEAT, 1994]. An emerging technique is holometric metrology, where surfaces are measured in their entirety. This is a fast and accurate means of measuring the entire surface profile [BOSCH, 1995b].

2.3   Computer Aided Geometric Design

Machining technology needs a representation of the part to be machined in an understandable format. As CNC hardware improved, Computer Aided Geometric Design (CAGD) developed, where previously, physical models of splines and surfaces were employed [BOSCH, 1995a]. Farin discusses the theoretical background to CAGD [FARIN, 1990], while Gerald and Wheatley discuss the mathematical principles involved [GERALD, 1994].

There are a number of geometric engines which are commercially available. These are software libraries, containing CAGD functionality which can be used for commercial or academic use. The three main competitors are ACIS® from Spatial Technology Inc. [SPATIAL, 1996], Parasolid from EDS [EDS, 1996], and DesignBase from Ricoh Corp. Many standard CAD packages also develop their own modelling engine. These are all software based, however Direct-X® is hardware driven, and may prove to challenge these software graphics engines, in speed and effectiveness [LEDOUX, 1996]. Each engine has its relative pros and cons, but choosing a particular geometric kernel is dependent on the flexibility and functionality needed. ACIS® is seen as a viable geometric engine [MEDLAND, 1992], [RAHMAN, 1992], [BRAID, 1997], and is used in this work.

2.3.1 ACIS®

ACIS® is a solid modeller, allowing wire-frame and surface model representation to be integrated [SPATIAL, 1997a]. Parametric boundary representation (B-rep) is the concept ACIS® adopts, allowing geometry and topology to be represented separately.

Geometry defines the points, curves and surfaces of the model, working with sculptured surface geometry based on Non-Uniform Rational B-Splines, (NURBS). Construction geometry is concerned with the mathematical definition of geometric objects, whereas model geometry is involved with model management, transformations and attribute support, such as save and restore.

Topology is concerned with the spatial relationship between geometric entities, an entity being the most basic ACIS® object. This topology takes the form of the data structure, seen in figure 2.1. Following this topology, data points are represented as *vertices*. The modelling process involves representations using the appropriate topology, culminating at a surface model representation as a *body*. This explicit B-rep method forms a hierarchy of higher dimensional to lower dimensional forms of: boundary, shell, faces, loops, edges, and curve edges bounded by two vertices [MILLER, 1993].

```
                          ┌──────────┐
                          │   BODY   │
                          └────┬─────┘
                               │
                          ┌────▼─────┐
                          │  LUMPS   │
                          └────┬─────┘
                               │
                   ┌───────────▼───────────┐
                   │        SHELLS         │
                   └──┬──────────┬──────┬──┘
                      │          │      │
         ┌────────┐   │   ┌──────▼────┐ │
         │ FACES  │   │   │ SUBSHELLS │ │
         └───┬────┘   │   └──────┬────┘ │
             │        │          │      │
         ┌───▼────┐   │          │  ┌───▼────┐
         │ LOOPS  │◄──┼────────► │  │ WIRES  │
         └───┬────┘   │          │  └───┬────┘
             │        │   ┌──────▼───┐  │
             └────────┼──►│ COEDGES  │◄─┘
                      │   └──────┬───┘
                          ┌──────▼───┐
                          │  EDGES   │
                          └──────┬───┘
                          ┌──────▼───┐
                          │ VERTICES │
                          └──────────┘
```
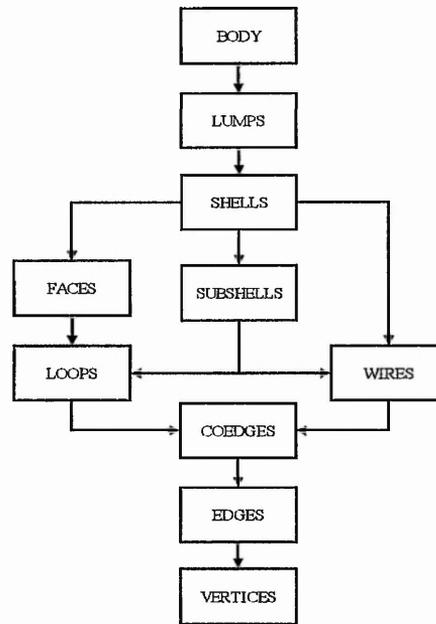
Figure 2.1. ACIS® topology [SPATIAL, 1997a].

All ACIS® surfaces, such as lofted and interpolated surfaces, have a parameterisation scheme defined for them. This results in a *body* with the topology type *spline*. This is a fairly computationally intensive structure used to define smooth sculptured surfaces, compared with analytic surface types. Analytic surfaces, such as plane, cone, sphere, and torus are not considered parametric surfaces. ACIS® 3.0 introduced the concept of net surfaces, creating a surface model from arrays of bi-directional curves, where the surface parameterisation is taken from the parameterisation of the curves. This proves to be useful in areas of Reverse Engineering (RE) [SPATIAL, 1997b].

2.3.2   Modelling Techniques

Modelling techniques include implicit analytical methods related to Constructive Solid Geometry (CSG), an alternative method of solid modelling [PRATT, 1990]. CSG defines solids in terms of Boolean combinations of solid 3D volumetric primitives, such as cylinders, cones and spheres [BESL, 1985], utilising a CSG binary tree whose terminal nodes are primitive solids, and non-terminal nodes are regularised Boolean operations [MILLER, 1993]. Implicit methods are closer to the concept of CSG and solid modelling, however suffer from a lack of free-form surface design techniques

[NEILSON, 1993]. However, implicitisation allows the determination of an implicit equation from a parametric equation, with inversion as the reverse process [SEDERBERG, 1985b]. As well as the B-rep and CSG methodologies, spatial occupancy is a volume-based method of CAGD, using voxels rather than pixels [BESL, 1985]. However, most CAGD systems use a rectangular array of parametric bi-polynomial patches based on a wire-frame model, which is used to approximate a smooth surface [JONES, 1988].

2.3.3   Fundamentals of Parametric Modelling

The parametric method of curve and surface representation is associated with spline functions. The term 'spline', commonly used in CAGD, originates from the law of beam theory. This allows the curvature and slope of a drafting rod to be continuous, where a physical rod can be bent, and held in place using weights and springs [GERALD, 1994]. The basis of modelling is fitting curves through points, where curves can either pass directly through each point, known as interpolation, or can be a best-fitted curve of the points, known as approximation. Interpolation of points result in spline curves, which are usually presented as B-splines. Polynomial equations are used widely to represent splines in CAGD. The basic forms of polynomial equations can be seen below:

- Linear equations are of the form: $y = a_0 + a_1 x$
- Quadratic equations have the form: $y = a_0 + a_1 x + a_2 x^2$
- Cubic equations have the form: $y = a_0 + a_1 x + a_2 x^2 + a_3 x^3$

Point data interpolation is needed for curve generation, where curves are fitted to points, P_i, with a parameter value t_i. This allows interpolating curves to have continuity between curve segments, involving functions such as tangency and curvature, discussed later. Cubic polynomials are the lowest order which can provide continuity of position and slope at a point where two curve segments meet [MEDIONI, 1987]. The highest power of a polynomial is known as its degree.

Fitting a polynomial through points forms a solution to the interpolation problem. Least-squares approximation finds a polynomial that is more likely to approximate the true

values. There are various methods for finding the best-fit through a set of data points, however, in all cases, the deviation of the curve from a set of points must be minimised. The sum of the derivatives can be minimised, as can the sum of the errors. However, minimising the sum of the squares of the errors is an acceptable method. Least-squares principles give a unique set of data, concurring with maximum likelihood principles [DUFFIE, 1985]. Algorithms have been developed which can optimise the parameters by solving the least-squares minimisation problem [SARKAR, 1991b]. Cubic splines are fitted to successive segments, allowing interpolation of data points. This form of polynomial causes the same slope and curvature at adjoining points, where the tangency and curvature of curve segments are described using continuity conditions. Piece-wise continuity involves using continuous curve segments to create a curve, using piece-wise polynomial interpolation. There are two main types of continuity, discussed below:

C^n continuity refers to the continuity of the nth derivatives of the underlying equations. Thus, the magnitude and direction of the nth derivative are continuous. There are a number of continuity constraints:

- C^0 continuity, where the $zero^{th}$ derivatives are the same at their intersection.

- C^1 continuity, where the first derivatives, or tangents, are identical.

- C^2 continuity, where the second derivatives agree. Because curvature is a function of the first and second derivatives, the curvature is continuous if curves are C^2 [SPATIAL, 1997a].

G^n continuity refers to the continuity of geometric properties. Here, only the direction of the nth derivative must be continuous. G^n allows parameterisation to achieve the desired continuity, as this changes the magnitude of the vectors. Again, there are a number of continuity constraints:

- G^0 continuity, where the $zero^{th}$ derivatives are the same at their intersection, but changing the parameterisation of one of the entities does not affect its position.

- G^1 continuity, where the direction of the tangent vectors are identical. By changing the parameterisation of a curve or surface, one can affect the magnitude of the tangent vectors without affecting the direction.

- G^2 continuity, where the direction of the second derivatives are identical. The parameterisation of one of the entities can be altered to get the geometric curvatures to agree, independently of parameterisation [SPATIAL, 1997a].

If a curve has a particular degree of continuity, all points on the curve's interior hold continuity of at least that degree, where the derivative level, n, refers to its degree of continuity.

Parameter values can be termed as interpolating nodes, where apart from the linear case, there is no linear relationship between the parameter and the arc length. There are three forms of parameterisation, outlined below:

- Uniform equal increment, where the node distribution is not related to the data points.

- Cumulative chord length, which is a better method, where the cumulative chord length is proportional to the distance between measured points [FARIN, 1990].

- Centripetal, which has been shown to be an improvement on the previous two methods, by losing the 'overshooting' associated with chord length parameterisation [LEE, 1989].

Parameter optimisation can be used to reduce the fitting error of data points. The number of interactions required for the optimisation process decreases as the number of patches increases [SARKAR, 1991b]. Curves are defined and parameterised in one direction, t, where $0 \le t \le 1$, represented as:

$x = x(t)$
$y = y(t)$
$z = z(t)$

A surface is parameterised in both u and v directions, where $0 \le u \le 1$ and $0 \le v \le 1$, represented as:

$x = x(u,v)$
$y = y(u,v)$
$z = z(u,v)$

There are many parametric CAGD methods for curve and surface design including Bézier and B-spline [FARIN, 1990], Coons [WANG, 1997b], Ferguson [BEZIER, 1972], Gregory [GREGORY, 1986], and Hermite methods [DUFFIE, 1985]. Ferguson and Coons developed their pioneering works based on interpolation theory [HOPPE, 1996]. Each method displays attributes suited to a particular set of conditions, but also has associated problems [SEILER, 1996]. Many curve and surface design methods involve interaction between the designer and the modelling system in a user-guided system [BARTELS, 1994]. Parametric spline and surface methods are discussed in the following sections.

2.3.4   Spline Methods

The most popular curve and surface techniques which have developed over the last 20 years involve the parametric methods of Bézier/B-spline approximation and Hermite/Coons interpolation [PIEGL, 1988]. Bézier curves and surfaces were developed by de Casteljau at Citroen, and Bézier at Renault [FARIN, 1990]. Despite the fact that de Casteljau developed his work before Bézier, it was Bézier who published his work first, hence his name is referred to in these areas. Bézier curves are used as the basis of much CAD work, first developed in the 1960s. They allow curvature control based on the node tension, approximating the data points, with the major advantage of allowing local changes, rather than a global effect. As Bézier curves are developed using a numerically stable polynomial method, they are used in many CAD systems. In many cases the terms Bézier and B-spline are interchangeable, as both are not generally interpolating splines.

When a smooth curve is formed, the internal strains within the spline are minimised. Wang et al. discuss that the energy form of a curve can have a greater impact on the curve than parameterisation [WANG, 1997a]. Minimisation of this strain energy is based on the squared principal curvatures for bi-cubic B-spline surfaces. This strain is used as the basis of geometric smoothness. Tension can involve the integral of a weighted sum of the first and second parametric derivatives. To mimic this behaviour, mathematical splines must use piece-wise polynomials of at least degree three (cubic).

Cubic splines fit a smooth curve through points, based on these earlier drafting techniques. This usually takes the form of a Ferguson, or parametric spline [MORETON, 1991]. This has a cubic polynomial between knot intervals, which form segments that are joined together, with two continuous derivatives, where each knot is a point on the curve.

B-spline polygons define a B-spline curve, but B-spline curves can be generated as an interpolating spline curve. Knot vectors allow the control points to be interpolated or approximated, where nodes control the curve, but are not on the curve. In the cubic case, the coefficient, b_k, is a basis weighting factor and is constant from point to point, for a set of four points. Approximation through four points P_0, P_1, P_2, and P_3 only creates a B-spline in the region of the inner two points. For the cubic case, start and end segments are formed by using sets of P_0, P_0, P_0, P_1, and P_{n-1}, P_n, P_n, P_n, respectively. This weighted sum creates a B-spline curve, as seen in figure 2.2.
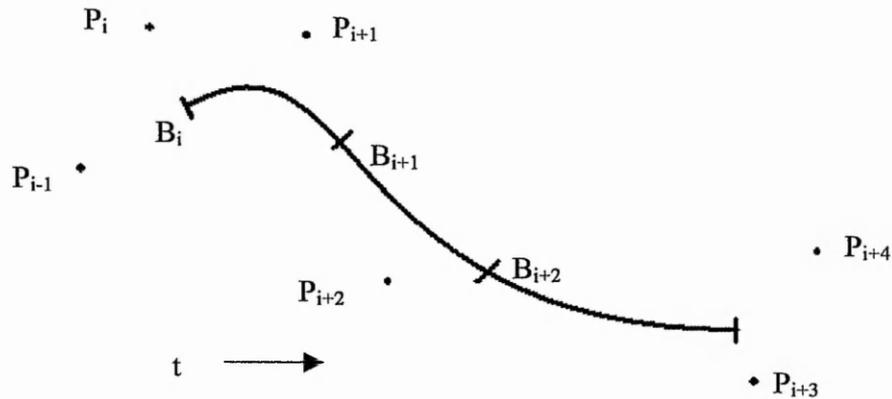
Figure 2.2. Generation of continuous B-spline segments.

This allows B-splines to have start and end knot multiplicity, where the degree of the curve determines the number of knot points at the start and end of the curve. Thus, continuity of a curve involves 'marching' along a curve one point at a time, discarding the first point. This forms a new set of four points. The equations for the weighting factors allow first and second degree continuity, where P_{i-1}, P_i, P_{i+1} and P_{i+2} are used to form B_i. This continues until the end segment is reached. Continuity is maintained by

the control points on the shared start and end of segments. Yau and Chen use rational B-splines to aid data reduction, by approximating complex geometry more accurately than pure polynomials [YAU, 1997]. As long as multiple knots can be contained in the B-spline, a Bézier, or piece-wise Bézier curve can be represented. To achieve smoothness, a B-spline can be converted into a cubic Bézier curve by inserting knots of appropriate multiplicity, using Lee's centripetal parameterisation scheme. Bézier curves are guaranteed only to be C^0 continuous, but achieve higher continuity if control points are suitably positioned [BARTELS, 1994]. Hermite interpolation bases curve fitting on point data and derivative data, such as tangent vectors, where continuity between the connected segments is achieved using the end tangent of one segment as the start tangent of the next segment. However, cubic B-spline curves are more stable than piece-wise cubic Hermite interpolated curves.

Geometric continuity is a measure of smoothness, which can be more appropriate than parametric continuity for CAGD. From this, Beta-splines were developed specifically for computer graphics [BARSKY, 1993]. Beta-splines are more general than B-splines, due to geometric rather than parametric continuity, for which they are tailored. This allows bias and tension factors to be taken into account as G^2 cubic beta-splines with uniformly spaced knots. β^1 and β^2, bias and tension respectively, allow extra control over the curve's shape [GOODMAN, 1986]. Work on other modelling methods has been done, where Sederberg has used tetrahedral algebraic patches, which can have advantages over more conventional free-form parametric surface patches, as they can be of a lower degree [SEDERBERG, 1985a].

Non-rational B-splines and Bézier curves are special cases of NURBS, which allow an exact representation of circular arcs. NURBS can approximate all known CAD surfaces and splines maintaining C^2 continuity [CHEN, 1997]. Most CAD systems now use this representation of B-splines. In 3D cases, underlying splines are used as the basis for surface fitting.

2.3.5   Surface Methods

A surface is the locus of a curve that is moving through space and thereby changing its shape [FARIN, 1990]. CAGD surface methods involve creating and joining adjacent surface patches into a smooth, total surface representation, taking into account continuity conditions. These parametric surfaces are invariant with respect to coordinate transformations [SARKAR, 1991b]. A single B-spline patch can only represent simple topological surfaces, thus complex surfaces are defined by a network of B-spline patches. Corner compatibility is maintained, and thus is tangent continuity, in areas where a patch corner is surrounded by four patches. The surface is described by a set of vertices forming a mesh. The surface follows the shape of this defining mesh, and does not pass through any interior nodes of the mesh, where a network of Bézier patches uses control points to generate a surface [FARIN, 1990]. Modelling systems can represent surfaces with patches bounded by Bézier curves, a special case of B-Spline curves [BARTELS, 1994].

Surfaces can be constructed using methods analogous to Bézier and B-splines. A problem common to all patch types is that the domain of the patches surrounding a single patch cannot be assumed to belong to a common plane domain [GREGORY, 1986]. This means the vector continuity maintains inter-patch continuity. As two cubic B-splines are needed (in the u and v directions), a bi-cubic surface is created, involving sixteen points to create one surface patch. A smooth surface is defined as a network of tensor product B-spline surface patches. This creates a control net, defining the underlying surface, as seen in Figure 2.3.
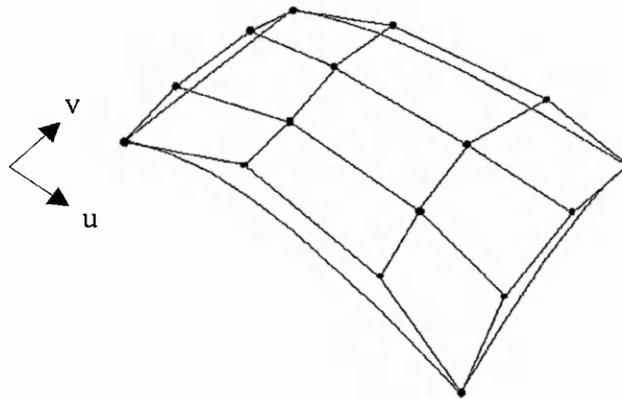
Figure 2.3. Bézier surface and control net.

A NURBS surface is a B-spline element, consisting of smoothly connected Bézier patches. Cubic Bézier surface patches are defined by control points, and Hermite surface patches are defined by interpolating points, but are mathematically equivalent [SEILER, 1994].

Hermite interpolation can use a transfinite blending function interpolant, where the interpolant matches an infinite set of data [GREGORY, 1985]. The shape of a surface can be altered by changing the coefficients of the patches making up the surface. Bi-cubic Hermite surface patches are modified using the method of least-squares fitting. This works towards allowing a new surface to fall on the given data points. This method finds the distance between a point and a surface patch, and obtains a new surface based on the parameter value of the point closest to the given point [DUFFIE, 1985].

Coons patches and tensor product composite surfaces are commonly used in CAGD applications [BESL, 1985]. Coons/Gordon patches differ from B-spline methods as they are based on data points, rather than control points. They are defined by boundary curves, and can be in B-spline, Bézier, or Hermite form. Blending functions are involved across the surface, which can be seen in Figure 2.4. B^1 is a blending function for $V_0(u)$ and $V_1(u)$, and b^2 is a blending function for $U_0(v)$ and $U_1(v)$. Each blending function gives a surface, interpolating two curves of the patch. This gives two different

surfaces, based on two boundary curves each. Subtraction of the bilinear interpolant of the four boundary curves is necessary to obtain the correct surface patch blending.
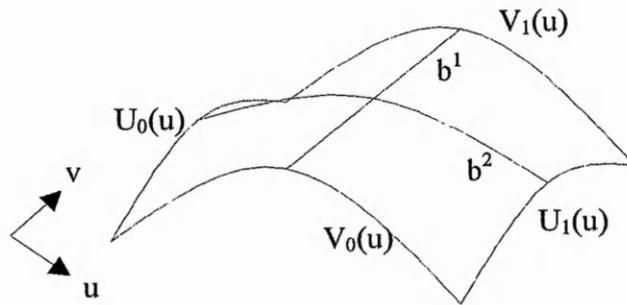
Figure 2.4. Coons patch with blending functions.

Coons/Gordon surface patches are defined by the boundary curves and twist vectors, whereas Ferguson and Gregory patches are defined by boundary curves. For C^2 continuity, control over second normal derivatives and consistency of three twist derivatives is needed [JONES, 1988].

Gregory patches use a blending function interpolant to define a boundary curve and cross-boundary tangent vectors. This boundary can be in a Bézier form, but is often in the Hermite form. Gregory patches do not require the definition of twist vectors, and can also be n-sided, hence are a very useful patch type [GREGORY, 1974], shown in Figure 2.5.
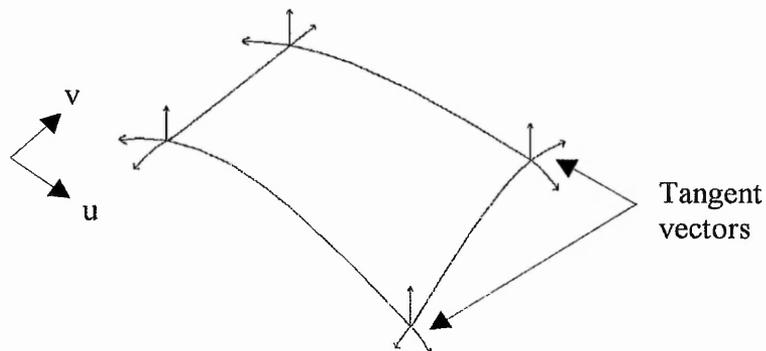
Figure 2.5. Gregory/Charrot patch, showing tangent directions.

A surface patch is generated using boundary edge data and tangent derivatives at the start and end of each boundary edge. Two blending functions are used, namely Brown-Little and Gregory/Charrot methods [GREGORY, 1986]. These methods interpolate the data by calculating the radial direction at each edge from the given boundary data. The Gregory/Charrot method creates interpolants in the V_i and U_i directions, which correspond to interpolants along the radial directions, but differ in parameterisation.

Most current surface modellers are constrained to using four-sided patches. Degenerate four-sided patches can be used, where two edges have tangent continuous edges at the ends they meet, however can cause distortion [STORRY, 1990]. This makes it difficult to match the boundary to a contiguous surface patch with tangent continuity. A quadrilateral surface patch is not always sufficient to be used in all design situations, as all elements must meet four to a corner. Due to this, triangular elements have been developed [HALL, 1990]. Parametric modelling can allow rectangular or triangle patches, however, rectangular patches can cause problems in representing certain objects [NEILSON, 1993]. This depends on the object to be modelled, and available data.

Triangular patches were first considered by de Casteljau in 1963 [BOEHM, 1985]. Models in computer graphics are often represented as triangular meshes, where a triangular mesh is a piece-wise linear surface consisting of triangular faces pasted together along edges, which can preserve discontinuity curves, introducing local regions [HOPPE, 1996]. Three-sided patches are often necessary, in particular with a 'suitcase' corner [GUAN, 1997]. Triangular patches are seen as a useful modelling technique for relatively flat surfaces [SUH, 1994]. These can be in Bernstein-Bézier form, where the hexagonal array of control vertices is analogous to B-spline vertices giving piece-wise cubic C^1 triangular patches [FARIN, 1982]. Triangle Steiner surface patches can join with slope continuity allowing a free-form piece-wise polynomial surface. Steiner surfaces have an implicit equation of degree four, but conversion to parametrically defined surfaces is possible with relative ease. Work by Boehm shows a refinement stage for the formation of a refined triangular net, converging to the spline surface, indicating a potential direction for improvement of triangular patches [BOEHM, 1985].

Peiro et al. generate unstructured triangular meshes on surfaces with defined boundaries [PEIRO, 1990].

2.4   Surface Segmentation and Feature Recognition

Surface-surface intersections are a common and important problem [HOUGHTON, 1985]. Common methods of dealing with composite surfaces at edges involve filling n-sided holes, which cannot easily be done automatically. This includes the corner patches, necessitating the use of triangular patches [BARNHILL, 1974]. The stylist traditionally must define patches that intersect each other along object boundaries, adding fillets, where necessary [BEZIER, 1974]. Non–four-sided patches are also used for blending surfaces. Continuous blending surfaces can link two surfaces applied to filling non-four-sided 'holes' [SCHICHTEL, 1993]. Recursive subdivision, involving n-sided surfaces can be used to improve the intersection problems associated with adjacent regions of four sided patches [STORRY, 1990]. Seiler has developed a methodology to recursively sub-divide patches into smaller patches, improving surface fitting, maintaining four sided patches [SEILER, 1994]. Associated problems of examining surface-to-surface intersections are envisaged to play a part in the trimming of a surface to a boundary or a plane. There are a number of techniques, presented by Patrikalakis [PATRIKALAKIS, 1993].

A major area of current research is involved with the determination of continuous and discontinuous regions, analysing curve and surface curvature. This aims to decompose a global surface into local regions of similar type, or determine surface boundaries by means of edge detection. This has the general term of feature recognition. A subdivision-based intersection method which is independent of surface type has been developed [HOUGHTON, 1985].

Very few automatic feature recognition systems use the CSG system, as it derives from interpreting CSG trees, thus features can be constructed in several ways. More use B-rep topological and geometric aspects, such as shape of faces, face connectivities, and angular relationships [TRABELSI, 1993]. Segmentation is usually done manually, by the reverse engineering operator [PUNTAMBEKAR, 1994, cited in CHEN, 1997]. One

of the earliest automated feature recognition systems was developed by Grayer in 1975 [TRABELSI, 1993]. Most works pertaining to the problem of surface segmentation are image-based. There are two main types of segmentation; edge-based and region-based, discussed below.

2.4.1 Edge-based Segmentation

Edge-based segmentation requires the detection of boundary discontinuities [CHEN, 1997]. These discontinuities in the digitised data are often known as corners or edges, where a corner is defined as a point where curvature goes through a discontinuity or extremal value [MEDIONI, 1987]. Edges can be defined into five categories, denoting forms of discontinuity [BESL, 1986], outlined below.

Step edges involve a change in range, with range images, defining discontinuities in depth values. Figure 2.6 shows a step edge.

Figure 2.6. 2D step edge.

Roof or crease edges account for discontinuities in the surface normal [GHOSAL, 1993]. These can be concave or convex, as seen in Figure 2.7. Step and crease edges both occur at a point of maximum curvature.

Figure 2.7. 2D convex and concave roof/crease edges.

Smooth ramp edges denote curvature discontinuity [GHOSAL, 1993]. These can also be concave or convex, as shown in Figure 2.8.

Figure 2.8. 2D convex and concave ramp edges.

Edge-based segmentation methods commonly detect boundaries between different regions using difference measurements, such as intensity gradient magnitudes on neighbouring pixels [GHOSAL, 1993]. Many works base segmentation on edge detection, where image-processing techniques are used [SARKAR, 1991a]. Surface segmentation can involve edge detection methods of range image data [ZHAO, 1997]. Djebali et al. obtain jump edges, highlighting discontinuities in range images [DJEBALI, 1994]. Edge-based methods suffer as extensive post-processing may be needed. Edge maps are often open, thus edge-based methods suffer from broken edge conditions and spurious edge points [GHOSAL, 1993]. These methods also have problems in roof and ramp edge detection, where a small depth variation leads to edge delocalisation. Due to these problems, many works focus on straight and circular boundaries [GHOSAL, 1993]. Range image segmentation, aimed at feature-based RE, results in overlapped pixels, thus there is no clean boundary between clustered pixels of the same type [FITZGIBBON, 1997]. Segmentation of 3D contours can involve curvature and torsion. Kehtarnavaz and deFigueiredo decompose boundaries into curve segments using B-spline data smoothing. This aims to obtain breakpoints on the contour, thus does not look at surface segmentation [KEHTARNAVAZ, 1988].

2.4.2   Region-based Segmentation

Region-based segmentation involves determining the surface characteristics by analysing surface curvature. Curvature is defined as the rate of change of the slope [MEDIONI, 1987]. A 3D surface point has two directions of curvature, known as primary and secondary curvatures (k_1 and k_2, respectively) [FARIN, 1990]. Gaussian and mean curvature are local second order surface characteristics that have invariant properties and represent intrinsic and extrinsic surface geometry, respectively [BESL,

1986]. Gaussian curvature has the first fundamental form of a surface defined by $x(u,v)$, which is invariant to surface parameterisation changes, translation and rotation. This measures the small amount of movement on the surface at a point (u,v) for a small movement in parameter space (du, dv). Mean curvature, and also k_1 and k_2, are of the second fundamental form, which is dependent on the embedding of the surface in 3D space. This measures the correlation between the change in the normal vector and change in the surface position. Differential geometry states that the first and second fundamental forms uniquely determine local surface shape. The principal curvatures, k_1 and k_2 are analytically equivalent to the mean and Gaussian curvature pair. However, principal curvatures are associated with direction, but mean and Gaussian curvature are not. Gaussian curvature is more sensitive to data noise than mean, which is less sensitive to noise than k_1 and k_2 [BESL, 1986]. Gaussian and mean curvature are used to interrogate the surface, allowing classification of surface types. This area is discussed further in chapter 4.

Region-based segmentation involves region growing/merging, clustering or partitioning. Region-based methods are robust in a noisy environment [GHOSAL, 1993]. Besl and Jain are seen as pioneers in the curvature-based decomposition of surfaces, where many methods are point-based for segmenting range data [HOFFMAN, 1987], [BESL, 1988]. Region growing involves seed regions, which are grown by merging neighbouring regions that have similar characteristics [GHOSAL, 1993]. Clustering is the most common region-based segmentation method, where pixels are partitioned into several clusters, based on approximate equality of surface properties. However, a main disadvantage is that generally *a priori* knowledge of the number of local surfaces present is needed. Clustering can either cause different regions to be grouped together, or over-segmentation, where adjacent similar regions are partitioned [GHOSAL, 1993]. Most region growing methods are highly dependant on the selection of seed regions. Besl and Jain base seed region growing on a variable-order concept, starting with the fitting of a planar surface, segmenting both range and intensity images. Low-order bivariate polynomials can be used to approximate a range image, estimating Gaussian and mean curvature, then applying a seed region method. The range image is decomposed into one of eight surface types, detecting edges and surface area [BESL,

1986]. Algorithms do not always yield ideal high quality edges between regions, and some pixels are left unlabelled [BESL, 1988]. Han et al. extract certain types of surface for 3D object recognition using range information. This concentrates on manmade parts containing simple shapes such as planes, cylinders, and spheres [HAN, 1987].

Rapid segmentation into planar regions has been achieved, based on range data [TAYLOR, 1989]. Henderson and Bhanu represent 3D data as a set of planar faces, taken from range data images. Initially, three very close non-collinear points are used to create a seed plane. Region growing of faces is determined by looking at the set of points lying in the plane of these three points, modelling as polyhedra, followed by tests for convexity and narrowness [HENDERSON, 1982]. This is applied to scene analysis, providing a model for 3D objects, and matching unknown objects with the model, resulting in a description of the surface of 3D objects, in terms of either the points or segmented faces. Generalised cylinder extraction from range images involves step-edge extraction. Axis points are extracted and polynomial curves are fitted through the surface, constructing cross sections. Sweeping rule estimation follows, allowing the generalised cylinders to be output in VRML (Virtual Reality Modelling Language) format [DION, 1997].

Tanaka and Ikeda use spherical correlation, based on principal curvatures in face recognition. This is based on the directions of concave and convex surfaces, where principal curvatures are used to determine surface types, concentrating on ridge and valley surface types [TANAKA, 1996]. A needle diagram is an image with defined surface normals at every point. Sethi and Jayaramamurthy use this, [SETHI, 1984], working towards object recognition, obtaining a Gaussian image of the scene by mapping all the surface normals onto a unit sphere which is centralised at the origin. Characteristic contours are used, based on the locus of the dot product of the surface normal, with reference to a central reference vector. Regular surfaces will give families of contours, which are used to identify types of surface. A Hough transform is used to identify the shapes of contours, giving the identity of the underlying surface.

Ghosal and Mehrotra form a hybrid or integrated method of segmentation, using both feature extraction and region growing [GHOSAL, 1995]. Surface patches are extracted

from range data using an Artificial Neural Network (ANN) connectionist architecture. This involves competitive region growing using a Kohonen self organising ANN, via clustering of feature space. Surface features are extracted and image points are grouped by local competition between surface features [GHOSAL, 1995].

2.5   Machining Methods

3D machining technology of sculptured surfaces improved with Computer Numerically Controlled (CNC) hardware in the 1950s. Traditional CNC machining techniques used linear interpolation, where a curved cutter path is approximated by straight line segments, based on normal vectors, tangent vectors and radii of curvature. These segments connect Cutter Location (CL) points on the curve, however there is a trade-off in accuracy and computation by approximating a parametric curve by a series of linear segments. The use of a ball-nosed cutter, and small step sizes minimises this error, however sculptured surfaces are represented as linear sections [KIM 1988]. Much of the underlying technology of Numerical Control (NC) is discussed in terms of the UNISURF CAD/CAM work [BEZIER, 1972].

More recently, new parametric methods are becoming more popular [YANG, 1994]. 3-axes machines with ball-nosed cutting tools are often used for the manufacture of sculptured surfaces, due to the potential high curvatures present in such surfaces [OLIVER, 1993]. In most cases, the manufacture of a curved surface necessitates the use of a ball-nosed mill, however, this can decrease the speed of milling, due to the smaller effective cutting area, compared to flat end-mills. The use of an inclined flat end-mill can increase this manufacture time, as more material can be removed at each pass [VICKERS, 1989]. Flat end-mills are easier to make and have a more effective material removal rate, however, these can only be used for surfaces with low curvature and often utilise machines with more than three axes. Smith developed a knowledge-based system for process planning for machine selection, machining strategy and parameters, such as tool size and spindle speed, minimising user intervention [SMITH, 1990]. Developments have been made in software tools specifically for the manufacture

of free-form surfaces, allowing the real-time generation of NC control blocks [BROOMHEAD, 1986].

In order to prepare a machining job, a part-program is necessary. Automatically Programmed Tools (APT) style algorithms have been used to generate tool paths for NC machines [GUNASEKERA, 1989]. This involves the creation of a part surface, and a drive surface, which guides the tool. A check surface is also used, which limits the extents of the tool path [HANSEN, 1988]. These work in conjunction with the part surface in the generation of tool paths. Ideally, the tool moves with continuous contact with the part surface. This is not possible as NC machines use linear interpolation, within an allowable tolerance and step length [BEZIER, 1972].

Modern machining programs utilise the G-code system, which defines the cutter path co-ordinates, and tool size and speed. Meander, zig-zag or spiral milling cycles are often used, generating machine paths for manufacture. Part-programs generate CL points, which determine the cutting path. With ball-nosed cutting tools, this is the centre of the tool end. The Cutter Contact (CC) point is offset from this by the tool radius. This offsetting can result in gouging.

2.5.1 Gouging

A common problem at the machining stage is gouging interference, occurring where the resulting offset surface contains offset errors, resulting in 'loops'. This unwanted cutter interference occurs where the cutter radius is greater than the curvature of the surface. Offset surfaces can be problematic, especially when dealing with free-form surfaces. Degeneracies are introduced at higher values of offset distance, occurring mainly at concave regions of curves and surfaces [SARKAR, 1991b]. Self-intersection curves of a collapsed offset surface are independent of surface type and applicable to continuous parametric surfaces [AOMURA, 1990]. Pham discusses a survey of offset curves and surfaces and works towards detecting and dealing with types of degeneracies [PHAM, 1992]. In the 2D case, as with pocket milling, there is the need for 2D offsetting of CC data points, generating an optimum sequence of points [SUH 1990]. Figure 2.9 shows the potential gouging effect of tool compensation.
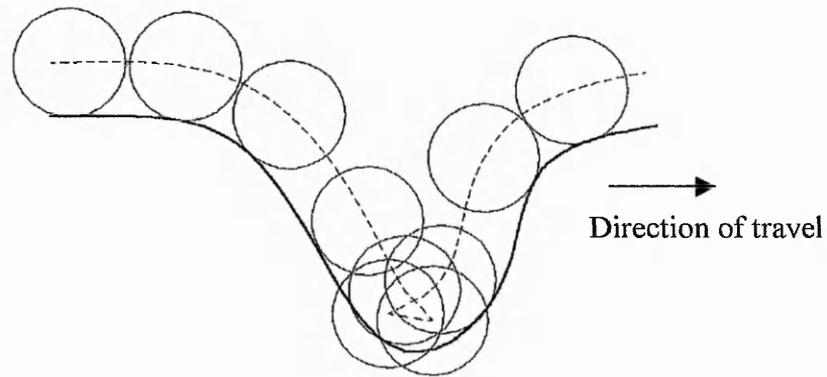
Figure 2.9. Gouging interference.

Gouge detection can be achieved by using linear curve approximation to calculate local chordal deviation, calculating CL points [OLIVER, 1993]. If the surface to be milled has discontinuous tangents, the offset surface may have 'holes', causing problems with concave regions. Offset curves often self-intersect, as seen above. This occurs where the principal radius of curvature is less than the offset distance [OLIVER, 1993]. Simulations can aid the gouge detection of a potential part-program, reducing costs of raw materials. As discussed above, free-form machining often needs a ball-nosed cutter. This shaped tool is the cause of cusp production.

2.5.2   Cusps

Using a ball-nosed tool, there is one contact point between the surface to be cut and the surface of the tool. Thus, furrows are machined, separated by ridges [BEZIER, 1972], often known as cusps [IP, 1991]. This is dependent on the size of the tool to be used and the step-over distance at the tool path stage. Figure 2.10 demonstrates this ridge, or cusp production.
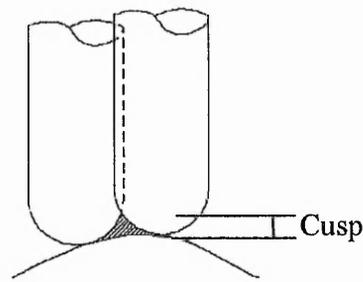
Figure 2.10. Cusp production by ball-nosed cutting tools.

The roughing stage will cause these, where a relatively large radius tool is used at a relatively large step-over distance. Figure 2.11 shows the effect of this gouging on a machined surface. The aim of the finishing stage is to remove these, by using a smaller tool with closer machining paths, often known as the tool interval [SUH 1990].
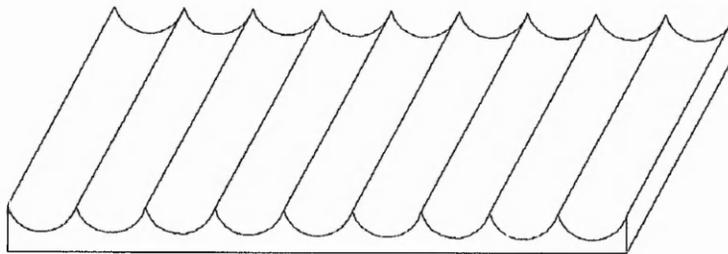
Figure 2.11. Resulting cusps on a machined surface.

There are associated errors with CNC machines themselves. Command errors are deviations of the servo commands, whereas tracking errors are deviations of the machine output from the command references [YANG, 1994]. Machining errors come under the two categories of dynamic errors and quasistatic 'errors of relative position based on the machine tool structure', including loading and thermally induced strains [FERREIRA, 1986]. Ferreira works towards compensating for quasistatic machine errors, modelling the geometric error of three–axes machines. Thermal states are stored and used to build a model relating the change in coefficients to the thermal state and history of the machine [FERREIRA, 1986].

2.6   Integrated Methodologies for Reverse Engineering (RE)

Earlier sections have discussed the background to the main stages of RE, discussed as single processes. Many works involve RE, where the various stages of data collection, modelling, segmentation and machining are implemented. Weir et al. divide the RE process into the three stages of:

- Surface data collection

- Data segmentation

- Surface fitting [WEIR, 1996].

Whereas Varaday give the phases of RE as:

- Data Capture

- Pre-processing

- Segmentation and Surface Fitting

- CAD Model Creation [VARADAY, 1997].

These deal with Part-to-CAD RE, where the result is a CAD model, derived from physical data. RE is broadly defined as the creation of the computer-based model from an existing physical prototype [BIDANDA, 1994]. However, the full RE process also includes surface machining, thus a degree of compatibility is necessary between CAD and CAM stages. IGES (Initial Graphics Exchange Specification) can be used to integrate CAD and CAM [KISHINAMI, 1985]. This is a popular neutral file format, however STEP (STandard for the Exchange of Product Data) aims to improve upon IGES, working towards greater integration between CAD and CAM [SIVAYOGANATHAN, 1993].

In a RE system, a potential CMM data point modelling environment can operate as either an on-line, or off-line system. On-line modelling fully integrates data collection and model generation. As data is collected, each point can be directly represented in real time. The CMM has a direct input to the CAD environment, where 2D and 3D profiles can be plotted, creating cubic splines from the 3D data [GUPTA, 1993]. This

concentrates on manual CMMs, designed for small organisations, and is particularly useful for the preparation of 2D CAD drafting drawings from a physical part. Chen et al. discuss the uncertainty of probe approach, developing a method of on-line CMM data collection. This determines the optimum sampling rate, involving on-line polynomial prediction, however is limited to point-to-point data collection [CHEN, 1992]. Real-time data validation is the main benefit of an on-line system.

The off-line processing of data, and the generation of a free-form surface model are not computationally intensive, thus are completed in a matter of seconds, depending on the size and complexity of the underlying CMM data. This involves the two independent stages of data collection and modelling. CMM data is collected from the object and the total CMM data-set is saved to a file. This concludes the data collection stage. This file is then used in an off-line mode to view and manipulate the CMM data. Simulation is a good application for graphical workstations in an off-line mode, preventing any risk of collision of expensive machinery. Off-line programming, allowing inspection of a CAD representation also plays a large part in CMM training, for similar reasons [ANON., 1996].

2.6.1 Surface Generation from Measured Data

In the realms of RE, CAGD methods are utilised in the fitting of data points. Many CAD systems can involve long processing times, due to the huge amounts of point data necessary for surface generation [KREJCI, 1995]. Many surface generation methods take the input of optically retrieved data. Hoppe generates a smooth surface from an original image of a physical object [HOPPE, 1996]. Mason uses an optical method of data collection, generating cloud data, which must be thinned before input to a CAD system, via IGES [MASON, 1990]. Balendran et al. use a machine vision method to detect flaws on automobile body panels, representing a typical slowly varying free-form surface. This is based on the principle of reflection of light, where the 3D information is used to create a best-fit surface [BALENDRAN, 1989]. Zheng and Harashima generate a 3D wire-frame model from range image data, involving triangulation [ZHENG, 1994]. They calculate a mean square curvature, based on the normal curvature, which detects

dominant points to represent the surface, generating a triangle-based wire frame. This method is insensitive to noise [ZHENG, 1994]. Garcia and Basanez approximate a triangular mesh of control points with smooth surfaces, taking into account uncertainty estimations associated with data points. Modelling methods generally ignore the uncertainty of data [GARCIA, 1996].

Contact methods of data collection, utilising CMM technology, can also be used to generate a surface model. Fang et al. obtain a best-fit surface from CMM data, using Artificial Neural Networks (ANN) to aid the RE process by reconstructing surfaces as a 3D CAD model [FANG, 1997]. The network learns the relationships between the parametric variables and the points by a supervised back-propagation process, which aims to minimise errors. Convergence is dependant on the curvature of the surface, where a smaller radius is more difficult to converge [FANG, 1997]. Seiler et al. use constrained least-squares methods to create a surface model from CMM data [SEILER, 1996]. Cubic B-splines are created from CMM scan data, where B-spline control polygons are found using Gaussian least-squares error norm. Calculating patch boundary curves that cut across the scan lines involves conversion to Bézier curve segments. This allows subdivision of the B-spline, thus unequal numbers of segments can occur on each curve. This resolves the problem where scan lines have unequal segments, used for patch boundary formation. Once patch boundaries are found, tangent continuity (C^1) is achieved using Hermite blending functions across each patch. Interior patch data points can be collected in a model refinement stage. The created surface model is dependent on the original patch shape and size. Also, differing data points taken from the same surface, results in a slightly different surface model. This method involves a return to the CMM, for the collection of additional patch interior points [SEILER, 1996].

Menq and Chen use CMM data collection of sculptured surfaces to form surface models, which in turn aims to improve the inspection path [MENQ, 1996]. Curves are passed through ordered data points taken from sculptured surfaces. This forms a curve made up of a series of polynomial arcs, equivalent to a Bézier curve. These curves are continuous in tangency and curvature, after elevation to degree five. The created surface patches have continuous tangent vectors across the patch boundaries. Their work looks

at improving the accuracy of a CAD model by improving the data collection stage, using surface information in the generation of an improved measurement path. Probing vectors and collision-free paths are important, as well as determining the positions of measured points. They use an iterative method to improve on the data collection stage by altering the probing vectors, based on known surface normals. This allows for improved probe radius compensation, thus improving the CAD model, but involves a number of data collection iterations [MENQ, 1996]. Spyridi and Requicha also use scan data to develop improved inspection paths, based on a solid model, taking into account surface normals to improve probe direction and orientation [SPYRIDI, 1994]. These can be developed in an off-line mode [HERMANN, 1997].

2.6.2 Segmentation of Measured Data

As part of the RE process, segmentation divides the measured points into areas for various individual features. CAD modelling identifies geometric features from measured points and merges identified features into a complete CAD model. Ma and Kruth divide RE into the two tasks of surface digitisation and model construction [MA, 1998]. Model construction involves segmentation and CAD modelling. They have developed a semi automatic system, using NURBS curves and surfaces. The process starts with digitised points, where features are measured with a CMM, rather than the total surface. They apply least-square fitting, parameterising the measured points. The measured points are subdivided into areas for features, involving a large amount of user interaction in the generation of a surface model. The process of parameter optimisation improves parameterisation of the fitted surface, but results in a much longer processing time [MA, 1998]. Sarkar and Menq represent a scanned object with multiple surfaces, detecting shape changes [SARKAR, 1991a]. Laplacian-Gaussian edge operators detect changes in curvature of B-spline surfaces, derived from point-to-point CMM data. They discuss the need for an interactive form of knot insertion, at areas of high curvature. They use a surface intersection algorithm, which uses continuous B-spline curves to connect the intersection points. Shyamsundar and Gurumoorthy construct a model of a part from points measured on the part boundary, inputting vertices. This is done in such

a fashion that it is assumed that the point data is clustered for each measured face [SHYAMSUNDAR, 1996].

Chen and Liu use CMM cloud data segmentation based on NURBS. The data is sliced in three orthogonal directions, where the 2D NURBS are examined for maximum curvature, determining object boundaries. This simplifies 3D segmentation to a 2D problem. There is no clustering of points within the detected boundary domain, thus this work does not look at the surfaces, but at the boundary curves only [CHEN, 1997]. Trimming to a boundary is a useful method of surface refinement, involving determining the intersection of the surface with a closed curve. Lau et al present a method of 3D contour measurement [LAU, 1985]. In the case of boundary trimming at the CAGD stage, the simplest approach to obtaining this boundary is with a 2D cylindrical contact probe. Thus, the intersection of the boundary with the surface to be trimmed can be found without using 3D contour measurement. Unnecessary 3D scan data can be trimmed automatically, involving edge detection algorithms. The data is refilled using continuous non-uniform B-splines, thus approximating the gap allowing no discontinuities [LI, 1997].

2.6.3   Part Machining from Generated Surface

Traditionally, copy milling is used for reproducing a manually made model. The onset of CAGD technology allows machining data to be obtained from a surface model. Ip and Loftus base the surface machining stage on a generated iso-parametric surface model [IP, 1991]. This machining stage is an approximation process, relating the number of subdivisions, or parameter points of the surface model to file size. However, the use of constant step values in the u and v directions cannot guarantee an even distribution of the parameter points on the surface. This shows the need for better cutter path strategies to avoid cusps and interference problems, vital for accurate finish machining [IP, 1991]. Lai and Lu use least-squares minimisation to model a composite NURBS surface from data collected by a 3D scanner [LAI, 1996]. This surface model is then used to generate machining paths. This involves a method for parameter optimisation using surface blending. Their approach uses Gauss-Jordan methods and

Powell's method for parameter optimisation, by changing the parameter value so that the error vector becomes normal to the fitted surface. At the error determination stage, the parameterisation is seen as playing a part in data fitting inaccuracies. Having a method of parameter optimisation will reduce these errors and thus the overall error. Cubic and bi-cubic blending algorithms are also proposed for two-patch and four-patch blending, respectively. Bi-cubic blend surfaces at the boundary of four patches create a Coons bi-cubic surface model, which uses Hermite blending functions. Blending can reintroduce continuity into a model where necessary, in this case to tangent (C^1) continuity [LAI, 1996].

Lee et al. develop a system using least-squares to best-fit a surface to CMM data points, where adaptive path planning generates a cutter path [LEE, 1990]. This can be used to reduce gouging of a machined surface. A parametric surface is created using a least-squares iteration method, based on a large number of equidistant data points. This method closely follows the methods of Duffie and Feng [DUFFIE, 1985], by modifying bi-cubic patches, creating Ferguson patches, which are probe-compensated. Path planning is achieved one patch at a time, generating compensated cutter contact points. This can then be used to generate a cutter path for the global surface [LEE, 1990]. The parameterisation of the modelled surface is important, regarding the generation of tool paths [CATANIA, 1992].

CSG modelling can be used to deduce machine paths, where Choi et al. investigate compound analytic surfaces containing distinct features, calculating CL points [CHOI, 1988]. Stephenson and Smith base machining strategies on the results of a feature recognition stage. Surface curvature is deduced, defining features such as cylindrical fillets, spherical surfaces, and planes [STEPHENSON, 1991]. This allows an appropriate tool to be used for particular features. Stereolithography is an alternative technique of RE, where thin cross-sections of liquid plastic are layered on top of each other, until all the layers are joined, building up a whole part. A *UV* laser passes across the surface, causing the photocurable polymers of the plastic to harden [LOFTUS, 1991]. This process is also known as rapid prototyping.

2.7   Discussion

Machine errors, part errors and measuring errors all contribute to deviations in the RE process [SEILER, 1991], making it difficult to decompose the overall error. This present work is concerned with improving the Reverse Engineering (RE) process, concentrating on the generation and analysis of free-form and composite surfaces. A composite surface is defined as one containing obvious geometric entities, in the form of primitive surface types. An evaluation of the current technology in the area of RE shows a lack of methodology when dealing with composite surface models.

At the physical prototype stage, where a visually pleasing optimum smoothness is desired, the aesthetic properties of free-form sculptured surfaces can be difficult to ascertain. There are a number of methods discussed for the collection of 3D point data, traditionally involving fixed gauges, but more recently utilising the contact CMM. Optical non-contact devices are also used, resulting in range or intensity images. However, many of these methods concentrate on the data collection and modelling of free-form surfaces.

Due to the high degree of achievable accuracy, and the application of this thesis to the improvement of the overall accuracy of the RE process, this present work concentrates on contact CMM data collection. Despite the associated inspection time, compared with non-contact methods, the superior accuracy is preferred. This data is collected once, with no return to the part for extra data collection, as this may not always be possible. This data collection stage is discussed fully in chapter 3. The development of in-house automatic data collection routines utilise the CMES language, native to the LK CMM. This operates in an off-line scanning mode, as the input to the modelling stage of RE. Data collection is not limited to free-form surfaces, as much of the novel work presented in chapter 4 is based on the interrogation of composite surfaces.

ACIS® supports polynomial patches in formats used in CAD/CAM systems, such as bi-linear, bi-cubic, Bézier, and B-spline patches [SPATIAL, 1997a]. ACIS® supplies functions including spline interpolation and a number of defined surface generation methods, such as interpolated and lofted surfaces, involving arrays of data points to

directly model a surface. Choosing the most suitable surface generation method involves factors such as computational time and data file size, as well as accuracy. Many modelling systems deal with rectangular patches alone, as these are more suited to scan data, where patch boundaries are parallel to the uni-directional scan lines. However, three-sided patches are an alternative to four-sided patches, which can be used as blending surfaces to represent specific regions of a surface or fill n-sided 'holes'.

A methodology for the automatic generation of a C^1 continuous surface, based on four-sided Gregory/Charrot patches, is developed in this study. This is discussed fully in chapter 3. Most CAGD surfaces are free-form surfaces, with global continuity, which can cause fairing problems. However, there are no defined features or local surfaces. 'Bumps' and 'wiggles' are terms generally used in CAGD to qualitatively describe inaccuracies due to curve and surface fairing. This is mainly due to problems with optimising the parameterisation. At the Computer Aided Design (CAD) stage, the judgment of the designer is relied upon when generating surfaces, where model improvements usually involve manipulation of the surface's control points. Once the optimal parameterisation is set, the curve is assumed to be fair, however, this is not always the case. Minimisation of the energy of the curve or surface can offer a solution [VASSILER, 1996]. Additional data points can be used to minimise the energy of the curves, as inserting points at necessary areas improves the fairness of the curve. This can be achieved by calculating areas on the curve where there are few points, relative to chord length. In these areas, extra data points may increase the accuracy, reducing the undulations occurring due to cubic B-spline interpolation. Generalising the polynomial can also help. This introduces an extra degree of freedom, known as a tension parameter [FLETCHER, 1987]. Gaussian filters can be used to control the amount of smoothing, but involves computing fourth derivatives [MEDIONI, 1987].

Many model improvement schemes involve a high degree of user-intervention. Also many modelling methodologies and CAD systems do not offer a surface analysis and comparison stage. Thus, limited information can be available on the accuracy and efficiency of the process, [LEE, 1990]. In order to allow reliable assessment of a generated surface, this present study employs a novel deviation analysis methodology,

discussed in chapter 4. This acts as a method of model verification, highlighting the potential inaccuracies in the generated surface model.

The modelling of discontinuous surface-surface intersections using automated modelling methods is a problematic area that has not received much attention, especially when dealing with surfaces derived from CMM data. These methods include edge and region-based segmentation, however, many require interaction in the segmentation of boundary curves and surface edges. Much of the surface segmentation methods have been developed in the realms of image processing. Applying a surface segmentation methodology to data collected by the CMM is an area of novel research. There are many difficulties due to noisy data [TANAKA, 1996], which must be examined in order to provide a successful method. A major area of work developed as part of this thesis involves the implementation of a novel seed region growing method, which labels similar surface points with the same surface type label, discussed in detail in chapter 4.

At the machining stage, choosing the appropriate cutter size, based on surface curvature, can reduce errors, forming a process planning stage [SMITH, 1991]. Errors are often due to the geometry of the part, where errors lead to gouging or cusps. Thus, it is important that the choice of tool used must have a radius smaller than the minimum local concave surface radius [BROOMHEAD, 1986]. Cusps and loops occur where the radius of curvature is less than the cutter radius [KIM 1988]. These can be reduced by using closer paths or a cutter with different form or radius [IP, 1991].

This present work concentrates on Part-to-CAD RE, but discusses the machining stage, as the concluding stage of RE, optimising cutting parameters. Interrogating generated surface models, assessing accuracy and continuity deviation, can reduce errors at an earlier stage, optimising the creation of machining paths that have a reliable conformity with the desired surface properties. This is discussed in chapter 3.

2.8   Summary

The current technologies in the areas of data collection, surface modelling and segmentation, and machining have been investigated in this chapter. These separate activities are often integrated into the RE process. These have been discussed, and gaps in the knowledge base have been highlighted, offering enhancements to the current RE technology to be developed. This present work demonstrates the problems associated with Part-to-CAD RE, and offers novel solutions, aimed at improving the accuracy of a complex CAD model.

Part-to-CAD RE aims to accurately generate a CAD model from CMM data. This is proposed, with free-form surfaces, using C^1 continuous modelling techniques, automatically generating a network of patches which interpolate the CMM data points. However, this method shows problems when dealing with complex surfaces, which are highlighted using Deviation Analysis (DA). In the case of free-form data collection, the desired need for smoothness is evident, and this can be used to assess both data collection accuracy, and physical part continuity. The accuracy of CMM data can be confirmed on surface models where slight discrepancies would be very hard to detect. These inaccuracies may arise from the manufacture of the part, or from the inspection of the part. In both cases, confirmation that the manufactured surface is continuously smooth, and passes through defined points within defined thresholds, is a useful aid to quality assessment. The amount of data needed to generate a surface model within tolerances is also examined. This introduces a novel data partitioning module, which analyses the number of scan lines used, and the resulting deviations between the surface model and the CMM data. In the case of free-form surfaces, a single data-set can be verified, based on its best-fit surface. Smooth surface data can be used to highlight and reduce possible CMM data inaccuracies, as well as improve the original surface's continuity.

Surface inaccuracies mainly occur at edges, where discontinuities cannot be modelled adequately. As the automatic collection of data results in a continuous set of surface information, the resulting surface model is sculptured in nature, despite the original part being made up of a global composite surface, made up of local surfaces. The ability to

decompose this surface into regions is highly desirable. Various methods of surface decomposition, or segmentation, are available in the realms of image processing of range image data. However, decomposing surface models derived from CMM data is a novel area of research. This involves the generation of a seed point on the global surface model, which is then grown to form a region, where all surface points within that region have similar characteristics. This is based on Gaussian and mean curvature, detecting continuous surface areas and discarding discontinuities.

Chapter 3.

Data Collection, Modelling and Machining

3.1   Introduction

As discussed in previous chapters, conventional Reverse Engineering (RE) is made up of the three main stages of data collection, modelling and machining. Work carried out, which leads to the novel work discussed in chapter 4, is presented in the following sections. This allows the rapid generation of accurate part-programs from CMM data.

3.2   Data Collection

Manufacturing has always been constrained by a desired accuracy, within tolerances, especially with parts used in assemblies. Due to this, the accurate verification of manufactured parts is necessary for quality assurance and Statistical Process Control (SPC). Inspection technology has evolved in parallel with the manufacturing process, where parts are produced to a much higher tolerance, leading to the development of Computer Integrated Inspection, (CII), and Computer Integrated Manufacturing, (CIM). In the 1950s, electronic gauging in the form of measuring machines arose and formed the basis of today's Coordinate Measuring Machine (CMM). These are Computer Numerically Controlled (CNC) machines used for fast, flexible, and repeatable measurement of physical parts [BOSCH, 1995a]. These improvements in flexibility and accuracy lead to a decrease in inspection times and cost, benefiting industry.

This section discusses the functionality and application of the CMM in the realms of RE. The CMM used here at Nottingham Trent University's Manufacturing Automation Research Group (MARG), is the LK horizontal arm CMM, using a Renishaw PH9

sensor mount with a TP2 touch-trigger probe. There are a number of CMM configurations, such as moving arm, fixed bridge and cantilever, each suited to different tasks or part size [NI, 1995]. However, the components form a standard set.

3.2.1 CMM Main Components

The measuring system is composed of the 3-axes mechanical set-up, the probe unit, control unit and a Personal Computer (PC). The touch-trigger probe unit is based on high precision switches, breaking an electrical contact when touching the part [BUTLER, 1994]. This generates the impulse that records the position. Figure 3.1 shows a typical touch-trigger probe and mount.

Sensor Mount

Extension
Column

Probe Stylus
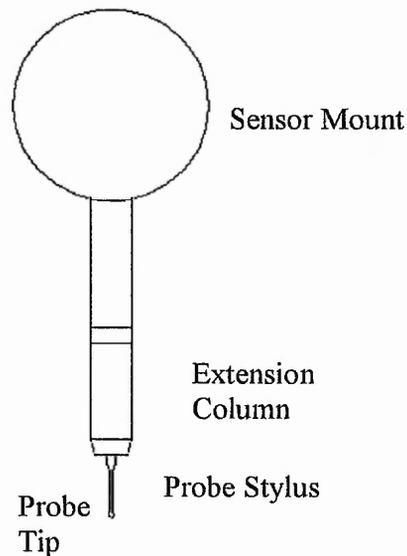
Probe
Tip

Figure 3.1. Touch-trigger probe components.

The control unit of the CMM incorporates a joypad with joysticks, which are used to move the probe manually within the bounds of the measuring machine envelope. This involves entering relevant commands into the PC to collect data. The CMM has become a very powerful metrology tool, where accessible dimensional information can be found from a physical part, applied to inspection and data collection.

3.2.2   Inspection and Data Collection

Inspection is concerned with quality control, where existing parts are checked for tolerance, compared with a desired result. This is particularly concerned with the repetitive task of validating a number of apparently identical parts. In many cases, this is automated, involving an initial manual teach mode. Here, the CMM is set to manual mode and controlled interactively, where one joystick controls the x and y direction and another joystick controls the z direction. Before a point can be measured, the user must access the PC terminal to input a command for the desired operation. This may involve the calculation of a dimension, such as the distance between two points, or the diameter of a hole. There then follow prompts for the required number of points to be taken, and the result is displayed on-screen. Each recorded point can be stored, or allocated a variable name for further usage. This manual process is well suited to the inspection of a few specific points or geometric shapes, however it can be time consuming and may be visually difficult, depending on the probe and part orientation. This teach mode programs the CMM to inspect a batch of similar parts, by first defining the position and size of the features to be inspected, such as holes or slots. The order these features are inspected in is important for successful collision avoidance. Similar parts can then be positioned in the same orientation, and the CMM will automatically inspect the features.

Where there is a need to collect data over a large area, in the case of obtaining surface information, the CMM can be programmed, allowing automatic data collection. Data collection usually refers to automatically measuring relevant regions of a part, with the simple intention of obtaining 3D point data. The CMM can be moved in all directions, but is restricted to measuring in the x-y, y-z or x-z working planes [IP, 1992], utilising point-to-point or scanning algorithms. Definitions between data collection and inspection can overlap, but in essence the goal of the CMM is the collection of 3D point information. In this work, the CMM is used as a data collection tool, automatically measuring a surface within defined boundaries, where the result is utilised further in a modelling stage, discussed later.

A physical prototype surface does not have any physical 'points', however the only way to represent a surface is by collecting a sufficient number of points to generate a surface

model. When data is collected from a surface, the result is a finite array of (x, y, z) Cartesian co-ordinates. However, theoretically a surface has an infinite number of virtual points that can be collected, thus any form of data collection can only obtain a finite sub-set of these surface points. Adequately dense collected surface data is assumed to be a true representation of this infinite set of points.

Before data collection or inspection can occur, adequate planning is essential, due to the high cost of measurement machinery, and in order to minimise inspection times for improved efficiency. The complexity of the physical surface to be measured determines many parameters, thus data collection strategies must be considered. The CMM is set-up and calibrated prior to the planning stage.

3.2.2.1 CMM Set-Up Procedure

Initially, set-up involves choosing an appropriate probe size, where a common probe diameter used is 1.95mm. The choice of probe size and stylus length is determined by the properties of the surface to be measured. The machine co-ordinate system is then initialised, by sending the probe to the 'home' position of (0,0,0). The probe is then calibrated by collecting a number of data points on the surface of a sphere of known diameter, determining the diameter of the un-calibrated probe tip. The CMM sensor mount, holding the touch-trigger probe, is free to move in x, y and z directions, and can be rotated in two axes. This allows the probe to be orientated in a number of positions, giving access to most features on a part. As the probe cannot be freely rotated in all directions, the part may need to be oriented accordingly. The first axis on the probe allows rotation in the x plane between -180° and +180° and the second rotational axis allows rotation in the y plane between 0° and 105°. Probe orientation planning is often neglected, but is an important aspect of the planning process [YAU, 1991]. Figure 3.2 shows two possible probe orientations.
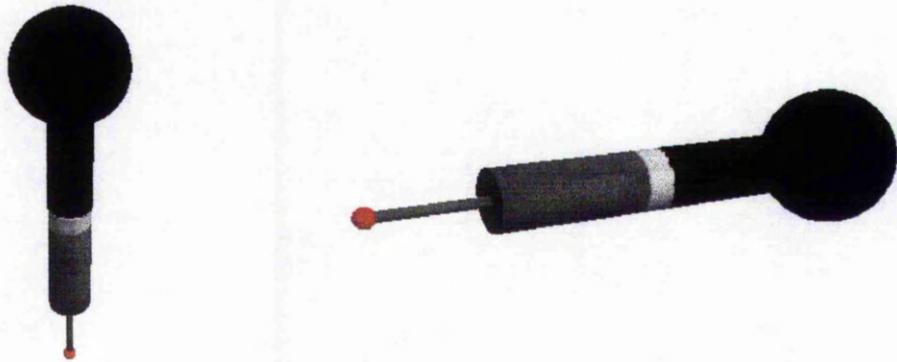
Figure 3.2. Common probe orientations.

The standard orientation is vertically down, parallel to the z axis. This work uses this standard orientation, collecting data from open surfaces oriented on the x-y plane, with the surface on top. The next set-up stage is to define the part co-ordinate system by allocating the x, y, and z axes, relative to the part in question. It is important to position the part so data can be collected from relevant regions. This includes sensible work-piece clamping, avoiding potential collisions. The work-piece co-ordinate system is defined by selecting intersecting planes, as seen in figure 3.3.
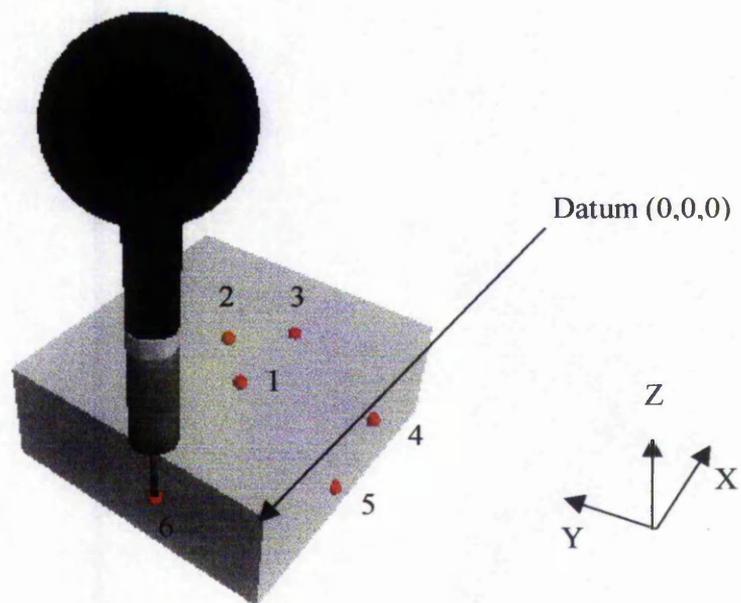
Figure 3.3. Axes determination and resulting work co-ordinate system.

The definition of six points in the order shown is necessary to determine the co-ordinate system and the direction of the axes. The datum is automatically placed at the convergence point of the three axes, but can be re-defined at a specific point in space or on a surface. All future collected points are recorded in relation to this part datum point. Once the initial set-up procedure is completed, there are a number of factors which need consideration in order to optimise the CMM operation. Many are established at the set-up stage, but some can be interactively determined on-line, prior to automatic data collection.

3.2.2.2 Automatic Data Collection

Rather than using the joy-pad, involving a large amount of human intervention, the data collection process can be automated by creating part-programs. These can range from user-interactive inspection programs to fully automated data collection programs. Part-programs can be written off-line by experienced personnel, allowing an interface with the CMM. A simple text editor can be used, and files are saved as text files with a .PRG extension, using the CMES (Co-ordinate Measuring) CMM language [LK, 1992]. In this work, to maintain a degree of user-interaction, generic programs have been written which allow specific parameters to be input. At program execution, the user is prompted to manually move the probe to record a start position and an end plane, as well as a clearance plane, essential for collision avoidance. These inputs are requested on-line, at the start of the generic part-program. The direction of data collection, the number of measurement paths along a plane, and the step-over distance are pre-determined in the program code. The probe then automatically collects data along the initial 2D plane, between the defined start and end points. A new path is then started, at a pre-determined step-over distance from the previous path. This forms a type of adaptable automation, usually employed for the collection of surface data, which results in a finite set of data points covering the part surface. This can be achieved in point-to-point or scanning modes. In both methods, data is collected within a rectangular domain.

Point-to-point data collection involves collecting data literally from one point to the next, at equidistant intervals. This is slow, due to the speed of probe approach, but results in the more accurate collection of discrete data points. This form of data

collection is useful as it simplifies the later model generation stage, as a regular grid of points is obtained, discussed further in subsequent sections. The probe travels in the defined direction, above the clearance plane, approaching a point above the surface defined in the x and y axes, then retracts in the z direction, contacting the surface. The probe location point is then recorded. Once contact has been made, the probe retracts to the clearance plane, before incrementing in the direction of travel to collect the next discrete point. Once the particular set of points has been collected in a plane, a defined step-over distance allows a parallel set of points to be collected. In this way, a regular grid of points is collected. However, this is a time consuming method, particularly with free-form surfaces with steep curvature, as the clearance plane must be specified at the highest point on the total object, with a defined approach speed. Figure 3.4 demonstrates this method, showing one pass across the surface.
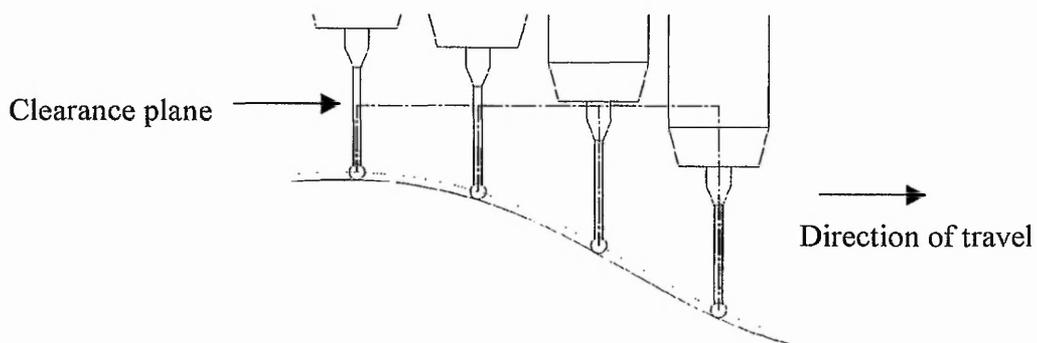
Figure 3.4. Point-to-point data collection.

Initial investigations with point-to-point data collection led to the conclusion that scanning algorithms should be developed to improve speed and surface fitting. For co-ordinate measurement, scanning is currently the most suitable method for acquiring points, at economically acceptable costs [WECKENMANN, 1998]. Scanning results in either uni-directional or bi-directional scan lines of data points, of a set step-over distance apart. The data is collected along a scan line at arbitrary intervals at a high density, using a 'pecking' action, which allows data to be collected much faster than the previous point-to-point method. Also, the data is much denser in the scan direction, thus fitting the part surface better. Adaptive scanning control ensures that the probe tip is in contact with the undefined surface at any change in work-piece shape [NI, 1995]. Bi-directional data collection minimises the need for parameterisation at the modelling

stage, as scan lines are collected with equal density in orthogonal directions on a surface, however, this method has an extended data collection time. Throughout this work uni-directional scanning is used, where the direction of the scan lines is sensibly chosen, depending on the topology of the surface, in order to minimise errors. In many cases, over-sampling is used to record excessive data in order to obtain more accurate data modelling. However, this must be weighed against having an extended data collection time and large data files. Surface scanning does not present any major problems, as long as care is taken that a solid surface actually exists between the start and end points of the scan lines. Deep slots or holes can cause problems, as they represent a break in the open surface. This can cause collisions with parts of the CMM other than the probe tip, where damage can easily occur. An accessible rectangular section of the surface must be present, within the bounds of the specified parameters, and an appropriate clearance plane must be defined. Figure 3.5 demonstrates the scanning method of data collection, showing a single pass across the object surface.


Direction of travel
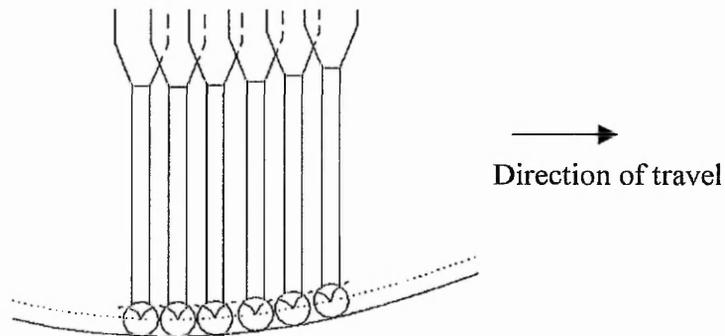
Figure 3.5. Data collection utilising the scanning method.

The most relevant section of a generic CMES scanning part-program file is shown below.

```
I1=5
I2=1
:ST
OP,'SCANNING LINE:',I2
#NS,Y,Z,Y\%Y2\+\N\%X1\%Y1\%Z1
DR
OP,'Lines Scanned;',I2
I2=I2+1
X1=X1+5
I1=I1-1
```

```
#MA,Z\%Z3
#MA,X,Y\%X1\%Y1
IF,I1,STO,STO,ST4
:STO
EP
OP,BE
ET
```

In this case, the program will start a scan line at the (x,y,z) co-ordinate defined on-line, and scan in the y direction, until it reaches the end plane, which is also defined prior to measurement. A defined step-over distance of 5mm in the x direction causes the probe to move to the relevant position for the next scan line, and resume scanning in the y direction. This process will continue until five scan lines of data have been collected. CMMs can be programmed to scan in a 'zigzag' fashion, allowing the end plane of one scan line to become the start plane of the next scan line. This is a minor embellishment to the scanning process, which is aimed at reducing inspection time. This is advantageous on very large objects, however on smaller objects, the time taken to return to the start plane is negligible.

The above generic program allows a degree of interaction within the automated measuring environment. The start point for uni-directional scanning, the extent of the scan lines in that direction, and the clearance plane are defined on-line before the program can execute. To have a true 'part-program', which is specific to a particular part in the same orientation, all moves are made relative to the datum point (0,0,0), with start, end, and clearance planes defined in the program code. Results from the data collection stage are displayed on-screen, and also saved as a CMES data point file, with the .DAT extension, a section of which can be seen below.

```
SCANNING LINE:    1
Number     Scan Raw Data
    Axis X     Axis Y     Axis Z        Direction Cosines

    1    -.003      .000     .017    .00000    .00000    .00000
    2     .000      .663     .014    .00000    .00000    .00000
    3     .000     1.095     .015    .00000    .00000    .00000
SCANNING LINE:    2
Number     Scan Raw Data
    Axis X     Axis Y     Axis Z        Direction Cosines

    1    10.000     .002     .053    .00000    .00000    .00000
    2     9.998     .660     .050    .00000    .00000    .00000
    3    10.001    1.105     .051    .00000    .00000    .00000
```

This data is in an uncompensated form, where the recorded location point is at the probe centre, rather than at the probe contact point. Due to this, data collected with a contact probe must have an associated stage of probe compensation at the modelling stage.

3.2.3   Probe Compensation

The spherical contact touch-trigger probe tip can range in diameter from 0.3mm to 8mm. The probe tip makes contact with the part surface on the sphere's circumference, however the recorded probe location point is taken as the centre of the sphere. The co-ordinate of the probe contact point on the surface must be calculated by offsetting the probe centre by the probe radius, as shown in figure 3.6. Probe compensation is carried out in the modelling stage, after generating a best-fit surface using the uncompensated data, discussed further in later sections.

Probe Location
point at probe
centre

Probe Contact
point with part
surface
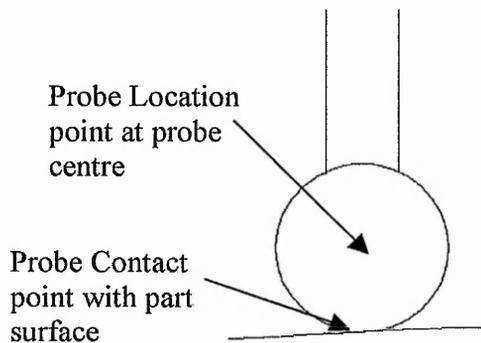
Figure 3.6. CMM data point compensation.

3.2.4   Data Collection Errors

It is vital to assess potential errors at the measuring stage, as this will affect the accuracy of the generated surface model. All data collection and inspection devices, including the CMM, are prone to inaccuracies which can be difficult to detect. A single data-set cannot be assessed alone, due to the collected data having no direct reference for comparison. The only verification method is to take multiple data-sets of the same object and then compare them. If the variance between these are within acceptable tolerances, then the data is deemed accurate and representative of the physical surface.

Due to the time consuming nature of CMM contact data collection, an initial data-set is assumed to be accurate. Where an optimum surface smoothness is desired, the modelling stage can be used to verify the CMM data-set, assessing continuity deviation [BARDELL, 1998c], [BARDELL, forthcoming]. This forms part of the surface model accuracy analysis stage, discussed in chapter 4. However, a good level of point sampling will result in accurate surface representation of all features present on the object inspected [IP, 1991].

There is a degree of measurement uncertainty with the collected data. As this data is recorded at the centre of the probe tip, offsetting is necessary at the modelling stage. This should occur in the exact normal direction of probe trajectory [SAHOO, 1992]. This may cause minimal errors at the surface generation stage. Uncertainty of the measuring process includes effects of the measuring environment, the measuring principle, the operator and the set-up/calibration stage [GRANT, 1995]. Measurement inaccuracies can be induced if contact with the surface has not been achieved in a direction normal to the surface. The compensation for probe diameter will be erroneous where the surface normal at the contact point does not lie on the working plane [IP, 1992]. This is often the case with surfaces with steep gradients, where data collection is automated. Seiler et al. discuss improving the accuracy of measuring complex surfaces by a closed loop inspection system [SEILER, 1991], involving interactive data collection and modelling with a return to the CMM to collect further data where necessary.

The probe trajectory must be controlled whilst approaching the surface, otherwise damage to the machine will occur. The speed of the measuring process determines the accuracy of the surface model, as a fast probe speed will result in fewer data points along a scan line. However, the desired accuracy must be balanced against the time spent on data collection. There can also be speed and accuracy problems due to the 'back-off' distance after the probe has pecked at the surface.

Inaccessible features, such as acute angles cannot be measured using a spherical probe. There may also be a limitation to objects that can be scanned, due to the length of the stylus causing unwanted collisions. This is the case with feature-based objects with deep

pockets or slots. It is assumed that the surface to be measured is of a solid material, with no holes, or breaks in the surface. This section discusses CMM contact measurement, however, certain objects would benefit from non-contact measurement, particularly where flexible materials are present.

As with all CNC machines, there are a number of external factors that affect the accuracy of a CMM, namely temperature, vibration and humidity. These conditions cannot be easily controlled in most industrial situations, but sensible use of surrounding machinery can minimise errors in data collection by trying to achieve a stable environment for inspection. Temperature deviations can be compensated for, with respect to the measuring equipment. Climate control, and vibration damping bases can be used to minimise these causes of error [WECKENMANN, 1998].

Once adequate CMM data has been collected, the modelling stage can commence.

3.3   Free-form Modelling of CMM Point Data

Traditionally, sculptured free-form surfaces have been used in the shipbuilding and aircraft industries, resulting in necessary aerodynamic properties [YAU, 1997], [KIM, 1988]. Due to improved manufacturing techniques, and a consumer driven market, there has been an increase in the use of sculptured surfaces in manufactured products. This is particularly the case with the automotive industry, where aesthetic properties are becoming as important as aerodynamic issues. Even household appliances, such as kettles, are now manufactured with sculptured surfaces. The definition of these surfaces can be difficult to specify, especially in cases where physical prototypes are manufactured by hand, but aesthetic and functional conditions must be satisfied [HOPPE, 1996]. In this work, a sculptured surface is defined as a free-form surface which is continuously smooth, with no distinguishable features or sudden deviations in the continuity. This differs from a complex composite surface, made up of separate distinguishable surfaces, intersecting at the surface boundaries.

The correlation between the prototype part and the generated surface must be maintained, within defined tolerances, in line with a functional part. This involves the

minimisation of any modelling errors, utilising an optimisation of modelling parameters. Where a physical surface is digitised, accurate assessment of the prototype model is necessary. As deduced from chapter 2, current RE technology is lacking in this area. Aesthetic qualities of visually pleasing surfaces introduce the term cosmetic quality [BALENDRAN, 1993], used to qualitatively describe the surface form. Slight flaws in a surface can be described in terms of cosmetic quality. In the case of sculptured surfaces, the CMM may detect flaws in the overall physical surface continuity, which will cause deviations in the generated best-fit surface. In some cases, these deviations are acceptable, as the generated surface model smoothes the CMM data, resulting in an ideal sculptured surface model, which is aesthetically pleasing.

It is vital that surface models are accurate, within tolerance, as these are often used in the manufacture of a reproduction part. This section discusses a Computer Aided Geometric Design (CAGD) method of automatically modelling CMM data collected from a physical surface, using a single probe orientation. This differs from a closed 3D surface, where changes in probe orientation are necessary at the measuring stage. Surface reconstruction is often used to define the problem of converting dense point sets into useful geometric models. The integration of data collection and modelling is termed Part-to-CAD Reverse Engineering (RE). In this work this utilises the functionality of the ACIS® CAGD development tool. This is developed in the object-oriented C++ language [HORTON, 1997]. A method of global surface generation is developed in this work, as existing ACIS® functions for surface generation cannot be confidently analysed. This is due to the unavailability of proprietary information on the internal CAGD mechanisms. This allows full transparency of the steps involved in the generation of a global surface model from CMM data. Programs are developed, linking to the appropriate libraries containing the CAGD functionality, using Microsoft Visual C++ version 5, integrating with ACIS® version 4.3. An Intel Pentium 133 Personal Computer (PC) with 64Mb is used, under a Windows® NT 4 operating system. CAD/CAM packages have evolved greatly over recent years, as has the processing power of PCs. This allows this computationally intensive CAGD work to be implemented on a standard PC, where traditionally powerful CAD workstations were needed. The automated free-form modelling method discussed in this section operates in

an off-line mode, involving an initial file conversion prior to the input of the CMM data file.

3.3.1   CMM Data Point Processing

Interoperability is a relatively new term to mean the ability for all CAD packages to equally share and translate data. However, whilst there are competitors in the CAD geometric engine area, this will never be a reality, due to incompatibility of data file formats [POTTER, 1997]. This problem has led to the development of standards such as STEP (STandard for the Exchange of Product Data) and IGES (Initial Graphics Exchange Specification), which work towards a greater integration between CAD and CAM [MAYER, 1987]. There are problems with IGES, such as excessive file size and the exchange of free-form information, which STEP aims to improve upon [SIVAYOGANATHAN, 1993]. In this present work, an intermediate file is created, extracting relevant data for input to the ACIS® modeller. The CMES .DAT file, discussed previously, is converted to a neutral .PNT format, which is created specifically for this work.

Due to the minimal co-ordinate data format, with the exclusion of headers and footers, this simplified file has the potential to be read by other modelling packages. Information on the number of scan lines, and the maximum number of points per scan line is also input, as a second file, with the file extension .EXT. A typical segment of a .PNT neutral file format is shown below, used as the input file for the ACIS® application developed in this work.

```
X -0.003 Y  0.000 Z  0.017
X  0.000 Y  0.663 Z  0.014
X  0.000 Y  1.095 Z  0.015
X 10.000 Y  0.002 Z  0.053
X  9.998 Y  0.660 Z  0.050
```

As an initial step, the ACIS® modelling environment converts and saves these points in a compatible file format. This can be a binary file with the extension .SAB, or a text file with the extension .SAT. Binary files have a smaller file size, however .SAT files are used in this work, as it is useful to have a readable text file. The .SAT file format

resulting from initial processing of a .PNT file is shown below. As discussed in chapter 2, these points are represented as entities.

```
201 0 6 0
7 Unknown 11 ACIS 3.0  NT 24 Wed Nov 25 13:13:29 1997
        -1 9.9999999999999995e-007 1e-010
point $6 -0.0030000000260770321 0 0.017000000923871994 #
point $7 0 0.66299998760223389 0.014000000432133675 #
point $8 0 1.0950000286102295 0.014999999664723873 #
point $9 10 0.0020000000949949026 0.05299999937415123 #
point $10 9.9980001449584961 0.6600000262260437 0.05000000074505806 #
End-of-ACIS-data
```

This .SAT file can be opened and viewed in an ACIS® environment. An example of a point-to-point data file, collected from a commercially available bottle, can be seen in figure 3.7. (Data collected courtesy of Renishaw).
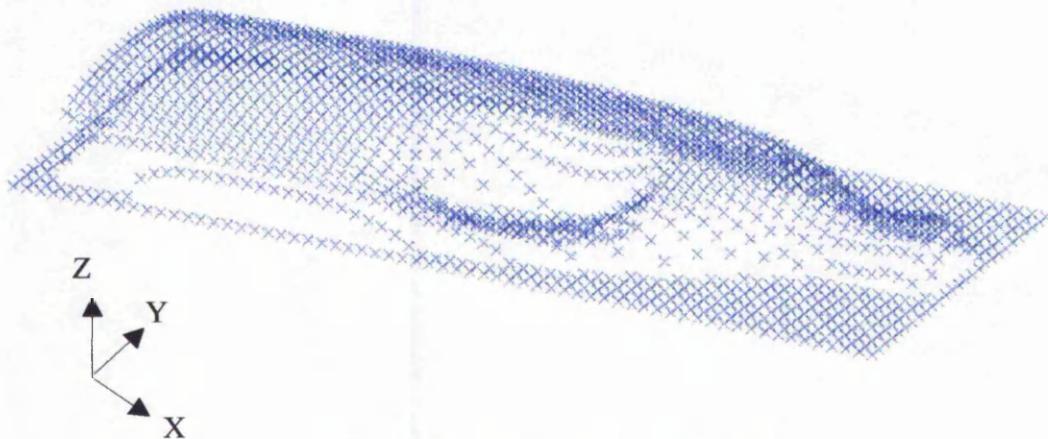
Figure 3.7. Point-to-point collected data.

This data was collected at 5mm intervals in the x direction, with a step-over distance of 5mm, resulting in a regular grid of data points. Figure 3.8 shows a photograph of a similar bottle, from which scan data is collected.
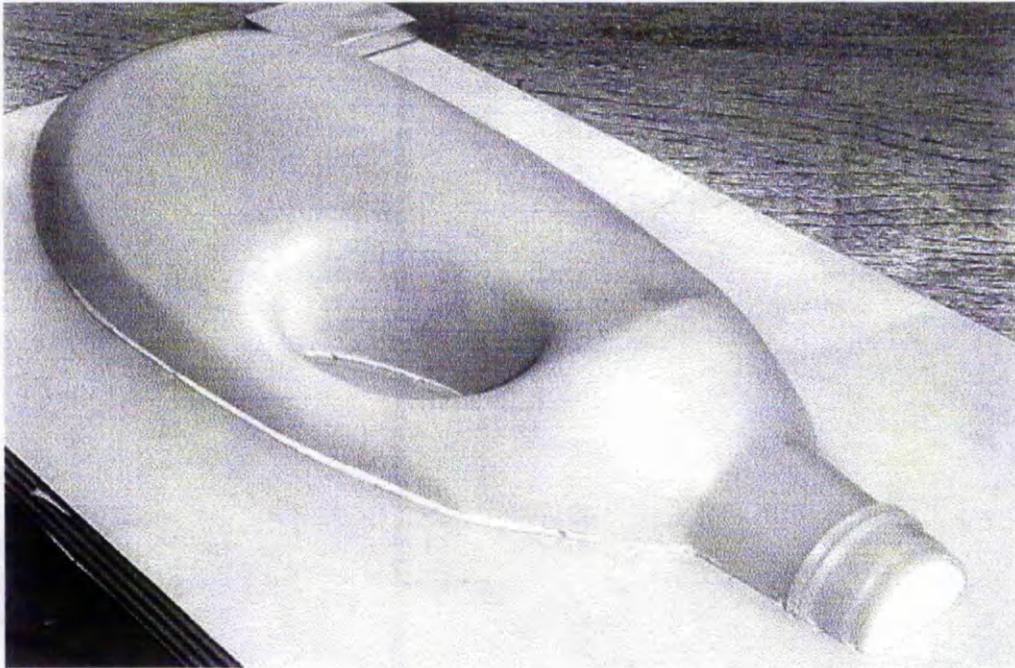
Figure 3.8. Photograph of bottle.

Scan data is collected from the neck region of this bottle, as this is a region containing complex surface-surface intersections. The scan line direction is parallel with the y-axis, with a step-over distance of 10mm. This is deemed a fairly sparse data-set, however it is used in a majority of this work to highlight modelling errors. Figure 3.9 shows this scan data.
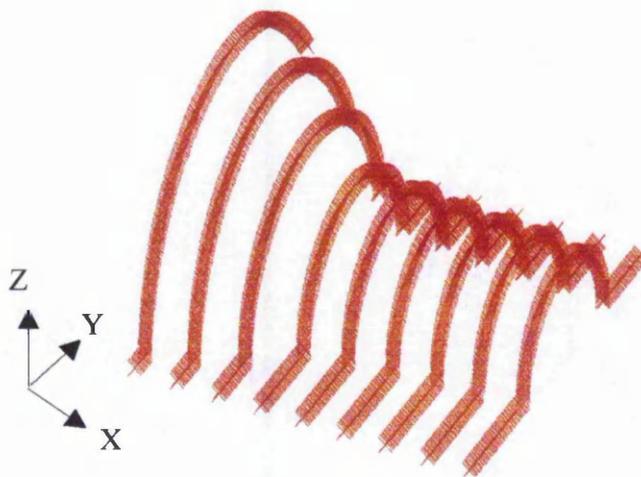
Figure 3.9. Scan data points.

This ACIS® representation of the uncompensated CMM data is the initial stage of free-form modelling. This data can be stored internally in array form, rather than being saved as part of the .SAT file. The .SAT files are viewed using the ACIS® Viewer software. The next modelling stage involves the interpolation of these CMM data points. Both point-to-point data and scan line data use the same interpolation methodology.

3.3.2   CMM Data Point Interpolation

Data is collected along parallel uni-directional lines. These are collected in a single direction, involving a return to the start plane at the end of each scan line. Each scan line of data is interpolated by a cubic B-spline, allowing continuity within the specified array of points forming a particular spline edge. These interpolated splines pass precisely through the CMM data points, and have null start and end vectors. Figure 3.10 shows the point interpolation of the scan lines, resulting in uni-directional second order B-splines.
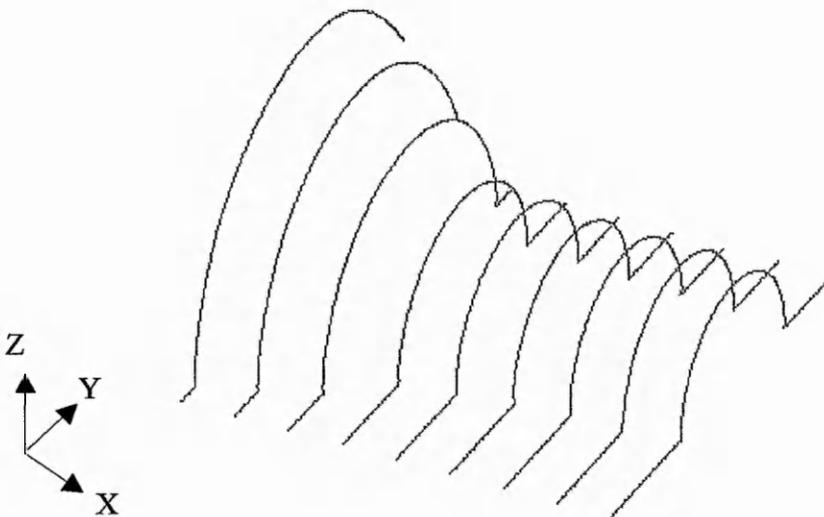
Figure 3.10. Uni-directional splines, interpolating the CMM points.

These splines have the same 'sense', thus have the same direction, due to the uni-directional nature of data collection. Zigzag, or meander, CMM scanning can be used, which improves inspection time, however it involves an extra processing stage, where alternate scan line directions must be reversed.

It is necessary to represent the 3D domain of co-ordinate points in parametric form, where each point is defined as $P(u, v)$. This involves the generation of a bi-directional spline network, approximating the CMM data points, from which the surface patch generation stage can proceed.

3.3.3   Bi-directional Spline Network Generation

Where data is collected in grid form, as with point-to-point data collection, obtaining a bi-directional spline network is a relatively straightforward task, as the actual CMM data points can be used for curve fitting in both u and v directions. Figure 3.11 demonstrates this, where the CMM data points are used directly, generating interpolating splines in both directions. However, this limits the effectiveness of the modelling stage, as the underlying surface model will rely on the density of the collected data.
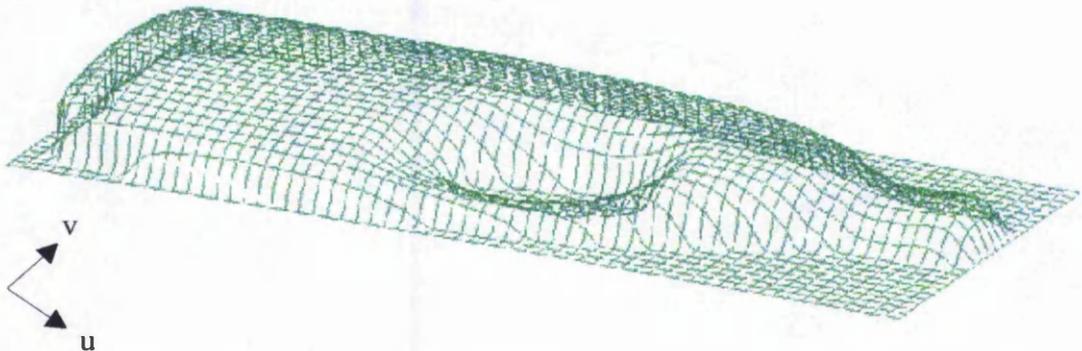
Figure 3.11. Network of bi-directional spline curves generated from point-to-point data.

As discussed previously, scan line data collection is preferred, which results in dense data points in the scan direction (u). The number of points on this line is arbitrary, depending on the speed of travel. To generate splines orthogonal to the uni-directional splines, it is necessary to introduce uniform parameter points along these splines. This involves chord length parameterisation, generating a defined number of parameter points along each spline. In this way, points between the CMM data points can be approximated, where necessary, and the actual CMM data points can be discarded, as parameter points along the spline can be utilised. Parameterised uni-directional B-splines specify the points on the splines as a function of the parameter u, where $0 \leq u \leq$

1, where u is the scan line direction. These parameter points are used for the generation of splines in an orthogonal direction. This is necessary, as CMM scan data is too dense to use, unlike point-to-point data. Also, there is an unequal number of points on each scan line. Figure 3.12 shows the generation of splines orthogonal to the u direction, interpolating parameter points created in the u direction. This orthogonal direction is defined as the v direction.
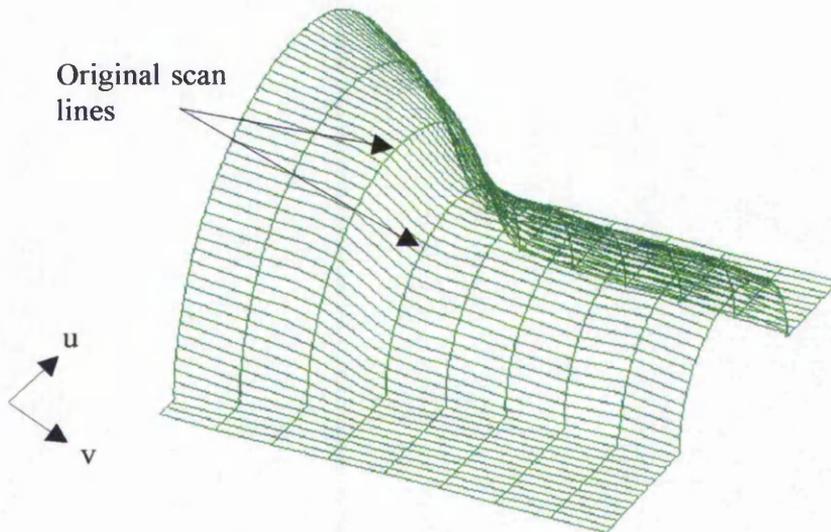
Figure 3.12. Generation of orthogonal splines, based on knot points in the u direction.

The number of parameter points employed in the u direction is user-defined, based on the required density. User-defined variables are input to the system, via a text file USR.USR. This file contains relevant information on the desired patch size and parameterisation. The effect of parameterisation and patch size is discussed in more detail towards the end of this section. Automatic parameter optimisation improves the parameterisation of the fitted surface, but results in a much longer processing time [MA, 1998]. The effect of the interpolation of the parameter points, generating splines in the v direction, can be seen more clearly from a top view of the same spline network, shown in figure 3.13.
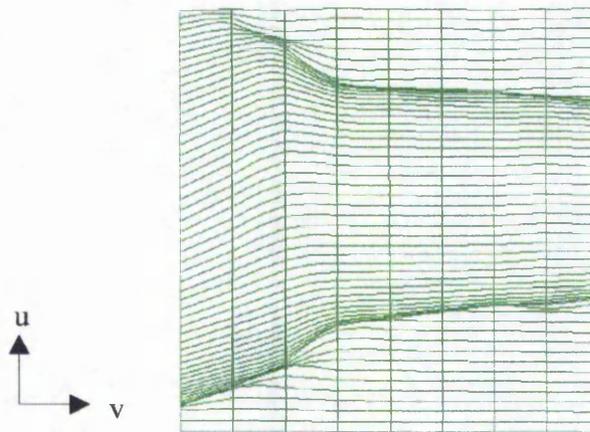
Figure 3.13. Top view showing parameterisation in u direction.

Due to the chordal length method of parameterisation, each parameter point is equidistant from the next, in terms of the length of each chord segment. For objects containing extreme curvature change, as in the above figures, this results in a compression effect, where the splines undergo deformation, and are non-symmetrical. The parameter points can be termed knot points, as they occur at the u and v spline intersections. The number of knot points is equal along each spline, independent of the length of the spline. This accounts for the non-symmetrical formation of the splines. It can be seen that the maximum number of knot points in the v direction is currently based on the number of scan lines used, thus any increase in parameterisation for improved surface fitting will only affect the density of knot points in the u direction, resulting in denser splines in this direction only.

The generation of a regular spline network involves parameterisation in the v direction, where $0 \leq v \leq 1$. This results in an iso-parametric spline network, where comparable chord length parameterisation is present in both u and v directions. Using the knot points generated in the v direction, the splines in the u direction are redefined, replacing the original splines interpolating the CMM data. This results in a uniform parameterisation in both u and v directions, maintaining a close approximation of the original CMM data points. The distance between parameter points is approximately equal, thus the number of knot points in the u and v directions can vary, depending on the dimensions of the surface in u and v. The generation of a bi-directional spline network is also essential for the calculation of tangency conditions at each knot point,

discussed later. Figure 3.14 shows the bi-directional re-parameterised spline network, and figure 3.15 shows the top view of the same object, highlighting the effect of chord length parameterisation in both the u and v directions. The compression phenomenon is now present in both u and v directions. This distorted parameterisation results in parameter lines that do not correspond with cross-sectional contours [STORRY, 1990].
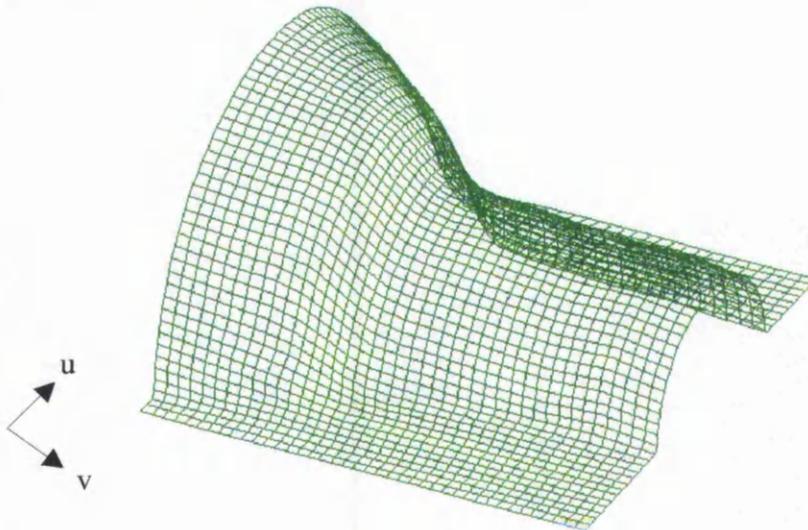
Figure 3.14. Bi-directional spline network, parameterised in u and v directions.
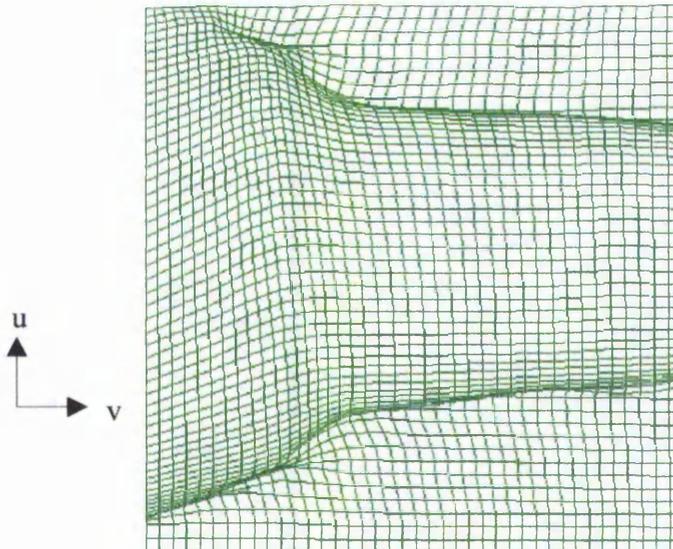
Figure 3.15. Top view of bi-directional spline network, parameterised in u and v directions.

The knot points can now be utilised in the generation of surface patches. This involves the knot point interpolants, rather than the actual interpolating splines. As discussed in chapter 2, a global surface is made up of many continuous patches. The user can define the size of each patch, and the number of knot points per patch. This determines the number of patches used to generate the global surface.

3.3.4 Patch Formation Fundamentals

A single patch is a function of u and v, forming an approximated bi-cubic spline surface patch with defined knots. Four interpolating Hermite splines are generated, interpolating a user-defined number of knot points, and a surface patch is formed from the closed loop of adjoining edges. The development of an appropriate patch formation methodology initially involves looking at the most basic patch conditions possible. The following sections discuss the evolution of the patch formation methodology developed in this work, demonstrated using a simple free-form surface. In the initial instance, knot points are used at the patch corners to generate planar patches.

3.3.4.1 Planar Patch Formation

Planar patches connect with adjacent patches at the patch boundaries but possess no intra-patch (within) or inter-patch (between) continuity. The result of using planar patches can be seen in figure 3.16. Each patch is defined by the four corner points, taken from knot points on the underlying iso-parametric spline network. Thus, each of the four patch boundary edges interpolate just two parameter points.
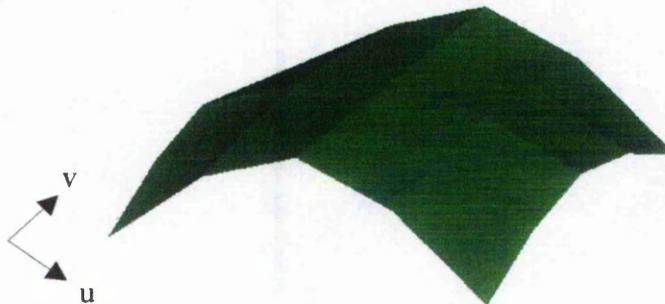
Figure 3.16. 4x4 planar patches.

If the patch size was smaller, each patch would seem to blend into the next, but in reality possess no continuity. As each patch is discontinuous and straight edged, this forms a method of surface faceting. Intra-patch continuity is the next constraint necessary for the generation of a smooth surface. This involves parameterising each patch boundary, allowing more parameter points per patch edge.

3.3.4.2 Intra-patch Continuity

Intra-patch continuity establishes curvature into the patch boundaries, where each patch boundary interpolates more than just the corner start and end points. This introduces intra-patch parameterisation, allowing larger patches to be used in the generation of a global surface. Figure 3.17 demonstrates this, where each patch boundary interpolates five parameter points. This results in C^0 continuity conditions [BARDELL, 1997].
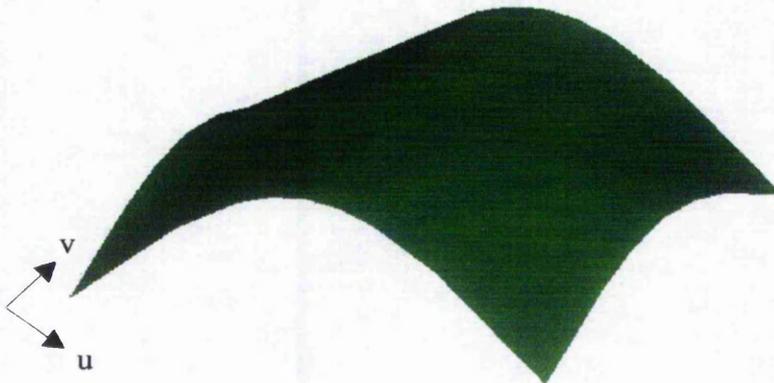
Figure 3.17. 2x2 C^0 continuous patches.

The four patches appear to blend into each other, forming inter-patch continuity, however this is not the case. This would be apparent with more complex surfaces. C^0 continuity conditions constrain the boundary edges to be adjacent, but no inter-patch tangency is present. In this case patch parameterisation is five, as seen in figure 3.18 showing the intra-patch parameter points for a single patch.
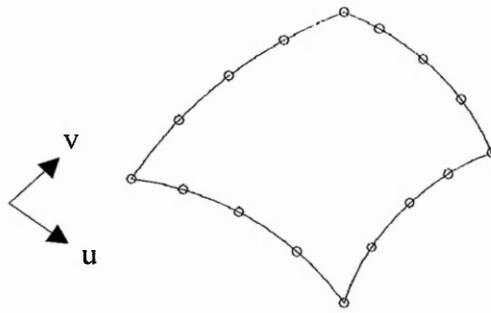
Figure 3.18. A surface patch, with a parameterisation of five.

This intra-patch parameterisation is defined by the number of knot points on an individual patch boundary. This determines the accuracy of the curve fitting to the CMM points. Optimising the parameterisation involves a trade-off between file size and accuracy. This C^0 continuity condition may be acceptable with smooth surfaces with low curvature, however the continuity constraints are not adequate for accurate generic free-form surface modelling. An ideal condition is to have C^1 continuous patches, where boundary tangency conditions are taken into account, allowing inter-patch continuity [FARIN, 1990].

3.3.4.3 Inter-patch Continuity

With C^1 continuity, the first derivatives, or tangents, are identical across the patch boundaries. These tangent conditions are calculated for each parameter point, in both u and v directions, utilising the bi-directional spline network. The resulting continuity constraints can be seen in figure 3.19, with positional and tangency continuity conditions, improving the approximation accuracy of the generated patches [BARDELL, 1998a].
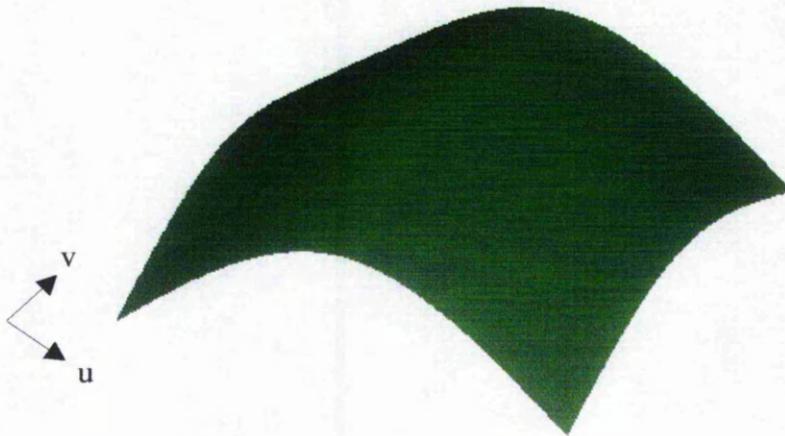
Figure 3.19. 2x2 C^1 continuous patches.

Visually, both C^0 and C^1 are similar, however are not mathematically equivalent. Using this level of continuity, adjacent patches are positional and tangency continuous. Figure 3.20 shows the principle of tangent continuity, where continuity of the internal patch is achieved, based on the curvature of the external boundary splines. C^1 continuity is obtained at the common boundaries with adjacent quadrilateral elements, as developed by Gregory and Charrot in 1980 [HALL, 1990].
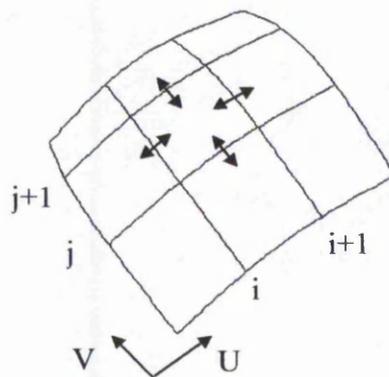
Figure 3.20. Inter-patch continuity.

Splines i and i+1 allow inter-patch continuity in the v direction, where splines j and j+1 allow continuity in the u direction. Positional and tangent inter-patch continuity is maintained, resulting in a network of C^1 continuous Gregory/Charrot patches.

The next stage involves generating a global surface from this patch network, where adjacent patches are merged, maintaining the continuity conditions present in the original spline curves. This patch network is often expected to be smooth, with at least tangent plane continuity (G^2). In most general cases a B-spline surface is defined as a network of tensor product B-spline surface patches, with seamless joints at adjacent patches, where the patches have the same knot vectors and order, and points are shared along the patch boundaries. Most 3D surface fitting of points either assume a simple topology surface type, or require user intervention in setting up the patch network.

3.3.5   Global Surface Generation

Cubic splines are used in the definition of patch boundaries, based on the bi-directional spline network interpolants. This results in a piece-wise polynomial patch network giving a parametric tensor product surface. The methodology for patch merging developed in this work involves recursively merging adjacent patches, first in the u direction, forming a single patch along the u direction, and then merging with adjacent patches in the v direction, summarised in figure 3.21 and described below.

13	14	15	16
9	10	11	12
5	6	7	8
1	2	3	4

v ▲
└─► u
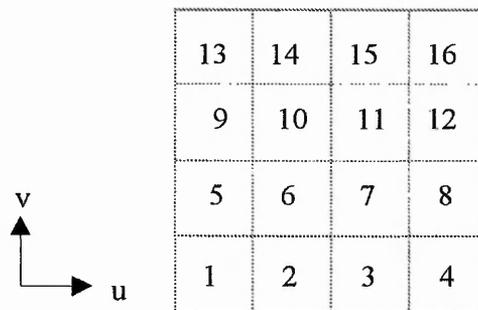
Figure 3.21. Adjacent patch merging.

Initially, patch 1 is merged with patch 2, forming a single patch, u1. This is then merged with patch 3, which again forms a single patch, replacing u1. This is merged with patch 4, completing the first patch merging in the *u* direction, resulting in a single patch made up of the original four patches. The same procedure takes place for patches 5, 6, 7, and 8, resulting in a single patch, u2. These two patches are then merged in the v direction,

forming a single patch v1. This process continues until the 16 individual patches have been merged into a single patch.

The number of patches in the u and v directions are calculated, based on the user-defined patch size. This is defined as patch resolution, which determines the accuracy of the resulting surface. If an inadequate patch size is used the patch resolution is low, resulting in high model deviations. This is discussed in chapter 4, involving surface model accuracy, computational time and size of file. Figure 3.22 shows the C^1 continuous patches used to generate a global surface model of the bottle seen earlier (wire-frame model). In this case, ten patches are defined in the u direction and eight patches in the v direction, with an intra-patch parameterisation of five. Figure 3.23 shows the rendered surface model of the same, where surface deviations are apparent.
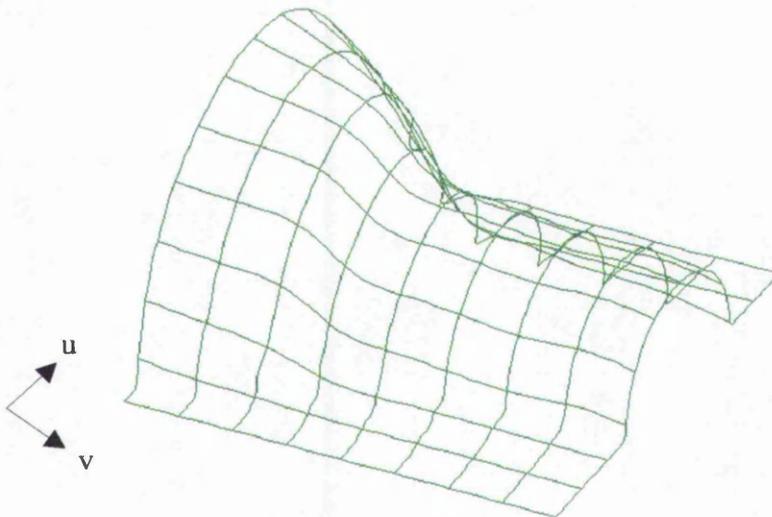
Figure 3.22. 10 x 8 C^1 continuous patches.
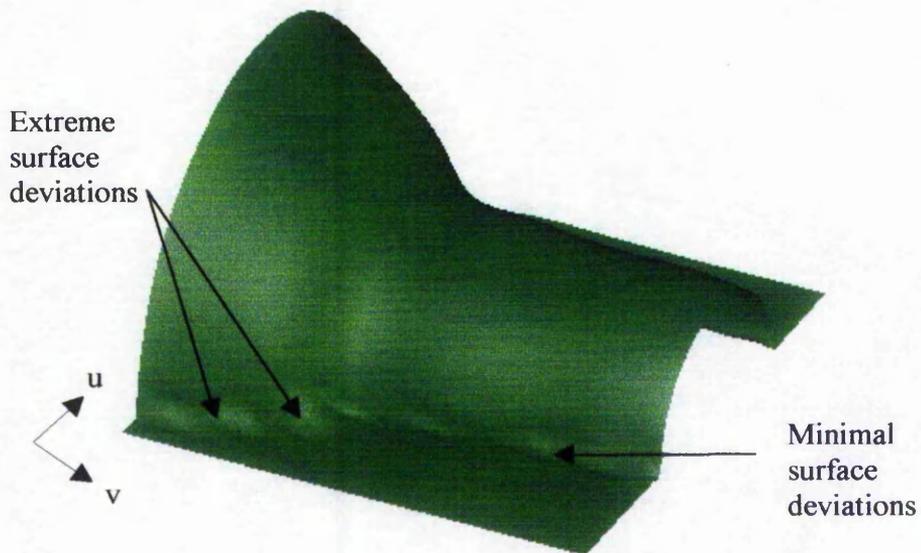
Figure 3.23. Global surface model.

It is at this stage, with a rendered surface model, that the major defect associated with automatic free-form modelling becomes apparent. This modelling error is compounded by the use of sparse scan data (at 10mm step-over distance). However, this is useful for the clarification of modelling errors of this type, representing regions of surface-surface intersection, where discontinuous conditions are desired. Minimal surface deviations occur where the surface-surface intersection is parallel to patch boundaries [BARDELL, 1998a], however the extreme deviations have more effect on the surface model accuracy. This forms the initial starting point of novel work discussed in chapter 4. The algorithm for generating a free-form global surface from CMM points is shown below.

> *Read USR.USR file for user-defined patch size and intra-patch parameter point*
> *density*
> *Read CMM scan line data-sets*
> *Calculate global parameterisation and number of patches needed*
> *For each scan line*
>   *Parameterise scan line data in u direction*
> *Fit orthogonal splines through u parameter points, and parameterise in v*
> *For each parameter point in v*
>   *Calculate tangent conditions in u direction*
> *Fit orthogonal splines through v parameter points, and re-parameterise in u*
> *For each parameter point in u*
>   *Calculate tangent conditions in v direction*
> *Generate patch boundaries in u and v, based on bi-directional spline network*

> *While patch domain in v direction, where v < maximum*
> > *If first row of patches, where v = 1*
> > > *Merge patches in u direction*
> > *Else*
> > > *Merge patches in u direction*
> > > *Merge previous row of patches with current row in the v direction*
> *Save global surface*

The resulting global surface model is based on uncompensated CMM data. As discussed previously, the CMM data is recorded at the probe centre, thus probe compensation must take place.

3.3.5.1 Probe Compensation

Initially, a global surface is generated from uncompensated CMM data, taken as the centre of the spherical probe tip (probe location point). Probe compensation involves offsetting the generated surface by the probe radius, normal to the generated surface. This results in an offset surface, demonstrated in figure 3.24.
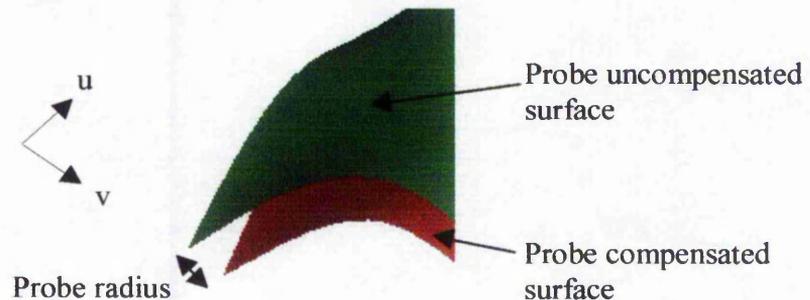
Figure 3.24. Principle of offset surface, compensating for probe radius.

Figure 3.25 shows the resulting offset surface for the bottle data, representing the actual part surface.
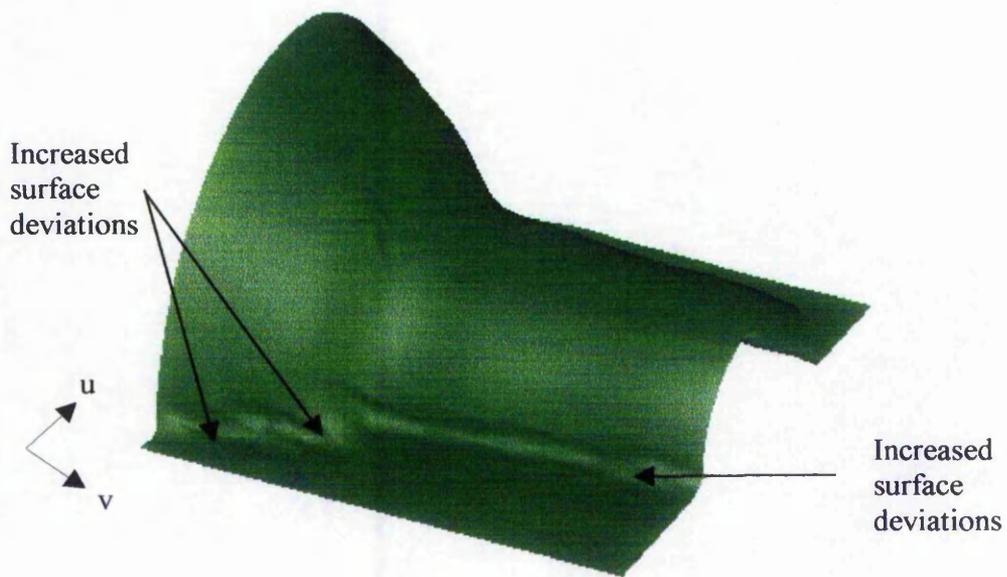
Figure 3.25. Generated offset surface, compensating for probe radius.

It can plainly be seen that the errors at the surface boundaries are more pronounced. This is due to the offset surface being generated from a surface model containing errors due to forced continuity constraints, occurring at regions of extreme curvature change. In simple free-form surfaces this problem rarely occurs.

The methods developed in this work for surface model generation utilise ACIS® functionality. The potential for internal modelling errors arising from computational inaccuracies with this modelling engine cannot be ascertained, however the general method of surface model generation is examined as the main source of errors.

3.3.6 Surface Modelling Errors

This section has discussed the development of a methodology developed for the generation of a global free-form surface, derived from CMM data points. It is important that sufficient data is collected, in order to reduce potential surface model errors. The accuracy of this generated surface model is paramount, thus it is important that this surface model is verified, assessing any errors which may arise. A main problem with generated surface models is the ability to verify the conformance to the underlying

CMM data. The accuracy of the surface model has a direct bearing on the accuracy of the reproduction part, where the full RE process is applied. Thus, it is important that a surface model has optimum conformance with the underlying CMM data, within tolerances.

Throughout this work, C^1 continuous surface models are maintained, based on the bi-directional network of cubic B-splines. This level of continuity is appropriate for this work, allowing accurate surface models to be generated, forming a best-fit surface of the CMM data. There is generally no need for higher continuity conditions for engineering purposes [SPATIAL, 1997b]. The accuracy of the surface modeller determines the difference between the actual surface geometry and the approximated surface geometry of a wire-frame model [IP, 1991]. Individual patches are merged together in a robust fashion, generating a global surface. At this stage, the accuracy of this generated surface is unknown, however, the integrity of a surface is more important than dimensional conformity [BALENDRAN, 1993].

There is always a compromise between the smoothness and accuracy of the final fitted surface or curve, where the level of fitting errors should be controlled at a level the user can accept [MA, 1998]. Using a large patch size will result in a small number of patches over the surface, which reduces fitting accuracy by introducing large approximation errors internal to the patches. As these patches are defined by the boundary curves, there is a large chance of features being lost, particularly where complex surfaces are modelled. An excessive patch resolution leads to increased computational time in the generation of accurate surfaces, and a large resulting file size. Potential efficient storage formats are being worked upon [HOPPE, 1996], however this work concentrates on the generation of ACIS® .SAT files. Data reduction is an important issue, where the balance between accuracy and model complexity is addressed, looking in particular at the required accuracy of the surface.

Judgement may be used to view the generated surface model and arbitrarily comment on the acceptability of the surface smoothness. Inaccuracies from data collection or modelling may be seen, but cannot be quantified. Due to the nature of free-form surfaces these regions of error are often missed. Modelling inaccuracies cause a deviation from the original CMM data. As discussed in chapter 1, surface models can be

classified into the two types of free-form and composite surfaces. Main errors arising from these are discussed separately below.

3.3.6.1 Free-form Surfaces

The assessment of the 'smoothness' of a physical surface is visually difficult, often relying on manual methods such as reflectance and hand feeling [BALENDRAN, 1993]. At the modelling stage, smoothing algorithms intrinsically improve the surface smoothness by approximating the data points. An adequate patch resolution and intra-patch parameterisation can be established to generate an acceptable surface model, depending on the surface model complexity. Where the CMM data is collected from a continuous, smooth object, both the nature of automatic CMM data collection, and automatic free-form modelling, cause minimal deviations. This occurs with global free-form surfaces generated automatically from continuously collected data, where the original surface definition can be smoothed [BARDELL, 1998c]. Figure 3.26 shows a free-form surface model, generated from artificial data, where any deviations are visually hard to identify.
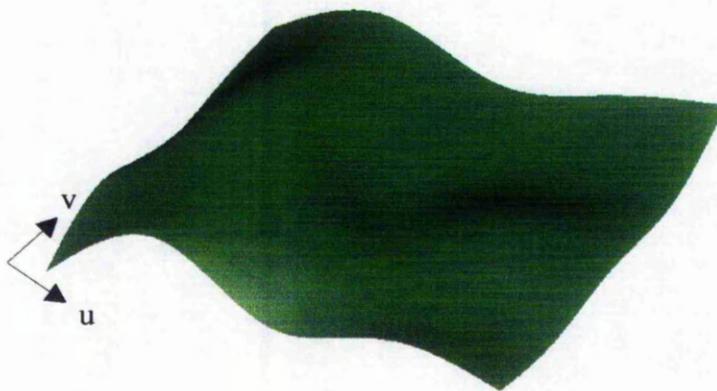
Figure 3.26. Typical free-form surface.

Where free-form surfaces are desired, this method of automatic modelling is computationally fast and accurate. However, an area of RE which has received limited attention to date involves the accurate modelling of CMM data collected from objects containing a number of different surfaces, defined as composite surfaces.

3.3.6.2 Composite Surfaces

A composite surface is defined as a global surface containing discontinuities, due to the intersection of different local surfaces. The automatic generation of a surface model does not lend itself to this type of object directly, as these surface-surface intersections are difficult to localise and model accurately. The free-form modelling of a CMM data-set containing discontinuities introduces deviations from the CMM data. These deviations from the desired modelled surface are due to the continuity conditions of the underlying bi-directional spline network constraining the patches, forcing continuous representation within the patch surface. This deforms the patch surface, causing patch scooping, which has been discussed briefly previously. Problems with automatic C^1 continuous modelling occur where areas of extreme curvature change are constrained, smoothing areas which should ideally be discontinuous surface-surface intersections. The combination of this, and the chordal parameterisation of the underlying splines, cause a degree of patch surface deformation. Patch boundaries are intact, however the internal patch surface is undergoing deformation. Fitting cross-splines through the parameter junction points can lead to smoothing problems in the other direction of the surface [PRATT, 1985], as seen in this work.

Figure 3.27 shows a schematic of how a 2D cross-section through this error region behaves, where continuity constraints affect the interpolation of the underlying parameter points. The desired modelling conditions are also shown in the lower part of the same figure, where the two curve segments are modelled with a discontinuous intersection.
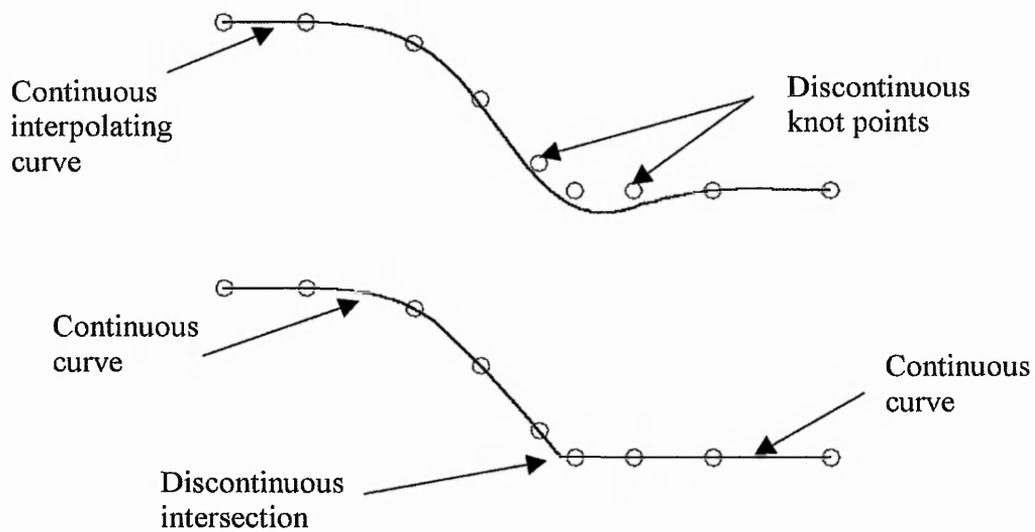
Figure 3.27. Forced continuity, and desired discontinuous conditions.

Any continuous cubic B-spline will display this behaviour. This is due to cumulative chord length parameterisation and the position of interpolated knot points. The spline must deform to allow a continuous best-fit through all the points. This phenomenon is typical of rectangular Bézier patches which do not handle cusps, where the wire-frame curves force a Bézier patch to have two tangent sides [SARRAGA 1990].

An alternative source of modelling errors occurs at the probe compensation stage. As discussed previously, the recorded CMM point is at the centre of the probe tip, thus the actual part surface must be generated by offsetting the surface model by the probe radius. Figure 3.28 shows an example of data collection at a discontinuous region (ramp edge).
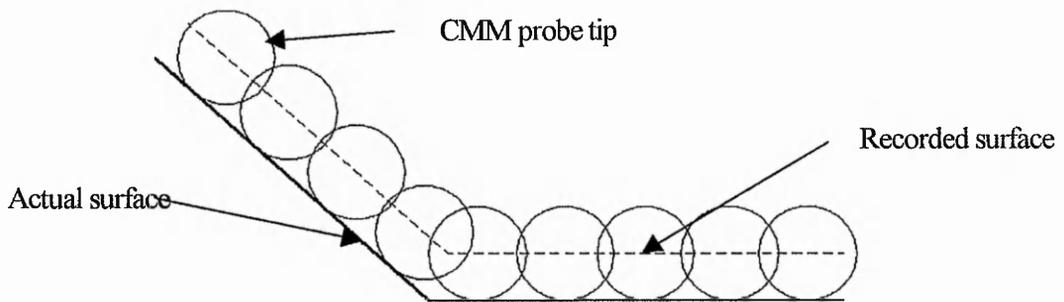
Figure 3.28. Data collection, showing actual, and recorded surface points.

This results in probe uncompensated data, containing a discontinuous edge. However, at the modelling stage, the discontinuities in the uncompensated data cannot be modelled using the automatic free-form modelling methodology developed in this work. Figure 3.29 shows a 2D schematic of the generated surface model derived from this data, and the resulting offset surface. This region is classed as an extreme curvature change.
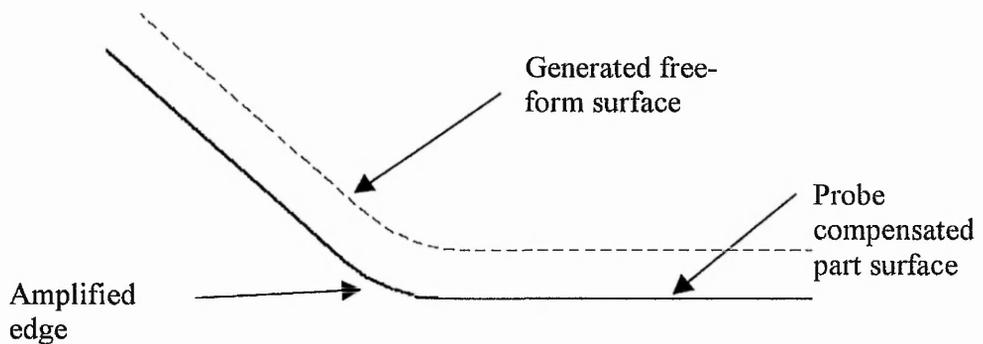
Figure 3.29. Free-form model and offset surface.

It can be seen that the best-fit smoothing, associated with free-form modelling, is amplified at the probe compensation stage, however it does not cause interference errors, due to the direction of curvature. Another problem involving surfaces containing extreme curvature change also occurs at the surface offset stage. Exact offset curves often exhibit degeneracies, due to self-intersections. Where a convex discontinuous

ramp edge is present these self-intersections may cause further errors. This occurs where the principal radius of curvature is less than the offset distance [OLIVER, 1993].

Extreme curvature is often present at the external boundary of the object, which can be trimmed, improving global surface accuracy by reducing these errors occurring at surface-surface intersections.

3.3.7 2D Surface Trimming

Trimming at surface boundaries is seen as a method of reducing the inaccuracies in modelling, due to sharp changes in curvature [BARDELL, 1998b]. This discards CMM data which causes discontinuities at the outer boundary of the measured object. In general cases, where a standard probe orientation is used, this allows data below or above an XY plane to be segmented from the rest of the data. This is necessary where the surface point data is collected with a rectangular boundary, but the actual object surface boundary is irregular. Preliminary results are shown below in figure 3.30, where excess scan line data is collected around the part.

Figure 3.30. Scan line data from a typical automotive part (data courtesy of LK Ltd.).

A trimming plane perpendicular to the z-axis can be defined, and in this case, data can be trimmed from above this plane. Figure 3.31 shows the trimmed surface model, with a reduction in modelling errors at the object boundary.
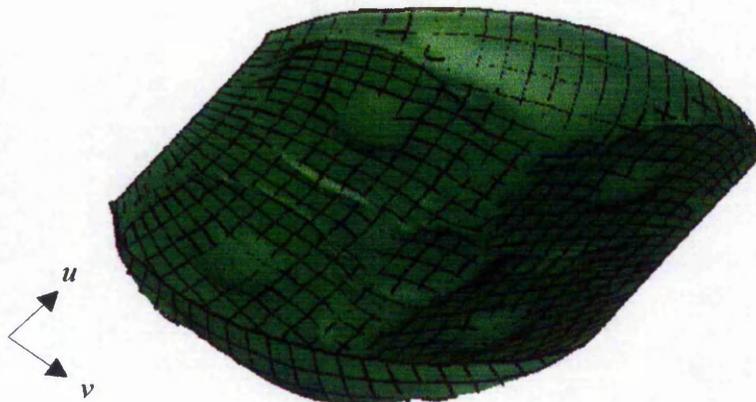
Figure 3.31. Trimmed surface model.

This discards unnecessary data on a 2D trimming plane, reducing errors at the object boundaries.

The RE process has the optional stage of machining, which is discussed in the following section.

3.4   Machining

This section discusses the development of a simple methodology for part-program generation, for the reproduction of a prototype object. This area is initially developed, however the present work does not focus on this machining stage. A reproduction part can be manufactured, based on the generated surface model methodology developed earlier. This is desirable, particularly where a mould of the physical prototype is required. This study involves the three-axis series 1 CNC Bridgeport milling machining centre within the manufacturing department. When a surface model is recreated in the RE fashion, the resulting CNC machined model is rarely an exact match [SEILER, 1994]. This is due to accumulated errors from the data collection and modelling stage, and also includes machining errors, such as tool radius compensation inaccuracies, discussed later. The generation of a physical reproduction part may also facilitate further RE process analysis. At the surface generation stage, the surface model is offset,

compensating for the CMM contact probe radius. In a similar manner, as a variety of ball-nosed cutters can be used with differing tool diameters, the generated surface model must be offset by the machine tool radius. However, the diameter of cutter shaft should be chosen, depending on surface geometry, when using a spherical milling cutter. This gives an offset set of data points, used for machine path generation for the final finishing pass across the surface.

3.4.1 Tool Radius Compensation

To generate the final pass for the reproduction part, the offset surface is equal to the cutter radius. Thus, it is necessary to progressively make rough cuts, removing waste material in a sensible manner. Roughing cuts are deduced, where a flat-end mill can be used, using a number of offset surfaces. The hardness of the material used and the complexity of the surface determine the number of passes necessary for roughing. Figure 3.32 shows the principle of surface offsetting, compensating for tool radius, and deducing the final finishing stage machine path surface.

Probe compensated surface

Tool compensated offset surface
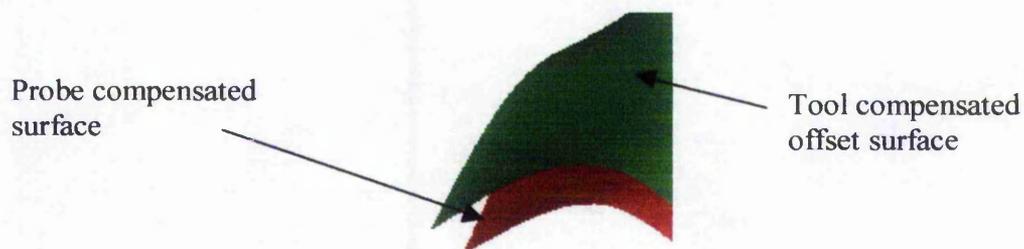
Figure 3.32. Surface model offset, compensating for tool radius.

Offset curves often self-intersect, occurring where the principal radius of curvature is less than the offset distance [OLIVER, 1993]. This is assumed to be correctly compensated for by the ACIS® geometric modeller, at the modelling stage. However, this area should receive further investigation, regarding the ACIS® modelling engine specifically. In particular, this problem may arise when dealing with offset composite surfaces. To calculate machine paths, this offset surface model is parameterised, to a

sufficient degree to accurately reproduce the surface. This involves the minimisation of cusps, achieved by the use of a sufficient step-over distance.

3.4.2   Tool Step-over Determination

Parameterisation influences the efficiency of the roughing process, thus a good surface parameterisation must be obtained at the modelling stage [CATANIA, 1992]. This involves defining parameter points at an adequate density to minimise cusp height, discussed in chapter 2. This is achieved in both the machine path direction, and the step-over distance, and is dependent on the size of tool used. The determined *uv* parameter points on the offset surface are used as Cutter Location (CL) points. The calculation of block size, based on the extents of the generated surface model in x, y and z directions is necessary, determining the minimum dimensions of stock material needed to machine the part. This is deduced, based on the extents of the generated machine points.

Figure 3.33 shows generated machine path CL points from a generated offset surface of the neck region of a bottle, forming the finishing stage. This data is optimised for an 8mm diameter ball-nosed cutter, offsetting the surface by 4mm, and checking the points are dense enough to minimise cusps.
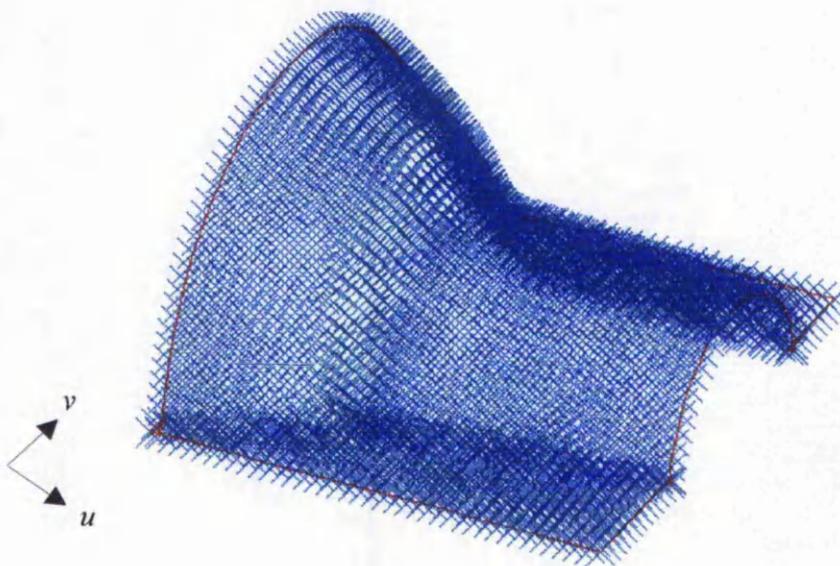
Figure 3.33. CL data for a reproduction part.

However, due to the nature of free-form surface modelling, classic surface intersection problems will be present. The accurate machining of these discontinuous regions of intersection necessitates the use of a flat end-mill, which also has associated problems [CATANIA, 1992]. The use of an 8mm diameter ball-nosed cutter may result in gouging problems. This work does not concentrate on improving global machine path generation, thus these generated paths are uni-directional. Many works, including [LEE, 1990], discuss the optimisation of path generation. In order to create a machined reproduction part, part-programs must be generated, allowing this machine data to control the motion of the cutting tool.

3.4.3   Part-program Generation

Part-programs are written in the standard 'G-code' notation, defining tool size and spindle speed, as well as coordinate information for the part to be machined. The benefits of CAGD become apparent when attempting to machine a complex surface from concept design, involving a high degree of expertise in deducing surface point coordinates. Thus, machine data is generally adapted from CAD model information, both in conventional engineering and RE. In this work, machine coordinate data is deduced from the generated free-form surface model, derived from CMM data. Below is a section of a generated part-program.

```
O1234
G21G40G80G9
      (LOAD TOOL 4.000000 MM BALL NOSE)
      T12M6
      G0G54G90X-10.0Y-10.0S1000M3
      G43Z10H12
      G1 F1000 X  0.000 Y  0.000
      Z  0.000
      X -0.010          Y        0.437          Z        1.969
      X -0.055          Y        2.419          Z        1.667
      :
      G00 Z55
      G01
      X  3.323          Y        0.258          Z        2.013
      X  3.289          Y        2.818          Z        1.877
      :
      G00 Z55
      G01
      G01Z10
      M5
      G0G28G91Z.0
      M30
```

3.4.4   Machining Errors

Machining errors are related to cutter deflections, datum errors, and classic gouging problems, as discussed in chapter 2, however, any errors from a previous stage of RE are passed to the next. Thus, determining errors from machining involves an appreciation of any errors that may arise at the data collection and modelling stages. With conventional RE, there is a degree of uncertainty regarding the conformity of the machined part to the prototype model.

A reproduced physical part may be used to assess the accuracy of the total RE process. However, it can be difficult to deduce at which stage of RE any potential surface errors occur. Starting from the original prototype, errors can be introduced at the measuring, modelling or machining stage. Data collection and machining involve mechanical processes, so the errors are expected to be more significant than the computational errors from surface fitting and offsetting. However, modelling errors can be deduced using Deviation Analysis (DA), which is discussed in full in chapter 4. These modelling errors are passed onto the machining stage. As well as testing the accuracy of the CAD model, this allows an insight into the overall errors in the process. In this present work, this forms a theoretical solution to machine error assessment.

Determining the errors in a reproduction physical part is a useful tool in engineering, particularly when dealing with Statistical Process Control (SPC). This error determination would involve the comparison of the original surface model and a Reverse Engineered Surface (RES) model, forming a New Model Analysis (NMA) stage.

3.4.4.1 New Model Analysis

This stage would involve inspection of the reproduction part, using the same probe diameter as the original part measurement, followed by surface model generation of the RES [BARDELL, 1998c]. Variance between these two CAD models highlights where data collection has been insufficient, or where the original physical surface had cosmetic quality flaws. The deviation of the generated RES from the original CMM data can then be deduced. This stage validates the correlation between the original surface

model and the RES. This acts as an indirect comparison of the models, utilising the DA stage. Direct surface model comparison involves defining reference points on each surface model, defined as localisation points. Geometric factors such as curve and surface equations can be used to recover the position of parts, for this localisation [SAHOO, 1992]. It is essential that the datum of the reproduction part is identical with the original part, at the data collection stage, negating any localisation problems. Furthermore, using the same probe diameter as before allows the probe uncompensated surface models to be used. Due to the nature of free-form surfaces, the determination of localisation points on a surface is not a trivial task, where free-form surface localisation algorithms involving transformations have been developed [HUANG, 1996], however these are not investigated here. At present, this NMA stage forms theoretical work, proposed as future developments to RE accuracy analysis.

3.5   Summary

The conventional RE process is made up of the areas of data collection, modelling and machining. The aim of RE is the generation of an accurate reproduction of the original physical prototype. Each stage of RE is discussed in this chapter, with emphasis on the maintenance of an accurate surface model. This theme is taken further in the development of novel enhancements to RE, discussed in chapter 4.

The CMM is dedicated to the collection of dimensional information. Having a single machine with the ability to accurately inspect any sized and shaped object, within limits, has obvious advantages, such as reduced costs and reducing space taken up by a number of inspection operations. The CMM has developed into one of the most accurate data collection methods, giving accuracy to 1µm. Care in selecting the correct variables, and taking into consideration the appropriate parameters, will reduce any potential inaccuracies. Measuring strategies are often ignored, and can be optimised to reduce the uncertainty of co-ordinate measurements. This involves the number and distribution of points [WECKENMANN, 1998]. Also, the selection of the direction of scan lines, relative to the topology of the surface to be scanned, can be important in order to avoid collisions.

In the realms of RE, the CMM is used for contact surface data collection, utilising uni-directional scan line technology. Surface scanning is a relatively new method, which is utilised throughout this work. This method has advantages over other methods discussed, such as speed and a closer fit to the part surface in question. Initial automated data collection methods looked at the point-to-point method. However, this results in a sparse data-set, and is time-consuming with surfaces needing a high clearance plane. After an appropriate probe calibration and machine set-up, generic CMES scanning programs are executed, which are written off-line. These control the direction of scan line, the number of scan lines to be collected, and the step-over distance, with the user defining a start point for the first scan line, and an end point, from which an end plane is determined for each scan line. A clearance plane is also defined on-line. Execution of the CMES code results in a 3D point file, which can then be used in the modelling stage.

The representation of CMM data involves the generation of a surface model. Initially, this involves converting the CMM data file to a neutral format, for input to the ACIS® modeller as point entities. After obtaining the point data in a suitable format, the modelling stage can proceed. Initial studies of ACIS® defined global surface methods, such as interpolated and net surfaces, show negligible differences from the method developed in this work. The internal functionality of the ACIS® functions for surface generation cannot be ascertained, thus in order to fully analyse and verify the surface generation stage, a Gregory/Charrot patch method has been developed. There are ACIS® defined surface generation methods, based on the definition of control points. However, this present work is based on generating surfaces from interpolated data. ACIS® has been used to interpolate probe uncompensated CMM data points, creating uni-directional B-splines. Parameterising these splines, designating the parameter points as knot points, allows splines orthogonal to the scan lines to be generated, creating a network of interpolating cubic B-splines with C^1 continuity. This spline network is used to form the boundary curves for adjoining surface patches. C^0 continuity is achieved where positional information is continuous. C^1 continuity allows an inter-patch tangent continuity at patch corners. In the realms of this work, continuity condition constraints allow C^1 continuity, giving second order splines and surfaces. Patch formation is based

on Gregory/Charrot patch methods, utilising Hermite interpolated data. The number of patches, and the internal parameterisation of these patches are user-defined, which is highly desirable as the parameterisation is critical to the resulting surface, and care must be taken to optimise this as much as possible. These adjacent patches are merged, or stitched together, approximating the original CMM data points and forming a single global surface. This surface must be offset, compensating for CMM probe radius.

The aim of the surface modelling stage is the generation of an accurate CAD representation of the CMM data points, useful for the generation of a reproduction part. The work developed here identifies problems associated with automatic free-form modelling. Patch resolution is an important issue, involved with the maintenance of model accuracy. Inadequate resolution, where large patches are used, can decrease the accuracy of the total model, due to the danger of 'lost features', as only information at the patch boundaries is known. Thus, the use of excessively large patches will result in an inaccurate surface model, as points internal to the patches will not coincide with the original data points, apart from on the patch boundaries.

As a surface model becomes more complex, the complexity of the underlying spline network increases. This is largely determined by the patch resolution used and intra-patch parameterisation, associated with the issue of data reduction, where an unnecessarily high patch resolution will lead to excessive file size and computational time, without justifying the surface accuracy improvement. However, the complexity of the underlying CMM points also contributes to the resulting surface model accuracy.

Free-form physical surfaces are ideally suited to this method of automatic surface generation. However, surface fitting undergoes deformations, incurring deviations from the desired shape, where extreme curvature change is present, as is the case with composite surfaces. Deviations have been shown to arise where the CMM data is discontinuous in nature, deforming the spline network used at the modelling stage. Modelling errors are partly based on an inadequate density of CMM data, but mainly are due to the modelling of discontinuities, using a free-form methodology. The modelling of composite surface data as a free-form surface highlights a number of drawbacks to the automatic method of modelling. This includes the intersections of two

or more differing surface types, resulting in a lack of precise control in the created surface model. As seen in this research, a major source of inaccuracy occurs at the edges, or boundaries, of surfaces. This is confirmed by Kawabe et al. [KAWABE, 1980]. Distortions in parameterisation will occur with automatic free-form modelling of point data. User interaction at the modelling stage is often relied upon to modify any inconsistent regions locally [STORRY, 1990].

Where a degree of surface conformity is necessary, in the case of composite parts, an adequate patch resolution is used to optimise the degree of accuracy required in the generated global free-form surface model. From this, surface information can be calculated for the creation of machine paths, involving the automatic generation of part-programs. These machine paths can then be used to control the CNC machining stage, reproducing the physical prototype part, if desired. This present work does not include this physical machining stage. Offset surfaces, both to compensate for probe radius and tool radius must be generated, resulting in the machine path data. The complexity of the surface will determine the density of the machine CL points, however regions of surface-surface intersection often have associated gouging problems. These errors arise from the free-form nature of the surface the CL points are derived from.

NMA is discussed as a theoretical method to analyse errors in the overall RE process, comparing deviations between the original prototype and the RES. This would utilise novel work developed in the area of Deviation Analysis (DA), discussed in chapter 4.

The results of the surface generation stage highlight the great need for surface model assessment, leading directly to the novel work discussed in chapter 4, where analysis of surface models is achieved, quantifying modelling errors. Initially, 2D trimming planes are used to reduce errors in complex surfaces, due to the data collection within regular, straight edged boundaries. This proved to be efficient, however, is it apparent that a 3D trimming methodology is necessary. A novel region-based surface segmentation methodology is developed from the global surface generation stage, where regions of deformation are discarded from the surface, allowing free-form modelling of local sub-surfaces, forming a 3D trimming stage. This utilises the seed region growing methodology, developed and discussed in chapter 4.

Chapter 4.

Enhancements to the Reverse Engineering Process

4.1   Introduction

The Part-to-CAD RE process, originating with a physical object and resulting in a free-form surface model is demonstrated and discussed in chapter 3. This involves the use of the CMM in the collection of 3D point data, automatic free-form model generation, and an optional machining stage. Errors arising from these stages are also discussed. This thesis aims to improve the accuracy of the generated surface model, which has been shown to possess regions where accuracy is compromised. Where free-form data is collected and modelled, locating and quantifying these errors is difficult. As physical surface complexity increases, in the case of composite objects, errors can be seen at surface-surface intersections, however they cannot be quantified.

It is essential that the generated surface is verified, giving the user confidence that the model is a reliable representation of the data. As well as the uncertainty in surface model accuracy, the amount of CMM data collected determines how reliable the resulting surface model is. In many cases, over-sampling at the data collection stage guarantees a surface model's accuracy. However, this involves extended data collection time, and the processing of a large amount of data, which vastly increases computational time. This increase in processing time may not be justified by the resulting accuracy of the surface model. In this work, free-form surface generation is automated, however there is a lack of precise control of the created surface model. There should be a balance between user interactivity and automation, particularly where the surface is made up of a number of separate surfaces which are difficult to localise automatically.

This chapter discusses improvements to the RE process, offering novel methods of analysing and refining the surface model, summarised in figure 4.1.
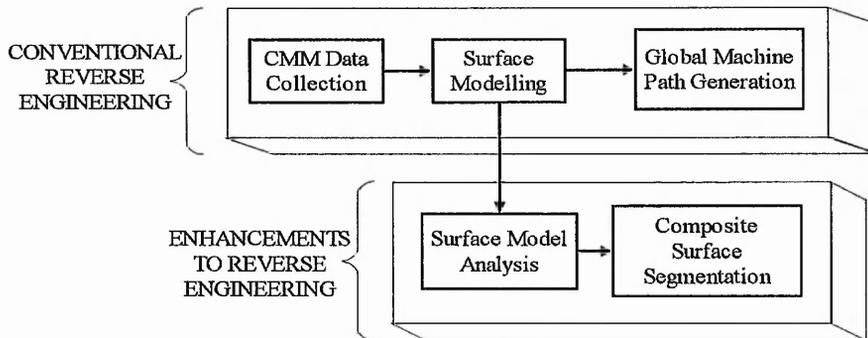
Figure 4.1. Conventional RE, with novel enhancements.

A surface model is derived from CMM data, which can be used to generate a machining part-program for the reproduction of a prototype model. Thus, the accuracy of this surface model is paramount. However, with conventional RE, there is no method of adequately quantifying either the generated surface model or the reproduction part surface. The introduction of a novel surface model analysis stage allows the quantifying and localisation of modelling errors. Model refinement may be necessary where discontinuities are present, forming a novel global surface segmentation scheme, concentrating on Part-to-CAD RE.

4.2   Accuracy Analysis and Surface Improvement

Visual analysis is a simple analysis stage involving a visually pleasing curve or surface. A fair amount of qualitative information can be attained from this stage. In particular, continuity conditions can be seen with degrees of smoothness, but this relies on the judgement and skill of the designer or user. This is only useful where aesthetic qualities are analysed, when verification is impossible. Numerical analysis involves positional and tangency continuity constraints, analysing data point interpolation. This involves both inter-point continuity, and inter-patch continuity, based on an appropriate parameter definition. Throughout the model generation stage, discussed in chapter 3, splines are maintained at C^1 continuity.

The accuracy of a generated surface is defined here as the correlation between the CMM data points and the generated surface model. This is determined by the parameterisation, involving the number of parameter or knot points per patch. The number and size of the continuous patches used also plays a part in the accuracy of the resulting global surface. This is defined as patch resolution. Simple free-form surfaces can be represented by far fewer patches than a complex composite model. However, there is an important trade-off between accuracy and file size, as a high surface model accuracy results in a high computational time and large file size. This is particularly the case at the surface analysis stage, where the analysis time is proportional to the complexity of the surface model. Data reduction is desired, where acceptable surface model accuracy is present with a minimal file size. The relationship between these two parameters is investigated in this work.

To deduce, with confidence, that a generated surface model adequately represents the underlying CMM data, a novel method of surface model analysis has been developed here, based on the deviation between the generated surface and the CMM data. This is necessary, as Part-to-CAD RE gives no information on the accuracy of the model. This analysis module determines the effect of parameterisation and patch resolution on the generated surface model. Theoretically, the spline network maintains a close approximation to the CMM points, particularly with free-form surfaces. This is proven in the Deviation Analysis stage.

4.2.1 Deviation Analysis

This stage confirms theoretical accuracies and visible inaccuracies, highlighting any surface deviations from the CMM data which may be present. Deviation Analysis (DA) determines the correlation between a surface model and the original CMM data points, by comparing the data and the resulting generated surface [BARDELL, 1998a]. The shortest distance between each CMM point and the surface model is calculated, and used to create a DA map. This is found by:

$$\text{Error}_{\text{deviation}} = Fp_i(u,v) - Dp_i(u,v)$$

Where:

$Fp_i(u,v)$ is the ith nearest fitted point on the surface

$Dp_i(u,v)$ is the ith CMM data point

The deviation error is the distance between the CMM data and the generated surface, calculated as a scalar distance, thus it does not have an associated direction. A close correlation between the CMM data points and the generated surface must be maintained, within a defined tolerance range. The DA stage highlights regions of the surface model which are outside this tolerance range, relative to the CMM data points. This is applied prior to the surface offset stage, compensating for probe radius.

A DA map is used to localise deviations on the surface model. The deviation error is calculated as a scalar, however the DA map plots the distance and direction of deviations on the model, and shows a 3D graph representing the distribution of deviations. This is plotted above each scan line, for every CMM data point. Due to the low magnitude of errors, compared with the dimensions of the surface model, the deviation graph is magnified ten-fold. This gives the user an immediate indication of the location and relative amount of deviation between specific CMM points and the best-fit surface. This acts as a global continuity analysis stage. This DA tool can be utilised differently, depending on the type of surface model. Firstly, global free-form surfaces are examined.

4.2.1.1 Free-form Surface Deviation Analysis

Where a physical surface is assumed to be free-form, there is a direct correlation between the data points, and the generated surface model, resulting in a very low deviation. Figure 4.2 shows a free-form surface, generated from artificially created point-to-point data. This involves writing a .PNT file directly, using a text editor.
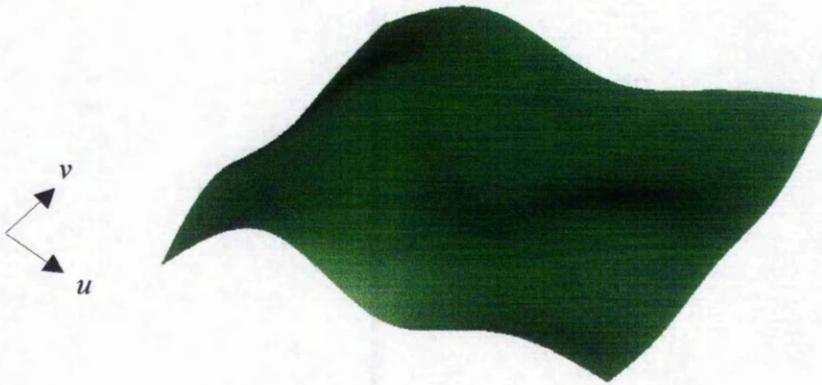
Figure 4.2. Smoothly varying free-form surface (5x5 patch resolution).

This free-form surface has optimum continuity, however, this can be very hard to confirm. DA can be used to check the correlation between the point data and the generated surface model, as seen in the deviation plot, shown in figure 4.3.
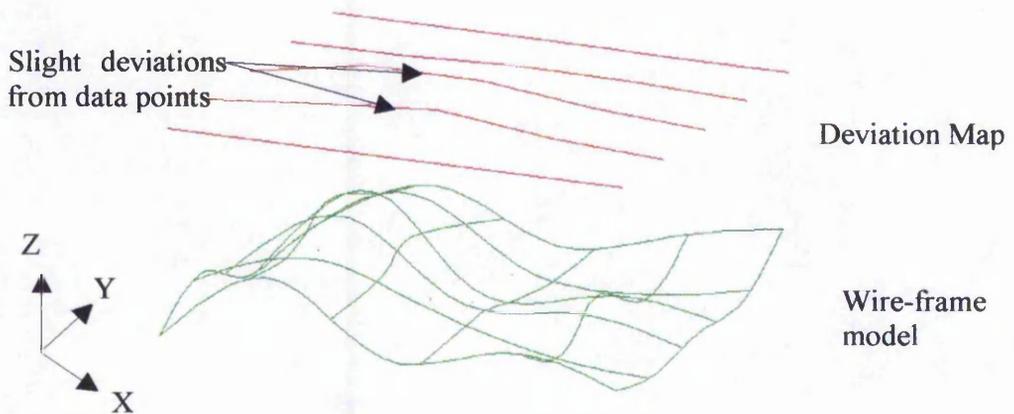
Figure 4.3. DA map, showing deviations between the data points and the generated surface model.

It can be seen that the first and last data-sets, and the first and last data points on each line, occurring at the global surface boundary, have a deviation of zero. This is due to direct surface interpolation at the end points of the bi-directional spline network, with null tangent conditions. This figure shows negligible deviation of the surface model from the data points, giving an average deviation from the point data of 0.003mm. This is achieved at a patch size of 8mm, with an intra-patch parameterisation of five. Despite

the smooth nature of the surface, the patch resolution and intra-patch parameterisation play a large part in the accuracy of the final model. This encompasses a comparative analysis of the effect of varying parameterisation, and patch size and frequency (resolution). Determining the best patch resolution generally involves visual analysis, increasing the intra-patch parameterisation and patch number until an acceptable surface is seen to be generated. However, despite the appearance of smoothness, it is unsure how this correlates to the actual data points.

This thesis aims to improve the reliability of a generated surface model, derived from composite surface CMM data specifically, where resulting modelling errors can be visualised, but not easily quantified, as discussed in chapter 3. DA can be utilised for the analysis of composite surface data, discussed below.

4.2.1.2 Composite Surface Deviation Analysis

The development of the DA stage allows deviations occurring at discontinuous regions to be localised, and quantified. Discontinuities cannot be represented, as the global surface model interpolates the CMM data automatically, generating a best-fit surface, causing the surface model approximation errors to reduce model accuracy for composite surfaces.

DA has been developed primarily for the analysis of composite surfaces containing discontinuities. These result in a 'scooping' at areas at extreme curvature change due to forced continuity constraints, discussed in Chapter 3. Figure 4.4 shows a free-form surface model, generated from CMM data taken from the neck region of a bottle, shown in chapter 3, which is a complex physical object containing discontinuities, described as areas of extreme curvature change.
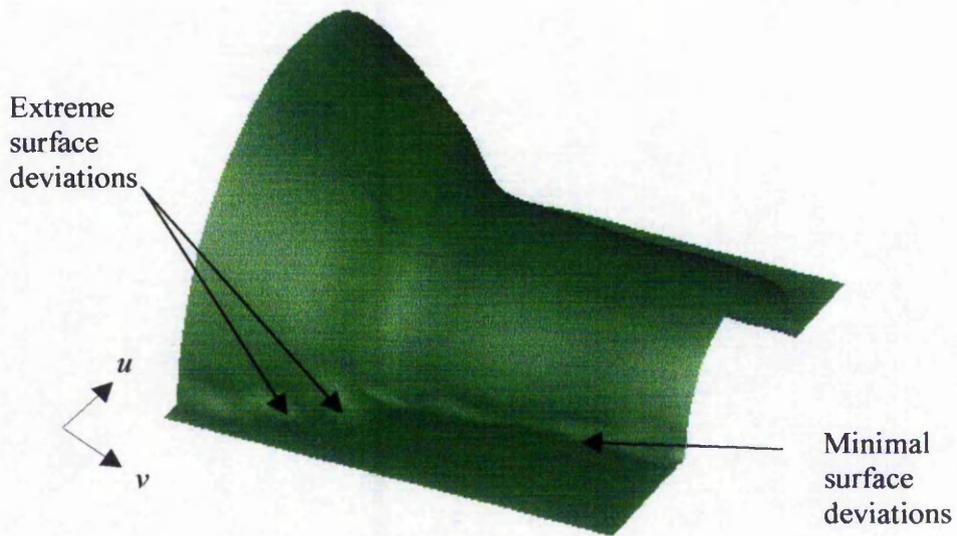
Figure 4.4. Automatically generated surface model (patch resolution 7 x 5).

From the surface model, it can be clearly seen where errors in the modelling of the data points lie. Figure 4.5 shows the initial results of DA, where the DA map highlights the exact location of these discontinuities, but also quantifies the deviations.
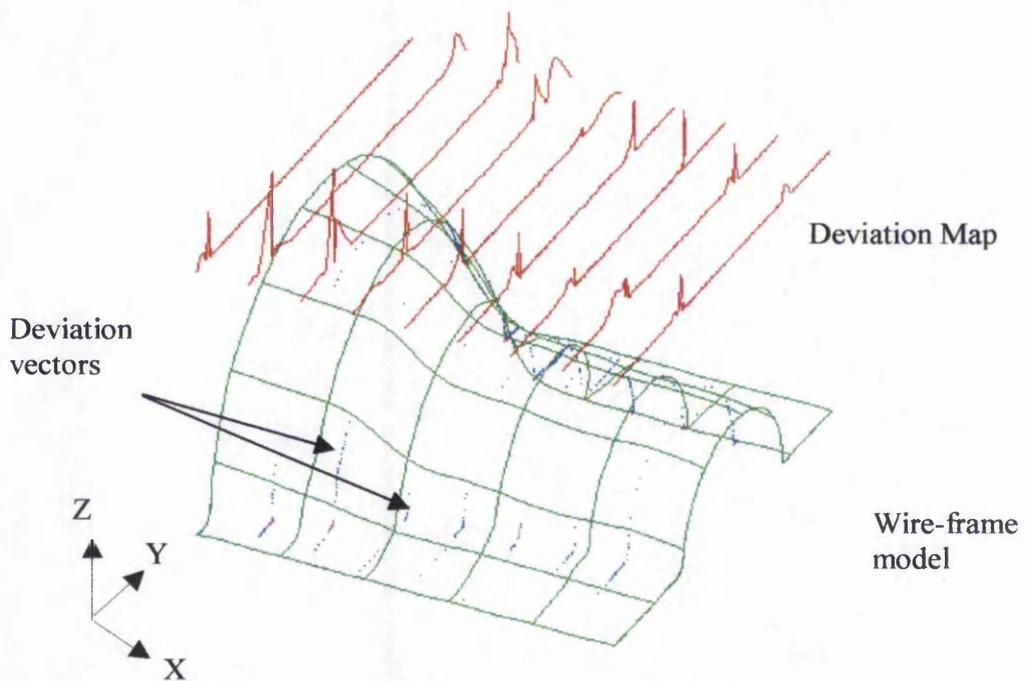
Figure 4.5. DA map and corresponding surface (patch resolution 7 x 5).

This is achieved at a patch resolution of 7x5, giving an average deviation of 0.086mm and a maximum deviation of 2.111mm. There is zero deviation where the surface is free-form in nature. However, at regions where different surfaces intersect, there are deviations. The CMM data is discontinuous here, however, the modelling method forces a continuous spline and patch network through this data. The correlation between surface deviation and extreme curvature change is apparent. Deviation vectors on the wire-frame model show the precise magnitude and direction of these deviations. As these are very low, they are hard to visualise, however these also have an associated tolerance range. Any deviations greater than a user-defined value, in this case 1mm, are flagged in magenta. Deviations of less than 1mm are shown in blue. Figure 4.6 shows a segment of this DA graph, where two scan data-sets are modelled, and are analysed for deviations. This gives a much clearer picture of the behaviour of the free-form modelling methodology, and the effect at regions of extreme curvature change.
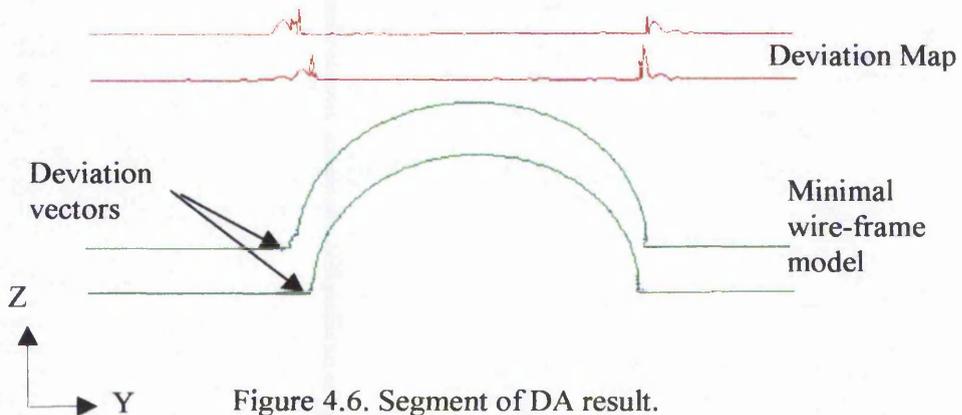
Figure 4.6. Segment of DA result.

The similarities of this to a curvature plot are apparent, discussed in more detail in subsequent sections. The deviation vectors are small, thus cannot be clearly seen. As a comparison with figure 4.5, a DA map is shown below in figure 4.7, with a higher patch resolution, resulting in a closer fitting surface model.
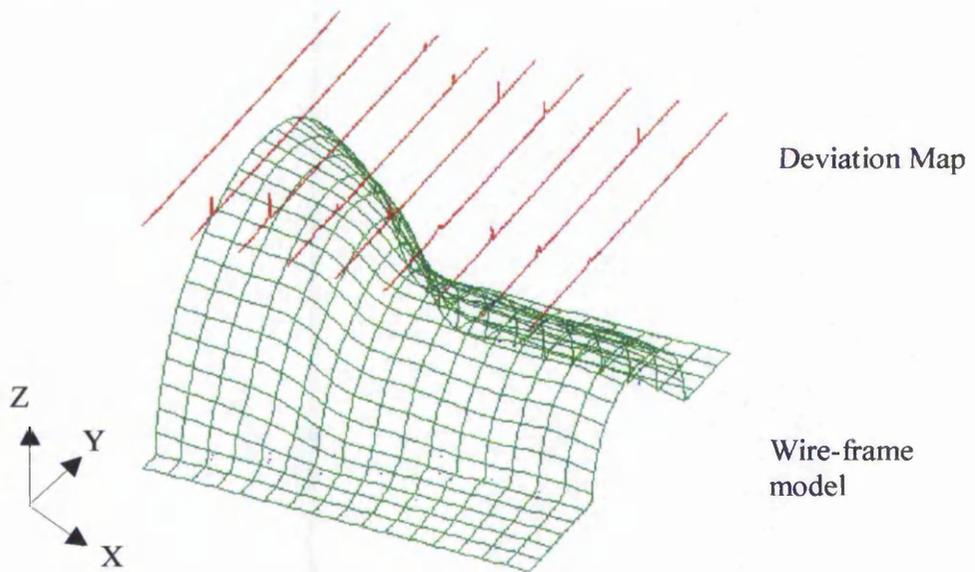
Figure 4.7. DA map and corresponding surface (patch resolution 23 x 16).

The results of DA show that as the size of patch increases, the deviations of the generated surface model from the CMM data also increase. A more detailed analysis of results is presented in chapter 5.

It is generally thought that the data collection stage should collect ample data, to guarantee a comparable generated surface model, despite the consequence of a long inspection time. However, this also results in a higher computational time for the generation of a surface from this data. A low parameterisation and patch resolution can simply approximate the surface model, performing less computation, but still uses the total data-set initially. However, there is a relationship between the amount of data used and the conformity of the surface model to the CMM data.

Minimising the data-set used to generate an accurate model within tolerance is an area which has received limited research. During the development work of the automatic surface generation methodology, it was found that the resulting accuracy did not always justify the amount of CMM data collected and then utilised. This is highly dependent on the required accuracy. Data-set partitioning is novel research aimed at optimising accuracy conditions, whilst minimising the amount of data required to generate an accurate surface model.

4.2.2   Data-set Partitioning

A common problem with the verification of Part-to-CAD RE is that comparative analysis is difficult. This differs from inspection, where data can be compared with a desired value. This involves the collection of multiple data-sets which can be compared. Data-set partitioning (DSP) allows the verification of a single data-set, based on the generated surface model. This aims to minimise the amount of data needed for the generation of a free-form surface, maintaining accuracy within defined tolerances. It is generally accepted that the complexity of the physical surface to be measured determines the density of data required to generate an accurate surface model. Planar surfaces require a minimal data-set to generate a corresponding surface model. With simple free-form objects, a reduction in the amount of CMM data collected may not vastly reduce the deviations of the resulting surface model. However, this is a purely qualitative statement, as there is currently no method to test this theory. Composite surfaces tend to require denser data, in order to correctly represent the features or surface boundaries. Generally, an arbitrary number of scan lines is taken, determined by the apparent complexity of the part. However, the collection of redundant data is an unnecessary use of the CMM. Thus, the relationship between the density of data, and the resulting surface model is unclear.

DSP introduces a method of investigating the effect of reducing the data-set, as part of the DA stage. The aim of DSP is to minimise data collection time, computational time, and file size, whilst maintaining the generation of an acceptable surface model. This will depend on the application of the part, in terms of functional constraints. This method is highly feature dependent, thus surfaces with many small features will need more data to depict the surface adequately. Using a high patch resolution to optimise the representation of small features may be redundant, as many small features cannot be inspected adequately using the contact CMM, due to the size of the probe. Also, after probe compensation, the offset surface is more likely to contain degeneracies.

As the first step of DSP, the CMM data is partitioned into two sets. One set is used to generate a surface model, and the DA stage can be used to quantify the correlation between the generated surface and this CMM data. The other set, defined as the

verification set, is also analysed by the DA stage, where the deviations between the surface model and the unused data can be deduced. The ratio of modelled scan lines to verification scan lines is defined as the DSP ratio.

Due to the continuous nature of free-form surfaces, a sufficiently best-fitting surface can be generated from a relatively sparse data-set. In this work, DSP is applied to composite surfaces due to the readily available dense data-sets, collected for accurate surface generation. It was envisaged that the DSP ratio would have an effect on the accuracy of the generated surface model. Results for two complex surfaces, shown in chapter 5, calculate deviations of the modelled sets at DSP ratios of 1:1, 2:1, 3:1, 4:1, and 5:1 (modelled sets : verification sets). Average and maximum deviations using different amounts of scan data has been found to have a negligible effect on the deviations of the modelled data and the generated model. Using the Renishaw bottle data at all DSP ratios, each verification set is 5mm from adjacent modelled sets, thus the underlying bi-directional spline network continuity constrains the unused data on either side. In this way, DSP analyses the effect of increasing the step-over distance to 10mm. The modelled data-set DA results of DSP are similar to that of the full data-set DA. This is due to the global continuity condition effect of the generation of a best-fit model.

There are many theoretical points on a surface. It can be deduced that there is a critical number of these points necessary to generate a surface model. This critical number is the minimum amount of data needed to generate a surface model to a desired tolerance. DSP aims to determine this critical data-set. This is initial work which looks at a maximum size of verification set at a DSP ratio of 1:1 (half the full data-set). Future work would investigate ratios where there is more verification data than modelled data, such as ratios of 1:2 and 1:5. In effect, this would change the scan line step-over distance at each DSP ratio, introducing more control of sparse data-sets. This preliminary study, building on the novel DA methodology, works towards the development of a method of predicting the accuracy of a resulting surface model, based on the density of data used.

4.2.3   Continuity Improvement of Free-form Surfaces

Despite an adequate patch resolution, generated best-fit surfaces may show deviations from the CMM data, highlighted by DA. However, with free-form surfaces, this can be advantageous [BARDELL, 1998c]. DA has been developed to show deviations between the CMM data and a surface model. However, with free-form surfaces, DA can be used to deduce the surface continuity improvement, where the greater the patch size, the greater the surface smoothness. Here, the DA plot can be interpreted to highlight regions where the CMM data is not optimally continuous, occurring where the original surface was not as smooth as once believed. What would normally be seen as modelling errors, are regions where compensation for optimum smoothness has occurred. Results demonstrating the effect of patch resolution on surface smoothness are presented in chapter 5. In this way, as well as highlighting deviations in free-form surfaces, DA can also be used to assess improvements to the smoothness of free-form surfaces. However, a sensible patch resolution must be maintained, otherwise the generated surface will have optimum smoothness, but will deviate widely from the data points. Often, this smoothing is done interactively by the user [RENZ, 1982]. This surface smoothing is useful where aesthetic qualities are desired in a hand-made physical prototype. This may be used to generate a reproduction part with improved smoothness.

Where optimum smoothness is desired, for aesthetic properties, this continuity improvement can be taken a step further, where potential machining point data can be analysed, demonstrating that an optimally smooth reproduction part will be generated. Machine cutter location (CL) points can be generated from the surface model, as discussed in chapter 3. As these machine paths are interpolating curves derived from the generated model, the deviations between these potential machining points and the generated surface model will be negligible. As discussed in chapter 3, the offsetting of a free-form surface amplifies the best-fit of discontinuous regions, adding errors to the overall RE process.

With free-form surfaces, it has been discussed that deviations between the surface model and CMM points account for deviations in continuity. This assumes adequate data collection density. If these deviations are relatively high, an alternative is to use the

'best-fit' generated surface to reproduce a second, smoother, physical surface [BARDELL, 1998c]. This would be appropriate where the original surface has been found to contain unwanted discontinuities, forming cosmetic quality issues. As the generated surface model is a best-fit of CMM points, machine points derived from the generated offset surface will also have improved continuity. Figure 4.8 shows the DA results of assessing these machined points derived from a best-fit surface.
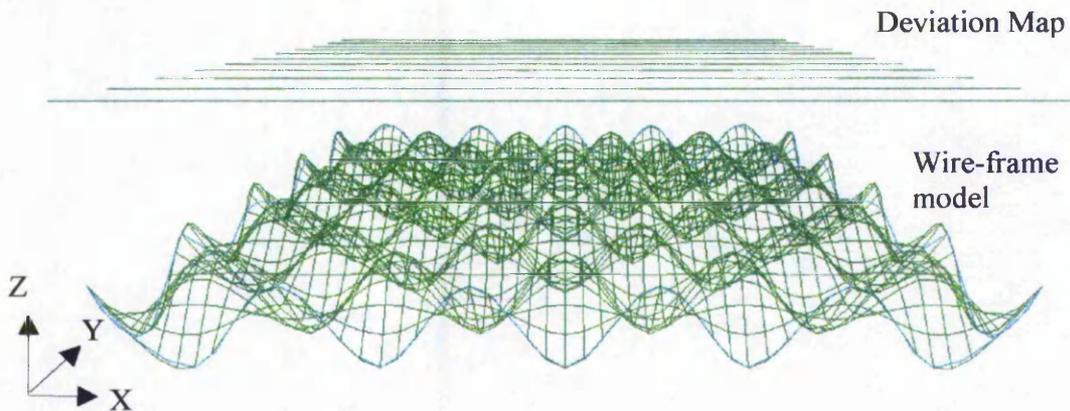
Figure 4.8. DA between machine points and generated surface.

It can be seen from the DA stage of the generated offset surface model and machined points, prior to machining, that the correlation between the machining data and the best-fit model has zero deviation. This shows the theoretical deviations of the potential reproduction part, where negligible deviations represent optimum smoothness, qualitatively defined as an improvement in overall continuity across the surface. This is very useful where the prototype was manufactured using traditional methods, relying on qualitative, rather than quantitative aspects.

Surface type recognition can be used as a region-based method of segmentation, discarding surface discontinuities, aimed specifically at composite surfaces.

4.3   Surface Type Recognition

This novel research is concerned with developing a methodology for improving the modelling of CMM data, in particular where discontinuous CMM data is collected. As demonstrated in chapter 3, CMM scan data is used to automatically generate a free-form

surface. Given an adequate CMM point data-set, a degree of user interaction is necessary, to determine the optimum patch resolution and intra-patch parameterisation. This aims to achieve the desired correlation of the surface model to the point data, whilst minimising the computational time and resulting file size. This reduces potential free-form modelling deviation errors. However the main source of modelling errors is caused by the complex nature of many objects. This is due to the original physical surface containing different surfaces that intersect in a discontinuous manner, forming crease, or roof edges. Determining the boundaries between these surfaces improves the accuracy of the resulting surface model, having a similar effect to 2D trimming, but in three dimensions. Most natural object faces are bound by crease edges, the identification of which is particularly difficult [HOFFMAN, 1987]. In many cases, reviewed in chapter 2, segmentation requires the detection of boundary discontinuities. The present work differs from this as it detects areas of free-form curvature, discarding any discontinuities. The introduction of a surface segmentation stage, as a 3D surface-trimming tool, acts as a model refinement stage. This improves the accuracy of a generated surface model at regions prone to errors, occurring at surface boundaries.

Industrial applications of this work include the generation of a visual representation of sub-surfaces making up a composite surface model, highlighting regions of the surface model which have inadequate CMM point data. This works towards the closer integration of data collection and surface modelling, seen as future research. Geometric properties can also be analysed, as can cosmetic quality flaws. Gaussian and mean curvature techniques form a method of interrogation, allowing the quality and smoothness of a surface to be ascertained [NIELSON, 1993]. These methods offer solutions to the generation of sub-surfaces, as a model refinement stage. This section demonstrates the development of a novel surface type recognition methodology, based on curvature, where the introduction of sub-surface domains of similar local surface type aims to decompose the global composite surface. This forms a number of steps, outlined in figure 4.9.

```
┌─────────────────┐
│  Global Surface │
│   Generation    │
└─────────────────┘
         │
         ▼
┌─────────────────┐
│    Curvature    │
│    Analysis     │
└─────────────────┘
         │
         ▼
┌─────────────────┐
│  Surface type   │
│   allocation    │
└─────────────────┘
         │
         ▼
┌─────────────────┐
│  Filtering and  │
│   Refinement    │
└─────────────────┘
         │
         ▼
┌─────────────────┐
│     Point       │
│   Clustering    │
└─────────────────┘
         │
         ▼
┌─────────────────┐
│   Sub-surface   │
│   Generation    │
└─────────────────┘
```
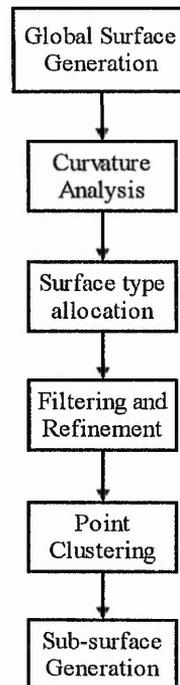
Figure 4.9. Process flowchart for curvature-based surface decomposition.

4.3.1 Surface Curvature Analysis

Once a free-form surface model has been generated, the preliminary stage involves analysing the surface curvature. This novel method of sub-surface determination uses point information to calculate surface curvature, where curvature is deduced at individual points on the surface. These points are theoretical, as there is no actual measurable point on a surface.

However, a 3D point domain must be derived from a surface in order to calculate curvature on a surface. This can be achieved by deriving a *uv* parameter point domain on the surface. The global surface is parameterised in *u* and *v* directions, where $0 \leq u \leq 1$ and $0 \leq v \leq 1$. Parameter points on the surface are defined at an adequate density, in both directions. From a preliminary investigation, the density of parameter points plays a vital role in local curvature analysis. A parameter point density of 2mm is sufficient to allow optimum analysis of local points, discussed in more detail later. Point-to-point CMM data can also be utilised, as long as a point density of 2mm is maintained. However, point-to-point data collection at this density is very time consuming. An

adequate parameterisation of the global surface is essential, in order to maintain a dense *uv* parameter domain, giving reliable calculations necessary for subsequent steps of surface type recognition. Figure 4.10 shows an example of this lattice of parameter points, defined as the *uv* parameter domain of the global surface.
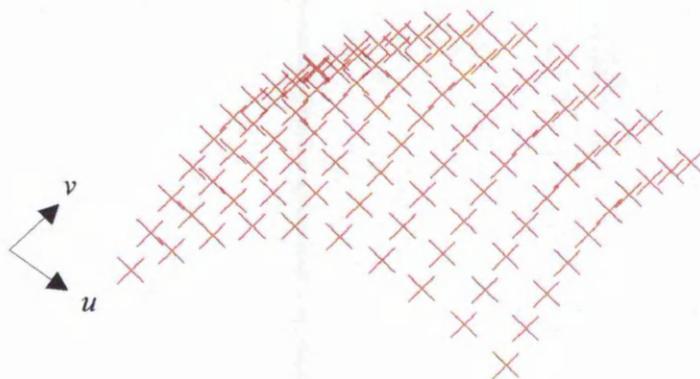
Figure 4.10. Global surface and *uv* parameter domain.

Each *uv* parameter point has two directions of curvature, known as primary and secondary curvatures (k_1 and k_2, respectively) [FARIN, 1990]. These are also known as maximum and minimum curvature, respectively as $k_1 > k_2$. Maximum and minimum curvatures occur for a pair of mutually orthogonal plane orientations [BARTELS, 1994]. By calculating the curvatures at each *uv* parameter point, global analysis of curvature can be effected, as seen in figures 4.11 and 4.12. These show maps of k_1 and k_2, respectively, for the surface model generated from the bottle data, seen earlier.
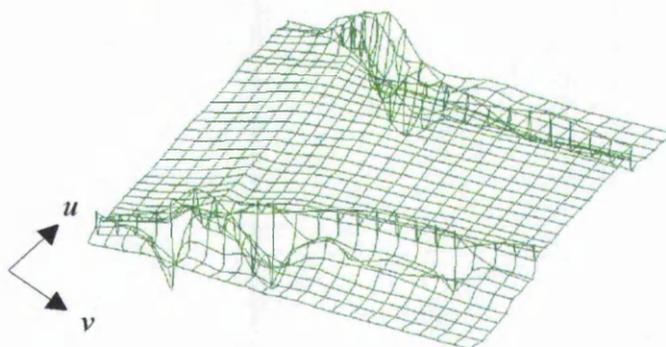
Figure 4.11. Primary curvature plot for generated bottle surface (scale x100).
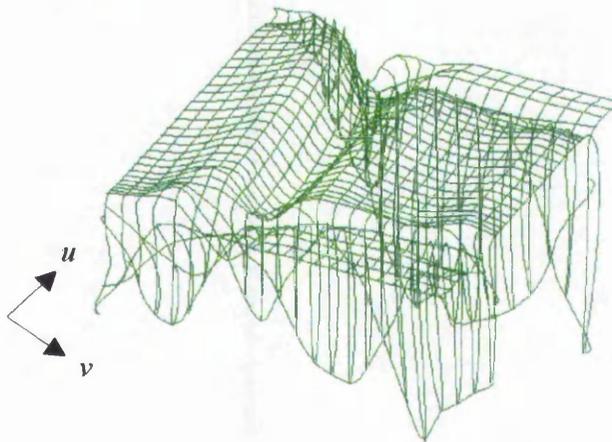
Figure 4.12. Secondary curvature plot for generated bottle surface (scale x100).

These figures demonstrate how the curvatures are distributed over the surface in each direction. The calculation of k_1 and k_2 are useful in the subsequent calculations for surface curvature. There are three main types of surface curvature used to deduce surface imperfections, known as Gaussian, mean, and absolute curvature [FARIN, 1990]. These are invariant surface characteristics [BESL, 1988]. In this work k_1 and k_2 are used to determine values for Gaussian and mean curvature. Gaussian curvature is commonly denoted as K, whereas mean curvature is denoted as H. This is adopted in this work, where Gaussian curvature is calculated by:

$$K = k_1 k_2$$

Mean curvature is calculated by:

$$H = (k_1 + k_2)/2$$

K can be used to analyse the global surface, where sudden changes in curvature are highlighted. The global surface is parameterised, as discussed above, and K is calculated for each parameter point, and plotted. Figure 4.13 demonstrates the K distribution over the global surface. This highlights surface discontinuities, present where differing surfaces intersect.
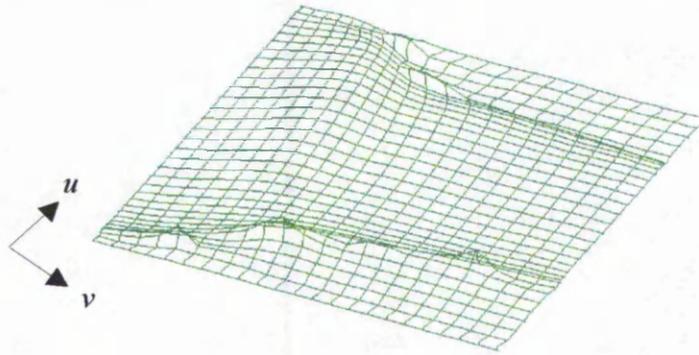
Figure 4.13. Gaussian curvature over global surface (scale x500).

This shows a correlation between DA and extreme curvature change, confirming that deviations between the CMM data and the generated surface model are due to extreme curvature change. A segment of the bottle data is used to show this effect more clearly, shown in figure 4.14.
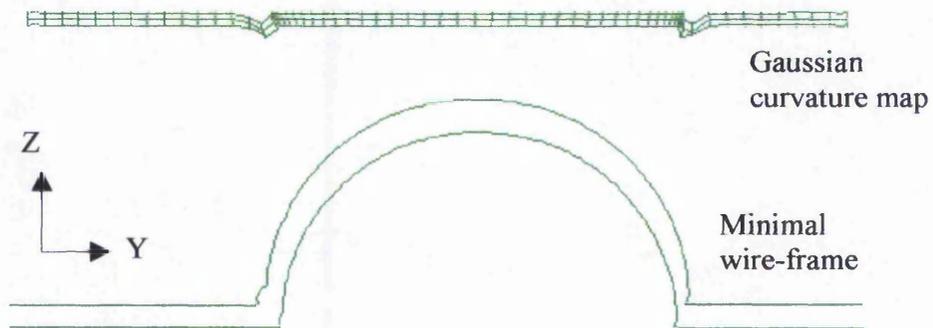
Figure 4.14. Gaussian curvature map, highlighting extreme curvature change.

This can be compared to figure 4.6, which is reproduced here as figure 4.15. As discussed earlier, the deviation errors are represented as scalar functions, thus the direction is irrelevant.
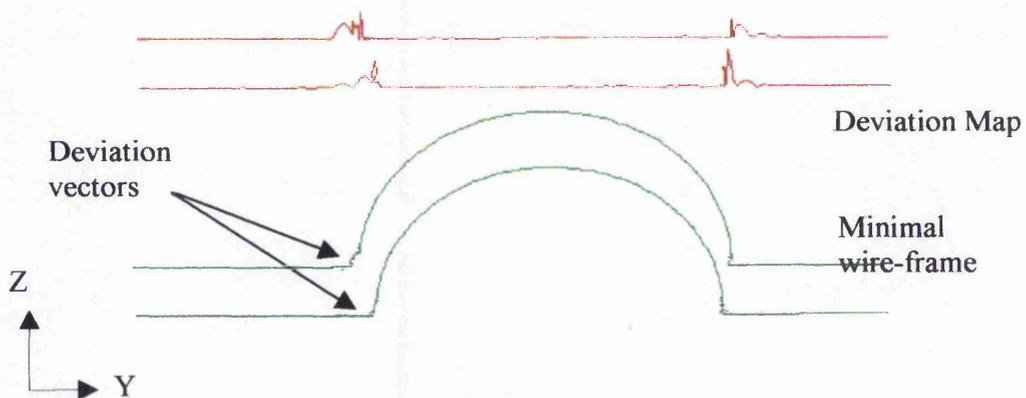
Figure 4.15. Segment of DA result.

The Gaussian curvature map shows the location of extreme curvature, and the DA map highlights these same regions as the major source of modelling errors. This offers two methods of identifying discontinuities in a surface model. A mean curvature plot is shown in figure 4.16, however is of limited use alone, as the combination of Gaussian and mean curvatures are used to deduce surface types.
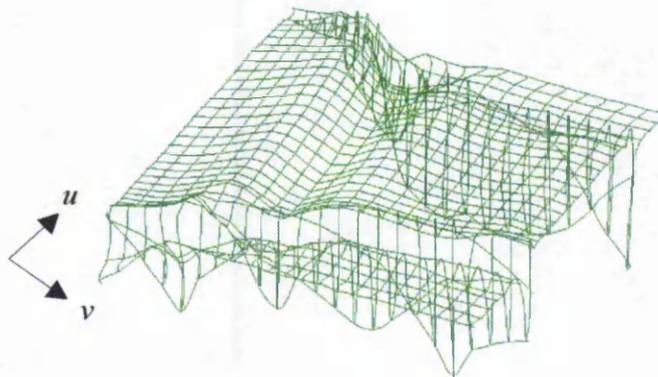
Figure 4.16. Mean curvature over global surface (x100).

The combined calculation of both K and H at surface parameter points is adopted in order to deduce the surface type at the point in question.

4.3.2 Surface Type Primitive Determination

All objects are represented by a set of primitives, the most basic being points, lines and surfaces [HOFFMAN, 1987]. The allocation of sub-surface types uses Gaussian (K) and

mean (H) curvature in the locality of a data point to associate one of eight possible surface type labels to that data point [BESL, 1990], [BALENDRAN, 1992]. This work aims to improve the modelling of a generated surface by discarding areas of discontinuity, forming a 3D surface-trimming tool. Thus, depending on the application, the actual allocated surface type may be irrelevant. This is particularly true where surface boundaries are sought. In the determination of surface types, the actual values of the Gaussian and mean curvature are unnecessary. The signs are used, determined by a threshold value, α, which is initially set to zero.

Table 4.1, shown below, demonstrates the methodology for determining the surface types, based on the values of k_1 and k_2, and the corresponding signs for Gaussian and mean curvature, where all points on the corresponding surfaces agree with the constraints deduced for each surface type. The eight surface types can be classified into being either convex or concave. Many works concentrate on the coarse classification of a surface type into planar (zero curvature), convex (positive curvature) or concave (negative curvature) types [HOFFMAN, 1987].

The surface models shown are generated from artificial point data. With adequate modelling parameters these surfaces are perfect, in terms of surface type description. Due to this, the values of k_1 and k_2 are used to calculate H and K, whose signs are then determined by α. In this case, the threshold value, α, is equal to zero. CMM noise interferes with this threshold value, which is discussed later. This work utilises the allocation of seven surface types, discussed below, in terms of specific surface type allocation, based on work by Besl and Jain [BESL, 1988], [BESL, 1990].

	Surface curvature		Directions of curvature		SURFACE TYPE	SURFACE MODEL
	Mean (H)	Gaussian (K)	K_1	K_2		
CONVEX SURFACE TYPES	$< \alpha$	$> \alpha$	$< \alpha$	$< \alpha$	Peak	
	$< \alpha$	$= \alpha$	$= \alpha$	$< \alpha$	Ridge	
	$< \alpha$	$< \alpha$	$> \alpha$	$< \alpha$	Saddle ridge $|k_1| < |k_2|$	
	$= \alpha$	$> \alpha$	-	-	None	-
	$= \alpha$	$= \alpha$	$= \alpha$	$= \alpha$	Flat	
	$= \alpha$	$< \alpha$	-	-	Minimal	-
CONCAVE SURFACE TYPES	$> \alpha$	$> \alpha$	$> \alpha$	$> \alpha$	Pit	
	$> \alpha$	$= \alpha$	$> \alpha$	$= \alpha$	Valley	
	$> \alpha$	$< \alpha$	$> \alpha$	$< \alpha$	Saddle valley $|k_2| < |k_1|$	
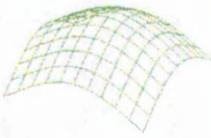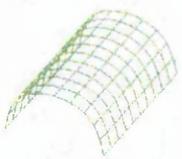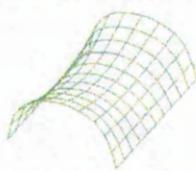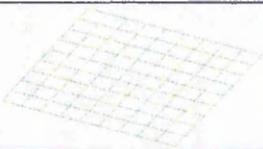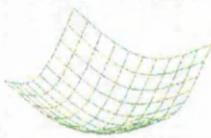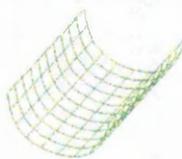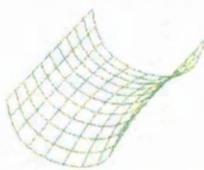
Table 4.1. Surface type labels, deduced from curvature values.

A planar surface forms an analytic type, where k_1 and k_2 values equal zero, resulting in zero values for H and K. Curved surface types also form analytic surfaces. Ridge and valley types form the *conical* analytic type, pit and peak form the *sphere* analytic type, and saddle ridge and saddle valley form the *torus* analytic type.

Convex surfaces, where mean curvature (H) is negative, alter depending on changing curvature in the k_1 direction, thus altering the sign of Gaussian curvature (K). Where K is also positive, an outer spherical surface is defined (peak surface type). With K equal to zero, an outer cylindrical surface is defined (ridge surface type). Where K is negative, an inner cylindrical surface is defined in the direction of primary curvature, and an outer cylindrical surface is defined in the direction of secondary curvature (saddle ridge surface type), where $|k_1| < |k_2|$.

In the case of concave surfaces, where mean curvature (H) is always positive, K determines the specific surface type, forming the inverse of the convex surfaces. A positive K value defines an inner spherical surface, giving both directions a concave curvature (pit surface type). Where K equals zero, an inner cylindrical surface is defined, defining the planar direction of the surface (valley surface type). Negative K defines an outer cylindrical surface in the k_2 direction, with an inner cylindrical surface in the k_1 direction, where $|k_2| < |k_1|$ (saddle valley surface type).

From table 4.1, six primitive curved surface types and a planar type are defined. There is also an eighth surface type, known as a minimal surface, which is a form of saddle surface [BESL, 1986]. Gaussian curvature is used to identify between saddle surfaces specifically [BARTELS, 1994]. This surface type allocation can be utilised to decompose a global surface model into constituent sub-surface types.

4.3.3   Global Surface Decomposition

This novel method of surface decomposition segments a global surface generated from CMM data into sub-surfaces containing points allocated as the same type. An object is often made up of a number of different surface types, intersecting at the surface boundaries. This method is based on the calculation of primary (k_1) and secondary (k_2)

curvatures at specific points on the surface, and the resulting signs for K and H. However, there are a number of factors which must be taken into consideration when developing this methodology. The combination of the sensitivity of the calculation for curvature, and the CMM data accuracy can result in an incorrect allocation of the desired surface type. This is due to the sensitive nature of curvature calculations, at a specific point, and 'noise' arising from CMM data. This leads to the necessary implementation of a filtering stage, allowing the correct surface type to be ascertained. In this way, the signs of K and H are determined using a threshold value, α, discussed fully below. This system can operate in an automatic or semi-automatic phase.

As presented in chapter 5, points on the global surface can be automatically allocated a surface type, based on a pre-defined threshold value. These point labels have no relationship with similar adjacent points, representing global surface type allocation. Despite the autonomous nature of this method, the sub-surface points may be allocated incorrectly. This method tends to segment the global surface into excessively small areas, and does not tackle the problem of clustering similar points.

To optimise the size of the sub-surfaces, the desired surface type can be input to the system, overriding the initial 'guess'. Using this surface type reference, the threshold value can be more precisely allocated, using the novel semi-automatic method of surface decomposition developed in this work. This involves seed region growing, which is discussed later, based on allocating local sub-surface labels, altering the threshold value to suit the desired surface type. This also acts as a method of point clustering. Table 4.1, shown previously, demonstrates how surface type allocation is initially based on the deviation of K and H from a threshold value, α, of zero. This threshold value of zero can be utilised with geometrically perfect surfaces, derived from artificial data, where deviations do not dramatically affect the values of curvature. However, CMM noise arises from physical surface imperfections, and the measurement accuracy, and can cause the surface type allocation to be hypersensitive.

4.3.4 Noise Arising from CMM Data

Due to the likelihood of an imperfect physical surface, particularly with forged parts, and the accuracy of 1μm for CMM contact probe data collection, fluctuations in the smoothness of the generated surface model often occur. With free-form modelling, the surface is smoothed as a best-fit model, partially reducing the CMM noise at an appropriate parameterisation [BARDELL, 1998c]. This leads to an improvement in the recognition of surface types, by minimising the curvature deviations present in the original CMM data. However, these deviations in the free-form models are still present. On a rendered free-form surface model these minimal errors may not be obvious, but the curvature analysis of the surface will cause these deviations to affect the results of the curvature-based surface decomposition methodology. The DA stage, developed earlier, highlights these areas, also corresponding to areas of extreme curvature change, in the case of composite surfaces.

Without a form of filtering, very few planar surfaces would be recognised as such, as each minimal deviation in the data-set would cause a deviation in curvature in the sub-surface domain. This would convert a potential planar surface into a curved surface type. The sensitive nature of local curvature analysis, with adequate parameterisation for surface segmentation, rarely supports the allocation of a global planar surface at a threshold value of zero. This necessitates a filtering method involving the calculation of an appropriate threshold value, α, allowing smoothing of the CMM data noise.

4.3.5 Threshold Value Determination

The curvature-based segmentation method results in the allocation of surface type labels, which are highly sensitive to curvature change. This is due to K and H being deduced as being greater or less than the threshold value, which has an initial value of zero. At this value of zero, positive and negative value allocation is straightforward, assuming no CMM noise. Figure 4.17 demonstrates the threshold value, α, and its effect on the signs of K and H.
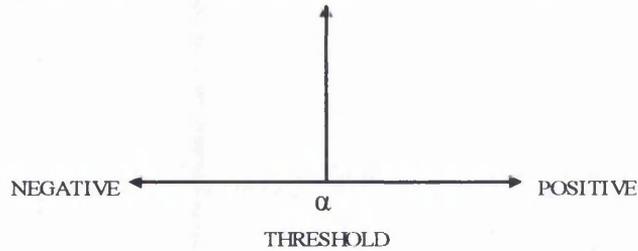
Figure 4.17. Threshold value of zero, and resulting sign allocation.

Filtering is necessary to determine an appropriate threshold value, in order to account for CMM data noise. This involves specifying the boundaries between positive and negative values for K and H, resulting in a correct surface type label. In effect, this widens the range for what is accepted as being equal to zero, allowing the desired allocation of positive and negative signs, as demonstrated in figure 4.18.
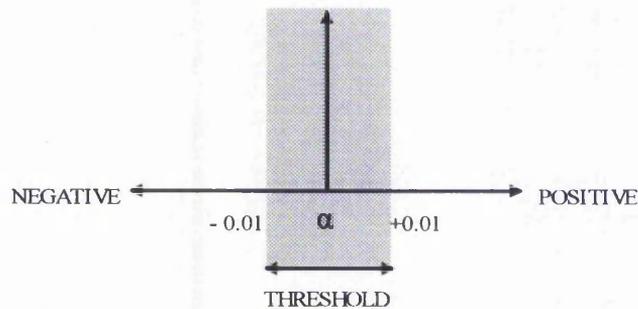
Figure 4.18. Threshold value widening, and resulting sign allocation.

The threshold value, α, acts as a filter on H and K. At 0.01, H and K are either <-0.01, >+0.01, or >-0.01 and <+0.01.This determines whether H and K are negative, positive, or zero. This works towards optimising the outcome of the surface type allocation phase, based on the signs of K and H.

In order to deduce the relevant threshold values necessary to allocate specific surface types, CMM data was collected from physical objects, manufactured to a tolerance of +/- 0.01mm, thus minimising the effect of physical imperfections. Three objects, of known surface type were used, and in each case, the threshold value was progressively increased from 0.0001 to 0.01. This corresponds to a threshold value, α, range from +/- 0.0001 to +/-0.01. These known surface types are taken from spherical, cylindrical and

planar physical objects, and free-form surfaces were generated from the CMM data. Each surface was then parameterised to contain one hundred points, in a grid of 10x10 uv parameter points. The local curvature signs of internal uv parameter points are calculated using Gaussian and mean methods.

The threshold value, α, is not directly related to the radius of curvature in a particular direction, as H and K are deduced from a combination of k_1 and k_2. However, α is based on the surface curvature for each type. By computing α, in order to generate the appropriate signs for H and K, the values of k_1 and k_2 also fall within the range of α. For example, where H or K are $< \alpha$ or $> \alpha$, k_1 or k_2 will also be $< \alpha$ or $> \alpha$, depending on the surface type. This is confirmed in table 4.1.

At each threshold value, α, the number of points allocated as spherical, cylindrical or planar is calculated, determining the optimum threshold value for correct surface type allocation. Within the scope of this experimentation, saddle and concave allocated surface types are ignored. The surface type allocation process uses the method of automatically allocating all uv parameter points on the surface, using a fixed threshold value each time, as discussed previously. Figure 4.19 shows the surface model generated from CMM data taken from a spherical physical surface.
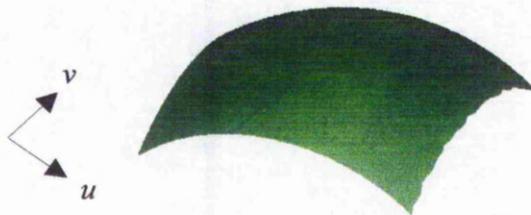
Figure 4.19. Spherical free-form surface model.

Graph 4.1 shows the results of filtering, increasing the threshold value from 0.0001 to 0.01.

Spherical (Peak) Surface with surface type labels
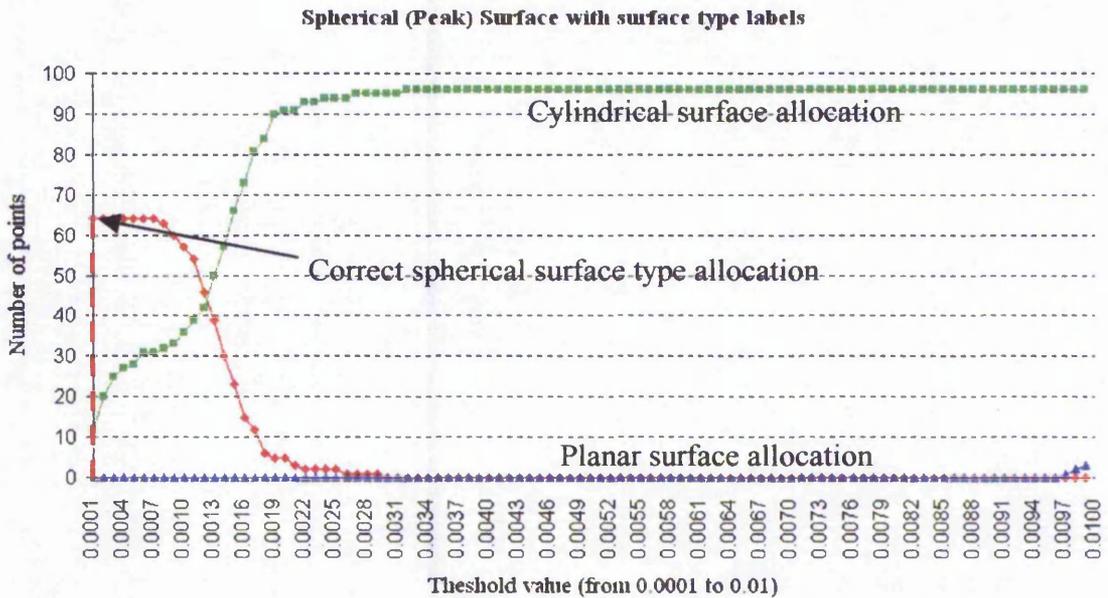
Graph 4.1. Result of varying threshold value for spherical surface type.

From the outset, all sixty-four internal surface parameter points are correctly recognised at a threshold value of 0.0001. The external boundary points on the surface cannot be labelled as spherical, as there is no surrounding neighbourhood of points, necessary for reliable curvature analysis. As the threshold value is increased, more surface points are recognised as a cylindrical surface type. Note that no points are allocated as planar until the threshold value approaches 0.01. This graph shows that the optimum threshold value for recognition of spherical surface types is at between 0.0001 and 0.0007.

Figure 4.20 shows the surface model generated from CMM data taken from a cylindrical physical surface.
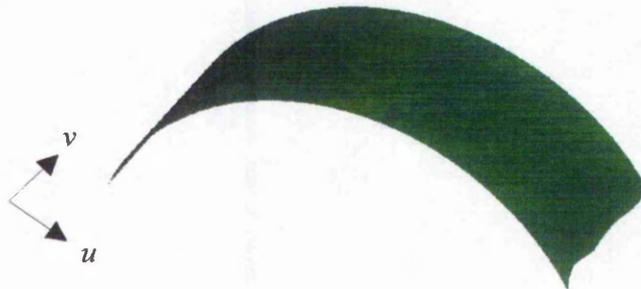
Figure 4.20. Cylindrical free-form surface model.

Graph 4.2 shows the results of filtering, increasing the threshold value from 0.0001 to 0.01.
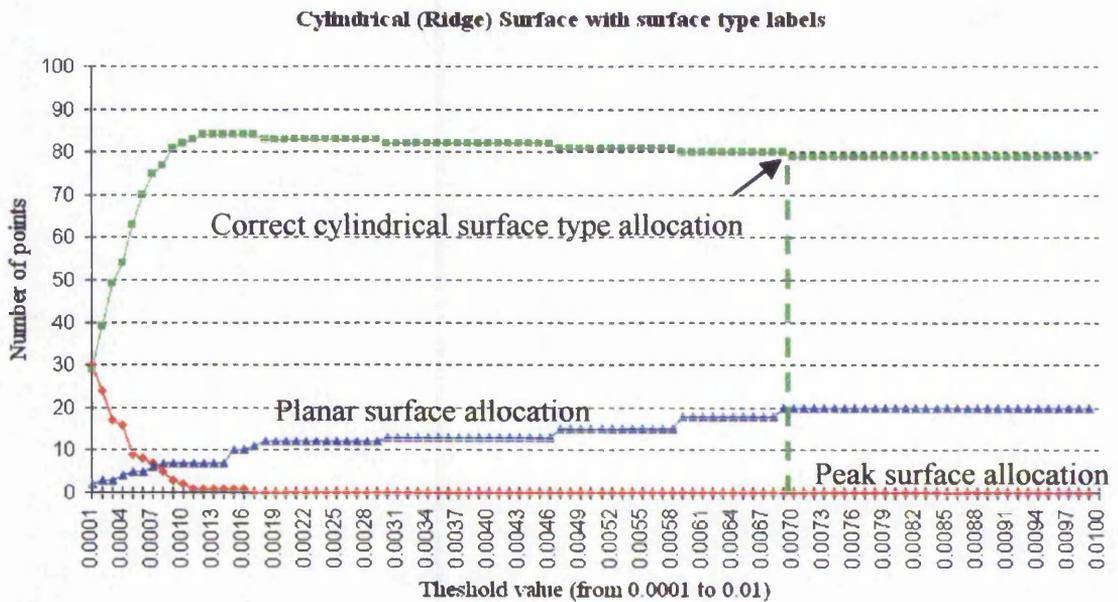
Graph 4.2. Result of varying threshold value for known surface type (cylinder)

Graph 4.2 demonstrates that at the initial threshold value of 0.0001, the surface type is indistinguishable, with an equal number of points being recognised as spherical and cylindrical. As the threshold value is increased, more surface points are correctly recognised as a cylindrical surface type, with the optimum number of cylindrical surface types (eighty) being correctly allocated at a threshold value in the region of 0.007. As cylindrical surface points are allocated based on the direction of curvature in one direction, two boundaries are correctly recognised, allocating eighty points. This demonstrates the effect of widening the threshold value range, until the signs of H and K allow correct surface type allocation.

Figure 4.21 shows the surface model generated from CMM data taken from a planar physical surface.
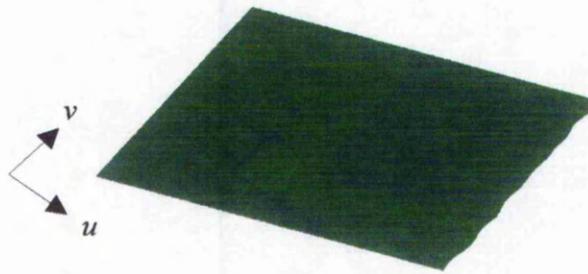
Figure 4.21. Planar free-form surface model.

Graph 4.3 shows the results of filtering, increasing the threshold value from 0.0001 to 0.01.
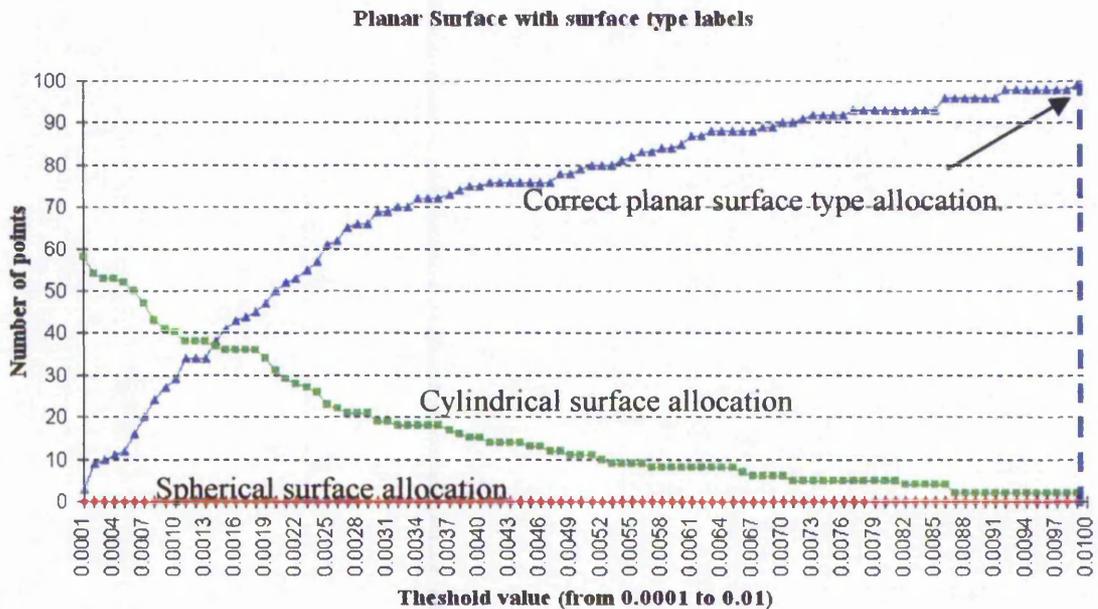
Graph 4.3. Result of varying threshold value for known surface type (planar)

In graph 4.3, the planar surface is initially recognised as mainly cylindrical. As the threshold value is increased, the surface points are correctly classified as a planar type, with one hundred points recognised at a threshold value of 0.01. Note that no points are recognised as a spherical type. At this threshold value, all points are correctly allocated, as planar surfaces are defined with zero curvature in both directions.

The determination of the threshold value, α, involves an iteration method of stepping through from 0.0001 to 0.01, until the desired surface type is allocated. As α increases,

the allocated surface type curvature decreases, thus α is inversely proportional to surface curvature conditions. Table 4.2 summarises the results of optimum surface type allocation, for known surface types.

		Physical Surface Type		
		Peak (Spherical)	Ridge (Cylindrical)	Planar
Surface type allocation	Peak (Spherical)	0.0001	0.0001	-
	Ridge (Cylindrical)	0.002	0.007	0.0001
	Planar	0.01+	0.01+	0.01

Table 4.2. Results of surface type recognition, allocating threshold value for known surface types.

The threshold value, α, has a profound effect on the resultant surface type allocation. At a α of 0.0001, peak surfaces are allocated. As α is relaxed, and the range widens to 0.007, one direction of curvature is redefined as having zero curvature, classifying a cylindrical surface type. As α is further relaxed to 0.01 and greater, both directions of curvature are allocated as zero, labelling the points as planar. The sensitivity of curvature analysis often results in an initial surface type allocation with curvature in two directions. Saddle surfaces also have curvature in two directions, and thus follow a similar pattern to peak surface types. Both saddle and peak/pit surfaces are allocated at a threshold value of 0.0001. Planar surfaces are rarely initially allocated as a peak type, as the sensitive nature of local curvature analysis, and CMM noise, is more likely to allocate saddle or ridge/valley surface types. Concave surfaces act in a similar manner, but the sign of mean curvature, H is reversed. This does not affect the threshold value.

In summary, for these three physical surfaces, taken as being dimensionally perfect, the CMM data results in a threshold value of 0.0001 for spherical, 0.007 for cylindrical, and 0.01 for planar (shaded cells in table 4.2). This filters the results for the calculations of H and K, based on the desired surface type. The corresponding surface allocation can then be given, using this threshold value at H and K calculations. It can be seen that some incorrect allocation may be possible, necessitating the use of user interaction in determining surface type allocation. This demonstrates the need for a curvature filtering method to compensate for the CMM noise, despite assumed 'perfect' physical surfaces being used. Artificially generated data-sets, resulting in geometrically accurate surface

models, as shown previously in table 4.1, do not need this form of filtering, where a threshold value of zero can be used.

Where a composite global surface is present, containing more than one surface type, general clustering of surface types is not possible. In order to develop this filtering methodology for a global surface comprising of a number of different surface types, the optimum type and size of sub-surfaces can be determined using the seed region growing method, discussed below.

4.4   Seed Region Growing

Initially, a single *uv* point on the global surface is chosen to be the seed point. The user defines this, based on the parameter value in the *u* and *v* direction, displayed in array form. It is sensible to choose a point central to the required sub-surface. For optimum surface label allocation, parameter points should be 2mm apart at the most, allowing points surrounding the seed point to be used to generate an initial 3x3 seed region domain. This minimises the size of intersection voids, discussed later. This neighbourhood of points surrounding the central point has a profound effect on the surface type allocation procedure of the central point, thus a sufficient point density is essential for optimum representation. The immediate nearest neighbourhood of surrounding points is used to create a seed region domain. Where the seed point is given as (u,v), the seed region domain is defined by the neighbourhood of surrounding points, allocated labels corresponding the points of the compass, as seen in figure 4.22.

NW *(u-1,v-1)*	N *(u,v-1)*	NE *(u+1,v-1)*
W *(u-1,v)*	SEED *(u,v)*	E *(u+1,v)*
SW *(u-1,v+1)*	S *(u,v+1)*	SE *(u+1,v+1)*

Figure 4.22. Seed region *uv* parameter point domain.

As an initial step, an interpolating surface is generated, utilising these eight boundary points. Figure 4.23 shows a typical initial seed region domain (wire-frame model), used to allocate the central point a surface type label.
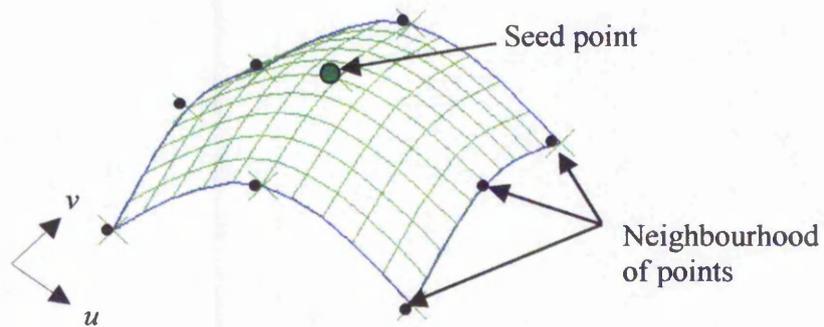
Figure 4.23. Seed region domain.

The generation of a seed region domain allows k_1 and k_2 to be calculated, at the central seed point. From this, K and H are calculated, deducing the surface type label for this central seed point, representing the local conditions of the seed point. In the above figure, this allocation would result in a peak surface type for the seed point. Adequately dense parameterisation of the global surface allows reliable allocation of the surrounding points with the same type label as the seed point. The assumption that the surrounding eight points are of the same type as the central seed point is validated by the density of the points being less than 2mm, and the fact that the seed point is selected at a region on the surface where points are expected to be of the same type. This parameter density guarantees that any local curvature change in the surface is accounted for. The ACIS® function for deducing k_1 and k_2, from which the surface type is allocated, requires the input of a surface and a point on the surface. Thus, as this deduced surface type is based on the seed region surface generated from the neighbourhood of points, an assumption is made that all these nine points are of the same type. Once the central seed point of the seed region domain has been successfully allocated, the nine neighbouring points are automatically allocated. The seed region domain is dense enough to make this assumption reliably. This seed region domain forms the basis for the seed region growing methodology developed in this work. The next stage of sub-surface type allocation involves the expansion of this seed region domain. If the assumption made is incorrect, the seed region domain will not be expanded, and a new seed point must be selected.

Seed region growing is based on expanding this initial seed region domain, clustering points of the same surface type as a sub-surface. Compared with automatic surface type allocation at a fixed threshold value, discussed earlier, it is preferred that a global surface is segmented into sub-surfaces, one surface at a time. This allows for the maximum area for a particular sub-surface to be found, using appropriate threshold values for each, depending on the surface type. This is particularly useful where two adjacent sub-surfaces intersect with tangent continuity, allowing the dominant surface to be expanded first, giving the largest possible sub-surface.

The seed region domain type label is based on calculations of k_1 and k_2 for the generated surface, and the resulting signs for H and K. This is initially calculated at a threshold value of zero. If this is not the desired surface type, the preferred surface label is input by the user. The system then recursively tests the point at various threshold values, until the surface is labelled with the desired type. There are cases where reallocation of a defined type is not possible. This occurs where the initial seed point is recognised as a convex surface type, thus cannot be reallocated as a concave type. The inverse of this also applies. Where this occurs, due to user-error, the system resets the threshold value and prompts the user to input another desired surface type. All surface types can be reduced to a flat type, by increasing the range of the threshold value.

As this seed region type allocation may rely on inputting a surface type prior to testing, it reduces the automation of the segmentation process, but vastly increases the resulting sub-surface domain size, and guarantees the correct surface type allocation. A minimum threshold value is deduced, which allocates the correct surface type label. The algorithm used to calculate the threshold value for the initial seed point surface label is given below:

> *Input position for seed, as uv parameter point*
> *If seed and neighbouring points are not already allocated a surface type*
>   *Generate seed region domain surface*
>   *Calculate H and K at threshold value of 0.0*
>   *Deduce surface type*
>   *If surface type = required*
>   *Use this threshold value*
>   *Else*
>   *Input required surface type*

For threshold value = 0.0001 to 0.1, in steps of 0.01
Calculate H and K at current threshold value
If surface type = required
Use this threshold value
If surface type ≠ required
Threshold value = 0.0
Return to input required surface type
Else
Return to input uv parameter position for new unallocated seed

The seed region growing methodology involves increasing the area of this initial seed region domain in a recursive manner, generating a local sub-surface domain. Points adjacent to the seed region points are individually 'tested' to determine whether they are of the same surface type as the seed region, at the same threshold value. This is determined by calculating k_1 and k_2 at each point, deducing H and K and the corresponding surface type. If this point fulfils the conditions to be included as part of the current sub-surface, it is added to the set of existing sub-surface points. This procedure continues in an anti-clockwise manner around the seed region points, recursively adding points to the seed region surface domain, creating a sub-surface domain. This method will conclude when tested points cannot be allocated as the seed point surface type. Using this methodology, a sub-surface will never grow beyond its actual boundary. Figure 4.24 shows a schematic of the seed region domain, defined in *u* and *v*.
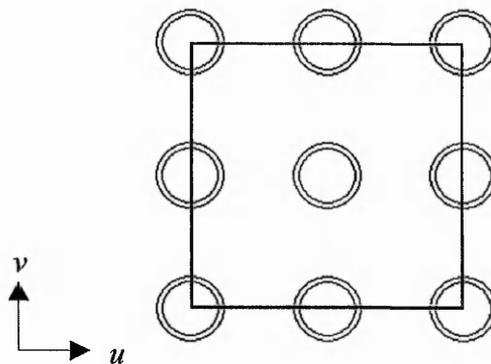
Figure 4.24. Initial seed region domain.

This initial stage of seed region growing originates with the seed region domain neighbourhood. The algorithm recursively tests points in the North, West, South and

East directions respectively. Each of the eight neighbours of the central seed are allocated as a seed point, aiming to grow the seed region domain into a sub-surface domain, where each is used to test adjacent points only. In each of the four directions, individual points are tested, comparing the deduced surface type with the original seed region surface type, and is either accepted or rejected. Seed region growing in the North and South directions are tested in an Eastern direction, from u-1 to u+1, and West and East seed region growing is achieved in a Southern direction, from v-1 to v+1. This is explained in more detail below. In each case, the shaded point is allocated as the current seed point.

Firstly, points are tested North of the highlighted point, in the order shown in figure 4.25 a. K_1 and k_2, and thus the surface type, are calculated at points 1, 2 and 3. If this type matches the seed surface type (shaded), the points are added to the seed region domain, initialising the generation of a sub-surface domain.
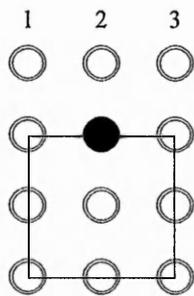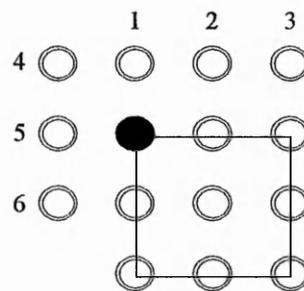
Figure 4.25 a.   Figure 4.25 b.

The sub-surface domain is then extended in a Westerly direction. This involves a new seed point being used to extend the sub-surface, testing points 4, 5 and 6 (figure 4.25 b). The next neighbour is allocated as the seed point, allocating point 7, as shown in figure 4.25 c.
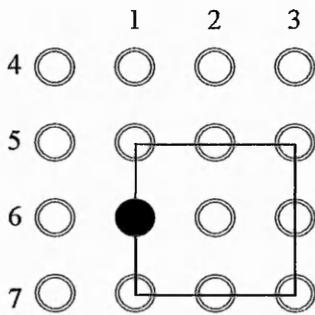
Figure 4.25 c.
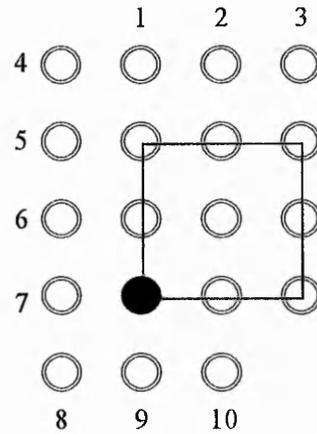
Figure 4.25 d.

Points in a Southerly direction are then tested. The new seed point allocates points 8, 9 and 10 (figure 4.25 d). The next seed point is used to test point 11, shown in figure 4.25 e.
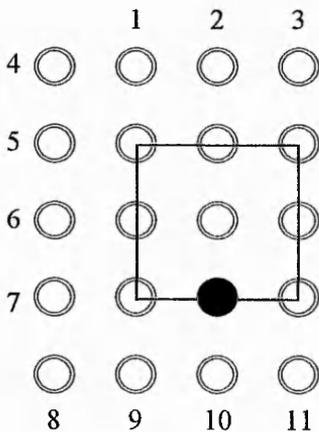
Figure 4.25 e.
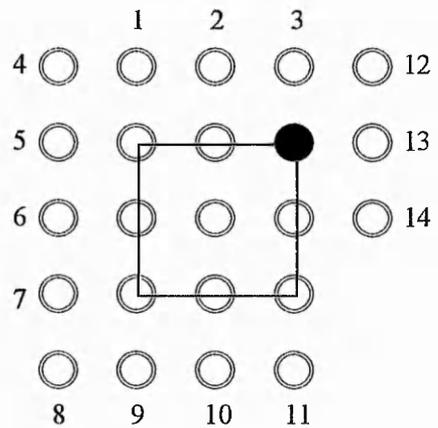
Figure 4.25 f.

Figure 4.25 f shows the next seed point allocated, which tests points 12, 13 and 14 (figure 4.25 f). The next seed point allocates point 15 (figure 4.25 g).
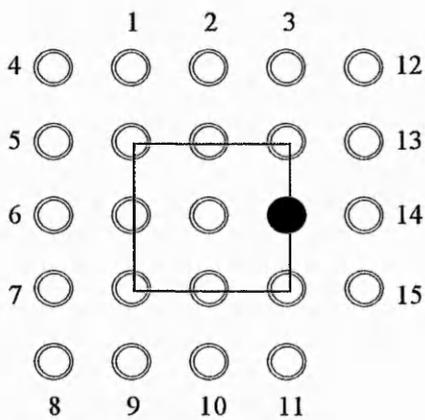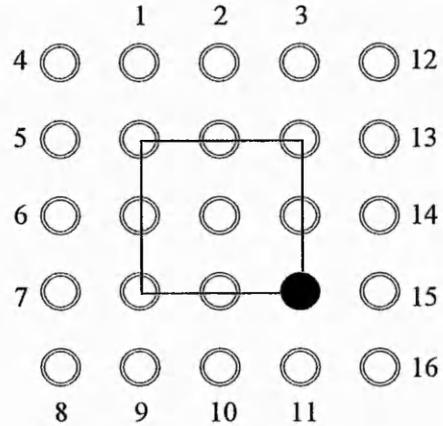
Figure 4.25 g.   Figure 4.25 h.

The conclusion of the first iteration involves the testing point 16, shown in figure 4.25 h. Point 1 on the allocated sub-surface domain is then used as the new seed point, and the recursive algorithm continues. The algorithm for the seed region growing methodology is given below, starting with the desired seed region allocation at a calculated threshold value. This algorithm also refines the sub-surface, discussed in the following section.

> *Extend in N direction*
> > *Find point adjacent to North seed region surface boundary*
> > *Calculate surface type*
> > *If type = seed*
> > *Add point to surface type array*
> > *Else*
> > *Convert threshold value, so type = seed*
> > > *If change in threshold value < initial threshold value*
> > > *Add point to surface type array*
> > > *Return threshold value to initial value*
> > > *Else*
> > > > *Discard point*
> > *Allocate surface type array to sub-surface*
> *Extend in W direction*
> > :
>
> *Extend in S direction*
> > :
>
> *Extend in E direction*
> > :
>
> *Recursive call to Extend in N direction*

There are cases where the current threshold value will reject a point, termed a 'rogue' point, which should be included in the sub-surface. This is due to excessive noise, causing a cosmetic deviation in the surface model, greater than the current threshold value can filter. This necessitates a refinement stage, further testing how 'close' the rejected rogue point is to the seed region domain surface type.

4.4.1 Sub-surface Refinement

In order to cluster points with similar surface labels, as a pre-cursor to the generation of sub-surfaces, it may be necessary to reassign some surface labels, based on each points' neighbourhood. In this way, the labelling procedure is error-checked. This is necessary, as in some cases a particular point label may differ from its neighbours, due to the sensitive nature of curvature analysis causing minimal local fluctuations in the surface, affecting cosmetic quality. For example, whilst growing a ridge (cylindrical) sub-surface, an adjacent point may be recognised as being a local saddle ridge, where it actually forms part of the larger cylindrical surface.

As discussed previously, the threshold value, α, is deduced in order to affect the signs of H and K, and does not have a direct relationship with either k_1 or k_2, taken individually. Sub-surface refinement involves altering α, based directly on k_1 or k_2, in order to reallocate a surface type label. Thus, α is based on the value of k_1 or k_2, rather than using the iteration method to find the desired type. This novel procedure takes the surface label of the rogue point and deduces the threshold value needed to convert the surface label to that of the seed point (required type). Using the above cylindrical case, a ridge surface is defined by $H < \alpha$ and $K = \alpha$, resulting in $k_1 = \alpha$ and $k_2 < \alpha$. This is verified in table 4.1, shown above. A saddle ridge surface is defined by $H < \alpha$ and $K < \alpha$, resulting in $k_1 > \alpha$ and $k_2 < \alpha$. In order to convert a saddle ridge to a ridge, the current threshold value, α, is modified to equal k_1. This results in H and K conditions for the allocation of a ridge surface. In other cases, in order to modify the surface type label, the threshold value is adjusted by a small amount, denoted as δ, to be greater or less than k_1 or k_2. The effect of this is to reallocate a surface type label of the current point. Table 4.3 shows the reallocations possible, and the action necessary for this

reallocation, where α is equal to the current threshold value, and δ is a negligible small value (0.0001), used to modify the signs of the resultant K and H values.

		Rogue point					
		Peak	Ridge	Saddle ridge	Pit	Valley	Saddle valley
Desired sub-surface allocation	Peak	N/A	$\alpha = k_1 + \delta$	$\alpha = k_1 + \delta$	-	-	-
	Ridge	$\alpha = k_1$	N/A	$\alpha = k_1$	-	-	-
	Saddle ridge	$\alpha = k_1 - \delta$	$\alpha = k_1 - \delta$	N/A	-	-	-
	Flat	-	$\alpha = (k_1 + k_2)/2$	-	-	$\alpha = (k_1 + k_2)/2$	-
	Pit	-	-	-	N/A	$\alpha = k_2 - \delta$	$\alpha = k_2 - \delta$
	Valley	-	-	-	$\alpha = k_2$	N/A	$\alpha = k_2$
	Saddle valley	-	-	-	$\alpha = k_2 + \delta$	$\alpha = k_2 + \delta$	N/A

Table 4.3. Method of rogue point reallocation, based on changes to threshold value, α.

Changing the threshold value in this fashion reallocates the surface type of the rogue point to that of the current seed region type (desired type). A surface type can only be altered to a similar type, in terms of convexity or concavity. Only ridge or valley rogue points can be modified to a flat type, as all other modifications involve changes to both k_1 and k_2. This is achieved by modifying the threshold value to equal the average of k_1 and k_2. Where a rogue point is initially allocated as a flat surface type, allocation to a new type is not possible, as this basic surface type cannot be converted to any other type by altering α alone. The reallocation of a rogue point surface type label must undergo validation, before the modification is accepted. This involves a comparison of the change in threshold value with the original threshold value at the initial seed point.

Worked Examples

Given the scenario that a flat sub-surface is being grown from an initial seed region, where the threshold value, $\alpha = 0.01$, points are tested in all directions. A point is tested, and found to be a valley type. Rather than rejecting it, threshold conditions are modified, resulting in the allocation of a flat surface type. The tested point has $k_1 =$

0.0286, and k_2 = -0.0006. Gaussian curvature is calculated by $K = k_1 k_2$, giving a result of K = -0.000. Mean curvature is calculated by $H = (k_1 + k_2)/2$, giving a result of H = 0.0141. Thus, at a threshold value of 0.01, $K = \alpha$, and $H > \alpha$, which allocates a valley surface. Conversion to a flat type is achieved by modifying α to equal $(k_1+ k_2)/2$, giving 0.0141, denoted as α^1. Thus, now $K = \alpha^1$ and $H = \alpha^1$ (flat). The change in threshold value, $\Delta_{threshold} = \alpha^1 - \alpha$, giving 0.0041. Determination of whether the point is accepted or rejected is made by comparing the change in threshold value with the original threshold value. If $\Delta_{threshold} < \alpha$, the point is accepted, as the change is negligible. In this example the point is accepted with the modified surface type label. A similar situation arises, where a valley surface is allocated with k_1 = 0.0408 and k_2 = 0.0041. Here, the calculation of $(k_1+ k_2)/2$, gives α^1 = 0.0225. $\Delta_{threshold} = \alpha^1 - \alpha$, gives 0.0125. In this case $\Delta_{threshold} > \alpha$, thus the point is rejected.

The outer boundary points of the current sub-surface are the last points to be checked for inclusion, using this rogue point reallocation method. Once complete, this represents the extent of the sub-surface in that direction. Where the difference, $\Delta_{threshold}$, is acceptable, the point is included in the sub-surface domain, as the reallocated surface type. The threshold value is then returned to the original threshold value and the next point is tested. This process concludes once the sub-surface cannot be extended in any direction.

4.5   Sub-surface Assessment and Generation

Following the allocation of points to sub-surfaces, the cosmetic quality can be analysed, where any local deviations are highlighted. This shows where the physical surface has flaws which are translated, via CMM data, to the surface model. This is a useful application of surface interrogation where surface deviations from physical parts are visually inspected for aesthetic requirements [BALENDRAN, 1993]. At the initial sub-surface generation stage, all points within a defined sub-surface are of the same type, however, the differences in radii are unknown. Potential fluctuations in radii can form aesthetically displeasing dents or peaks. Assessment of local curvature can be used to analyse the aesthetic quality of the underlying points of the sub-surface. This occurs

prior to sub-surface generation. Surface decomposition segments the global surface into a number of sub-surfaces of specific surface type. However, a sub-surface may not have a uniform radius. For example, a cylindrical sub-surface may have a slowly varying surface radius, thus not possessing a constant global radius. After sub-surface generation, a further assessment of the geometric tolerance of the resulting surface can occur, where the radius of curvature is used to determine the uniformity of the surface model. This forms an extension to the main objective of sub-surface generation, further analysing the resultant surface.

4.5.1   Local Quality Assessment

When a sub-surface domain has been extended to its limit, all points on this sub-surface are validated, based on the principal radii of the seed region, given by the reciprocals of k_1 and k_2:

$$r1 = \frac{1}{k_1} \text{ and } r2 = \frac{1}{k_2}$$

A user-defined tolerance range, based on surface radius, is used to determine the tolerance of fit for local points. This calculates the radius of curvature at each point on the sub-surface, determining whether the radius is outside this tolerance range. This is deduced by comparing the radius of the point in question with the radius of the initial seed point, calculating the difference between the two. The point is not discarded, if found to deviate outside the tolerance, but is flagged as being outside of this tolerance. This is used to highlight cosmetic quality defects in the sub-surface. The results of surface decomposition, shown in chapter 5, contain examples of cosmetic flaws in the generated sub-surface. Once a complete sub-surface has been grown and validated, it is deemed to be an acceptable sub-surface domain. The clustered *uv* parameter points making up this region can be interpolated, forming a sub-surface.

4.5.2   Single Sub-surface Domain Representation

A single sub-surface is a local free-form surface, extending to the sub-surface boundary, which is often irregular. This may cause degenerate surface boundaries, particularly

with sub-surfaces with concave boundaries, despite the underlying sub-surface points being correct. This is demonstrated in the following figures. Figure 4.26 shows uni-directional spline fitting in the u direction, through the sub-surface points.
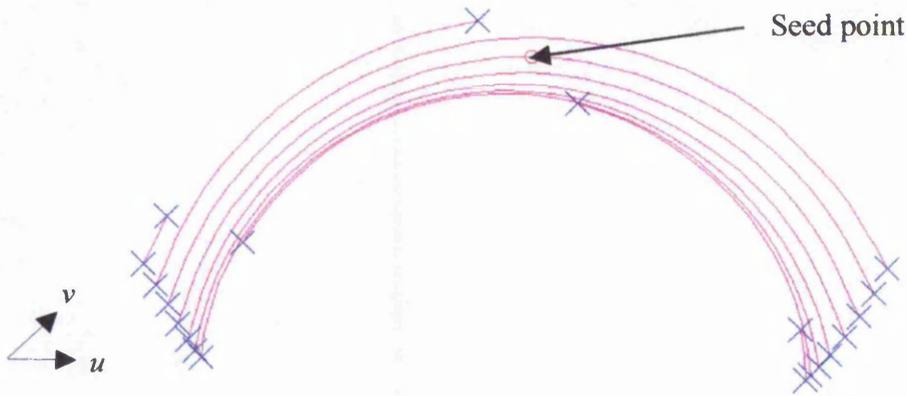
Figure 4.26. Uni-directional spline fitting through sub-surface points.

The internal sub-surface points are not shown, but the start and end points of each spline are highlighted. It can be seen that there is a vast difference in the length of these interpolating splines. Figure 4.27 shows orthogonal splines fitted through these start and end points, forming the sub-surface boundary in the v direction. It can be seen that the nature of continuous spline fitting through these end points causes a degenerate surface boundary.
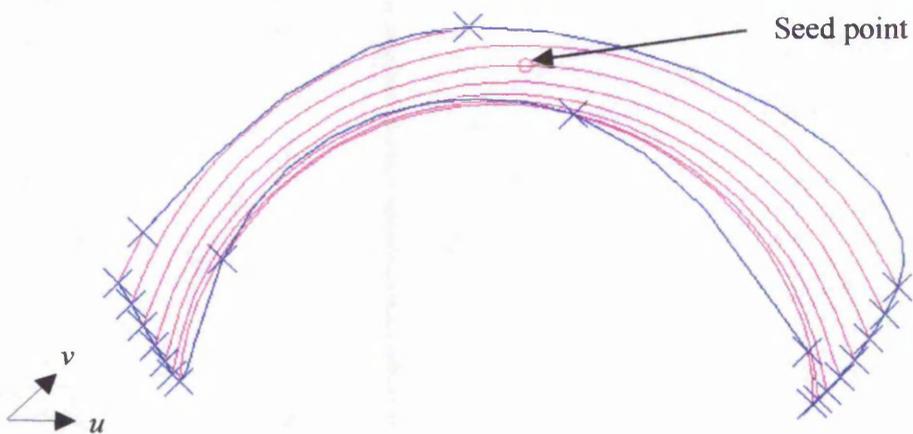
Figure 4.27. Orthogonal spline fitting through start and end points.

Due to this, the underlying sub-surface points and uni-directional splines are used to display the results of global surface decomposition, rather than the generated sub-surfaces themselves.

Once a sub-surface has been successfully grown, the global surface decomposition process continues, allowing another seed point to be input to the system, until the global surface has been segmented into unique sub-surfaces. Sub-surface points, which are allocated a surface type by previous seed region growing, cannot be used as a new seed point, or be reallocated by the seed region growing of an adjacent sub-surface. Appendix I shows the program flowchart for the curvature-based surface decomposition application. Results of global surface decomposition using seed region growing are presented in chapter 5.

There may be inter-sub-surface points between the sub-surface boundaries, due to the points in question being of an indeterminate type. These unallocated points form an *intersection void*. A fillet, often defined as a degenerate patch, is traditionally inserted in regions such as these intersection voids, by the CAD operator [BEZIER, 1974]. Depending on the success of the curvature-based surface decomposition and filtering stage, intersection voids will vary in size. These regions require discontinuous modelling, seen as a post-processing 'healing' stage, which is beyond the scope of this present work. Intersections to be added later, create a surface model with no intersection voids, allowing both continuity and discontinuity conditions to be modelled. This can be achieved using a compatible CAD package, such as AutoCAD. There will always be a minimum intersection void between two sub-surfaces, representing the discontinuous surface-surface intersections which caused the original global model inaccuracies highlighted by DA. These remaining points can be allocated a surface type, at a user-defined global threshold value, however these are generally of a type based on the deformed surface model, 'belonging' to neither of the adjacent surfaces.

4.5.3   Geometric Surface Assessment

As discussed previously, the surface decomposition process can be used to assess cosmetic quality, by analysing local changes in radius of curvature. This can be found

by calculating the maximum and minimum principal radii throughout the sub-surface. Additional initial research is made into the assessment of the geometric properties of the generated sub-surfaces. This involves the analysis of tolerance of form, aiming to determine the geometric properties of the surface. This takes the assessment of cosmetic quality a step further, where the total sub-surface radius is analysed for conformity, rather than comparing deviations in curvature with the seed point. The desired geometric tolerance determines the accuracy of the part, in terms of its functionality [BSI, 1993]. A geometric tolerance defines the size and shape of a tolerance zone in which the feature fits. Tolerance of form involves aspects such as straightness, flatness, roundness, and the profile of line or surface. Tolerance of orientation involves parallelism and angularity. Location tolerances are used to define symmetry and position [GAO, 1994]. Generally, B-rep surface models are not suitable for representing tolerances, as they are not feature-based. However, tolerance of form, or more specifically tolerance of a surface profile, can be used to assess and define sub-surfaces as features. This describes the roundness or flatness of the surface, or can define 'runout' [BSI, 1993]. A tolerance zone is associated with the profile of the surface, as shown in figure 4.28, in the case of a cylindrical surface. Offset surfaces can be used to describe this tolerance zone [SARKAR, 1991b].
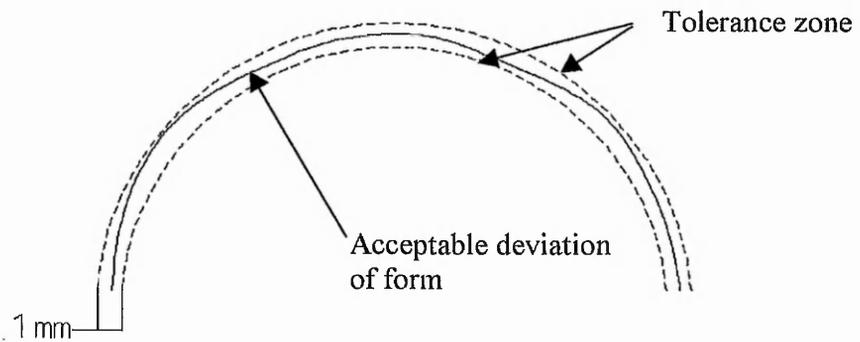
Figure 4.28 Tolerance zone of 1mm, for a cylindrical surface.

This defines the desired accuracy as +/- 0.5mm. To determine the geometric tolerance of cylindricity, a section of a cylinder, with a 12.5mm radius, manufactured to an accuracy of +/- 0.01mm is used. The surface model generated from this object is shown previously in figure 4.20. From this, the bilateral geometric tolerance for the surface

profile can be deduced. This involves calculating the radius of curvature, after probe compensation, for all *uv* parameter points on the surface. This utilises the cosmetic quality assessment methodology, discussed previously, aiming at quantifying the deviations of these irregular sub-surface regions. The average radius for all the local parameter points is then calculated.

Initial results are shown in table 4.4, for a number of patch resolutions. This aims to assess the effect of patch resolution on global geometric tolerance.

Patch Size (mm)	Average Radius (mm)	Average Error (mm)
2	12.971	+ 0.471
3	12.616	+ 0.116
5	12.412	- 0.088
7	12.477	- 0.023

Table 4.4. Preliminary results for radius of generated surface model.

The calculation of average surface radii is initially based on local seed regions, resulting in local curvature. However, calculating the upper and lower ranges of radii, in order to define the resulting tolerance zone for the generated surface, can cause irregularities. For a surface model defined at a patch size of 5mm, the geometric tolerance is found to be 5mm, where results of radius of curvature vary from 11.5mm to 16.5mm, despite giving an average radius of 12.412mm. This gives a close correlation to the actual physical surface diameter of 12.5mm. This large tolerance zone is due to calculations of local curvature, k_2, at each sub-surface point, and the resulting radius. As smaller patches are used, this tolerance zone increases. At a patch size of 2mm, the range of radius varies from 8.5mm to 17.5mm. Depending on the application, these errors may be acceptable, such as an average error of +0.47mm at a patch size of 2mm, where an optimum patch size of 7mm gives the smallest tolerance zone, and an average error of 0.023mm.

It is assumed that the data collection stage and surface offset of the generated surface yield optimal results. This can be confirmed by performing DA on the surface, and also by the calculation of average local curvature. However, results show that the tolerance

zone is reasonably large. ACIS® is used to calculate k_1 and k_2 for a given parameter point on the given surface, however the locality of the surface used to calculate curvature is unknown. Further investigation is necessary to determine a methodology for global geometric assessment. An extension to this initial research would be the calculation of global curvature, necessitating future research. This involves the conversion of the spline surface to an analytical type, necessitating the good estimation of local curvature.

4.6   Summary

This chapter has investigated novel methods of enhancing the RE process. Many works involving this process do not adequately analyse the generated surface model and the reproduction physical part, as discussed in chapter 2, as it is often assumed that there will be a high degree of correlation throughout the RE process. However, this can depend on the complexity of the physical surface, the CMM data density, and the surface generation method. Physical factors in data collection and machining often cause the most errors. The accuracy of a generated surface model depends on the definition of the intra-patch parameterisation and patch resolution. These are determined by the complexity of the surface, and are user-definable.

Accuracy analysis highlights areas on a generated surface model which do not conform to the underlying CMM data. This can be applied to industry, where surface models are generated within tolerances, maintaining an optimum patch resolution and corresponding file size. Regions of deviation are localised and quantified using deviation analysis (DA), which is a novel method of determining the accuracy of generated free-form models. Here, a comparison is made between the CMM data points and the surface model, recording any deviations which occur. These deviations are caused by the surface parameterisation, patch resolution and the complexity of the surface model, and are highlighted in a deviation graph. Free-form physical prototypes result in deviations at the modelling stage due to continuity deviation, rather than modelling errors, where a sensible patch resolution is applied.

Where the original physical surface contains discontinuities, these deviations occur at regions where discontinuities are modelled as free-form surfaces. In this way, deviations show free-form modelling errors due to a low patch resolution, and surface model deformations, due to discontinuous local surface-surface intersections. Investigation of this area works towards optimising patch resolution and patch size, minimising surface complexity and resulting file size, whilst maintaining an acceptable correlation of the surface to the underlying CMM points. This leads to the generation of an accurate surface model, which can be used for further design processes, or in the reproduction of a physical reproduction part, completing the RE process. This reproduction stage is outside the realms of this present work. Results of DA show that the accuracy of a surface model is highly dependant on the complexity of the underlying CMM data, in terms of the definition of continuous and discontinuous regions. Errors, expressed as deviations between the surface model and the point data are quantified and localised. This allows the deduction of an adequate surface definition, based on acceptable tolerances. The accuracy of the surface model is proportional to the file size, thus optimising the patch parameterisation depends on the application of the data file.

Data-set partitioning (DSP) is a further method used to analyse the surface model. This method is based on creating a sub-set of the original data, which is then used to generate a surface model. The remaining verification data-set is then compared with the surface model. This deduces the potential reduction in surface model accuracy, with a reduction in the number of scan lines used. Results of DSP show the effect of the amount of data collected on the accuracy of the resulting surface. Where scan lines of data are not used at the modelling stage, adjacent scan lines that are used maintain a correlation with the surface model. This is due to global continuity conditions across the bi-directional spline network generating a best-fit surface, approximating the intermediate scan lines. The required accuracy is needed to predict the amount of data necessary, determined by the patch resolution. The effect of using less data, by having an increased step-over distance between scan lines, results in a much reduced accuracy where a small patch size is used. At larger patch sizes the step-over distance has less of an effect. The results of DSP show that the deviations of the verification sets from the surface model increase in magnitude at larger patch sizes. This effect is due to the increased smoothness of the

surface at these larger patch sizes. The size of the deviation increase, however, compared to the deviations of the full data-set, is reduced at larger patch sizes. Thus, a reduction in CMM data used has less effect on surface model deviations at low patch resolution. Further work is needed in order to accurately predict the resulting accuracy of a surface, based on the density of available CMM data.

Where continuous physical surfaces are present, free-form model generation can be used to improve surface smoothness. DA shows any continuity deviation, and an adequate patch resolution can be used to reduce irregularities in smoothness. Rather than assessing and flagging local cosmetic quality defects, the global smoothness can be improved. Results of this stage lead to improved smoothness in the surface model derived from CMM data. This surface model can be used to generate machine path points, at the appropriate tool radius compensation. Part-program generation, based on these machine points may be utilised in the reproduction of a part which is smoother than the original. This is desired where qualitative properties are more relevant than functional and dimensional constraints. However, this machining stage is not pursued in this present work.

Model refinement is necessary to improve the appearance and accuracy of a surface model, shown to contain deviations from CMM data, quantified in the DA stage. Areas of extreme curvature change can be prone to inaccuracies from data collection, but the nature of free-form surface fitting accounts for the highest deviation.

A novel surface type recognition approach has been used to decompose a free-form surface generated from CMM data, determining the corresponding sub-surface types. It is possible to automatically allocate surface labels to a global surface, based on a single predefined threshold value. However, the CMM data accuracy, causing noise, and the fluctuation in local surface curvature, tend to give unique properties to a surface model. Using a constant threshold value throughout the global surface leads to excessive segmentation of surface types, due to the effect of slight curvature change on the surface. Results of this successfully allocate surface points a surface type label, however do not cluster these points as a local sub-surface.

Curvature-based surface decomposition has been developed as a 3D surface segmentation tool, specifically aimed at surfaces derived from CMM data. This involves a novel seed region growing methodology of surface expansion, shown to successfully segment a global free-form surface into local sub-surfaces, using appropriate threshold values. Clusters of points of the same surface type are then interpolated, generating sub-surfaces. Due to the potential irregular boundaries of these sub-surfaces, there may be surface interpolation inaccuracies, however the actual points labelled are well defined within the sub-surface boundary. This curvature-based method also forms a cosmetic quality assessment stage, where points on the surface which do not conform to the rest of the surface, based on a local radius tolerance, are highlighted. The generated sub-surfaces do not have a common boundary, which is beneficial when applied to composite surfaces, as modelling errors at surface-surface intersections are reduced. These regions need 'healing' to introduce discontinuous intersections between sub-surfaces. This process is seen as an additional procedure, filling the intersection voids by utilising appropriate multiple surface intersection routines, common to many good CAD packages. Results of curvature-based surface decomposition involve the successful segmentation of a global surface containing different surfaces of unknown type, into a number of local sub-surfaces of known surface type. This can be applied to the analysis of sub-surface types, and the identification of regions of the surface model which have inadequate CMM data. This is useful where further data can be collected, improving the accuracy at these regions.

Further analysis of the generated surface model is possible, investigating geometric tolerance of fit. This analyses the sub-surface, calculating deviations of form, rather than deviations from the CMM data. Accurately machined objects are necessary for this. Results of this investigation show that the generated surface model for physically 'perfect' parts, to the manufactured tolerance, can be accurately modelled. The local curvature at points on the surface can cause a relatively large tolerance zone, depending on the patch size used. However, this still results in an overall radius displaying a very close correlation with the actual radius of the original part. A very small patch size, such as a patch size of 2mm, will cause excessive local fluctuations in the surface. The calculation of noise-sensitive k_1 and k_2 highlight these fluctuations. The deduction of

radius of curvature, based on the global radius, would compensate for these local fluctuations, necessitating further research.

This work allows a visual representation of the individual sub-surfaces derived from the global surface model, which is useful at the design verification stage. The seed region growing methodology results in clearly defined sub-surfaces of the same surface type, where any cosmetic quality flaws are detected, allowing steps to be taken to improve the surface. The analysis of geometric properties is particularly relevant to the evaluation of hand-made prototypes. This also applies to the detection of regions on the surface where inadequate data has been collected, due to extreme curvature change in the surface profile. This work aims to improve the accuracy of the modelled surface by minimising the errors due to extreme curvature change. The determination of sub-surfaces also works towards the conversion to analytical surfaces, which would vastly reduce the file size and computational processing time. This conversion is seen as future research.

Results of these novel enhancements to RE are presented in chapter 5.

Chapter 5.

Experimental Results of Novel Work

5.1   Introduction

This chapter is based on the results obtained from the novel work discussed in chapter 4. As discussed in chapter 3, composite surfaces cannot be accurately modelled. The novel work discussed in chapter 4 aims to analyse the accuracy of these surface models, and offers a method of surface model accuracy improvement, utilising the surface type recognition methodology. Three composite surfaces are used to demonstrate these results, including sections on Deviation Analysis (DA), Data-set Partitioning (DSP), and automatic and semi-automatic surface segmentation. Initially, free-form deviation analysis is presented.

5.2   Deviation Analysis

5.2.1   Free-form Surface Deviation Analysis

Figure 5.1 shows a free-form surface, generated from artificially created point-to-point data.
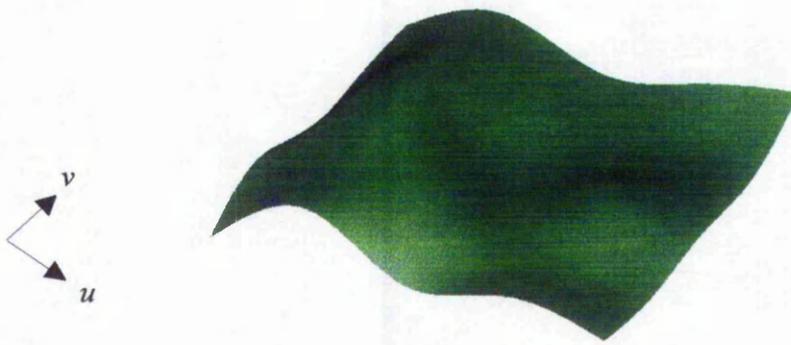
Figure 5.1. Smoothly varying free-form surface (5x5 patch resolution).

A typical DA graph is shown in chapter 4, as part of the discussion of the DA methodology. DA has been performed at various patch resolutions, which is summarised in table 5.1.

Patch parameter -isation	Patch size (mm)	Number of patches (U x V)	Ave. Deviation (mm)	Max. Deviation (mm)	File size (Kb)
5	5	9x8	0.001	0.004	548
5	10	4x4	0.004	0.036	133
5	11	4x3	0.060	0.549	102
5	12	3x3	0.277	1.301	79
5	15	3x2	0.301	2.260	56
5	20	2x2	0.351	3.504	40

Table 5.1. Patch resolution and corresponding deviations.

These results can be plotted, showing the relationship between average deviation and patch size, shown in graph 5.1.

Deviation Analysis
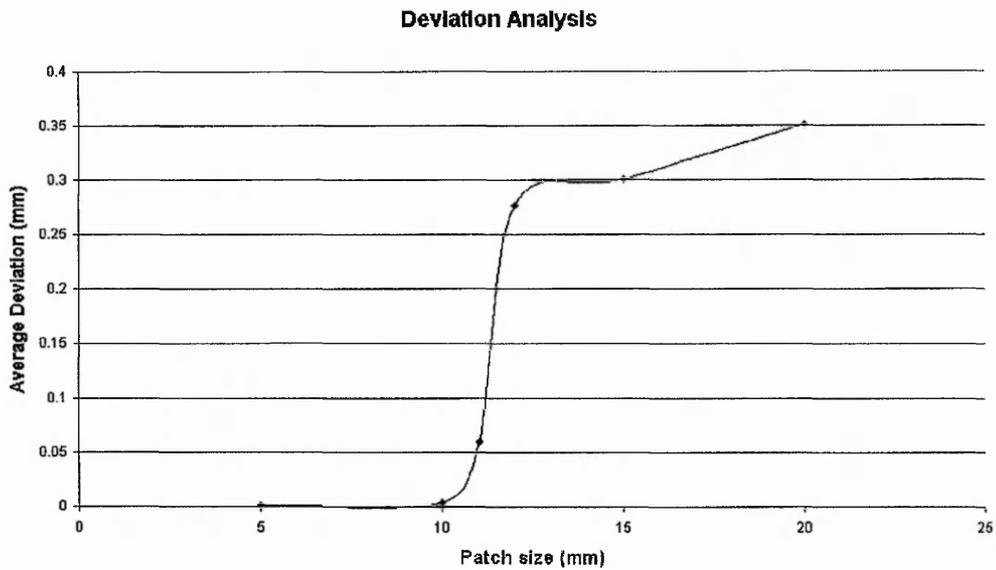
Graph 5.1. Relationship between average deviation and patch size.

Results show that the average deviation is minimal at a patch size in the region of 5mm to 10mm. As the patch size increases, the deviations increase. This can be compared with the effect of patch size on file size, shown in graph 5.2, where file size decreases as the patch size increases, relating to the decrease in the number of patches and surface complexity.
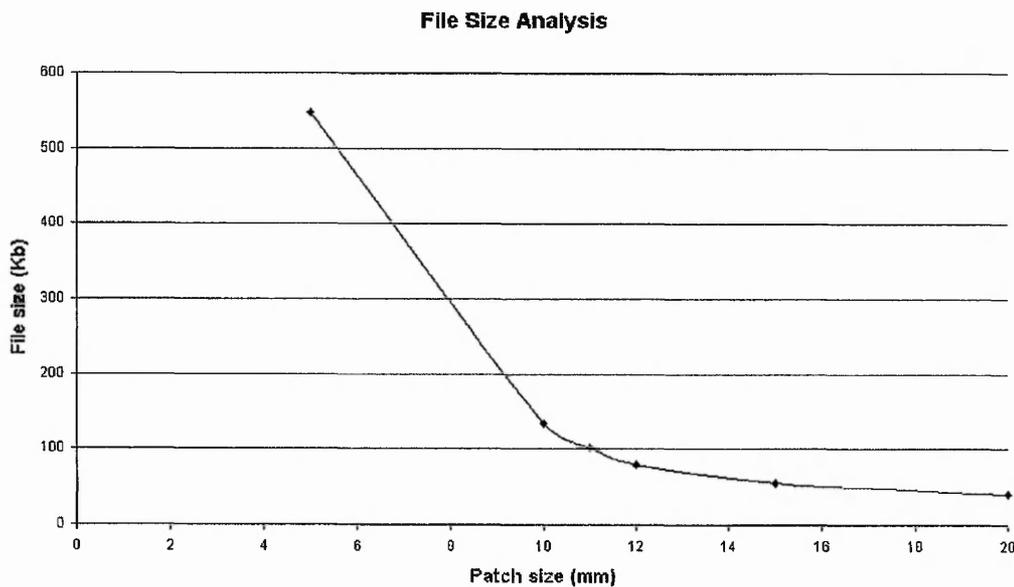
File Size Analysis

Graph 5.2. Relationship between file size and patch size.

However, DA is specifically aimed at analysing deviations of composite surfaces, presented in the following section.

5.2.2   Composite Surface Deviation Analysis

The effect of patch resolution on average deviations and file size for three complex physical surfaces are presented below. These surfaces are progressively more complex, generated from CMM data taken from complex physical objects containing discontinuities, described as areas of extreme curvature change.

5.2.2.1 Bottle Neck

Figure 5.2 shows a surface model of the neck region of a bottle. CMM scan data was collected at a step-over distance of 10mm
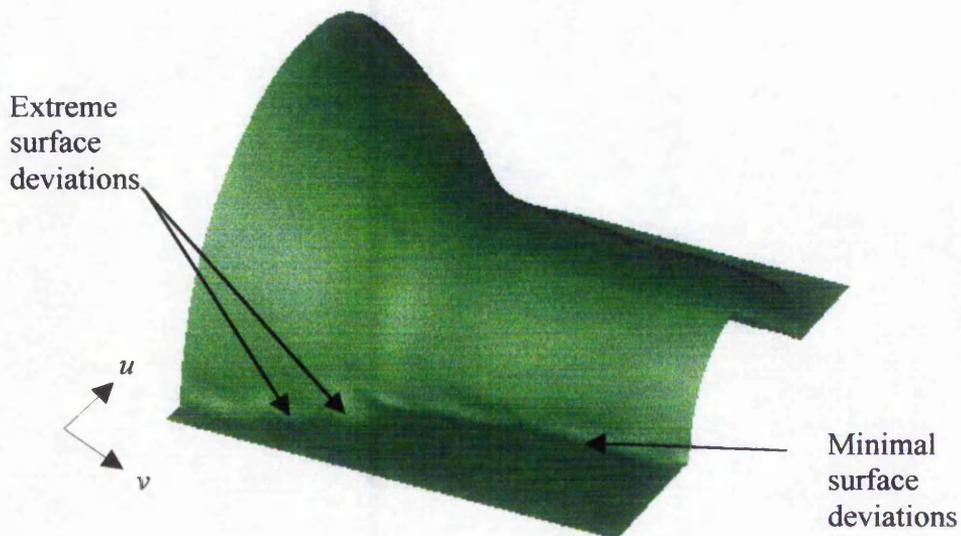
Figure 5.2. Automatically generated surface model (patch resolution 7 x 5).

Typical DA graphs are shown in chapter 4, as part of the discussion of the DA methodology. Table 5.2 shows results for varying patch resolutions for this surface model, aimed at minimising the deviations.

Patch parameter -isation	Patch size (mm)	Number of patches (U x V)	Ave. Deviation (mm)	Max. Deviation (mm)	File size (Kb)
5	5	23x16	0.007	0.608	2,698
5	6	19x13	0.010	0.446	1,850
5	7	17x11	0.013	0.564	1,413
5	10	11x8	0.025	0.716	683
5	13	9x6	0.056	1.575	430
5	15	7x5	0.086	2.111	287

Table 5.2. Patch resolution and corresponding deviations.

In a similar fashion to table 5.1, for a free-form surface, the greater the number of patches, the lower the deviations are. Graph 5.3 plots the patch size against the average deviation.
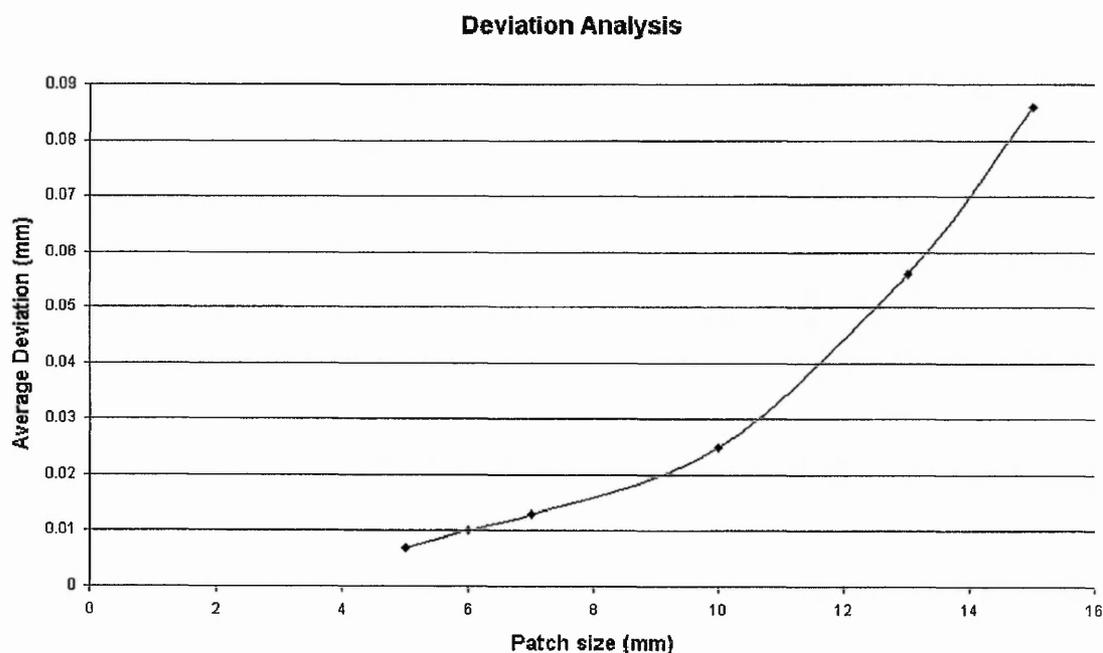
Graph 5.3. Relationship between deviation and patch size.

This can be compared with the graph of the effect of patch size on the resulting file size, shown in graph 5.4.

File Size Analysis
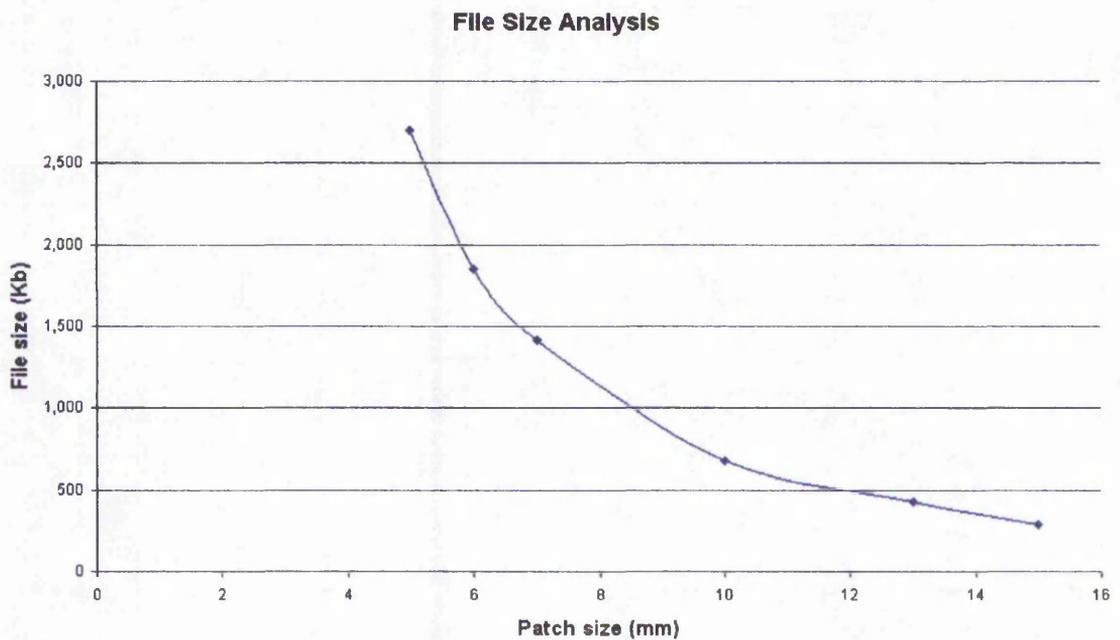
Graph 5.4. Relationship between file size and patch size.

5.2.2.2 Bottle

Figure 5.3 shows the interpolating splines generated from point-to-point CMM data collected at a step-over distance of 5mm.
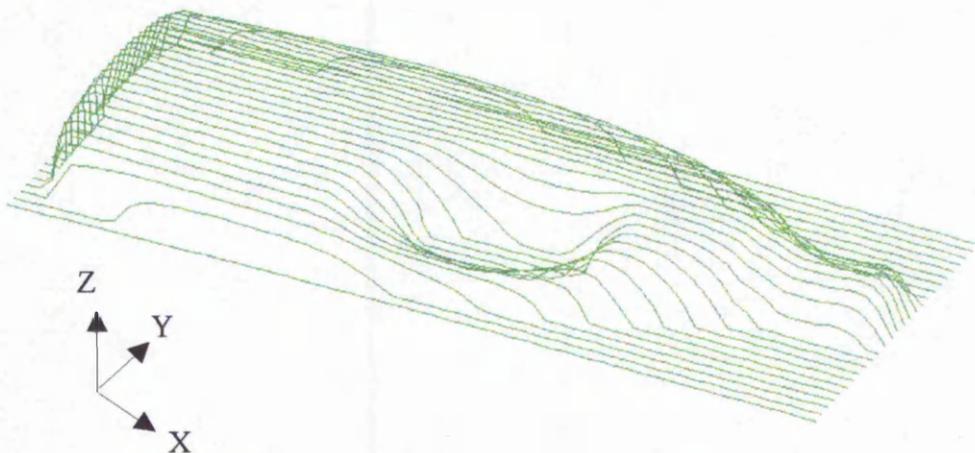
Figure 5.3. Interpolated point-to-point data taken from a bottle.

Figure 5.4 shows a typical surface model.
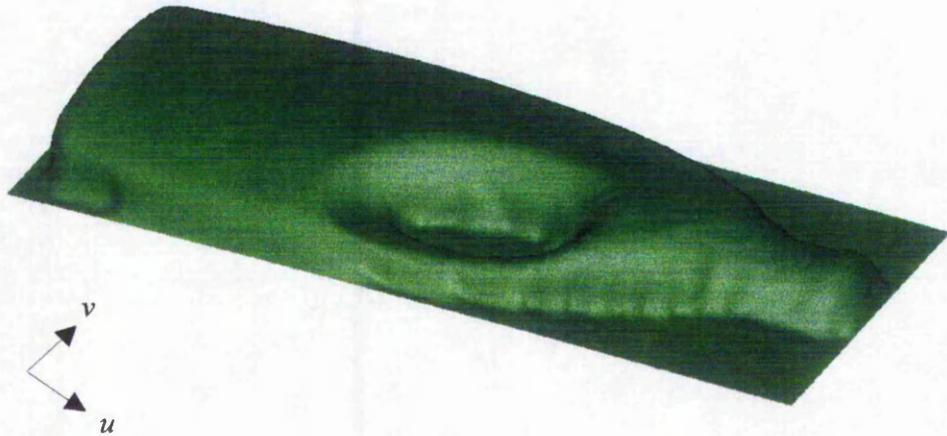
Figure 5.4. Free-form surface model for point-to-point data taken from a bottle (38 x 13 patch resolution).

A typical DA graph is shown is figure 5.5.
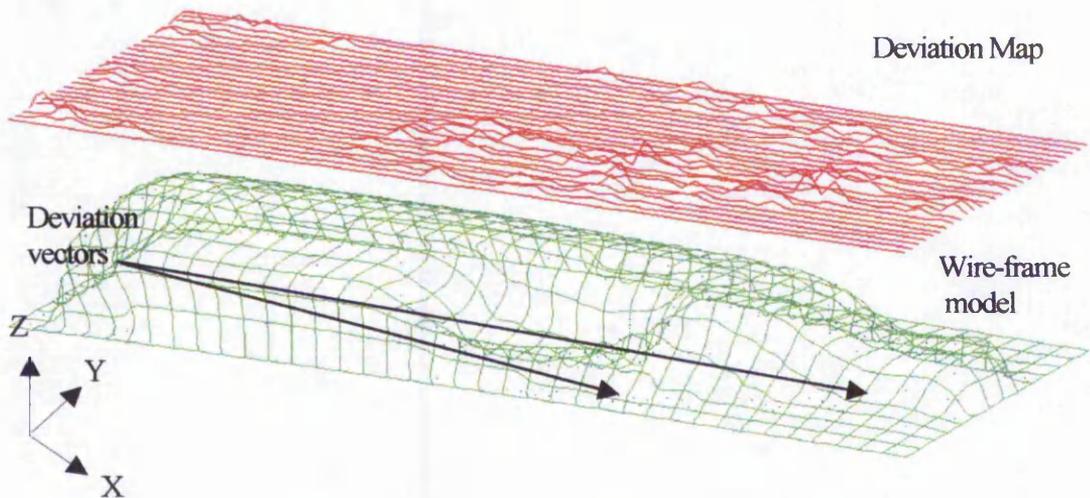
Figure 5.5. Deviation Analysis Graph (38 x 13 patch resolution).

DA results at various patch resolutions are shown in table 5.3.

Patch parameter -isation	Patch size (mm)	Number of patches (U x V)	Ave. Deviation (mm)	Max. Deviation (mm)	File size (Kb)
4	9	42x14	0.031	0.967	2,879
4	10	38x13	0.039	0.923	2,426
4	12	31x10	0.068	1.767	1,539
4	15	25x8	0.104	2.115	1,005
4	20	19x6	0.173	2.667	585
4	25	15x5	0.270	4.369	392
4	30	12x4	0.407	5.891	257

Table 5.3. Patch resolution and corresponding deviations.

The relationship between patch size and deviation and patch size and file size are demonstrated in the following graphs.
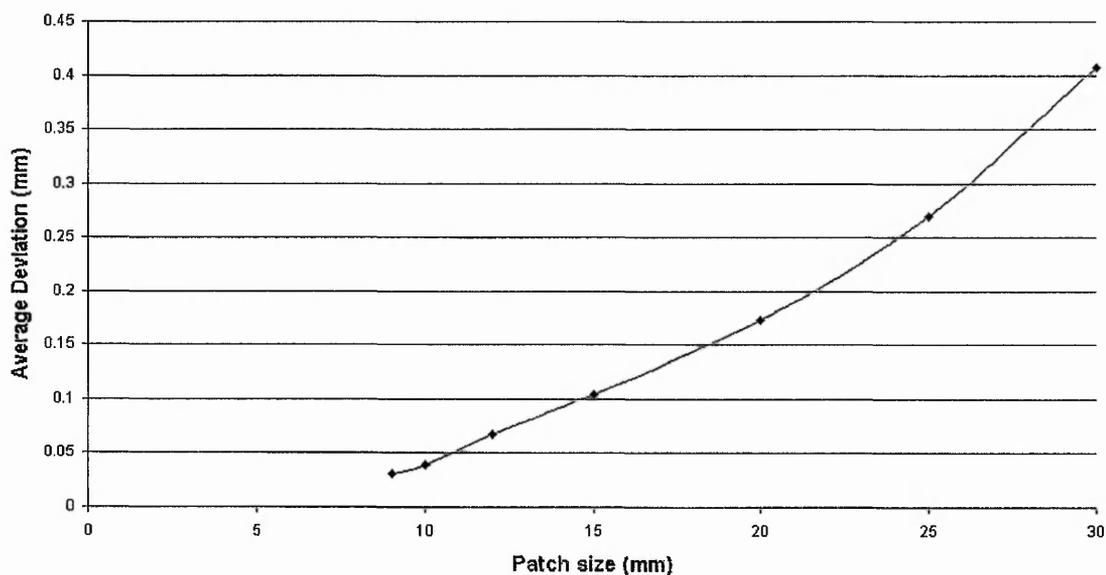
Graph 5.5. Relationship between deviation and patch size.

File Size Analysis
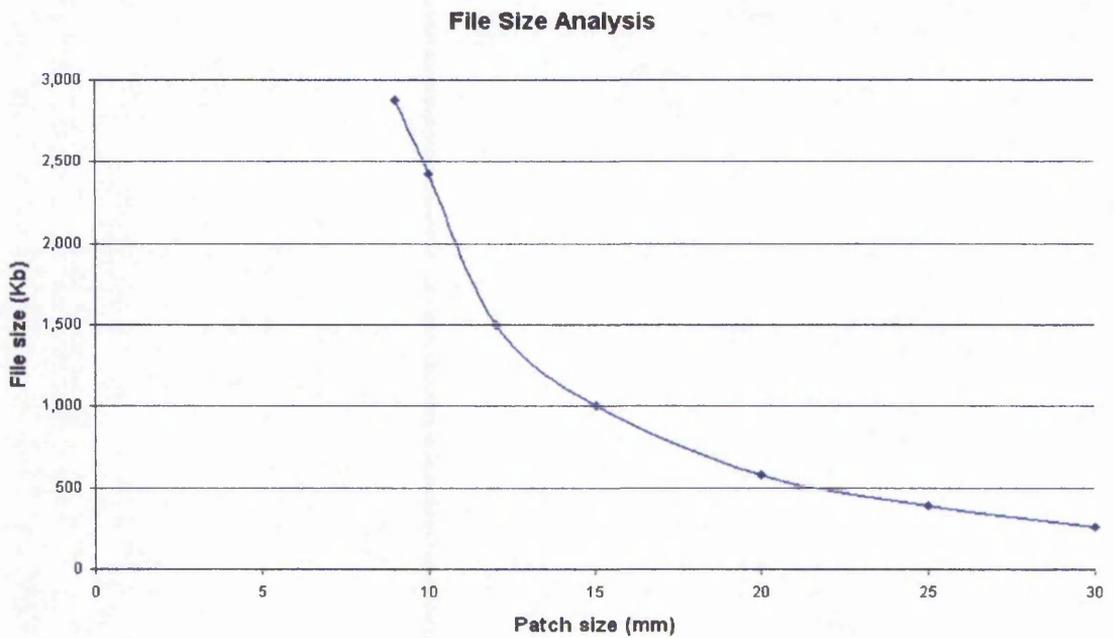
Graph 5.6. Relationship between file size and patch size.

5.2.2.3 Face Mould

Figure 5.6 shows a photograph of a more complex surface, which is a mould of a face (mould courtesy of Star Trek®, Paramount Pictures).

Figure 5.6. Photograph of face mould.

Figure 5.7 shows interpolating splines generated from CMM data collected from this object. In this case, scan line data was collected at a step-over distance of 2.5mm. Due to the complex nature of this surface, many concave regions, such as the eyes and mouth have features smaller than the probe diameter, thus accurate data is unobtainable from these regions.
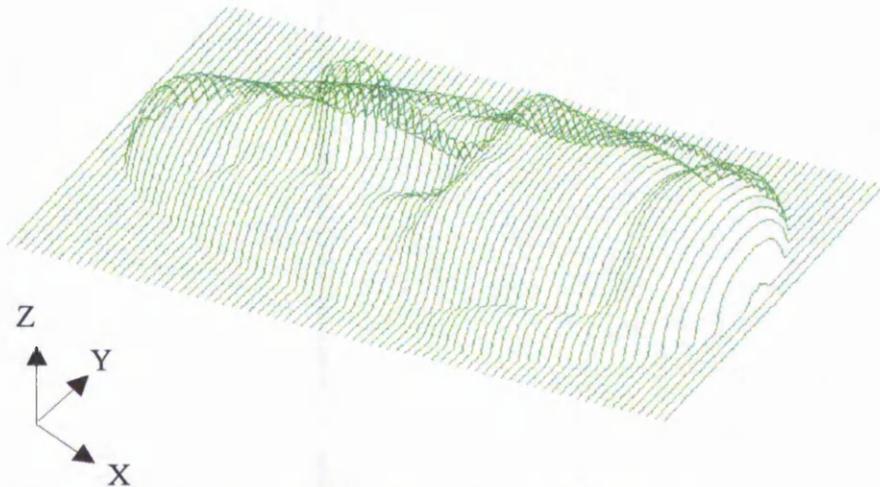
Figure 5.7. Interpolated scan line data taken from a face mould.

Figure 5.8 shows a typical surface model of the data.
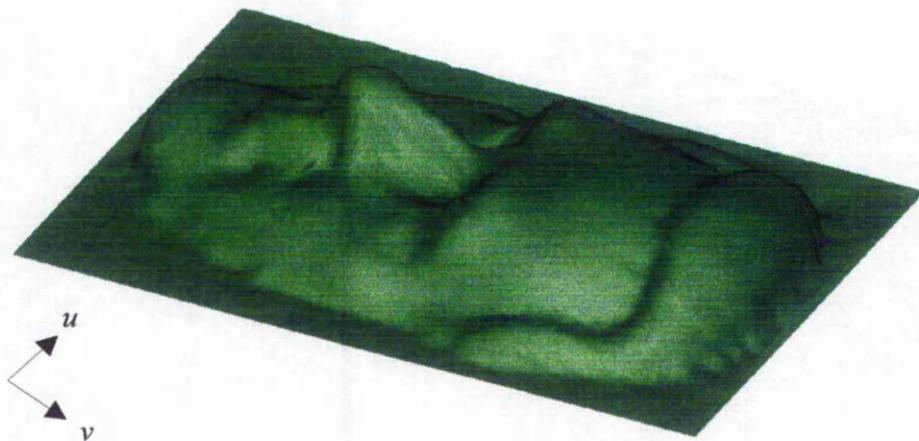
Figure 5.8. Free-form surface model for scan data taken from a face mould (17 x 19 patch resolution).

The DA graph of this surface model is shown in figure 5.9.
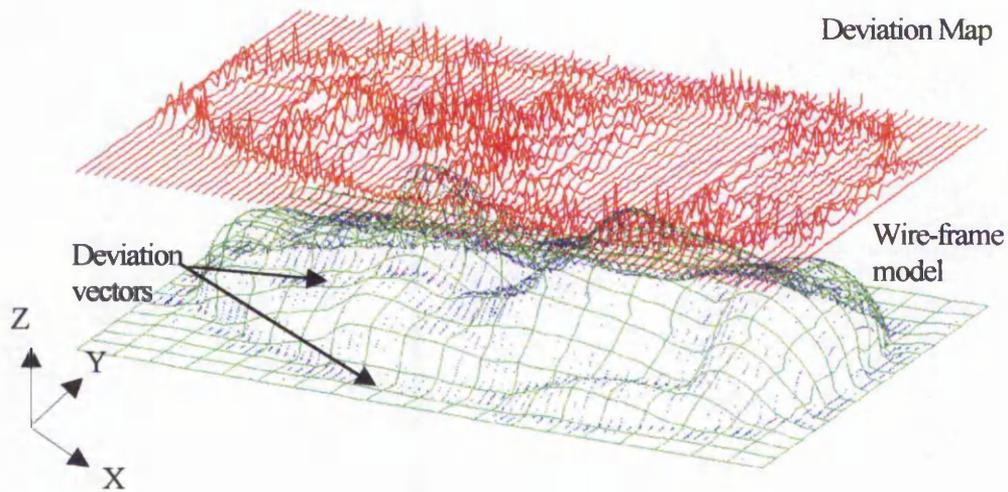
Figure 5.9. Deviation Analysis Graph (17 x 19 patch resolution).

Varying patch resolution alters the deviations, and file size, as shown in table 5.4.

Patch parameter-isation	Patch size (mm)	Number of patches (U x V)	Ave. Deviation (mm)	Max. Deviation (mm)	File size (Kb)
3	7	25x27	0.054	1.223	2,097
3	8	21x23	0.078	1.541	1,513
3	9	19x21	0.089	1.655	1,257
3	10	17x19	0.122	1.684	1,024
3	12	14x15	0.153	2.132	677
3	14	12x13	0.194	3.106	510
3	16	10x11	0.280	2.807	366

Table 5.4. Patch resolution and corresponding deviations.

Graph 5.7 shows the relationship between patch size and average deviation.

Devaition Analysis
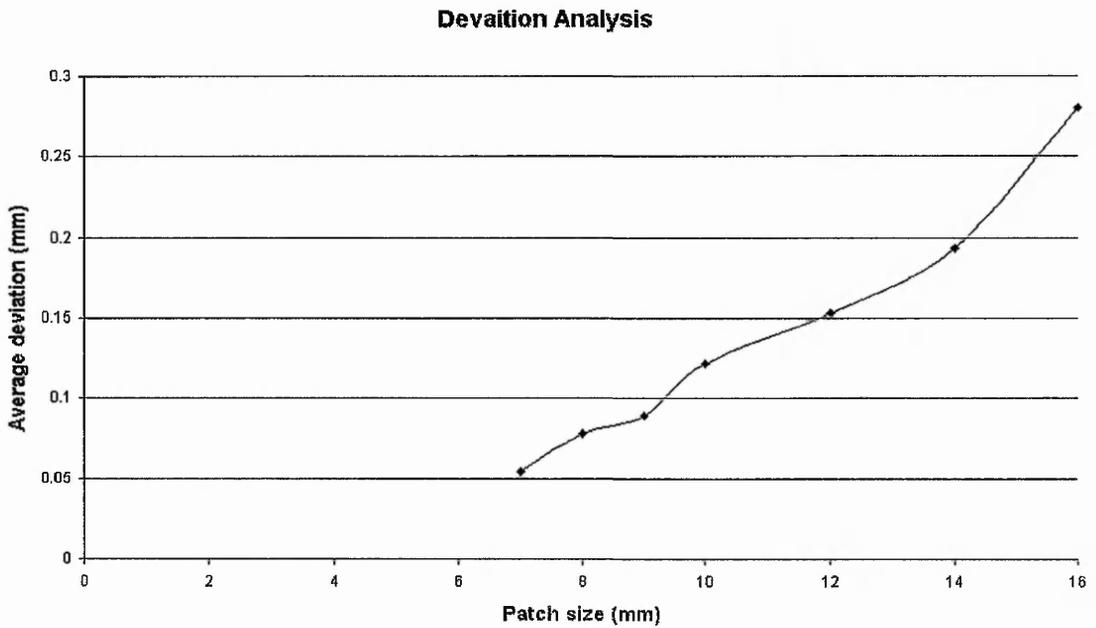
Graph 5.7. Relationship between deviation and patch size.

This can be compared with the graph of the effect of patch size on the resulting file size, shown in graph 5.8.

File Size Analysis
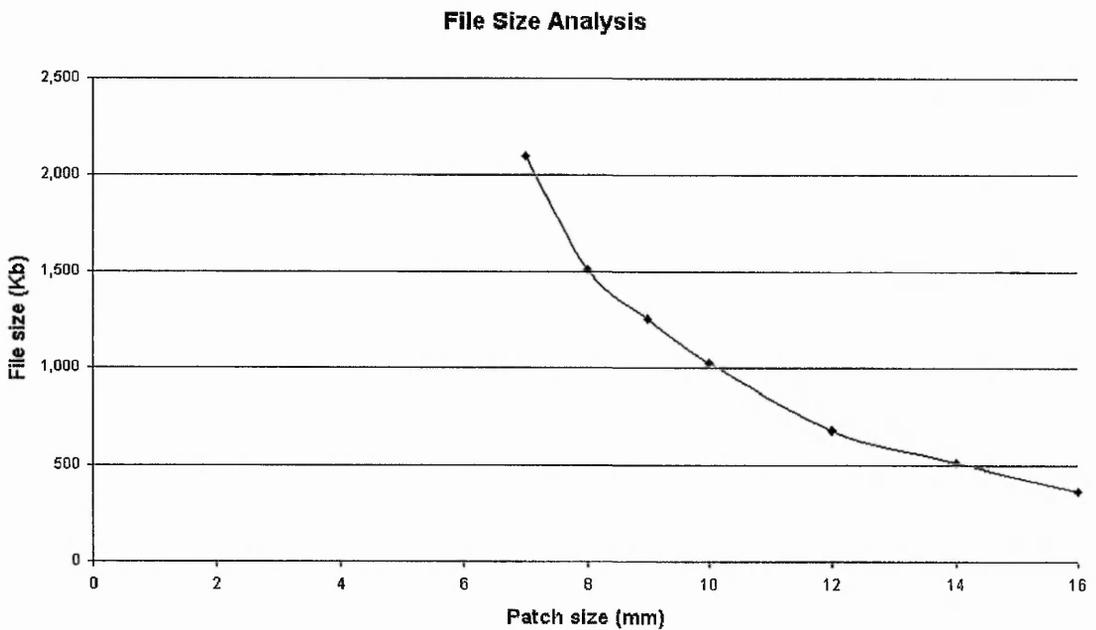
Graph 5.8. Relationship between file size and patch size.

5.2.3 Summary of Results

Computational time for the generation of surfaces is negligible. In all cases, the patch size is proportional to the resulting surface accuracy, and inversely proportional to the file size. Results presented show a decrease in deviation errors with a smaller patch size, however this incurs a file size increase. Results of this nature can be used to determine an adequate patch resolution, which will result in a surface model with acceptable deviations from the CMM data.

5.3 Data-set Partitioning

Data-set Partitioning (DSP) aims to analyse the effect of the amount of data used at the surface generation stage. This stage quantifies the reduction in surface model conformity where less data is used, utilising verification data-sets, which are a sub-set of the full data-set. The model conformity is also related to the patch resolution of the generated surface. Dense data is required for this stage, thus results are based on the Renishaw bottle and the face mould, as the bottle neck surface is generated from a data-set which is too sparse.

5.3.1 Bottle

In order to relate the amount of CMM data used to the resulting surface model accuracy, a number of results are taken at various patch sizes and DSP ratios. Table 5.5 shows Data-set Partitioning (DSP) for the Renishaw bottle data at a 9mm patch size, where the full data-set gives average deviation of 0.031mm and maximum deviation of 0.967mm. This occurs where the initial data step-over distance was 5mm, and was increased to 10mm where verification sets were introduced.

DSP Ratio	Data-set used	Ave. Deviation (mm)	Max. Deviation (mm)
1:1 (14:13)	Modelled	0.021	0.630
	Verification	0.456	4.668
2:1 (19:8)	Modelled	0.029	0.533
	Verification	0.329	2.880
3.5:1 (21:6)	Modelled	0.029	0.896
	Verification	0.317	2.794
4:1 (22:5)	Modelled	0.037	0.701
	Verification	0.391	3.157
5:1 (23:4)	Modelled	0.034	0.879
	Verification	0.330	2.641
Mean Average	Modelled	0.030	0.728
	Verification	0.365	3.228

Table 5.5. DSP and corresponding DA results at patch size of 9mm (41x14 patch resolution).

For the modelled sets, the mean average deviation is 0.030mm. (0.728mm for maximum deviation). This is very similar to the resulting deviations when the full data-set was used. The average deviation for the verification set is 0.365mm (maximum 3.228mm). Comparing the results of DA for the full data-set and the modelled data-sets at various DSP ratios shows that the mean values are comparable. Thus, the effect of the DSP ratio on the modelled set deviation is negligible. In the remaining results, this modelled data-set analysis is unnecessary, and thus omitted.

Table 5.6 shows DSP for the bottle data at 12mm patch size, where full data-set gives average deviation of 0.068mm and maximum deviation of 1.767mm.

DSP Ratio	Data-set used	Ave. Deviation (mm)	Max. Deviation (mm)
1:1 (14:13)	Verification	0.463	4.662
2:1 (19:8)	Verification	0.340	2.867
3.5:1 (21:6)	Verification	0.324	2.756
4:1 (22:5)	Verification	0.399	3.206
5:1 (23:4)	Verification	0.345	2.631
Mean Average		0.374	3.224

Table 5.6. DSP and corresponding DA results at patch size of 12mm (31x10 patch resolution).

For the verification sets, the mean average deviation is 0.374mm. (3.224mm for maximum deviation).

Table 5.7 shows DSP for the bottle data at 15mm patch size, where full data-set gives average deviation of 0.104mm and maximum deviation of 2.115mm.

DSP Ratio	Data-set used	Ave. Deviation (mm)	Max. Deviation (mm)
1:1 (14:13)	Verification	0.471	4.659
2:1 (19:8)	Verification	0.354	2.794
3.5:1 (21:6)	Verification	0.354	2.909
4:1 (22:5)	Verification	0.416	3.482
5:1 (23:4)	Verification	0.364	2.711
Mean Average		0.392	3.311

Table 5.7. DSP and corresponding DA results at patch size of 15mm (25x8 patch resolution).

For the verification sets, the mean average deviation is 0.392mm. (3.311mm for maximum deviation).

Table 5.8 shows DSP for the bottle data at 20mm patch size, where full data-set gives average deviation of 0.173mm and maximum deviation of 2.667mm.

DSP Ratio	Data-set used	Ave. Deviation (mm)	Max. Deviation (mm)
1:1 (14:13)	Verification	0.495	4.664
2:1 (19:8)	Verification	0.387	2.771
3.5:1 (21:6)	Verification	0.384	3.360
4:1 (22:5)	Verification	0.449	3.381
5:1 (23:4)	Verification	0.387	2.608
Mean Average		0.420	3.357

Table 5.8. DSP and corresponding DA results at patch size of 20mm (19x6 patch resolution).

This gives the average deviations for the verification set as 0.420mm (maximum 3.357mm).

Table 5.9 shows DSP for the bottle data at 30mm patch size, where full data-set gives average deviation of 0.407mm and maximum deviation of 5.891mm.

DSP Ratio	Data-set used	Ave. Deviation (mm)	Max. Deviation (mm)
1:1 (14:13)	Verification	0.670	5.580
2:1 (19:8)	Verification	0.563	4.618
3.5:1 (21:6)	Verification	0.573	3.622
4:1 (22:5)	Verification	0.676	5.805
5:1 (23:4)	Verification	0.589	3.345
Mean Average		0.614	4.594

Table 5.9. DSP and corresponding DA results at patch size of 30mm (12x4 patch resolution).

For the verification sets, the mean average deviation is 0.614mm. (4.594mm for maximum deviation).

Table 5.10 shows the results of the mean average deviations at various patch sizes, as compared to the average deviations of the full data-set.

Patch size (mm)	Mean Ave. Deviation of verification sets (mm)	Ave. Deviation of full data-set (mm)	Magnitude of error increase
9	0.365	0.031	11.774
12	0.374	0.068	5.500
15	0.392	0.104	3.769
20	0.420	0.173	2.428
30	0.614	0.407	1.509

Table 5.10. Magnitude of mean average deviation increase of verification sets, compared to average deviation of full data-set.

The results of the relationship between patch size and magnitude of error increase is plotted in graph 5.9.

Verification set Deviation
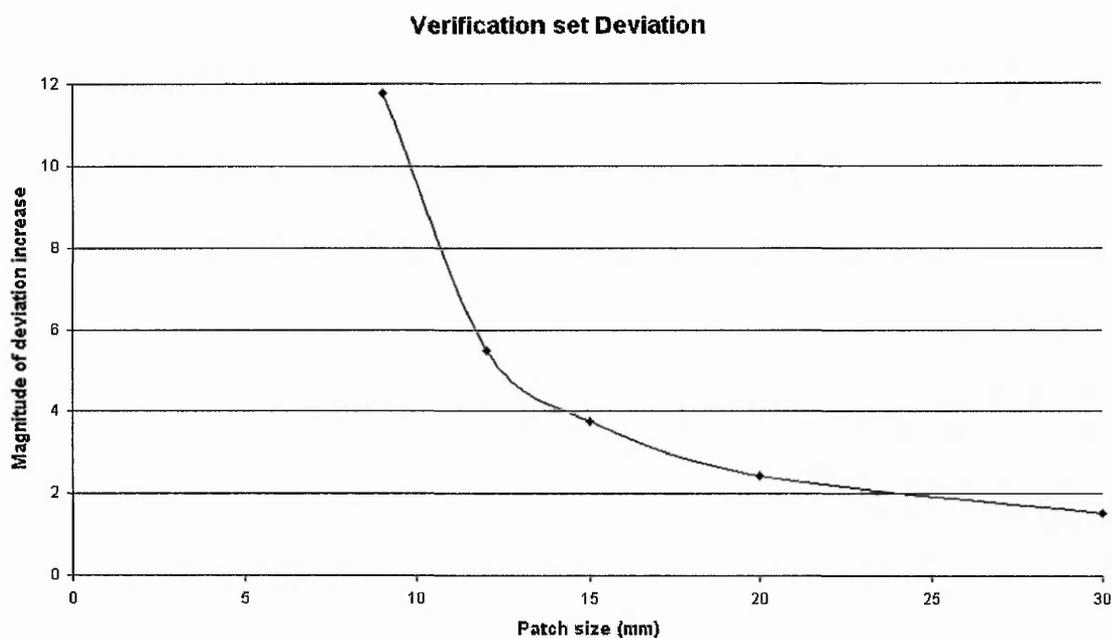
Graph 5.9. Relationship between DSP and patch size, and the resulting deviations of the surface model from the unused CMM data.

Similar DSP results are presented for the face mould.

5.3.2　Face Mould

Here, DSP, at all ratios results in the use of scan data at a step-over distance of 5mm, at the modelling stage, where the full data-set has a step-over distance of 2.5mm. Again, a number of results are taken for various patch sizes and DSP ratios. Table 5.11 shows DSP for the face data at 7mm patch size, where full data-set gives average deviation of 0.054mm and maximum deviation of 1.223mm.

DSP Ratio	Data-set used	Ave. Deviation (mm)	Max. Deviation (mm)
1:1 (39:38)	Verification	0.137	1.706
2:1 (52:25)	Verification	0.129	1.532
3:1 (58:19)	Verification	0.136	1.527
4:1 (62:15)	Verification	0.137	1.512
5:1 (65:12)	Verification	0.122	1.511
Mean average		0.132	1.558

Table 5.11. DSP and corresponding DA results at patch size of 7mm (25x27 patch resolution).

For the verification sets, the mean average deviation is 0.132 mm. (1.558mm for maximum deviation).

Table 5.12 shows DSP for the face data at 8mm patch size, where full data-set gives average deviation of 0.078mm and maximum deviation of 1.541mm.

DSP Ratio	Data-set used	Ave. Deviation (mm)	Max. Deviation (mm)
1:1 (39:38)	Verification	0.152	1.784
2:1 (52:25)	Verification	0.149	1.694
3:1 (58:19)	Verification	0.147	1.528
4:1 (62:15)	Verification	0.156	1.40
5:1 (65:12)	Verification	0.140	1.40
Mean average		0.149	1.561

Table 5.12. DSP and corresponding DA results at patch size of 8mm (21x23 patch resolution).

For the verification sets, the mean average deviation is 0.149mm. (1.561mm for maximum deviation).

Table 5.13 shows DSP for the face data at 9mm patch size, where full data-set gives average deviation of 0.089mm and maximum deviation of 1.655mm.

DSP Ratio	Data-set used	Ave. Deviation (mm)	Max. Deviation (mm)
1:1 (39:38)	Verification	0.161	2.422
2:1 (52:25)	Verification	0.153	2.340
3:1 (58:19)	Verification	0.160	2.271
4:1 (62:15)	Verification	0.163	2.291
5:1 (65:12)	Verification	0.143	2.270
Mean average		0.156	2.319

Table 5.13. DSP and corresponding DA results at patch size of 9mm (19x21 patch resolution).

For the verification sets, the mean average deviation is 0.156mm. (2.319mm for maximum deviation).

Table 5.14 shows DSP for the face data at 10mm patch size, where full data-set gives average deviation of 0.122mm and maximum deviation of 1.684mm.

DSP Ratio	Data-set used	Ave. Deviation (mm)	Max. Deviation (mm)
1:1 (39:38)	Verification	0.173	1.811
2:1 (52:25)	Verification	0.163	1.673
3:1 (58:19)	Verification	0.168	1.691
4:1 (62:15)	Verification	0.167	1.673
5:1 (65:12)	Verification	0.153	1.365
Mean average		0.165	1.643

Table 5.14. DSP and corresponding DA results at patch size of 10mm (17x19 patch resolution).

For the verification sets, the mean average deviation is 0.165mm. (1.643mm for maximum deviation).

Table 5.15 shows DSP for the face data at 12mm patch size, where full data-set gives average deviation of 0.153mm and maximum deviation of 2.132mm.

DSP Ratio	Data-set used	Ave. Deviation (mm)	Max. Deviation (mm)
1:1 (39:38)	Verification	0.198	2.164
2:1 (52:25)	Verification	0.205	2.296
3:1 (58:19)	Verification	0.204	2.166
4:1 (62:15)	Verification	0.212	2.196
5:1 (65:12)	Verification	0.193	2.127
Mean average		0.202	2.190

Table 5.15. DSP and corresponding DA results at patch size of 12mm (14x15 patch resolution).

For the verification sets, the mean average deviation is 0.202mm. (2.190mm for maximum deviation).

Table 5.16 shows DSP for the face data at 14mm patch size, where full data-set gives average deviation of 0.194mm and maximum deviation of 3.106mm.

DSP Ratio	Data-set used	Ave. Deviation (mm)	Max. Deviation (mm)
1:1 (39:38)	Verification	0.237	3.306
2:1 (52:25)	Verification	0.239	3.189
3:1 (58:19)	Verification	0.245	2.377
4:1 (62:15)	Verification	0.254	3.256
5:1 (65:12)	Verification	0.187	2.169
Mean average		0.232	2.859

Table 5.16. DSP and corresponding DA results at patch size of 14mm (12x13 patch resolution).

For the verification sets, the mean average deviation is 0.232mm. (2.859mm for maximum deviation).

Table 5.17 shows DSP for the face data at 16mm patch size, where full data-set gives average deviation of 0.078mm and maximum deviation of 1.541mm.

DSP Ratio	Data-set used	Ave. Deviation (mm)	Max. Deviation (mm)
1:1 (39:38)	Verification	0.313	2.786
2:1 (52:25)	Verification	0.311	3.136
3:1 (58:19)	Verification	0.313	2.782
4:1 (62:15)	Verification	0.324	2.854
5:1 (65:12)	Verification	0.319	2.826
Mean average		0.316	2.877

Table 5.17. DSP and corresponding DA results at patch size of 8mm (21x23 patch resolution).

For the verification sets, the mean average deviation is 0.316mm. (2.877mm for maximum deviation).

Table 5.18 shows the results of the mean average deviations at various patch sizes, as compared to the average deviations of the full data-set.

Patch size (mm)	Mean Ave. Deviation of verification sets (mm)	Ave. Deviation of full data-set (mm)	Magnitude of error increase
7	0.132	0.054	2.448
8	0.149	0.078	1.910
9	0.156	0.089	1.753
10	0.165	0.122	1.352
12	0.202	0.153	1.320
14	0.232	0.194	1.196
16	0.316	0.280	1.139

Table 5.18. Magnitude of mean average deviation increase of verification sets, compared to average deviation of full data-set.

In this case, less CMM data and varying patch size does not have as great an effect on the resulting deviations of the data from the surface model, as compared to the Renishaw bottle, however the trend is the same. This is due to the complexity of the surface, and the initial density of the data. Graph 5.10 shows the results of the relationship between patch size and magnitude of error increase.

Verification set Deviation
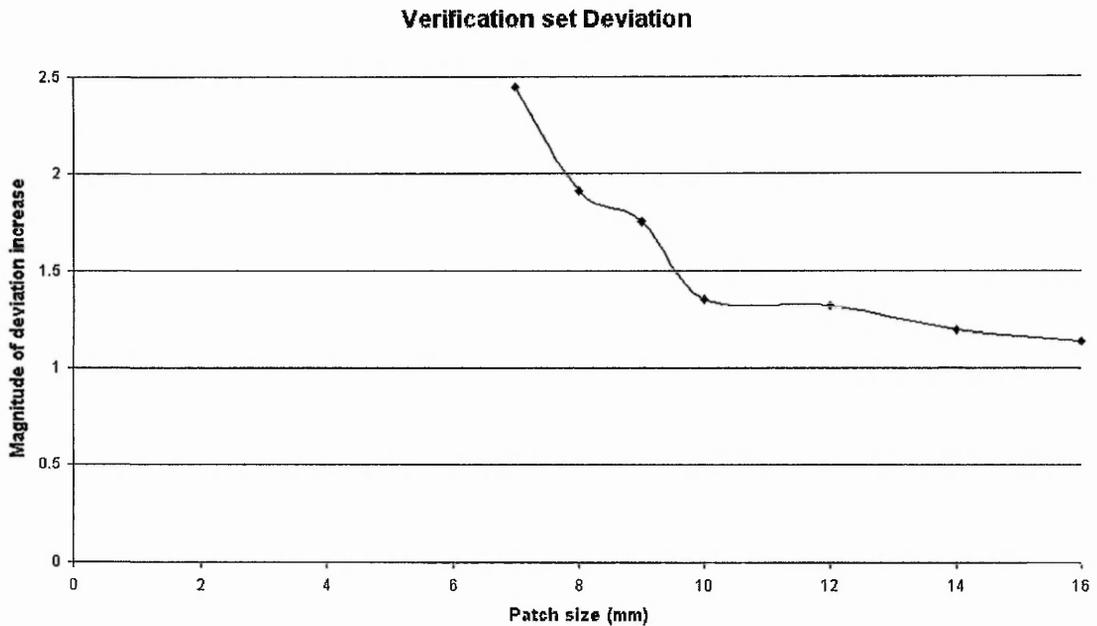
Graph 5.10. Relationship between DSP and patch size, and the resulting deviations of the surface model from the unused CMM data.

5.3.3   Summary of Results

DSP aims to predict the accuracy of the resulting surface, based on the amount of CMM data used. Partitioning the full data-set into a verification and modelled set works towards a method of quantifying the relationship between amount of data and resulting surface model conformity. DA of verification sets, at various patch resolutions, allow this relationship to be established. Results show that as the size of the patch increases, verification set deviations increase. This concurs with the full data-set deviations increasing as the patch size increases. However, the magnitude of deviation increase reduces as patch size increases. Thus, the effect of using less CMM data is reduced at lower patch resolution, which is quantified by DSP.

5.4   Surface Model Improvement

Where free-form surfaces are present, DA can be used to highlight regions where the original surface was not as smooth as once believed. This surface smoothness can be quantified using DA, where the generated surface model represents an ideal smooth surface, dependant on patch resolution. Figure 5.10 shows a free-form surface, generated from artificial data, which is complex in nature.
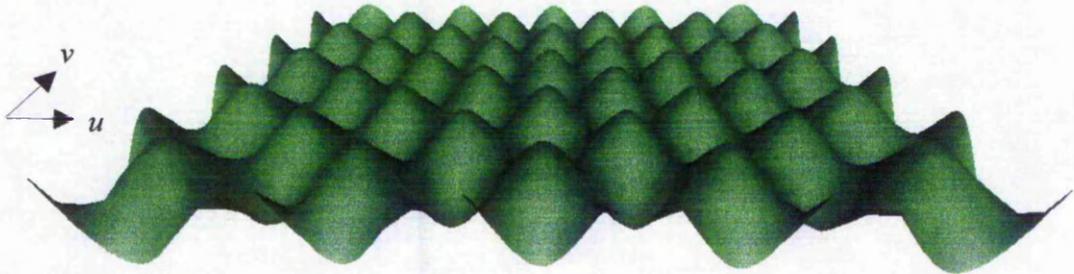
Figure 5.10. Free-form surface model, generated from artificially created data (11 x 11 patch resolution).

The excessive resulting curvature helps demonstrate the use of the DA tool for assessment of surface improvement, applied to free-form surface models. The deviation plot can be seen in figure 5.11, for this surface. Surface deviations are low, thus this deviation plot is scaled by a factor of ten. The actual deviation vectors on the wire-frame model are too small to be seen clearly here.
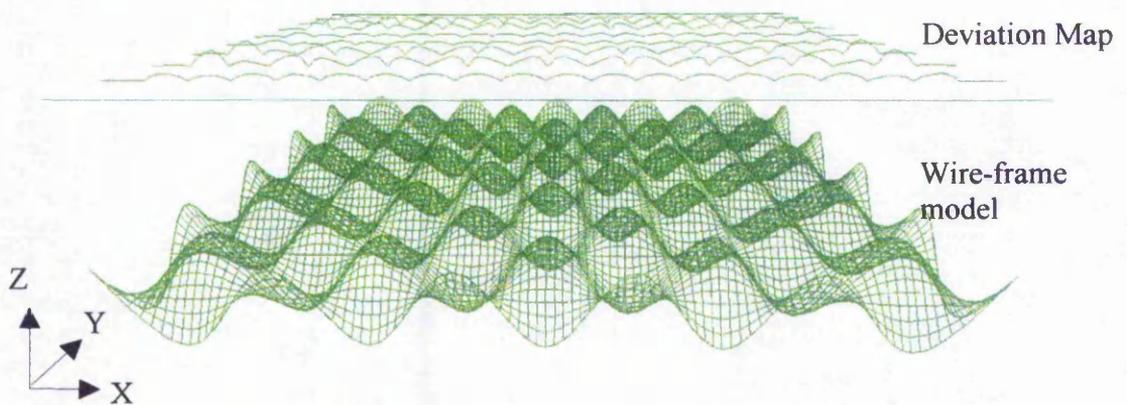
Figure 5.11. Deviation analysis results, between the data points and the generated free-form model.

Table 5.19 shows the deviations between the point data and the generated surface, at different patch resolutions. This forms a model calibration stage, where the minimisation of the surface deviation can be balanced with the desired smoothness.

Patch parameter -isation	Patch size (mm)	Number of patches (U x V)	Ave. Deviation (mm)	Max. Deviation (mm)	File size (Kb)
5	3	48x44	0.005	0.016	15,295
5	6	24x22	0.054	0.188	3,881
5	8	18x16	0.191	0.618	2,130
5	9	16x14	0.253	0.874	1,664
5	11	13x12	0.434	1.257	1,006

Table 5.19. Patch resolution and corresponding deviations.

As with the previous application of DA, graphs show the trends for the effect of patch size on deviations and file size. However, optimising the deviations is not of importance here, as these deviations imply an improvement in continuity. Graph 5.11 demonstrates this.
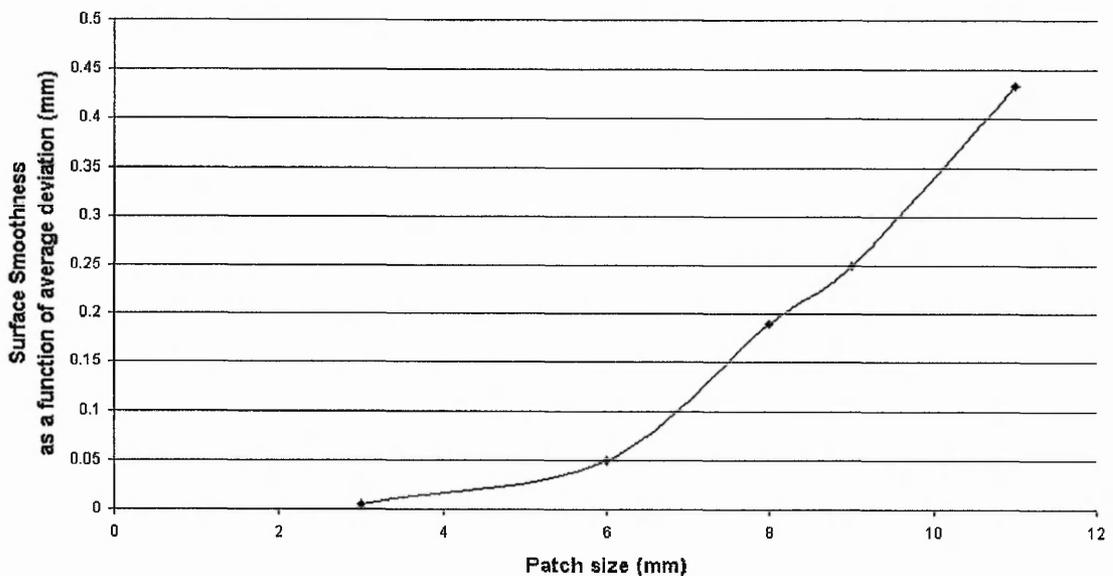
Graph 5.11. Analysis of smoothness as a function of average deviation.

5.4.1   Summary of Results

Graph 5.11 shows how the surface smoothness increases with patch size. This can be used to assess improvements to the qualitative aesthetic properties of surface smoothness. Continuity constraints within the best-fit surface cause approximation deviations, which can be minimised by reducing the patch size, or increasing the parameterisation per patch.

5.5   Global Surface Decomposition

5.5.1   Automatic Surface Type Allocation

Surface types can be allocated to global surface points using a constant threshold value. This is seen as a coarse determination, based on curvature, however similar points are not clustered together. This forms the initial stage of surface type recognition, prior to the seed region growing methodology. Two composite surface models are used here to demonstrate the results. The bottle neck represents a sparse data-set taken from a complex object with four distinct surface types. The face mould is a much more complex object.

5.5.1.1 Bottle Neck

Figure 5.12 shows the automatic surface type allocation at a threshold value of zero, where, a surface which may be preferred to be segmented as a cylindrical sub-surface, is excessively segmented into peak and saddle ridge sub-surfaces. This highlights the effect of CMM noise, and deviations in the physical surface, on the sensitive surface curvature calculations.
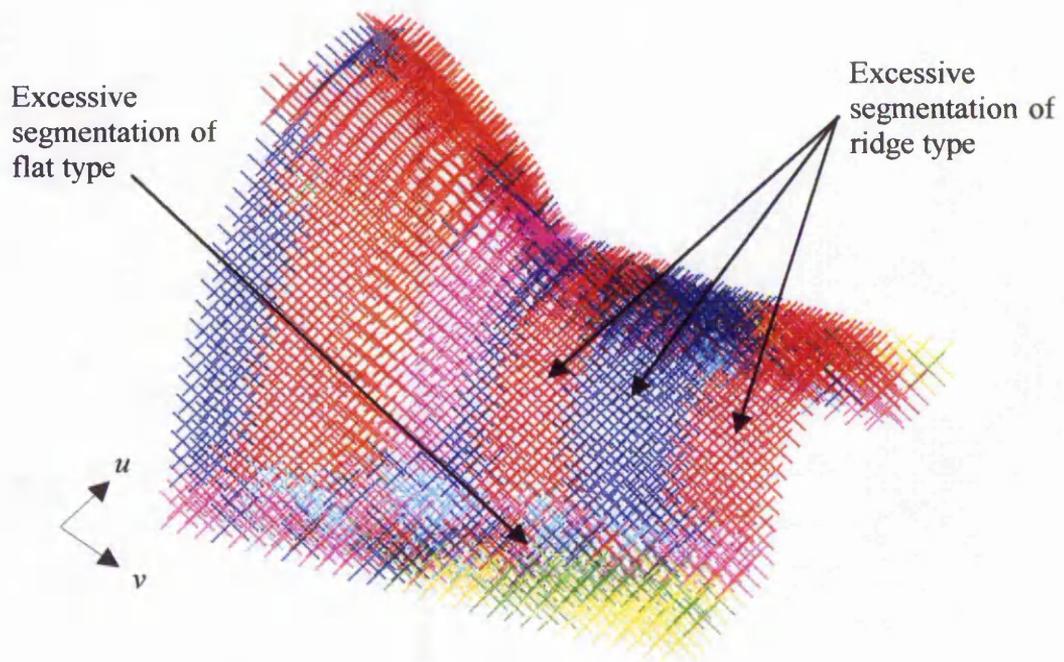
Excessive segmentation of flat type

Excessive segmentation of ridge type

u

v

Key:
COLOUR	SURFACE TYPE LABEL
RED:	PEAK SURFACE
GREEN:	RIDGE SURFACE
BLUE:	SADDLE RIDGE SURFACE
BLACK:	FLAT SURFACE
CYAN:	PIT SURFACE
YELLOW:	VALLEY SURFACE
MAGENTA:	SADDLE VALLEY SURFACE

Figure 5.12. Results of automatic surface type allocation at a threshold value of 0.0.

5.5.1.2 Face Mould

Figures 5.13 and 5.14 show the automatic surface type allocation at a fixed threshold value. The planar region has been separately segmented using the seed region growing method, which is presented in the following section, to highlight the face area.

Key:

COLOUR	SURFACE TYPE LABEL
RED:	PEAK SURFACE
GREEN:	RIDGE SURFACE
BLUE:	SADDLE RIDGE SURFACE
BLACK:	FLAT SURFACE
CYAN:	PIT SURFACE
YELLOW:	VALLEY SURFACE
MAGENTA:	SADDLE VALLEY SURFACE
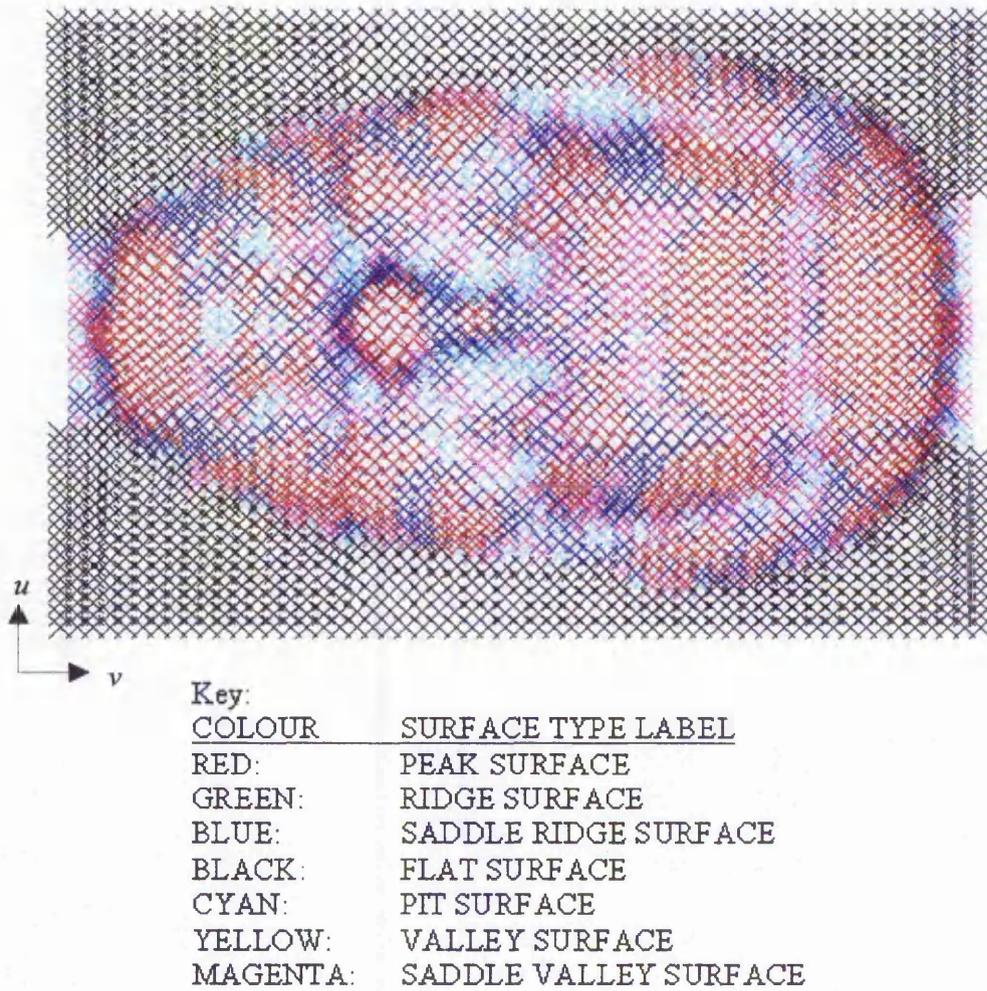
Figure 5.13. Automatic surface type allocation of face region at threshold value of 0.0.

Key:
COLOUR   SURFACE TYPE LABEL
RED: PEAK SURFACE
GREEN: RIDGE SURFACE
BLUE: SADDLE RIDGE SURFACE
BLACK: FLAT SURFACE
CYAN: PIT SURFACE
YELLOW: VALLEY SURFACE
MAGENTA: SADDLE VALLEY SURFACE
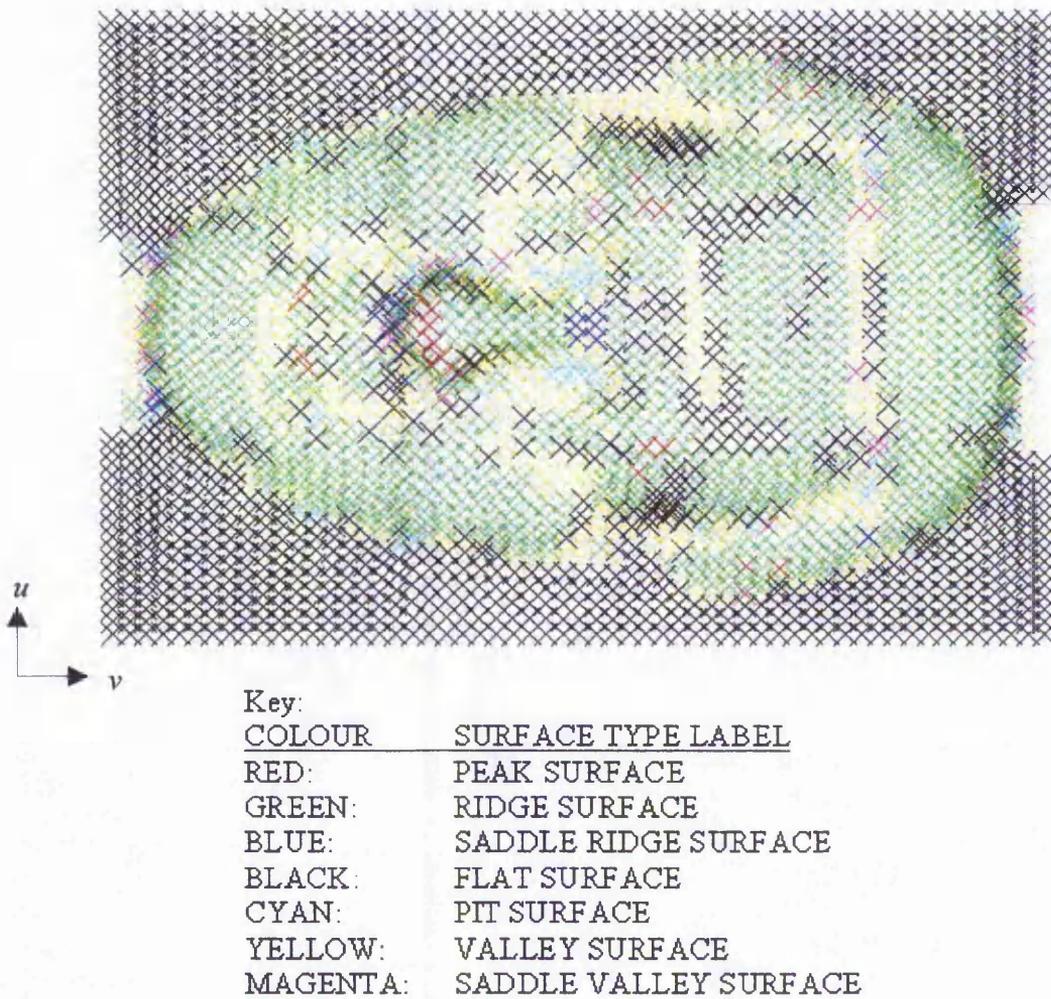
Figure 5.14. Automatic surface type allocation of face region at threshold value of 0.01.

5.5.2   Seed Region Growing

It can be seen from the previous two segmentation results, that a variable threshold value is desired, in order to accurately segment the global surface into sub-surfaces.

5.5.2.1 Bottle Neck

Figure 5.15 shows the results of curvature-based surface decomposition, utilising seed region growing. In this case, in order to highlight the intersection voids, degenerate

boundaries are modelled. This also shows points which are flagged as a different colour to the sub-surface (peak), highlighting points where cosmetic quality is compromised.
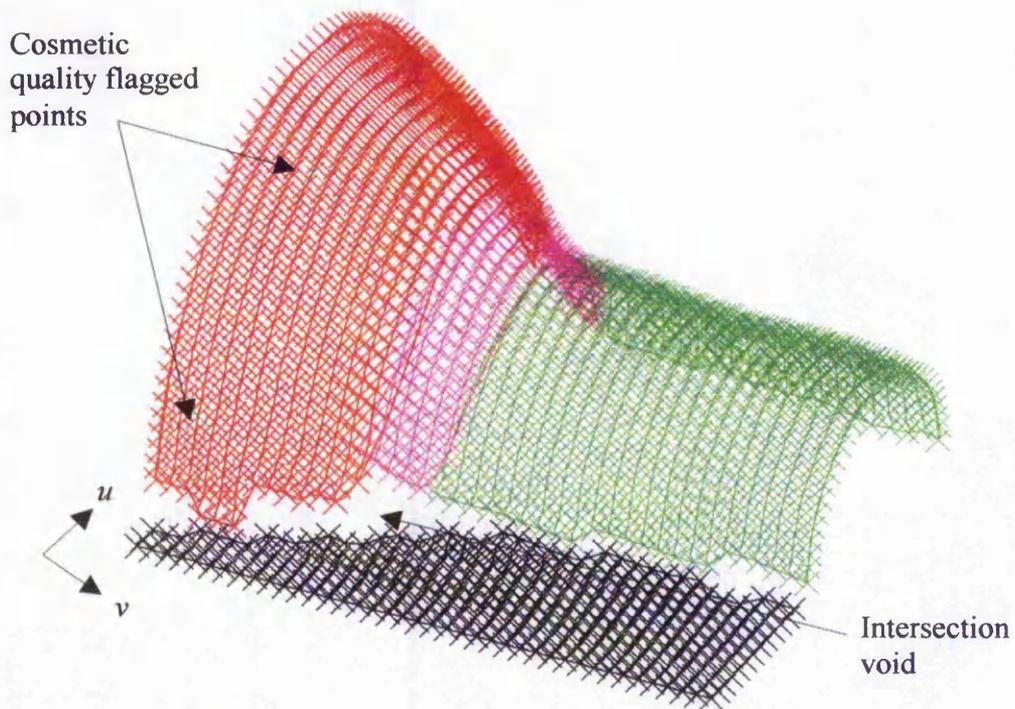
Key:

COLOUR	SURFACE TYPE LABEL
RED:	PEAK SURFACE
GREEN:	RIDGE SURFACE
BLUE:	SADDLE RIDGE SURFACE
BLACK:	FLAT SURFACE
CYAN:	PIT SURFACE
YELLOW:	VALLEY SURFACE
MAGENTA:	SADDLE VALLEY SURFACE

Figure 5.15. Result of global surface decomposition, with intersection voids.

The results of surface segmentation are also saved to a text file, allocating a number code to each surface type, shown in figure 5.16.

```
55500111111111111111111111111111111111111111111111111111
55500111111111111111111111111111111111111111111111111111
55501111111111111111111111111111111111111111111111111111
55551111111111111111111111111111111111111111111111111111
55551111111111111111111111111111111111111111111111111111
55551111111111111111111111111111111111111111111111111111
55550001111111111111111111111111111111111111111111111111
55555001111111111111111111111111111111111111111111111111
55555001111111111111111111111111111111111111111111111111
55555001111111111111111111111111111111111111111100000
55555500111111111111111111111111111111111111111111000
55555550111111111111111111111111111111111111111111000
55555550001199911111111111111111111111111111111111000
55555550000099999999999999999911111111111111111111000
55555550000099999999999999999999999999999911999991100000
55555555500009999999999999999999999999999999999990000000
55555555500099999999999999999999999999999999990005555
55555555550022999999999999999999999999999999990005555
55555555555502222222222222222229999999999999999900555555
55555555555502222222222222222222222222299999999900555555
55555555555502222222222222222222222222222222555555555
55555555555552222222222222222222222222222222255555555
55555555555552222222222222222222222222222222255555555
55555555555552222222222222222222222222222222255555555
55555555555552222222222222222222222222222222255555555
55555555555552222222222222222222222222222222255555555
55555555555550222222222222222222222222222222255555555
55555555555552222222222222222222222222222222255555555
55555555555552222222222222222222222222222222255555555
55555555555552222222222222222222222222222222255555555
55555555555552222222222222222222222222222222255555555
55555555555552222222222222222222222222222222255555555
55555555555552222222222222222222222222222222255555555
55555555555550022222222222222222222222222222255555555
55555555555550022222222222222222222222222222255555555
55555555555550022222222222222222222222222222255555555
55555555555550222222222222222222222222222222255555555
55555555555550222222222222222222222222222222220555555555
55555555555550222222222222222222222222222222220555555555
```

Key:

NUMBER	SURFACE TYPE LABEL
0:	INTERSECTION VOID
1:	PEAK SURFACE
2:	RIDGE SURFACE
3:	SADDLE RIDGE SURFACE
5:	FLAT SURFACE
7:	PIT SURFACE
8:	VALLEY SURFACE
9:	SADDLE VALLEY SURFACE

Figure 5.16. Result of global surface decomposition, with no point allocation at

intersection voids.

Labels of zero (0) highlight the intersection voids, where no surface type label is allocated. Figure 5.17 shows the result of global surface decomposition, where points falling in these intersection voids are allocated a surface type label at a threshold value of zero.

Key:
COLOUR   SURFACE TYPE LABEL
RED: PEAK SURFACE
GREEN: RIDGE SURFACE
BLUE: SADDLE RIDGE SURFACE
BLACK: FLAT SURFACE
CYAN: PIT SURFACE
YELLOW: VALLEY SURFACE
MAGENTA: SADDLE VALLEY SURFACE

Figure 5.17. Result of global surface decomposition, with point allocation at intersection voids.

Figure 5.18 shows the top view of the same.

u

v

Key:
COLOUR	SURFACE TYPE LABEL
RED:	PEAK SURFACE
GREEN:	RIDGE SURFACE
BLUE:	SADDLE RIDGE SURFACE
BLACK:	FLAT SURFACE
CYAN:	PIT SURFACE
YELLOW:	VALLEY SURFACE
MAGENTA:	SADDLE VALLEY SURFACE

Figure 5.18. Result of global surface decomposition, with point allocation at intersection voids (top view).

5.5.2.2 Face Mould

Figure 5.19 shows results of global surface segmentation of the face mould.
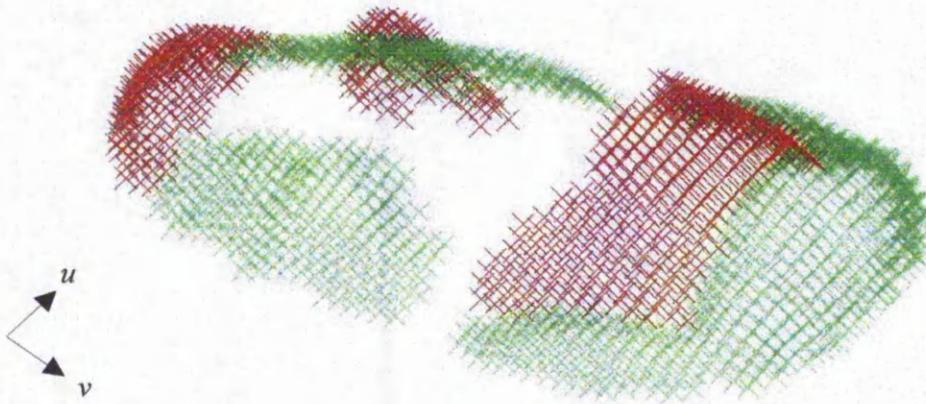
u

v

```
Key:
COLOUR          SURFACE TYPE LABEL
RED:            PEAK SURFACE
GREEN:          RIDGE SURFACE
BLUE:           SADDLE RIDGE SURFACE
BLACK:          FLAT SURFACE
CYAN:           PIT SURFACE
YELLOW:         VALLEY SURFACE
MAGENTA:        SADDLE VALLEY SURFACE
```

Figure 5.19. Segmentation of main regions of face.

Figure 5.20 shows the top view of the same.
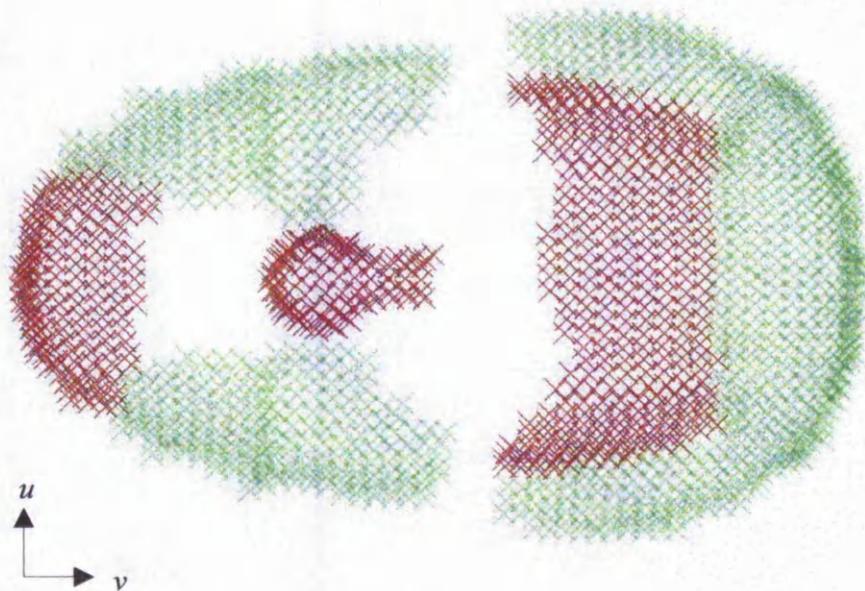
Key:
```
COLOUR          SURFACE TYPE LABEL
RED:            PEAK SURFACE
GREEN:          RIDGE SURFACE
BLUE:           SADDLE RIDGE SURFACE
BLACK:          FLAT SURFACE
CYAN:           PIT SURFACE
YELLOW:         VALLEY SURFACE
MAGENTA:        SADDLE VALLEY SURFACE
```

Figure 5.20. Segmentation of main regions of face (top view).

5.5.3 Summary of Results

Automatic surface type allocation at a constant threshold value can be used to find surface type labels of a global surface. However, this does not cluster similar surface types, and does not take CMM noise and surface model fluctuations into account. The seed region growing methodology is used to generate sub-surfaces containing surface points of the same surface type label, taking CMM noise into account. This is seen as an effective methodology to decompose a global surface into its constituent sub-surface types, where similar points are clustered as a sub-surface, and a cosmetic quality assessment takes place.

Chapter 6.

Conclusions and Future Developments

6.1   Introduction

Reverse Engineering (RE) is a useful tool in industry, where a physical prototype may be accurately reproduced. This involves surface digitisation and part-program generation, via a surface modelling stage. Due to the relevance to engineering, many methodologies have been developed in this area, concerning the integration of Computer Aided Design (CAD) and Computer Aided Manufacture (CAM) processes. Important factors for an integrated system are cost, speed, accuracy, reliability, and compatibility. Often, RE concludes with the generation of a surface model, rather than a reproduction part. Chapter 2 of this thesis discussed the current RE technology, highlighting associated problems and areas of further improvement to the knowledge base.

There are a number of methods available for digitising a physical part, however all measuring devices have a degree of error, or accuracy uncertainty. The CMM is used throughout this work. Despite being a more traditional CNC-based metrology tool, it is still the most accurate, however it incurs lengthy inspection times. Programs, written using the native CMES language, automatically control the CMM, collecting data from a physical prototype. This is discussed in chapter 3. In this work, programs have been created to automatically collect data from any surface, where start point, clearance plane, direction of uni-directional scan lines, step over distance, and end point are all defined prior to data collection. Point-to-point programs are also developed, but the increased time for data collection means that the scan line methodology is preferred. Complex physical prototypes can cause problems at the data collection stage, where

incorrect probe direction can cause slippage of the probe tip, giving erroneous data. However, sensible use of part orientation and an adequate scan line density can reduce these potential errors, resulting in an optimum data-set.

The data collection stage allows an adequate quantity of data to be collected. In most cases, a large quantity of data is collected. However, this adds computational time to surface model generation, thus initial work has been done to investigate the relationship between data-set size and model accuracy, allowing an optimum amount of data to be used, which minimises data collection time. A method of fitting a surface to this data is developed and discussed in chapter 3, based on uni-directional CMM scan lines. An understanding of the ACIS® modelling environment allowed the relationship between conventional Computer Aided Geometric Design (CAGD) techniques and ACIS® geometric functionality to be developed.   ACIS® is a development tool containing CAGD functionality. Within the scope of this work, ACIS® is used to represent CMM data points, and generate a best-fit surface model which approximates these points. This utilises spline functions for the interpolation of CMM points, and surface functions for the generation of Gregory/Charrot patches from the generated bi-directional network of splines. Surface functions are also used to generate the initial seed region domain, at the surface decomposition stage.

The aim of Part-to-CAD RE is to accurately generate a surface model from CMM data. This is achieved using C^1 continuous modelling techniques. However, this method shows problems when dealing with complex, composite physical surfaces, as the resulting CMM data will contain discontinuities. A composite surface is defined as one containing obvious geometric entities, or surface primitives, whereas a free-form surface is of a more continuous nature. The modelling stage has traditionally been based on sculptured models. Thus, RE has been applied to the accurate reproduction of sculptured parts. Only recently have a few works emerged, investigating the modelling of composite surfaces derived from CMM data, involving a segmentation stage. A high degree of user-interaction, in the surface model generation of a part is a major limitation to the application of RE to composite surfaces.

The automatically generated free-form surface may be further utilised to create a reproduction part, forming the CAM stage of RE. This involves deducing 3D surface information from the surface model, and generating a part-program for a CNC machine to accurately reproduce the physical prototype. This physical machining stage is not implemented in this work.

The novel work discussed in this thesis has been developed to enhance the conventional RE process. This is particularly concerned with improving the modelling of global composite surfaces. Original objectives have been reached, which resulted in the investigation and initial development of secondary objectives. The novel contributions to the field of RE are discussed in the following sections, summarised in figure 6.1.
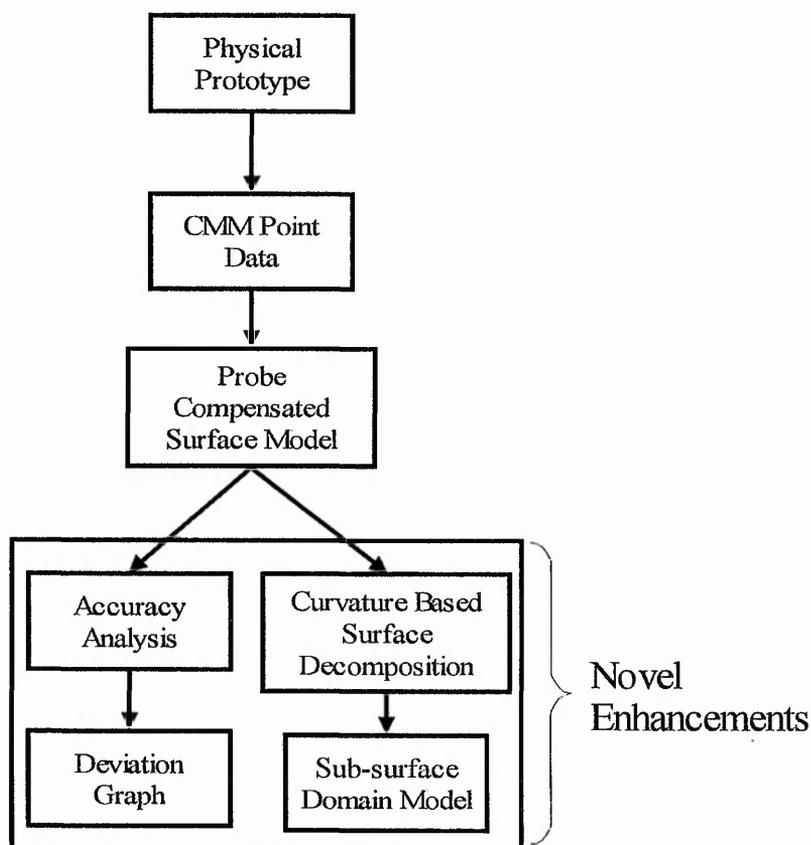
Figure 6.1. Novel improvements to the RE process developed in this study.

6.2   Novel Improvements to Reverse Engineering

Novel improvements to RE are concerned with surface assessment, verifying the generated free-form model. The results of this accuracy analysis stage lead to a novel method of surface segmentation, aimed at improving the modelling of composite surfaces.

6.2.1   Accuracy Analysis of Free-form Surfaces

Quality assessment is achieved by a Deviation Analysis (DA) module, which allows model verification, highlighting potential inaccuracies between the CMM points and the generated surface. In the case of physical free-form surfaces, this permits the verification of a single data-set, based on the generated best-fit surface. Any deviations which are present are due to CMM error or an inadequate patch resolution.

With correct calibration, data collection tools are assumed to be accurate, although problems may occur which cannot be detected. The conventional way to check for the accuracy of a data collection tool is by taking repeated results, and comparing them within tolerances. The integration of data collection with the modelling stage can act as a data verification stage, where assumptions are made about the original physical object, such as optimum continuity conditions. When an acceptable patch resolution is present, the best-fit surface represents an improvement in the underlying surface smoothness. In the case of data collected from a free-form physical object, the desired need for smoothness is evident, and free-form surface generation can be used to assess both data collection accuracy, and physical part continuity. This study allows the accuracy of CMM data to be confirmed on surface models where slight discrepancies would be very hard to detect. These inaccuracies may arise from the manufacture of the part, or from the inspection of the part. In both cases, confirmation that the manufactured surface is continuously smooth, and passes through defined points within defined thresholds, is a useful aid to quality assessment.

6.2.2 Accuracy Analysis of Composite Surfaces

DA is primarily developed to highlight areas of inaccuracy arising from the modelling of a composite surface as a free-form model. This stage highlights areas of extreme curvature change, determined by deviations between the CMM data and the surface model. Modelling CMM data as a free-form surface can increase surface model variance, where regions of the model do not conform to the underlying CMM data points. The use of an appropriate parameterisation and patch resolution will optimise the accuracy of the surface model. However, the modelling of a composite surface as a free-form surface highlights a number of drawbacks to this automatic method of modelling. This involves the modelling of intersections between two or more different surfaces, introducing extreme curvature change to the free-form model. Deviations occurring in these regions correspond with results of curvature analysis. The resulting DA of composite physical models leads to the development of a novel surface decomposition stage.

6.2.3 Data–set Partitioning

A further novel stage to DA is data-set partitioning (DSP), where the full CMM data-set is not used at the model generation stage. Initial results differed from expected results, thus developments have been made as further research. A portion of the data-set, known as a verification sub-set, is used to assess deviations in the generated surface model. This process is developed as an investigation into the important issue of data reduction, where the complexity of a surface model (and thus file size and computation time) does not justify the improved accuracy. This examines the relationship between the amount of CMM data used, and the resulting model accuracy. There is no knowledge of how an increased data-set improves the generated surface model accuracy. This work analyses the need for a reduction in CMM data, whilst maintaining adequate model accuracy, to within defined tolerances. Results show that a reduction in data used, by increasing the step-over distance between scan lines, dramatically affects the accuracy of the resulting surface, where a high patch resolution is used. At a lower patch resolution, the decrease in accuracy is less pronounced. Further work is necessary to investigate this

phenomenon, relating the step-over distance to the size of patch, aiming to predict the accuracy of a surface model, based on the density of the initial data-set.

6.2.4 Curvature-based Surface Decomposition

Curvature-based surface decomposition is a novel method of segmenting the global surface generated from CMM data. This method uses seed region growing to allocate surface types to clusters of points on the global surface, optimising the size of the generated sub-surfaces, based on surface curvature. Points classified as the same type, after curvature analysis, filtering, and refinement, are independently modelled as sub-surfaces. Areas which occur at extreme curvature change, are omitted, introducing intersection voids in the surface model. These occur where two or more different surface types intersect. Results show the successful decomposition of global surface models, resulting in sub-surfaces of known type. This verifies the sub-surface types making up a composite surface model, where regions of surface model deviation, caused by extreme curvature change, are identified. This highlights regions of a surface model which have reduced accuracy, due to free-form modelling deviations or insufficient CMM data, as well as allowing a clear representation of a global surface's constituent sub-surface types.

6.2.5 Analysis of Sub-surfaces

Generated sub-surfaces contain uv surface points which have been allocated the same surface type label. Verifying the cosmetic quality of these points detects any very slight discrepancies at a local level, based on curvature. These points, whilst still forming part of the sub-surface, display a radius of curvature which is out of a specified tolerance range. Flagging these points in a colour different to the rest of the sub-surface allows any potential CMM errors, or errors in the physical part surface to be highlighted. This is analogous to the manual methods of cosmetic quality assessment, such as glove feeling, where dents, peaks or valleys are detected by experienced personnel.

The curvature-based surface decomposition method developed in this work aims to segment a global surface into a collection of sub-surfaces with minimal intersection

voids. This novel research has been taken a step further, by the initial development of a geometric analysis module. Geometric tolerance of form is used to determine the overall deviation of a total surface profile from the physical prototype. At present, this further research examines the geometric tolerance of a cylindrical surface, based on the radius of curvature at local points. Results show that the local curvature of a generated surface fluctuates increasingly, as the patch size is decreased. This is partly due to the more constrained surface smoothness and the density of the *uv* point domain. Initial results of this research determine the need to convert spline surfaces to analytical types, where global curvature can be calculated to a more acceptable degree. Further investigation into the locality of the curvature calculation should also occur.

6.3   Future Developments

This work has developed enhancements to the RE process. There are areas of further research which would build upon the work carried out here, which are discussed below, in terms of the individual components of RE. The CMM is used for data collection and inspection, however this study is not concerned with improving or optimising this stage. In order to improve the accuracy of the data collection stage, the use of bi-directional scan lines is an alternative to uni-directional scanning. However, this will significantly increase the length of time for scanning.

The generation of inspection paths with defined surface normals is possible using the generated global surface model. This can form a 'teach' mode where sparse data is initially taken, and surface normals are deduced. These can then define the probe trajectory, improving the accuracy of the collected data, for the full data collection process. Known surface information can be used to determine the directions the probe can approach the part, and then select the shortest route, depending on the current position of the CMM, and any obstacles that may be present. Some work has been done in this area by Spyridi and Requicha [SPYRIDI, 1990]. This is useful where surface information is to be inspected for a number of similar objects. The planning of an optimum, collision-free inspection path can minimise inspection times and increase model accuracy. This would allow the optimum sequence of feature measurement, to

minimise the distance travelled and the probe orientation changes. Probe trajectory modification can take place if a collision is evident. Thus, complex objects with multiple features can have an inspection plan, based on speed and distance travelled, avoiding obstacles.

It is envisaged that integrating contact and non-contact stages in the data collection stage will gain the benefits offered by both methods of inspection. Some work has been done in this area by Cheng and Menq [CHENG, 1995]. The novel method of surface segmentation developed in this study relies on a high density of data collected, thus it is well suited to optical, non-contact scanning. However, the effect in the reduction in accuracy would involve further investigation. Integrating contact with non-contact methods is an area of viable research, speeding up the data collection process, however maintaining accuracy where necessary.

The use of the segmented surface model can be used to obtain a more accurate path plan for the CMM, where, rather than taking 'blind' continuous scan lines in a defined direction, data collection can be feature-based. In this way, priority can be given to surface intersection points, and complex areas, and minimal data can be collected from known surface types such as planar areas. Intersection voids, which are not modelled, can have data collected specifically, where a return to the CMM is a feasible option. This would allow an adequate amount of data to be collected from these specific areas, improving the modelling stage. These points can be used to 'heal' the surface model, introducing discontinuities. This would involve a closer integration between data collection, modelling, and analysis. In a similar way, non-contact data collection could be used to rapidly collect sparse data and generate a coarse global surface segmentation, highlighting regions of extreme curvature change. These regions could then have accurate data collected using the contact CMM data collection method. This would 'guide' the CMM to regions of interest, filling generated intersection voids with extra data, aimed at improving overall surface model accuracy.

A full comparative study of the ACIS® global surface generation functions with the method developed in chapter 3 is hindered by the lack of proprietary information on the methodologies behind the functions. As this is a commercially available CAGD

package, it is assumed that the functionality is accurate. However, analysis of the functionality would allow confirmation of the conformance of resulting surfaces, and the surface analysis tools developed in this work.

Restricting the modelling system to one patch shape, as is common, can have disadvantages. Thus, using surface patches of varying shape and size aims to improve model accuracy. In cases of extreme curvature change, a major problem occurs when the surface model curvature is not orthogonal to the patch boundaries. The use of differing patch orientation can improve model accuracy to a certain degree. For example, oblique object boundaries may determine the type of patch which should be used, where an oblique edge will be more closely approximated by an oblique patch than an orthogonal patch [BARDELL, 1998a]. Results from this investigation show that parallel edges allow orthogonal continuity across patches. Square or rectangular patches, parameterised in u and v can model data collected in a u or v direction. However, diamond shaped patches alone, parameterised in s and t, cannot be used to model an object measured in u and v. At the boundary of the object, triangular patches are needed, which are functions of uv and st. Initial attempts to rectify this problem involved the formation of triangular patches, with the aim of improving boundary edge continuity. Further investigation into using four sided oblique patches, and three sided patches form future work, where the integration of different patch shapes could lead to improved accuracy.

The reconstruction of surfaces that contain discontinuities such as creases and corners would vastly reduce the deviations in surface model accuracy due to the free-form modelling approach. Improved modelling of edges would result in a more accurate correlation with CMM data, but would still be continuous, where ideal conditions are discontinuous intersections. Inserting extra knot points at regions of high curvature, based on a pre-defined curvature value, would improve the modelling at these regions. A preliminary algorithm for this is shown below.

> *Parameterise scan line, $0 < u < 1$.*
> *Calculate curvature at parameter points, u*
> *Where curvature $> VALUE$*
>   *Find previous and next parameter points*
>   *Parameterise between these parameter points*

> *Insert new parameterised spline segment into original spline*
> *Until reach end of spline*

This would introduce an unequal number of knot points per scan line, thus would necessitate modifications to the modelling methodology discussed in chapter 3.

The original objective of surface model analysis was the development of a DA tool to reliably analyse the fit of the surface model to the underlying CMM points. Data-set partitioning (DSP) extends this research, examining the relationship between the scan line density and the resulting acceptance of the surface model. This is based on deviations of verification data-sets, where the patch size determines the reduction in surface fit accuracy. Further research is necessary to extend this tool to a reliable surface model accuracy prediction aid. This includes an investigation into DSP ratios where more verification data is used, further increasing scan line step-over distance. This should be compared with the partitioning of data in the scan line direction.

With composite models, results from the DA stage highlight CMM points that are outside the desired deviation for free-form modelling. These points are not modelled after global surface decomposition, residing between generated sub-surfaces. These CMM points exist at the intersection voids and can be included in the relevant sub-surface. Future research aims to extend the sub-surface boundaries using CMM data directly, rather than the free-form surface model. Discontinuous surface-surface intersection algorithms can be used to fix the resulting sub-surfaces, if necessary, joining them at their boundaries. This would be seen as an interactive post-processing stage, necessitating a CAD Graphical User Interface (GUI) for surface selection, and tools for surface extension and trimming. This would allow the user to add discontinuous surface-surface intersections, such as fillets or chamfers. Allowing the total surface recognition process to be automated, including the introduction of discontinuous intersections, is outside the realms of this present work. A method of automatic surface type allocation, filtering CMM noise by deducing appropriate threshold values for each sub-surface, would allow each cluster of similar points to be automatically modelled as a sub-surface, over the global surface. This involves the optimum allocation of the seed region surface type, which could potentially be achieved using an Artificial Neural Network (ANN). The selection of the initial seed region is still envisaged to be an interactive stage, which is ideally suited to a GUI, where the

growing method can also be graphically viewed within an ACIS® environment in real time. As an aid to training, and also to minimise usage of hardware, such as the CMM and the CNC milling machine, a GUI also lends itself to the development of graphical simulations for data collection and machining stages.

The recognition of sub-surface types can be taken a step further, allowing feature recognition, based on the surface type boundary. This present work has highlighted the type of sub-surface, but no information is available on the resulting shape of sub-surface. This may involve the use of Hough transforms for the recognition of these sub-surface boundaries. The automatic allocation of surface types, on a global scale, as a coarse alternative to seed region growing is discussed in chapter 4. Surface type labelling works towards the determination of surface boundaries, as well as surface regions. This deserves future attention.

Initial investigations into assessing geometric tolerances show the need for further studies into the methods of local radius analysis. A comparative study between the functionality of ACIS® and other CAGD applications is beyond the scope of this present work. Future work would involve developing methods to plot tolerance zones on the generated surface model, where trends may be apparent. Analysis of the global curvature of the surface may necessitate the conversion of the spline surface to an analytical CAD entity surface. This would allow geometric tolerance analysis based on the radius of the total sub-surface, rather than of the local sub-surface points. The conversion of parametric sub-surfaces of known surface type to an analytic representation would vastly reduce the size of the resultant file. The analysis of surface profile form works towards this, where information on the global curvature of sub-surfaces is necessary, as well as the sub-surface type. Converting surface type sub-surfaces to CAD entities would also work towards faster processing and analysis time, as ACIS® parametric spline surfaces are far more complex than analytical surface types. This could be taken further for the conversion to neutral file-formats, such as STEP.

Accurately reproducing a physical prototype made up of composite surfaces has received limited attention. The introduction of discontinuities in a CAD surface will

cause problems with tool offsetting and tool interference. In the case of free-form modelling, these discontinuities are represented as extreme changes in curvature, which traditionally cause problems at both the surface offset stage and machining stage. Where extreme curvature change caused gouging at the machining stage, these degenerate regions, occurring at surface-surface intersections are discarded by this present work of surface segmentation. Curvature-based surface decomposition results in a number of free-form sub-surfaces. Each sub-surface may be machined individually, using an appropriate ball-nosed cutter. This allows the best tool, based on the surface curvature, to be determined, giving the maximum material removal rate. This is similar to feature-based machining, but is based on surface type. Interference at surface-surface intersections is avoided, due to these regions being discarded from the surface model. This is defined as the gouging problem. Where the density of the machine points are greater than the machine radius, only small cusp production is envisaged between sub-surfaces. However, this depends on the size of the intersection voids. This forms a theoretical solution to reducing gouging. The development of techniques to overcome the machining problems at these regions, utilising flat end-mills is seen as viable future research. Initial developments in accuracy analysis work towards analysing the total RE process, including the machining stage, utilising New Model Analysis (NMA). This is seen as future work which would perform DA on the CMM data collected from a reproduction part, and compare the results with the DA results of the original surface model.

The manufacturing industry, as with many other industries, is concerned with the continual improvement of products and services. RE is a tool which will improve, as new technologies emerge. The present work, discussed in this thesis, investigates current technology, and works towards continual improvement, by developing novel methods to enhance the existing RE process. Areas have been highlighted, and work has been implemented, which aims to improve the understanding of the cause of errors and inaccuracies, and develop methods of reducing them to acceptable levels.

References

[ANON., 1996]	Anon., 1996, 'Simulation for CMM training', *Quality Today*, July, pp. 35-36.
[AOMURA, 1990]	Aomura, S., and Uehara, T., 1990, 'Self-intersection of an Offset Surface', *Computer Aided Design*, vol. 22, no. 7, pp. 417-422.
[ARONSON, 1996]	Aronson, R., 1996, 'Forward Thinkers take to RE', *Man Engineer*, November, pp. 34-44.
[BALENDRAN, 1989]	Balendran, V., Sivayoganathan, K., and Al-Dabass, D., 1989, 'Detection of Flaws on Slowly Varying Surfaces', Proceedings of the 5th *National Conference on Production Research*, pp.82-85.
[BALENDRAN, 1992]	Balendran, V., Sivayoganathan, K., and Howarth, M., 1992, 'Sensor Aided Fettling', *Proceedings of the 8th National Conference on Manufacturing Research*, pp.132-136.
[BALENDRAN, 1993]	Balendran, V., 1993, 'Cosmetic Quality of Surfaces: A computational approach', *PhD. Thesis*, Nottingham Trent University.
[BARDELL, 1997]	Bardell, R., Balendran, V., and Sivayoganathan, K., 1997, 'Representing Surfaces from CMM Data', *Proceedings of the 13th National Conference on Manufacturing Research*, pp.22-26.
[BARDELL, 1998a]	Bardell, R., Balendran, V., and Sivayoganathan, K., 1998, 'Optimising Surface Modelling Techniques', *Proceedings of the Mechanics in Design International Conference*, pp. 771-779.
[BARDELL, 1998b]	Bardell, R., Sivayoganathan, K., and Balendran, V., 1998, 'Refinement and Modelling of CMM Data', *Proceedings of the 14th National Conference on Manufacturing Research*, pp.759-764.
[BARDELL, 1998c]	Bardell, R., Balendran, V., and Sivayoganathan, K., 1998, 'Accuracy Analysis of 3D Data Collection and Free-form Modelling Methods', *Proceedings of the 7th International Scientific Conference, Achievements in Mechanical and Materials Engineering - AMME*, pp. 33-36.
[BARDELL, forthcoming]	Bardell, R., Balendran, V., and Sivayoganathan, K., 'Accuracy Analysis of 3D Data Collection and Free-form Modelling Methods', *Journal of Materials Processing Technology, special issue from Achievements in Mechanical and Materials Engineering - AMME'98*.
[BARNHILL, 1974]	Barnhill, R., 1974, 'Smooth Interpolation over Triangles', *Proceedings of the 1st International Conference on Computer Aided Geometric Design*, pp. 45-70.
[BARSKY, 1993]	Barksy, B., 1993, 'Rational Beta-splines for Representing Curves and Surfaces', *IEEE Computer Graphics and Applications*, vol. 13, no. 6, pp. 24-32.

[BARTELS, 1994]   Bartels, R., and Warn, D., 1994, 'Experiments with Curvature-Continuous Patch-Boundary Fitting', *IEEE Computer Graphics and Applications,* September, pp.64-73.

[BESL, 1985]   Besl, J., and Jain, R., 1985, 'Three-Dimensional Object Recognition', *Computer Surveys,* vol. 17, no. 1, pp.75-145.

[BESL, 1986]   Besl, P., and Jain, R., 1986, 'Invariant Surface Characteristics for 3D Object Recognition in Range Images' *Computer Vision, Graphics, and Image Processing,* vol. 33, pp. 33-80.

[BESL, 1988]   Besl, P., and Jain, R., 1988, 'Range Image Segmentation', *Algorithms, Architectures and Systems,* ed. H. Freeman, Academic Press.

[BESL, 1990]   Besl, P., 1990, 'The Free-Form Surface Matching Problem', *Machine Vision for 3D Scenes,* Academic Press, Inc.

[BEZIER, 1972]   Bézier, P., 1972, *Numerical Control - Mathematics and Applications,* (Translated by Forrest, A., and Pankhurst, A.) Wiley & Sons Ltd.

[BEZIER, 1974]   Bézier, P., 1974, 'Mathematical and Practical Possibilities of UNISURF', *Proceedings of the 1st International Conference on Computer Aided Geometric Design,* pp. 127-152.

[BEZIER, 1990]   Bézier, P., 1990, 'Style, mathematics and NC' *Computer Aided Design,* vol. 22, no. 9, pp. 524-526.

[BIDANDA, 1994]   Bidanda, B., and Hosni, Y., 1994, 'Reverse Engineering and its Relevance to Industrial Engineering: A Critical Review', *Computers Ind. Engng.,* vol. 26, no. 2, pp. 343-348.

[BOEHM, 1985]   Boehm, W., 1985, 'Triangular Spline Algorithms', *Computer Aided Geometric Design,* vol. 2, pp. 61-67.

[BOSCH, 1995a]   Bosch, J., 1995, 'Evolution of Measurement' in *Co-ordinate Measuring Machines and Systems.* Edited by Bosch, J., © Marcel Dekker, Inc.

[BOSCH, 1995b]   Bosch, J., 1995, 'Future Trends', in *Co-ordinate Measuring Machines and Systems.* Edited by Bosch, J., © Marcel Dekker, Inc.

[BRAID, 1997]   Braid, I., 1997, 'Non-local Blending of Boundary Models', *Computer Aided Design,* vol. 29, no. 2, pp. 89-100.

[BROOMHEAD, 1986]   Broomhead, P., and Edkins, M., 1986, 'Generating NC Data at The Machine Tool for the Manufacture of Free-Form Surfaces', *Int. J. Prod. Res.,* vol. 24, no. 1, pp. 1-14.

[BUTLER, 1994]   Butler, C., 1994, 'Probes for High Precision Dimensional Measurement', *Sensor Review,* vol. 14, no. 1, pp. 24-26.

[BSI, 1993]   British Standards Institution, 1993, Geometric Tolerancing and Dimensioning, BS 308, Part III.

[CASE, 1994]   Case, K., Gao, J., and Gindy, N., 1994, 'The Implementation of a Feature-based Component Representation for CAD/CAM Integration', *Proceedings Instn. Mech. Engrs.,* Part B, *Journal of Engineering Manufacture,* vol. 208, pp. 71-79.

[CATANIA, 1992]   Catania, G., 1992, 'A Computer-aided Prototype System for NC
                     Rough Milling of Free-form Shaped Mechanical Part-pieces',
                     Computers in Industry, vol. 20, pp. 275-293.

[CHE, 1992]   Che, C., 1992, 'Scanning Compound Surfaces with no Existing CAD
                     Model by Using Laser Probe of a Coordinate Measuring Machine
                     (CMM)', *Proceedings of SPIE,* vol. 1779, pp. 57-67.

[CHEN, 1992]   Chen, Y., Tang, J., and Wu, S., 1992, 'Automatic Digitization of
                     free-form Curve by Coordinate Measuring Machines', *Symp. of
                     Engineered Surfaces, ASME,* vol. 62, pp. 113-125.

[CHEN, 1997]   Chen, Y., and Liu, C., 1997, 'Robust Segmentation of CMM Data
                     Based on NURBS', *Int. J. Adv. Technol.,* vol. 13, pp. 530-534.

[CHENG, 1995]   Cheng, W., and Menq, C., 1995, 'Integrated Laser/CMM System for
                     the Dimensional Inspection of Objects Made of Soft Material', 1 *Int.
                     J Adv Manuf. Technol.,* vol. 10, pp. 36-45.

[CHOI, 1988]   Choi, B., Lee, C., and Jun, C., 1988, 'Compound Surface Modelling
                     and Machining', *Computer Aided Design,* vol. 20, no. 3, pp.127-136.

[DION, 1997]   Dion, D., Laurendeau, D., and Bergevin, R., 1997, 'Generalised
                     Cylinders Extraction in a Range Image', *Proceedings Int. Conf. on
                     Recent Advances in 3D Digital Images and Modelling,* pp. 141-147.

[DJEBALI, 1994]   Djebali, M., Melkemi, M., and Vandorpe, D., 1994, '3-D Range
                     Images Segmentation Based on Deriche's Optimum Filters', *IEEE
                     Int. Conf. Image Processing,* vol. 3, pp. 503-507.

[DMIS, 1995]   DMIS, 1995, CAM-I Dimensional Measuring Interface Standard,
                     Revision 3.0 National Standards Committee.

[DUFFIE, 1985]   Duffie, N., and Feng, S., 1985, 'Modification of Bicubic Surface
                     Patches Using Least-Squares Fitting Techniques', *Computers in
                     Mechanical Engineering,* September, pp. 57-65.

[DUNCAN, 1989]   Duncan, J., and Law, K., 1989, 'Natural Surfaces and Data
                     Collection', in *Computer Aided Sculpture,* pub. Cambridge
                     University Press.

[EDS, 1996]   EDS, 1996, *'EDS Unigraphics Announces Release of Parasolid V.8',*
                     pub. Parasolid Sales.

[ELMARAGHY, 1987]   ElMaraghy, H., and Gu, P., 1987, 'Expert System for Inspection
                     Planning', *Annals of the CIRP,* vol. 36, no. 1, pp. 85-89.

[FANG, 1997]   Fang, M., Chen, D., and Zhu, B., 1997, 'Model Reconstruction of
                     Existing Products Using Neural Networks for Reverse Engineering',
                     IEEE International Conference on Intelligent Processing Systems,
                     pp. 396-400.

[FARIN, 1982]   Farin, G., 1982, 'Designing C^1 Surfaces Consisting of Triangular
                     cubic Patches', *Computer Aided Design,* vol. 14, no. 5, pp. 253-256.

[FARIN, 1990]   Farin, G., 1990, *Curves and Surfaces for Computer Aided Geometric
                     Design, A Practical Guide,* 2nd. Ed., Academic Press.

[FERREIRA, 1986]   Ferreira, P., and Liu, C., 1986, 'A Contribution to the Analysis and Compensation of the Geometric Error of a Machining Center', *Annals of the CIRP*, vol. 35, no. 1, pp. 259-262.

[FITZGIBBON, 1997]   Fitzgibbon, A., Eggert, D., and Fisher, R., 1997, 'High-level CAD model acquisition from range images', *Computer Aided Design*, vol. 29, no. 4, pp. 321-330.

[FLETCHER, 1987]   Fletcher, G. and McAlister, D. ,1987, 'An Analysis of Tension Methods for Convexity Preserving Interpolation', *IEEE Computer Graphics and Applications*, vol. 7, no. 8, pp. 7-14.

[GAO, 1994]   Gao, J., Case, K., and Gindy, N., 1994, 'Geometric Elements for Tolerance Definition in Feature-Based Product Models', *Proceedings of the 10th National Conference on Manufacturing Research*, pp. 264-268.

[GARCIA, 1996]   Garcia, M., and Basanez, L., 1996, 'Efficient Free-form Surface Modelling with Uncertainty', *Proceedings of the IEEE Int. Conf. On Robots and Automation*, pp. 1825-1830.

[GERALD, 1994]   Gerald, C., and Wheatley, P., 1994, *Applied Numerical Analysis*. 5th ed. Addison-Wesley Publishing Company Inc.

[GHOSAL, 1993]   Ghosal, S., and Mehrotra, R., 1993, 'Segmentation of Range Images: An Orthogonal Moment-Based Integrated Approach' *IEEE Transactions on Robotics and Automation*, vol. 9, no. 4, pp. 385-399.

[GHOSAL, 1995]   Ghosal, S., and Mehrotra, R., 1995, 'Range Surface characterization and Segmentation Using Neural Networks', *Pattern Recognition*, vol. 28, no. 5, pp. 711-727.

[GOODMAN, 1986]   Goodman and Unsworth, 1986, 'Manipulating Shape and Producing Geometric Continuity in Beta-spline Curves', *IEEE Computer Graphics and Applications*, vol. 6, no. 2, pp. 50-56.

[GRANT, 1995]   Grant, 1995, 'Financial Evaluations', in *Co-ordinate Measuring Machines and Systems*. Edited by Bosch, J., © Marcel Dekker, Inc.

[GREGORY, 1974]   Gregory, J., 1974, 'Smooth Interpolation without Twist Constraints', *Proceedings of the 1st International Conference on Computer Aided Geometric Design*, pp. 71-87.

[GREGORY, 1985]   Gregory, J., 1985, 'Interpolation to boundary data on the simplex', *Computer Aided Geometric Design*, vol. 2, pp. 43-52.

[GREGORY, 1986]   Gregory, J., 1986, *'N-Sided Surface Patches'*, The Mathematics of Surfaces, ed. J. A. Gregory.

[GUAN, 1997]   Guan, Z., Ling, J., Tao, N., Ping, X. and Rongxi, T., 1997, 'Physics based Deformable Curves and Surfaces', *Comput. and Graphics*, vol. 21, no. 3, pp. 305-313.

[GUNASEKERA, 1989]   Gunasekera, J., 1989, *CAD/CAM of Dies*, ed. John Wiley & Sons, pub. Ellis Horwood Ltd.

[GUPTA, 1993]   Gupta, V., and Sagar, R., 1993, 'A PC-based System Integrating CMM and CAD for Automated Inspection and Reverse Engineering', *Int. J. Manuf. Technol*, vol. 8, pp. 305-310.

[HALL, 1990] Hall, W., and Hibbs, T., 1990, 'Continuous, quadrilateral, and triangular surface patches', in *Applied Surface Modelling,* ed. Creasy & Craggs, pub. Ellis Horwood Ltd.

[HAN, 1987] Han, J., Volz, R., and Mudge, T., 1987, 'Range Image Segmentation and Surface Parameter Extraction for 3D Object Recognition of Industrial Parts', *Proceedings of IEEE Int. Conf. On Robotics and Automation,* vol. 1, March, pp. 380-386.

[HANSEN, 1988] Hansen, A., and Arbab, F., 1988, 'Fixed-Axis Tool Positioning with Built-in Global Interference Checking for NC Path Generation', *IEEE Journal of Robotics and Automation,* vol. 4, no. 6, pp. 610-621.

[HENDERSON, 1982] Henderson, T., and Bhanu, B., 1982, 'Three-point Seed Method for the Extraction of Planar Faces from Range Data', *Proceedings of Workshop Ind. Apps. of Machine Vision Res.,* May, pp. 181-186.

[HERMANN, 1997] Hermann, G., 1997, 'Feature-based Of-line Programming of Coordinate Measuring Machines', *IEEE Proceedings Conf. Intelligent Engineering Systems, INES,* pp. 545-548.

[HOCKEN, 1995] Hocken., R., 1995, 'Measurement Integration', in *Co-ordinate Measuring Machines and Systems.* Edited by Bosch, J., © Marcel Dekker, Inc.

[HOFFMAN, 1987] Hoffman, R., and Jain, A., 1987, 'Segmentation and Classification of Range Images' *IEEE Transactions on Pattern Analysis and Machine Intelligence,* vol. 9, no. 5, pp. 608-620.

[HOPPE, 1996] Hoppe, H., 1996, 'Progressive Meshes', *Computer Graphics (SIGGRAPH '96 Proceedings),* pp. 99-108.

[HORTON, 1997] Horton, I, 1997, *'Beginning Visual C++ 5',* pub. Wrox Press Ltd.

[HOUGHTON, 1985] Houghton, E., Emnett, R., Factor, J., and Sabharwal, C., 1985, 'Implementation of a Divide-and-conquer Method for Intersection of Parametric Surfaces', *Computer Aided Geometric Design,* vol. 2, pp. 173-183.

[HUANG, 1996] Huang, X., Gu, P., and Zernicke, R., 1996, 'Localization and Comparison of Two free-form Surfaces', *Computer Aided Design,* vol. 28, no. 12, pp. 1017-1022.

[IP, 1991] Ip, R., and Loftus, M., 1991, 'Free Form Surface Machining' *Proceedings of the 7th National Conference on Production Research,* pp. 345-349.

[IP, 1992] Ip, R., and Loftus, M., 1992, 'The Application Of Co-ordinated Metrology Techniques To Assess Free-Form Surfaces', *Proceedings of the 8th National Conference on Manufacturing Research,* pp.224-228.

[JONES, 1988] Jones, A., 1988, 'Nonrectangular Surface Patches with Curvature Continuity', *Computer Aided Design,* vol. 20, no. 6, pp. 325-335

[KATEBI, 1994] Katebi, M., Lee, T., and Grimble, M., 1994, 'Total Control of Fast Co-ordinate Measuring Machines', *IEE Proceedings Control Thery Appl.,* vol. 141, no. 6, pp. 373-384.

[KAWABE, 1980]   Kawabe, S., Kimura, F., and Sata, T., 1980, 'Generation of NC Commands for Sculptured Surface Machining from 3D-Co-ordinate Measuring Data', *Annals of the CIRP,* vol. 29, no. 1, pp. 369-372.

[KEAT, 1994]   Keat, J., Balendran, V., Sivayoganathan, K., and Sackfield, A., 1994, '3-D Data Collection for Object Recognition,' *Proceedings of the 10th National Conference on Manufacturing Research,* pp. 648-652.

[KEHTARNAVAZ, 1988] Kehtarnavaz, N., and deFigueiredo, R., 1988, 'A Framework for Surface Reconstruction from 3D Contours', *Computer Vision, Graphics and Image Processing,* vol. 42, pp. 32-47.

[KIM, 1988]   Kim, K., and Biegel, J. E., 1988, 'A Path Generation Method for Sculptured Surface Manufacture', *Computers Ind. Engng.,* vol. 14, no. 2, pp. 95-101.

[KISHINAMI, 1985]   Kishinami, T., Kanai, S., and Saito, K., 1985, 'MKS: Machining Kernel Software for CAM-System', *Annals of the CIRP,* vol. 34, no. 1, pp. 419-422.

[KREJCI, 1995]   Krejci, J., 1995, 'Application Software', *Co-ordinate Measuring Machines and Systems.* Edited by Bosch, J. © Marcel Dekker, Inc.

[LAI, 1996]   Lai, J., and Lu, C., 1996, 'Reverse Engineering of Composite Sculptured Surfaces', *Int. J. Adv. Manuf. Technol.,* vol. 12, pp. 180-189.

[LAU, 1985]   Lau, K., Duffie, N., and Bollinger, J., 1985, 'Automatic Contour Measurement for Three-dimensional Geometry', *Manufacturing Engineering Trans.* vol. 13, pp. 535-540.

[LAWRENCE, 1993]   Lawrence, P., 1993, 'Assessing and Using the Capability of a CMM', *Proceedings of the 9th Conference for Manufacturing Engineering,* pp. 400-404.

[LEDOUX, 1996]   Ledoux, S, 1996, 'Getting Started with Direct3D', *Microsoft Corporation.*

[LEE, 1989]   Lee, E., 1989, 'Choosing Nodes in Parametric Curve Interpolation', *Computer Aided Design,* vol. 21, no. 6, pp. 363-370.

[LEE, 1990]   Lee, A., Chen, D., and Lin, C., 1990, 'A CAD/CAM System From 3D Co-ordinate Measuring Data', *Int. J. Prod. Res.,* vol. 28, no. 12, pp. 2353-2371.

[LI, 1997]   Li, P., and Jones, P., 1997, 'Automatic Editing and Curve-fitting of 3D Surface Scan Data of the Human Body', *Proceedings of IEEE Int. Conf. On Recent Advances in 3D Digital Imaging and Modelling,* pp. 296-299.

[LK, 1992]   LK Ltd., 1992, PC CMES Command Language V.9. vols. 1, 2, Castle Donnington.

[LOFTUS, 1991]   Loftus, M., 1991, 'Aspects of NC Within Geometric Modelling Systems', *Proceedings of the 7th National Conference on Production Research,* pp. 47-51.

[MA, 1998]   Ma, W, and Kruth, J., 1998, 'NURBS Curve and Surface Fitting for Reverse Engineering', *Int. J. Adv. Manuf Technol.*, vol. 14 pp. 918-927.

[MASON, 1990]   Mason, F., 1990, '3D Surface Mapping Aids Programming', *American Machinist*, vol. 11 pp. 91-93.

[MAYER, 1987]   Mayer, R., 1987, 'IGES – One Answer to the Problems of CAD Database Exchange', *BYTE*, vol. 6, pp. 209-214.

[MEDIONI, 1987]   Medioni, G., and Yasumoto, Y., 1987, 'Corner Detection and Curve Representation Using Cubic B-Splines', *Computer Vision, Graphics and Image Processing*, vol. 39, pp. 267-278.

[MEDLAND, 1992]   Medland, A., Mullineux, G., and Rentoul, A., 1992, 'Measurement of Features By a Sample-Grid Approach', *Proceedings of the 8th National Conference on Manufacturing Research*, pp. 673-677.

[MENQ, 1996]   Menq, C., and Chen, F. L., 1996, 'Curve and Surface Approximation from CMM Measurement Data', *Computers Ind. Engng.*, vol. 30, no. 2, pp. 211-225.

[MILLER, 1993]   Miller, J., 1993, 'Incremental Boundary Evaluation Using Inference of Edge Classifications' *IEE Computer Graphics & Applications*, January, pp. 71-78.

[MORETON, 1991]   Moreton, D., Parkinson, D., and Wu, W., 1991, 'The application of a biarc technique in CNC machining', *Computer Aided Engineering Journal*, vol. 8, no. 2, pp. 54-60.

[NEILSON, 1993]   Nielson, G., 1993, 'CAGD's Top Ten: What to Watch', *IEEE Computer Graphics and Applications*, vol. 13, no. 1, pp. 35-37.

[NI, 1995]   Ni, J., and Wäldele, F., 1995, 'Co-ordinate Measuring Machines', in *Co-ordinate Measuring Machines and Systems*. Edited by Bosch, J., © Marcel Dekker, Inc.

[OLIVER, 1993]   Oliver, J., Wysocki, D., and Goodman, E., 1993, 'Gouge Detection Algorithms for Sculptured Surface NC Generation', *Journal of Engineering for Industry*, vol. 115, pp.139-144.

[PATRIKALAKIS, 1993]   Patrikalakis, N., 1993, 'Surface-to-Surface Intersections', *IEEE Computer Graphics and Applications*, vol. 13, no. 1, pp. 89-95.

[PEIRO, 1990]   Peiro, J., Peraire, J., and Morgan, K., 1990, 'The Generation of Triangular Meshes on Surfaces', in *Applied Surface Modelling*, ed. Creasy & Craggs, pub. Ellis Horwood Ltd.

[PENG, 1998]   Peng, Q., and Loftus, M., 1998, 'The Reverse Design Approach Based on Vision Information', *Proceedings of the Mechanics in Design International Conference*, pp. 806-815.

[PHAM, 1992]   Pham, B., 1992, 'Offset Curves and Surfaces: A Brief Survey', *Computer Aided Design*, vol. 24, no. 2, pp. 223-229.

[PIEGL, 1988]   Piegl, L., 1988, 'Hermite-and Coons-like Interpolants using Rational Bézier Approximation Form with Infinite Control Points', *Computer Aided Design*, vol. 20, no. 1, pp. 2-10.

[POTTER, 1997]   Potter, C., 1997, 'The Engines of Mechanical CAD', *Computer Graphics World*, vol. 20, no. 5, pp. 31-36.

[PRATT, 1985]   Pratt, M., 1985, 'Smooth Parametric Surface Approximations to Discrete Data', *Computer Aided Geometric Design*, vol. 2, pp. 165-171.

[PRATT, 1990]   Pratt, M., 1990, *'Surfaces in Solid Modelling'*, Applied Surface Modelling, ed. Creasy & Craggs, pub. Ellis Horwood.

[RAHMAN, 1992]   Rahman, W., Harun, W., and Case, K., 1992, 'Object-Oriented Feature-Based Design,' *Proceedings of the 8th National Conference on Manufacturing Research,* pp 294-298.

[RENZ, 1982]   Renz, W., 1982, Interactive Smoothing of Digitised Point Data, *Computer Aided Design,* vol. 14, no. 5, pp. 267-269.

[SAHOO, 1992]   Sahoo, K., and Menq, C., 1992, 'Localization of 3-D Objects Having Complex Sculptured Surfaces Using Tactile Sensing and Surface Description', *Journal of Engineering for Industry,* vol. 113, pp. 85-92.

[SARKAR, 1991a]   Sarkar, B., and Menq, C., 1991, 'Smooth-surface Approximation and Reverse Engineering', *Computer Aided Design,* vol. 23, no. 9, pp. 623-628.

[SARKAR, 1991b]   Sarkar, B., and Menq, C., 1991, 'Parameter Optimization in Approximating Curves and Surfaces to Measurement Data'', *Computer Aided Geometric Design,* vol. 8, pp. 267-290.

[SARRAGA, 1990]   Sarraga, R., 1990, 'Computer Modelling of Surfaces with Arbitrary Shapes', *IEEE Computer Graphics and Applications,* vol. 10, no. 2, pp. 67-77.

[SCHICHTEL, 1993]   Schichtel, M., 1993, 'G2 Blend Surfaces and Filling of N-sided Holes', *IEEE Computer Graphics and Applications,* September, pp. 68-73.

[SEILER, 1991]   Seiler, A., Sivayoganathan, K., Sackfield, A., and Chisholm, A., 1991, 'Close Loop Error Correction Using Co-ordinate Measuring Machine Data', *Proceedings of the 7th National Conference on Manufacturing Research,* pp.276-280.

[SEILER, 1994]   Seiler, A., 1994, 'Improved Methods of Reverse Engineering utilising CMM Scan Data.' *PhD Thesis,* Nottingham Trent University.

[SEILER, 1996]   Seiler, A., Balendran, V., Sivayoganathan, K., and Sackfield, A., 1996, 'Reverse Engineering from Uni-directional CMM Scan Data', *Int. Jnl. Advanced Manufacturing Technology,* vol. 11, pp. 276-284.

[SEDERBERG, 1985a]   Sederberg, T., 1985, 'Piece-wise Algebraic Surface Patches', *Computer Aided Geometric Design,* vol. 2, pp. 53-59.

[SEDERBERG, 1985b]   Sederburg, T., and Anderson, D., 1985, 'Steiner Surface Patches', *IEEE Computer Graphics and Applications,* vol. 5, no. 5, pp. 23-36.

[SETHI, 1984]   Sethi, I., and Jayaramamurthy, S., 1984, 'Surface Classification Using Characteristic Contours', *Proceedings of 7th Int. Conf. On Pattern Recog.,* pp. 438-440.

[SHYAMSUNDAR, 1996]   Shyamsundar, N., Gurumoorthy, B., 1996, 'Construction of Solid Model from Measured Point Data', *Proceedings of the IEEE Int. Conf. on Robots and Automation,* pp.1831-1836.

[SIVAYOGANATHAN, 1993]   Sivayoganathan, K., Balendran, V., Czerwinski, A., Keats, J., Leibar, A., and Seiler, A, 1993, 'CAD/CAM Data Exchange Application', *Proceedings of the 9th National Conference on Manufacturing Research,* pp.306-310.

[SIVAYOGANATHAN, 1994]   Sivayoganathan, K., Leibar, A., Balendran, V., 1994, 'Off-Line Programming for Co-ordinate Measuring Machines' *Proceedings of the 10th National Conference on Manufacturing Research,* pp. 678-682.

[SMITH, 1990]   Smith, G., 1990, 'From Computer Modelling to the Manufacture of Dies with Sculptured Contours', *Journal of Materials Processing Technology,* vol. 24, pp. 115-124.

[SMITH, 1991]   Smith, G., and Stephenson, H., 1991, 'The Selection of Optimum Tool Sizes for Three-axis and Multi-axis Machining of Highly Curved Features', *Proceedings of the 7th National Conference on Production Research,* pp. 316-320.

[SMITH, 1994]   Smith, G., Hill, T., Rockliffe, S., and Harris, J., 1994, 'Geometric Assessment of Sculptured Features', *Proceedings of the 10th National Conference on Manufacturing Research,* pp. 663-667.

[SPATIAL, 1996]   Spatial Technology, 1996, 'ACIS® Application Guide'.

[SPATIAL, 1997a]   Spatial Technology, 1997, 'ACIS® 3D Toolkit 3.0 Modelling Primer'.

[SPATIAL, 1997b]   Spatial Technology, 1997, 'Mechanical CAD Modelling with ACIS® 3.0'.

[SPYRIDI, 1990]   Spyridi, A., and Requicha, A., 1990, 'Accessibility Analysis for the Automatic Inspection of Mechanical Parts by Co-ordinate Measuring Machines', *Proceedings of the IEEE Int. Conference on Robotics and Automation,* pp. 1284-1289.

[SPYRIDI, 1994]   Spyridi, A., and Requicha, A., 1994, 'Automatic Programming of Co-ordinate Measuring Machines', *Proceedings of the IEEE Int. Conference on Robotics and Automation,* pp. 1107-1112.

[STEPHENSON, 1991]   Stephenson, H., and Smith, G., 1991, 'Efficient Machining Strategies Based on Recognition of Features on Free Form Surfaces', *Proceedings of the 7th National Conference on Manufacturing Research,* pp. 321-325.

[STORRY, 1990]   Storry, D., and Davies, R., 1990, 'Design of N-spline Patches using Recursive Subdivision', in *Applied Surface Modelling,* ed. Creasy & Craggs, pub. Ellis Horwood Ltd.

[SUH, 1990]   Suh, S., and Lee, K., 1990, 'NC Milling Tool Path Generation For Arbitrary Pockets Defined by Sculptured Surfaces', *Computer Aided Design,* vol. 22, no. 5, pp. 273-284.

[SUH, 1994]   Suh, S., and Lee, S., 1994, 'Compensating Probe Radius in Free Surface Modelling with CMM', *Proceedings of 4th Int. Conf. On Computer Integrated Manufacturing & Automation Technology,* IEEE Computer Soc. Press, pp. 222-227.

[TANAKA, 1996]   Tanaka, H., and Ikeda, M., 1996, 'Curvature-Based Face Surface Recognition Using Spherical Correlation – Principle Directions for Curved Object Recognition', *IEEE Proceedings of ICPR*, pp. 638-642.

[TAYLOR, 1989]   Taylor, R., Savini, M., and Reeves, A., 1989, 'Fast Segmentation of Range Imagery into Planar Regions', *Computer Vision, Graphics and Image Processing,* vol. 45, pp. 42-60.

[TEEUWSEN, 1989]   Teeuwsen, J., Soons, J., and Schellekens, P., 1989, 'A General Method for Error Description of CMMs Using Polynomial Fitting Procedures' *Annals of the CIRP,* vol. 38, no. 1, pp. 505-510.

[TRABELSI, 1993]   Trabelsi, A., and Carrard, M., 1993, 'Feature Recognition From 2D and 3D Modellers', *Computers in Design, Manufacture and Production,* pp. 210-216.

[VARADAY, 1996]   Varady, T., Martin, R., and Cox, J., 1997, 'Reverse Engineering of Geometric Models - An Introduction', *Computer Aided Design*, vol. 29, no. 4, pp. 255-268.

[VASSILER, 1996]   Vassiler, T., 1996, 'Fair Interpolation and Approximation of B-splines by Energy Minimisation and Point Insertion', *Computer Aided Design*, vol. 28, no. 9, pp. 753-760.

[VICKERS, 1989]   Vickers, G., and Quan, K., 1989, 'Ball-Mills Versus End-mills for Curved Surface Machining', *Journal of Engineering for Industry, Transactions of the ASME,* vol. 111, pp. 22-26.

[WANG, 1997a]   Wang, X., Cheng, F., and Barsky, B., 1997, 'Energy and B-spline Interproximation', *Computer Aided Design,* vol. 29, no. 7, pp. 485-496.

[WANG, 1997b]   Wang, L., Zhu, X. and Tang, Z., 1997, 'Coons Type Blended B-spline (CNBS) Surface and its Conversion to NURBS', *Comput. and Graphics*, vol. 21, no. 3, pp. 297-303.

[WECKENMANN, 1998]   Weckenmann, A., and Knauer, M., 1998, 'The Influence of Measurement Strategy on the Uncertainty of CMM-Measurements', *Annals of the CIRP,* vol. 47, no. 1, pp. 1998.

[WEIR, 1996]   Weir, D., Milroy, M., Bradley, C., and Vickers, G., 1996, 'Reverse engineering physical models employing wrap-around B-Spline surfaces and quadratics', *Proceedings of Instn. Mech. Engrs., Part B, Journal of Engineering Manufacture*, vol. 210, pp. 147-157.

[YANG, 1994]   Yang, D., and Kong, T., 1994, 'Parametric Interpolator versus Linear Interpolator for Precision CNC Machining', *Computer Aided Design,* vol. 26, no. 3, pp.225-234.

[YAU, 1990]   Yau, H., and Menq, C., 1990, 'The Development of an Intelligent Dimensional Inspection Environment in Manufacturing', *Japan-USA Symposium on Flexible Automation,* pp. 1059-1065.

[YAU, 1991]   Yau, H., and Menq, C., 1991, 'Path Planning for Automated Dimensional Inspection Using Co-ordinate Measuring Machines', *Proceedings of the IEEE Int. Conference on Robotics and Automation,* pp. 1934-1939.

[YAU, 1997]   Yau, H., and Chen, J., 1997, 'Reverse Engineering of Complex Geometry Using Rational B-Splines', *Int. J. Advanced Manufacturing Technology,* vol. 13 pp. 548-555.

[ZHAO, 1997]   Zhao, D., and Zhang, X., 1997, 'Range-Data-Based Object Surface Segmentation via Edges and Critical Points' *IEEE Trans. on Image Processing,* vol. 6, no. 6, pp. 826-830.

[ZHENG, 1994]   Zheng, W., and Harashima, H., 1994, 'The Automatic Generation of 3D Object Model Form Range Image', *IEEE Int. Conference on Acoustics, Speech and Signal Processing,* vol. 5, pp. 517-520.

[ZHOU, 1992]   Zhou, E., Harrison, D., and Link, D., 1992, 'The Application of In-Process Measuring Techniques', *Proceedings of the 8th National Conference on Production Research,* pp.219-223.

[ZHUANG, 1995]   Zhuang, B., Zhang, J., Jiang, C., Li, Z., and Zhang, W., 1995, 'Precision Laser Triangulation Range Sensor with Double Detectors for Measurement on CMMs', *Int. Soc. for Optical Engineering, Proceedings of SPIE,* vol. 2349, pp. 44-52.

Appendix I

Flow Chart

Main

Surface Segmentation ?

main_surf. new_curvature_arrays

grow. new_arrays

mainsurf. do_curvature_analysis

mainsurf. alloc_bounds

main_surf. save_final_gaus_map

Allocate remaining points?

mainsurf. alloc_remains

main_surf. del_curvature_arrays

grow. del_arrays

Set tolrance?

grow. get_patch_curvature

user. get_HK

user. colour_alloc

main_surf. displaysurf

intial choose_seed

grow. intial_sub_patch

user. seed_grow

Do Again ?

grow. extend

main_surf. alloc_bounds

grow. set_sub_surf_array

grow. get_patch_curvature

user. get_HK

user. colour_alloc

grow. confirm

Still growing ?

intial print_s_surf

grow. extend_N

grow. extend_W

grow. extend_S

grow. extend_E

grow. get_patch_curvature

user. get_HK

grow. re_allocate

user. colour_alloc

user. get_HK

Type same as seed ?

grow. alloc_types

Seed type OK ?

grow. get_patch_curvature

user. get_HK

user. colour_alloc

intial find_accuracy

grow. get_patch_curvature

user. get_HK

user. colour_alloc

grow. get_patch_curvature

user. get_HK

user. colour_alloc

Appendix II

Published Conference Papers

[BARDELL, 1997]   'Representing Surfaces from CMM Data', *Proceedings of the 13th National Conference on Manufacturing Research*, pp.22-26.

[BARDELL, 1998a]   'Optimising Surface Modelling Techniques', *Proceedings of the Mechanics in Design International Conference*, pp. 771-779.

[BARDELL, 1998b]   'Refinement and Modelling of CMM Data', *Proceedings of the 14th National Conference on Manufacturing Research*, pp.759-764.

[BARDELL, 1998c]   'Accuracy Analysis of 3D Data Collection and Free-form Modelling Methods', *Proceedings of the 7th International Scientific Conference, Achievements in Mechanical and Materials Engineering - AMME*, pp. 33-36.

[BARDELL, forthcoming]   'Accuracy Analysis of 3D Data Collection and Free-form Modelling Methods', *Journal of Materials Processing Technology, special issue from Achievements in Mechanical and Materials Engineering - AMME'98*.

Representing Surfaces from CMM Data.

R Bardell, V Balendran, K Sivayoganathan.

Department of Mechanical & Manufacturing Engineering,
The Nottingham Trent University, Nottingham, NG1 4BU

Abstract: Co-ordinate Measuring Machines (CMMs), are used in the inspection process for the precision collection of 3D data of physical parts. This point data can then be used in areas such as error estimation and reverse engineering.

Visually representing this data is highly desired, aiding simulation and modelling systems. This can be in the form of wire-frame models, with the ability to extend into surface and ultimately solid representations.

Extending this area to label local surfaces based on Gaussian and mean curvature is seen as a way of segmenting data to map to corresponding CAD entities. Obtaining the CAD entities that make up a physical part or component has its obvious advantages in the areas of reverse engineering and design.

This paper focuses on the current research involving the ACIS® Geometric Modeler to create surfaces from CMM touch trigger probe scanned data. Techniques are developed for edge and surface creation, building up a representation of the 3D data in visually understandable entities.

1   Introduction

A Co-ordinate Measuring Machine (CMM) can be thought of as a Cartesian robot with a probe tip instead of a gripper, or end effector. This is used in the inspection process for the precision collection of 3D data of physical parts. This may involve measuring of geometric features, or the scanning of boundaries or surfaces, resulting in co-ordinate point data. However, it would be of an advantage to have the data in a form similar to that used by CAD systems. Representing the scan data in a form that can be used by CAD systems is thus an important area of research, involving surface modelling and labelling.

2   Data collection

Contact measurement is performed, involving the touch-trigger spherical probe of the CMM. This allows a more flexible measuring of geometric features and shapes, from a pre-defined datum. Manipulation of the point data is concerned with the further representation of this data, involving curves and surfaces. Data can be collected using two main methods (a)Point to point and (b) Scanning. Both methods of data collection have been used to base the modelling stage upon. Point to point data collection has the advantage of being in a uniform grid-like form. This is useful in the surface generation stage. Scan data is denser, and will fit the measured surface closer. Data in this form is generally preferred.

2.1 Point to Point

Data is collected literally from one co-ordinate to the next, in a pecking action. This can be slow and tedious, but can result in a much more accurate positioning of data points. For example, a rectangular grid of points can be collected (Figure 1).
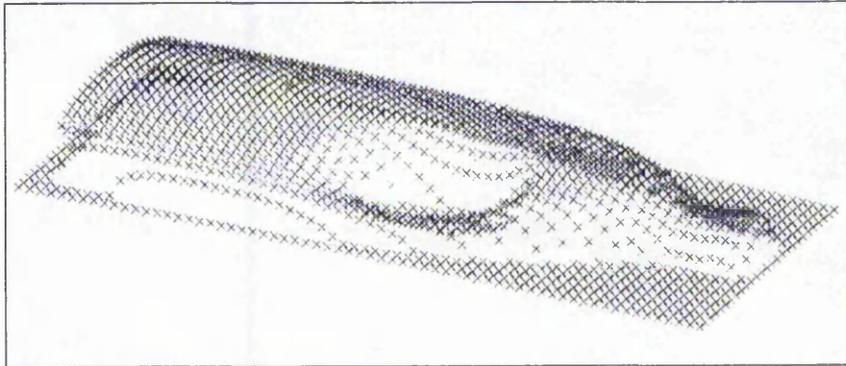

Figure 1.Grid of Collected Points.

2.2 Scanning

Scanning methods result in either uni-directional or bi-directional scan lines, of a set step distance apart. The data is collected along a scan line at arbitrary intervals at a high density. This process is much faster than Point to point data collection (Figure 2).
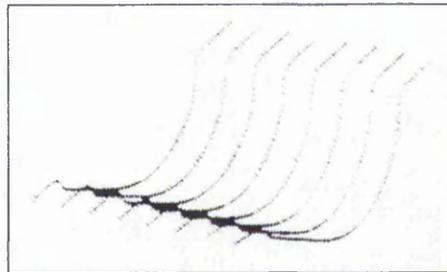
Figure 2. Uni-directional Scan Lines

2.3 Output File Format

There are a number of languages used in conjunction with the CMM. CMES (Co-ordinate Measuring Language) is specific to the LK Company Ltd. The format for the output data, using this CMES language, needs conversion software to create files capable of being viewed in the ACIS® environment. ACIS® is a geometric CAD development tool containing functionality necessary for this work.

More recently, the DMIS (Dimensional Measuring Interface Standard) language has been used, which, in this case, is capable of creating an output file in the native ACIS® text file format. Thus no file conversion is necessary. DMIS allows the portability necessary in the integration of CAD and CMMs, by its bi-directional communications [1]. This file format is compatible with some existing CAD packages, such as AutoCAD, and can be readily viewed in ACIS® applications. As the CMM collects data in a co-ordinate point form, this is all the output files contain. The ACIS® modeller can then used to represent this data in terms of curves and surfaces.

3 Modelling

Modelling of the measured part is the starting point in reverse engineering. As such, it is desirable to fully integrate modelling with the measuring process as much as possible. Inspection processes too can also benefit from these computer models.

3D boundary representations and definitions of the data point co-ordinates are achieved initially using wire-frame models which should have the ability to be fully rendered in real-time. The ability to model boundaries and surfaces using spline and surface patch technology is of importance to this work. ACIS® is being used in the representation of curves and surfaces to describe the surface model. The underlying principles of the modelling system use a Non Uniform Rational β-Spline or NURBS representation. This can be viewed as the ratio of two non uniform β-splines and is able to represent free-form curves and surfaces, conic curves, and quadric surfaces [2].

The modelling process can be broken down into three main stages.

3.1 Curve fitting

The first stage in tackling this problem involves building up curve representations of the data points. Bezier and β-Spline curves are often used for this purpose. In this way, points along the scan lines can be expressed as a cubic spline curve. This involves taking each scan line, and passing a spline through the points. Uni-directionally collected scan line data give parallel spline curves, whereas bi-directional scanning gives a network of spline curves. Curves are first generated using the same number of data points on each curve. In the initial case, using the grid data (Figure 3), and then scan data.
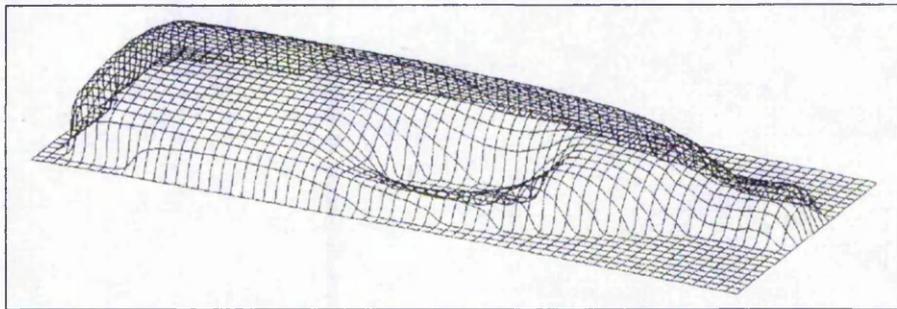

Figure 3. Network of bi-directional spline curves.

As inspection generally results in scan lines, the formation of a spline network from this data format is being examined. Once a spline network is present over the data points, the next stages of modelling are the same. The difference lies in the data collection techniques.

3.2 Patch creation

These bi-directional spline curves can be used to represent sub-surfaces, or patches, where the surface of each patch is enclosed within the regular grid lines of corresponding splines. Thus, initially, rectangular shaped patches are concentrated upon. Creating these patches involves forming a loop of sub-edges, enclosing a single patch. Each spline must interpolate the given data points with knot points forming the patch corners. Spline segments between these knot points are best-fits of the intermediate points. This is dependent on how close the curve must fit the data points. This must occur bi-directionally to allow a regular surface patch grid to be formed, where the corner points are the fixed knots. Collecting data in the point to point form readily lends itself to this technique of patch creation. In data collection using scan lines, least square approximations of the curves are necessary to attain bi-cubic surface patches.

3.3 Surface modelling using patch-to-patch continuity

Patch methods involve the connecting of adjacent patches, allowing the continuity conditions present in the original spline curves, to form a smooth bi-cubic surface. C^0 continuity is the minimum condition, allowing connection of the patch boundary edges [3]. As cubic splines are

being used, a continuity of at least C^2 should be maintained. There are various patch technologies often used, such as β-Spline, Coons [3], Bezier [4], and Hermite methods [5], each displaying attributes suited to a particular set of conditions, but also having associated problems [6].

At present, functions supplied with the ACIS® modeller are being used to convert part data collected using the CMM into curve and surface information. The resulting model can be analysed and viewed as a 3D object. Figures 4 and 5 refer to patches of differing sizes, covering the same surface, displaying C^0 continuity.
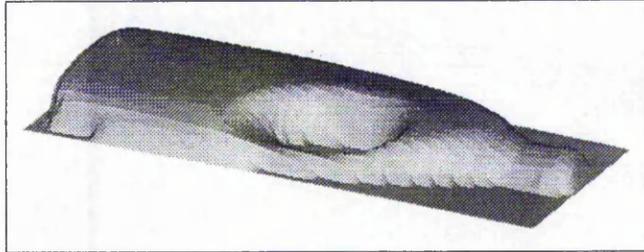
Figure 4. C^0 continuity with minimum patch size (64 x 26 patches covering surface).

A further stage which is desired is to convert the NURBS representations of the part into the CAD primitives CAD workstations actually use. This would aid reverse engineering in a Part-to-CAD stage immensely, reducing data sizes by converting the data into simpler representations, without losing any accuracy.
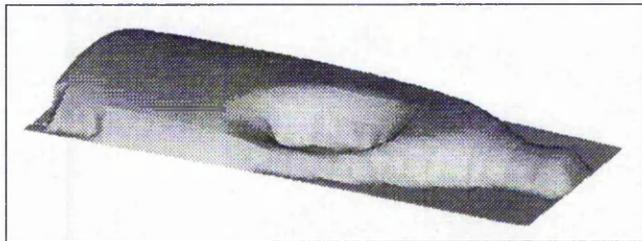

Figure 5. C^0 continuity with larger patch size (32 x 13 patches covering surface).

4   Curvature based Surface Decomposition

This alternative method of surface determination is also examined. This approach uses Gaussian and mean curvature in the locality of a data point to associate one of 8 possible surface type labels to that data point [7][8]. Several contiguous regions are formed by grouping points having the same surface type label. This operation effectively segments the surface into sub-surfaces. Local surface patches can be labelled according to their surface properties, based on the point data obtained. This area has applications where local surfaces based on Gaussian and mean curvature will allow a way of segmenting data to map to corresponding CAD entities.

This method relies on the high density of data collected, and thus is suited to optical, non-contact scanning. From the optical scan data, segmentation of the modelled surface can be achieved quickly and be used to determine where an accurate touch-trigger scan on critical data should take place. An area on the surface which has been determined as being planar would need very few data points, whereas an area of high curvature would need more detail. The collected surface data can then be classified as CAD entities. This leads to automation of the inspection process and a reduction of inspection time.

5 Conclusion and Future Work

Integrating CMM data collection with the modelling stage is of importance, in particular in the area of reverse engineering. This modelling stage involves creating accurate surface models from CMM point data. A further enhancement which is desired by industry is the conversion of the geometric model to the CAD entities, such that synthesied data can be fed into existing CAD systems for reverse engineering purposes.

Integrating non-contact and contact data collection is envisaged to greatly reduce data collection times, as well as increase the accuracy of the final model. This will be achieved using optical scanning techniques in conjunction with curvature based methods. Also, contact data collection techniques will be examined, incorporating bi-directional scan data collection and the methods discussed will be used together to create surfaces, and modify surface boundaries, where necessary.

6 Acknowledgements

7 References

1   Krejci, J; Application Software, *Co-ordinate Measuring Machines and Systems*. Edited by Bosch, J. Dekker 1995.

2   Barsky, B; Rational Beta-Splines for Representing Curves and Surfaces, *IEEE Computer Graphics & Applications*, pp 24-32. November, 1993.

3   Farin, G; *Curves and Surfaces for Computer Aided Geometric Design, A Practical Guide. 2nd. Ed.*, Academic Press, 1990.

4   Suh, S & Lee, S; Compensating probe radius in free surface modeling with CMM, *Proc. 4th Int. Conf. On Computer Integrated Manufacturing & Automation Technology*, pp. 222-7. IEEE, Comput. Soc. Press 1994.

5   Duffie, N & Feng, S; Modification of Bicubic Surface Patches Using Least-Squares Fitting Techniques, *Computers in Mechanical. Engineering*, September 1985.

6   Seiler, A, Balendran, V, Sivayoganathan, K, Sackfield, A; Reverse Engineering from Uni-directional CMM Scan Data, *Int Jnl Advanced Manufacturing Technology (11)* pp 276-284. 1996.

7   Besl, P.J; The Free-Form Surface Matching Problem, *Machine Vision for 3D Scenes*, Academic Press, Inc. 1990

8   Balendran, V, Sivayoganathan, K, Howarth, M   Sensor aided fettling, *Proceedings of the Eighth National Conference on Manufacturing Research*, pp.132-136.1992.

OPTIMISING SURFACE MODELLING TECHNIQUES

R. Bardell, V. Balendran and K. Sivayoganathan

Department of Mechanical & Manufacturing Engineering,

The Nottingham Trent University, Nottingham, UK.

ABSTRACT

Surface modelling techniques play a large role in Part-to-CAD engineering, an area of reverse engineering which is expanding due to the improved capability of existing modelling systems.

Representing point data, collected by a Co-ordinate Measuring Machine (CMM), in terms of wire-frame and surface models is seen as an important step towards improving surface model accuracy, as well as allowing the integration of data collection and modelling. Creating accurate surfaces whilst maintaining continuity conditions is a key aim of this work.

This paper focuses on current research, investigating the optimisation of surface model continuity, including error estimation as an essential stage in this process. Two methods of surface patch formation, using the ACIS® 3D Toolkit, are examined in conjunction with Gaussian and mean curvature techniques. These methods may improve the surface accuracy, particularly on key features of complex surface models. These are especially used in areas of extreme curvature change.

Keywords: Surface modelling, continuity, error estimation.

INTRODUCTION

A Co-ordinate Measuring Machine (CMM) is used for the precision inspection of physical parts, involving the measurement of geometric features, or the scanning of surfaces. This results in co-ordinate point data, which can be represented as a surface model. This visual representation can be used as a way of assessing the accuracy of the collected data. ACIS® is a geometric CAD development tool containing the functionality necessary for this work, in the form of C++ functions which can interface with an application. Figure 1 outlines this process.
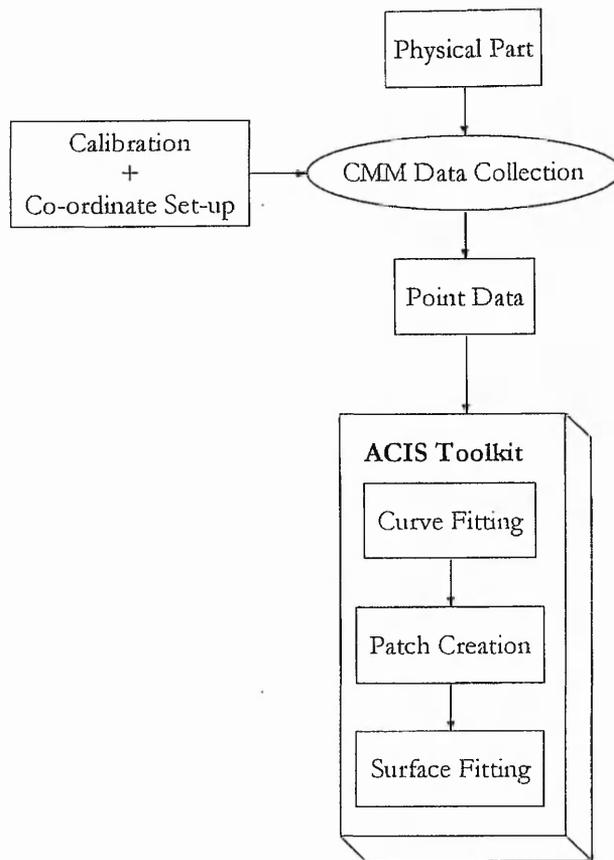
Figure 1: Outline of Part-to-CAD Process.

DATA COLLECTION USING THE CMM

Data can be obtained using two main methods; non-contact and contact measurement. Non-contact optical laser probes are mainly based on the principle of triangulation (Keat et al, 1992), (Zhuang et al, 1995). These are fast at inspecting, but the speed can compromise the accuracy. Other limitations are the size of the spot of the laser, and that only dark surfaces can be measured in stable, light conditions. These limitations result in non-contact CMM probes being rarely used at present. It is possible to have the CMM perform non-contact measuring, (Cheng and Menq, 1995). However due to these limitations, and the nature of this study, work concentrates on contact measuring.

Contact Probe CMM Fundamentals

Contact measurement involves the touch-trigger spherical probe of the CMM. This causes flexible measuring of geometric features and shapes, from a pre-defined datum. The probe is made up of a number of components which can be seen in Figure 2.

The measuring system components are the 3-axes mechanical set-up, the probe head, control unit and PC. The CMM used here, (in the Nottingham Trent University's Manufacturing Automation Research Group), is the LK horizontal arm CMM, using a touch-trigger probe. The sensor mount is attached to the CMM, and the probe tip is the part which actually touches the surface of the object to be measured. When this occurs, a point is recorded.
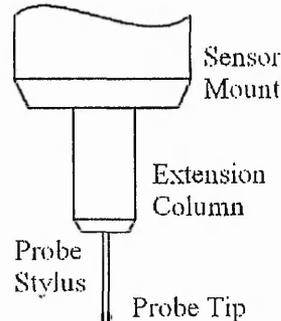
Figure 2: Contact Probe Components.

Data Collection Methods

Data collection can be achieved manually or automatically. Manual inspection can be tedious, depending on the complexity and size of the part to be measured. Its main advantage is that data can be collected at specific areas, without the need for any recursive processes or programming. In this case the CMM is controlled interactively, using a joy-pad and the user terminal.

Automatic inspection is more accurate than manual inspection, as the positioning of the CMM is more precise. This mode involves the creation of a part program. By generating part programs, the process is faster, more repeatable, and accurate, thus automatic usage of the CMM is preferred.

Two forms of automatic data collection are used in this work; (i) point to point and (ii) scanning.

Point to point data collection results in a rectangular grid of points collected from the part, by literally recording points from one co-ordinate to the next, as can be seen in Figure 3.
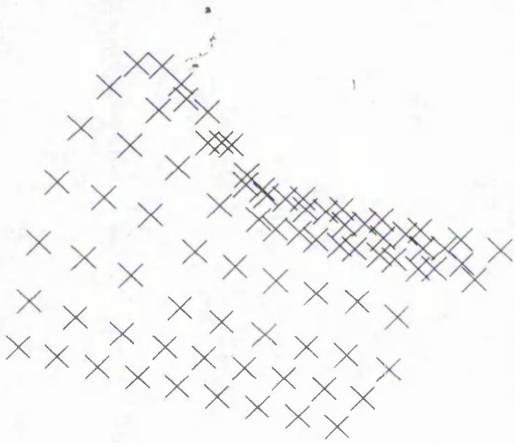
Figure 3: Point to point collected data.
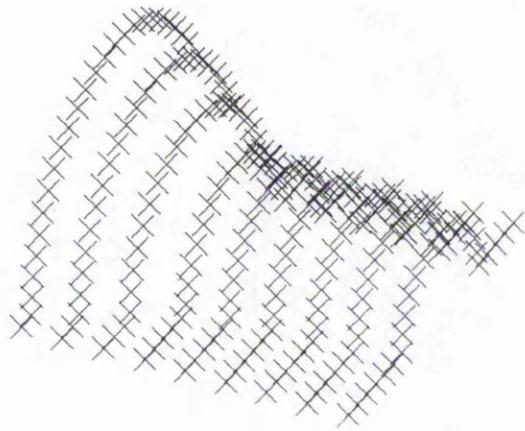
Figure 4: Scan data.

Scanning results in uni-directional scan lines, of a set step distance apart. The data points along this scan line are at arbitrary intervals, but at a high density. An example of this is seen in Figure 4.

The use of scan lines is a relatively recent development (Seiler, 1994) which allows data to be collected faster and denser than the previous point to point method of data collection. This denser data aids model accuracy where a complex surface is present, thus is generally preferred.

SURFACE MODELLING USING ACIS®

Solid modellers, such as ACIS® have proved to aid Computer Aided Geometric Design (CAGD) research in a number of areas (Medland et al, 1992), (Rahman et al, 1992). Boundary representation is used by ACIS®, where the geometry defines the points, curves and surfaces of the model, working with sculptured surface geometry based on Non-Uniform Rational B-Splines (NURBS), (ACIS, 1996). ACIS® allows wire-frame and surface model representations. Wire-frame models are defined by its edges and vertices, whereas a surface model can also define an object by its visible faces. It is this area of surface modelling which is of interest here.

Surface Modelling Fundamentals

CMM output results in point data in a Cartesian co-ordinate form. This point data forms the input to the modelling stage, where ACIS® is used to represent this data in terms of curves and surfaces. This modelling process can be broken down into three main stages:

- **Curve fitting**

The first stage involves interpolating the data points to form a continuous cubic spline. It is necessary to obtain a lattice or net of these splines, for the next stage of modelling, thus this curve fitting is done bi- directionally (Figure 5).

It is important to maintain the conjunction of knot points on intersecting curves, thus chord length parameterisation was performed, allowing the formation of curves which interpolate parameter points in both U and V directions where:

Figure 5: Network of spline curves.

$$0 \leq U \leq 1 \text{ and } 0 \leq V \leq 1$$

From this spline net, Bezier surface patches can be created.

- **Patch creation**

These spline curves can be used to approximate sub-surfaces, or patches, where the surface of each patch is enclosed within the boundary of four adjoining spline segments. Each spline interpolates the knot points on the corresponding patch boundary, with start and end points forming the patch corners. There are many surface patch methods such as Coons (Yau and Menq, 1990), Bezier (Suh and Lee, 1994), Hermite (Duffie and Feng, 1985) and Ferguson, (Lee et al, 1990). Each is suitable for different circumstances, however each also has associated problems (Seiler et al, 1996). Any created model needs to be validated and verified for accuracy, compared with the collected data and the original prototype, for acceptance. Faceting of the surface can be achieved by using the point to point data method of inspection, resulting in a surface patch model displaying C^0 continuity (Bardell et al, 1997). The model can be refined by introducing continuity within each patch, based on the parameterisation, approximating a C^1 continuous surface patch model. This can be seen in Figure 6.

Figure 6: C^1 Surface patch model.

- **Surface modelling**

Surface modelling involves connecting the adjacent patches using patch-to-patch continuity. This approximates the original spline curves' continuity, resulting in a smooth surface. A large area which CAD systems do not seem to have many operations in, is the surface analysis and comparison stage. This error mapping stage is essential to verify the models' accuracy, especially in the area of reverse engineering.

ERROR MAPPING

Accuracy is paramount, as surfaces are created based on accurate CMM point data, or from curves fitted through the point data. Accuracy analysis allows a comparison of the point on the fitted model with the corresponding digitised point. Tolerancing methods can involve determining the U and V values on a surface patch of size mxn which are closest to the i'th data point. A deviation analysis tolerancing stage is proposed where the correlation between original data points and points on a generated surface must be maintained, within defined tolerances. This is with the aim of estimating the surface model deviation error, as seen in equation (1).

$$Error_i = Fp_i(U,V) - Dp_i(U,V)$$

(1)

where:

Fp$_i$(U,V) is the i'th fitted point

Dp$_i$(U,V) is the i'th digitised point

Error analysis is a useful tool in the generation of accurate complex surface models, within tolerance. However, areas of a complex model can suffer inaccuracies from the patch formation stage. These modelling errors can be seen at the boundary in Figure 6. These errors can be classified as patch scooping inaccuracies. These areas at internal and external boundaries are caused by extreme curvature change.

MINIMISING EXTREME CURVATURE CHANGE ERRORS

This phenomenon is typical for rectangular Bezier patches which do not handle cusps where the patch boundary wire-frame curves force a Bezier patch to have two tangent sides (Sarraga, 1990). In order to improve boundary edge continuity, patch shapes other than rectangular patches, parameterised in a UV orientation, were investigated. The chosen patch shape was a diamond shaped patch, parameterised in a ST orientation. Many surfaces can be accurately modelled using the methods described here, using rectangle and diamond patches. However there are conditions where a curvature can change so sharply that usual patch methods will not suffice. Such areas are at internal and external boundaries, where a curved surface may abruptly meet a planar 'base' surface. An alternative proposed method is offered as a solution to this common problem; Gaussian and mean curvature methods.

Diamond Patch Creation

Diamond shaped patches were created, based on the original scan data. This formed similar steps to the formation of rectangular patches. However curve parameterisation occurred allowing the formation of curves which interpolate parameter points in both S and T directions, where:

$0 \leq S \leq 1$ and $0 \leq T \leq 1$

This is shown in Figures 9 and 10.
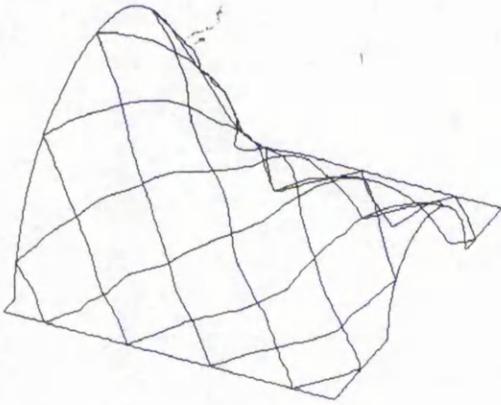
Figure 9: Network of spline curves.
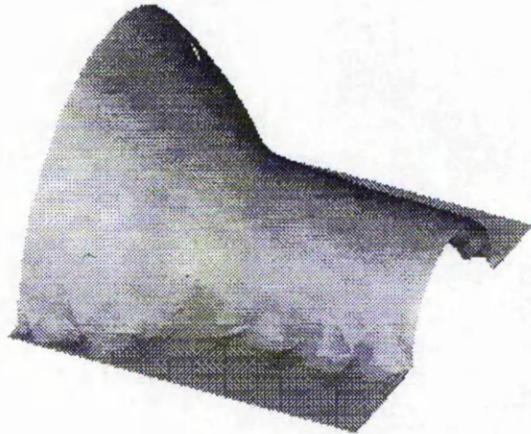
Figure 10: Surface patch model using diamond patches.

Gaussian and Mean Curvature Methods

As an alternative method towards a solution to this problem, it is proposed that complex surface modelling techniques will benefit from the use of Gaussian and mean curvature based decomposition. This allocates one of eight possible surface type labels to each data point (Besl, 1990), (Balendran et al, 1992). In this way, adjacent points of similar type label can be grouped together. This actively decomposes a total surface into sub-surfaces, allowing boundary edges to be defined. Each separate surface type can then be modelled separately, and then blended together, thus avoiding the associated problems with the extreme changes in surface curvature. The accuracy of point data at specific areas on a complex surface model is vital and this can be maintained by the surface being segmented into smaller areas. This could allow more accurate modelling, by assigning more detail to these areas of interest in the data collection stage.

CONCLUSION

With rectangular and diamond shaped patches, the resulting surface models show that parallel patch edges allow orthogonal continuity across these patches. Surrounding a patch corner with four-sided patches ensures correct corner compatibility conditions, resulting in continuity. These give satisfactory results on many surfaces, allowing the desired continuity. However, looking at an optimum surface modelling technique must include complex surfaces, in particular cases of high curvature change. This proves to be a problem when the surface model curvature is not orthogonal to the patch boundaries. The use of rectangular and diamond patches, depending on the underlying model, can improve

model accuracy to a certain degree. As well as these two methods of surface patch formation, Gaussian and mean methods of curvature based surface decomposition offer a solution, forming on-going research. It is envisaged that Gaussian and mean curvature methods, in conjunction with patch formation methods already used, will reduce the inaccuracies encountered previously. This method relies on the high density of data collected, and thus is suited to optical, non-contact scanning.

FUTURE WORK

Triangular patches are seen as a useful modelling technique for relatively flat surfaces. This corresponds with work done by Suh and Lee (1994). Using rectangular and diamond patch shapes to create a triangular patch with the correct surface properties would be a useful tool to surface modelling. Work by Boehm (1985) shows a refinement stage for the formation of a refined triangular net, converging to the spline surface, indicating a potential direction for improvement of triangular patches. Methods of surface trimming need to be investigated and compared as an alternative to Gaussian and mean curvature based techniques.

REFERENCES

ACIS®, 1996, *Application Guide*, Spatial Technology.

Cheng, W., and Menq, C., 1995 "Integrated Laser/CMM System for the Dimensional Inspection of Objects Made of Soft Material," *Int J Adv Manuf Technol,* 10 pp. 36-45.

Balendran, V., Sivayoganathan, K., Howarth, M., 1992, "Sensor aided fettling," *Proceedings of the Eighth National Conference on Manufacturing Research*, pp.132-136.

Bardell, R., Balendran, V., and Sivayoganathan, K., 1997, "Representing Surfaces from CMM Data," *Proceedings of the Thirteenth National Conference on Manufacturing Research*, pp. 22-26.

Besl, P.J.; 1990, "The Free-Form Surface Matching Problem," *Machine Vision for 3D Scenes*, Academic Press, Inc.

Boehm, W.,1985, " Triangular spline algorithms," *Computer Aided Geometric Design,* 2 pp. 61-67.

Duffie, N., and Feng, S., 1985, "Modification of Bicubic Surface Patches Using Least-Squares Fitting Techniques," *Computers in Mechanical Engineering*, September ed. pp. 57-65.

Keat, J., Balendran, V., Sivayoganathan, K., and Sackfield, A., 1992, "3-D Data Collection for Object Recognition," *Proceedings of the Eighth National Conference on Manufacturing Research,* pp. 648-652.

Lee, A., Chen, D., and Lin, A., 1990, "CAD/CAM system from 3D Co-ordinate Measuring Data," *Int. J. Prod. Res,* **28**, no. 12 pp. 2353-2371.

Medland, A., Mullineux, G., and Rentoul, A., 1992, "Measurement of Features By a Sample-Grid Approach," *Proceedings of the Eighth National Conference on Manufacturing Research,* pp. 673-677.

Rahman, W., Harun, W., and Case, K., 1992, "Object-Oriented Feature-Based Design," *Proceedings of the Eighth National Conference on Manufacturing Research,* pp 294-298.

Sarraga, R., 1990, "Computer Modelling of Surfaces with Arbitrary Shapes," *IEEE Computer Graphics & Applications* March ed. pp. 67-77.

Seiler, A., 1994, "Reverse Engineering and CMM," *PhD thesis,* Nottingham Trent University.

Seiler, A., Balendran, V., Sivayoganathan, K., Sackfield, A.; 1996, "Reverse Engineering from Uni-directional CMM Scan Data," *Int Jnl Advanced Manufacturing Technology,* **11** pp. 276-284.

Suh, S., and Lee, S.; 1994, "Compensating probe radius in free surface modeling with CMM," *Proc. 4th Int. Conf. On Computer Integrated Manufacturing & Automation Technology,* IEEE, Comput. Soc. Press, pp. 222-7.

Yau, H., and Menq, C., 1990, "The Development of an Intelligent Dimensional Inspection Environment in Manufacturing," *Japan-USA Symposium on Flexible Automation,* pp. 1059-1065.

Zhuang, B., Zhang, J., Jiang, C., Li, Z., and Zhang, W., 1995, "Precision Laser Triangulation Range Sensor with Double Detectors for Measurement on CMMs," *Int. Soc. for Optical Engineering, Proc. of SPIE,* **2349**, pp. 44-52.

Refinement and Modelling of CMM Data.

R. Bardell, K. Sivayoganathan and V. Balendran

ABSTRACT

The Co-ordinate Measuring Machine (CMM), is a Cartesian robot used to collect relevant data from physical parts. Representing this point data as a surface model is a major step in reverse engineering. However, surface model generation can cause inaccuracies, originating from both the data collection and modelling stages.

This paper presents a method of model refinement, based on trimming planes, using the ACIS® Toolkit as the geometric engine to perform this task. 2D trim planes are presented and a method of 3D boundary trimming is proposed.

1 INTRODUCTION

In its initial stages, the Reverse Engineering (RE) industry relies heavily on the accurate surface data acquisition of a physical prototype. The Co-ordinate Measuring Machine (CMM) has proved to be successful at this task, collecting point data to an accuracy of one micron (1). This 3D data is then applied to generating a surface model, in a Part-to-CAD stage. The accuracy of this model is paramount, relating to areas such as physical reproduction of CAD models, and accuracy analysis.

The accuracy of a created surface model can be improved, by implementing surface refinement methods as a means of reducing modelling errors. This in turn reduces machining errors.

2 REVERSE ENGINEERING

Conventional engineering involves the stages of concept design, using Computer Aided Design (CAD), and results in the creation of a physical part, via the creation of a machining part program, utilising Computer Numerically Controlled (CNC) machining.

RE is the reverse process, and can be defined as: 'Systematic evaluation of a product with the purpose of replication. This involves either direct copies or adding improvements to existing design' (2). RE comprises of three main areas, outlined in the following sections.

2.1 Data Collection using the CMM

3D point data is usually collected automatically, using either point to point or scanning methods. Scanning methods are usually preferred, having improved accuracy and speed due to the fast pecking action of the probe on the surface. CMM scanning takes place uni-directionally or bi-directionally across a surface, physically touching the part in question with a spherical probe.

A problem with contact probe data collection is the issue of probe compensation. Despite the fact that the probe makes contact with the surface on its circumference, the recorded point is taken at the centre of the probe. Thus the point on the actual surface differs from the recorded point by the probe radius. In the generation of a surface model, it is essential that this is taken into account by offsetting the surface by this probe radius.

In most cases, the collection of data involves placing the object on a planar 'bed'. This is due to most scanning algorithms requiring a regular quadrilateral boundary within which data is collected.

2.2 Data Modelling

The modelling of CMM data in this work is achieved using ACIS®, a CAD development tool which is interfaced using the C++ language. This results in a CAD surface model, based on the collected points. This process forms a number of stages.

Uni-directional scanning results in a series of parallel scan lines made up of dense data points. These scan points are interpolated, forming uni-directional spline curves as shown in figure 1. The quadrilateral boundaries as mentioned previously can be seen here by the extents of the excess data which is not needed.
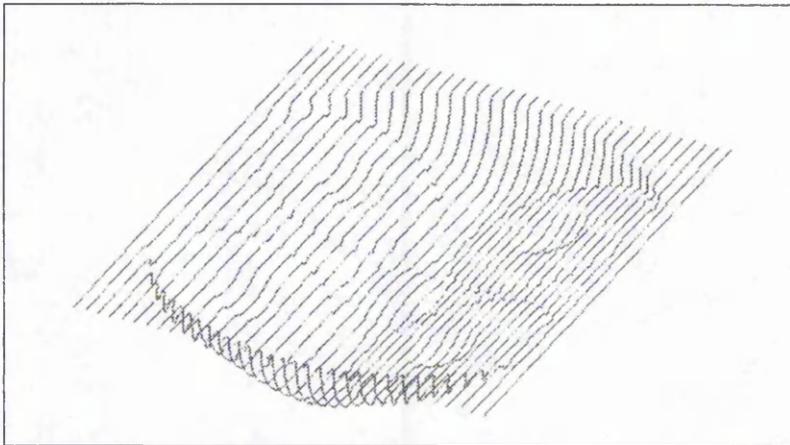

Figure 1 Uni-directional Scan Data Lines

(data collected by LK Ltd.)

Knot points are introduced at intervals along these splines in order to form perpendicular spline curves necessary for the generation of a spline network. From this spline network, patch boundary curves and tangent vectors are used to create a composite surface made up of tangent continuous (C^1) Gregory/Charrot patches.

The point to point method of data collection has the advantage of allowing the direct generation of a surface model from data points, without knot insertion (3). However this limits continuity conditions.

From a surface model it is possible to create machining paths in a CAD-to-Part stage, as well as analyse the generated surface for accuracy.

2.3 Machining

CAD surface information can be used to create part programs for CNC machines, causing the original measured part to be reverse engineered. As well as creating a physical model, this stage also forms an additional error determination stage, as inspection of this new model can take place.

It is important to assess a surface, as its accuracy cannot be assumed merely because accurate point data is used. Thus an accuracy analysis stage completes the RE process.

2.4 Accuracy Analysis

Surface assessment is a necessary step, both for aesthetic and functional properties (1). This usually takes the form of physical assessment, with contact inspection based on a reverse engineered model. However, assessing the CAD model can save time and money in the RE process. Basic numerical analysis involves positional and tangency continuity constraints, examining both inter-point and inter-patch continuity.

Deviation analysis allows the comparison of a point on the fitted model with the corresponding (closest) digitised point. The close correlation between original data points and points on a generated surface must be maintained, within defined tolerances, with the aim of estimating the surface model deviation. This stage also encompasses comparative analysis, where an optimum level of accuracy should be established, based on parameter optimisation.

3 MODEL REFINEMENT

It is not known if a set of data points will generate an adequate surface model until the modelling stage is complete. In some cases, if the data collected is inadequate, further data collection can take place. Often, however, it is unfeasible to return to a physical part once data collection has taken place. Where this is the case, a degree of manipulation of the data may be necessary to improve the surface accuracy.

Model refinement is possible at object boundaries, aiming to improve the accuracy of the model, at areas prone to errors. This involves the trimming and extension of surfaces to reduce the errors in modelling which occur due to high curvature change. These problems occur in both convex and concave areas on a surface, but in particular where data cannot be collected at concave corners approaching a right angle. This is due to the spherical nature of the probe. An additional problem is caused by the continuous nature of spline interpolation (4). This problem is highlighted in figure 2, where the surface deviates from its desired position at areas of high curvature change, resulting in a smoothing of the corner at the base of the object. Here all the collected data is wanted, thus it is necessary to refine the surface model at these areas to improve accuracy.
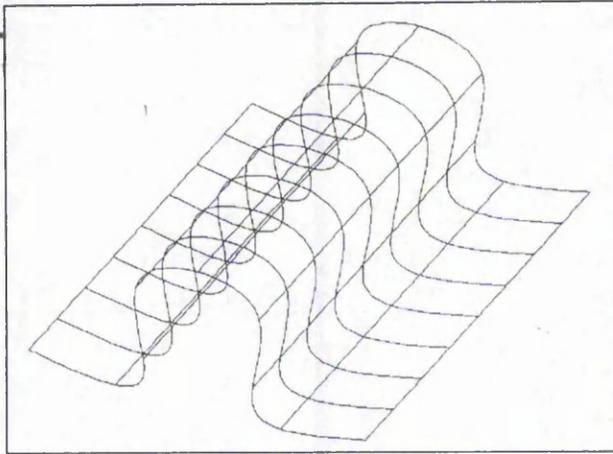
Figure 2 Surface Deviation

3.1 2D Boundary Trimming

There are two main applications for planar (2D) trimming.

1) In areas where minimal data was collected due to probing constraints at concave areas, causing surface deviations, as seen in figure 2.

2) Where the data collection stage requires quadrilateral boundaries around the object to be inspected, causing excess data, as seen in figure 1.

2D boundary trimming involves the automatic creation of a trimming plane at or near the base plane of the object. This refines the surface model by improving the surface accuracy at concave areas on the surface model where minimal data was collected. This reduces the surface deviation, improving the accuracy of the refined model, as compared with the original model.

This form of model refinement allows discontinuities such as sharp corners to be modelled, as seen in figure 3, where data is manipulated and remodelled.
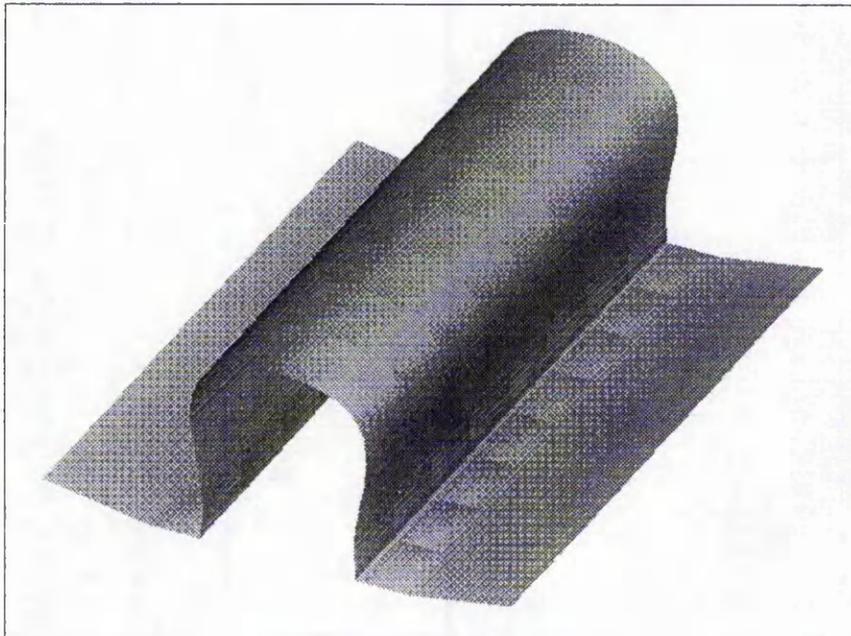

Figure 3 Refined Surface Model with Improved Data Fitting

In some cases excess data is modelled. This due to the nature of artificially creating quadrilateral boundaries around objects, as required for the data collection stage. This causes continuity problems as seen in figure 2, which would be reduced if data was trimmed to where data is actually needed. Figure 4 shows a refined surface model, where trimmed data is discarded, reducing the surface area. This greatly benefits the speed of accuracy analysis stages, as only wanted points are analysed for deviation.
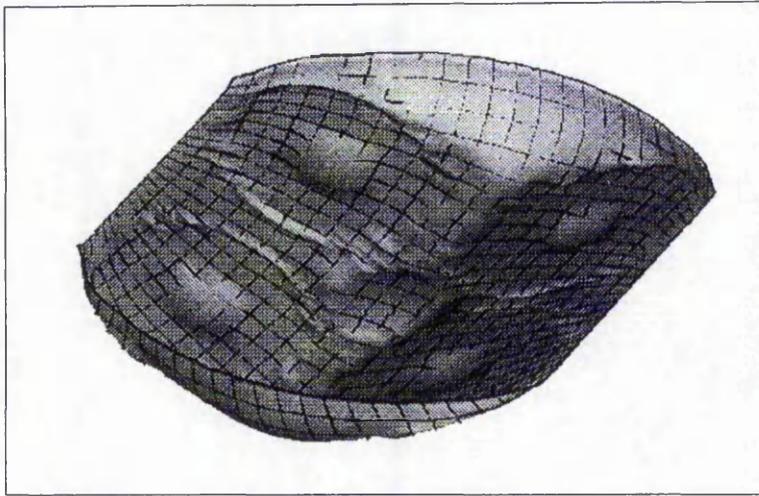

Figure 4   Refined Surface Model, with Discarded Excess Data

2D trimming is only effective with surfaces with a planar boundary. This is the case with most CMM scanned external boundaries, due to the need for a planar 'bed'. However, internal boundaries of features will inevitably have 3D boundaries.

3.2 3D Boundary Trimming

Creating 3D boundaries around internal features is proposed as a method of improving the accuracy of the overall model. This relies on segmenting the surface, creating 3D sub-surface trim boundaries. Each sub-surface can be trimmed along its corresponding boundary and then be modelled separately.

This uses the methods of Gaussian and Mean curvature based decomposition to create 3D boundaries from point data. Each data point is associated with one of eight possible surface type labels (5). These are given as peak, pit, ridge, valley, saddle ridge, saddle valley, flat and minimal (6). Automatic edge detection is then possible, and from this, surface refinement can occur.

4 CONCLUSION AND FUTURE WORK

Errors are expected at the data collection stage, and in most cases these are inevitable, such as collecting data from concave corners. In some objects, corners are present, but in many cases, corners are introduced into a data set due to the functionality of scanning routines. This involves unnecessary corners between the wanted object and the planar 'bed' necessary for scanning routines.

This paper shows how 2D trim planes can be used to improve the accuracy of a surface model by modifying data and introducing corners in areas where inadequate data was

collected. 2D trim planes can also be used to discard unnecessary data which is unavoidably collected by the CMM contact measuring method of unidirectional scan lines. This results in a reduction of the data set for processing tasks, such as accuracy analysis.

Gaussian and Mean curvature based methods aim to define internal boundaries, improving model accuracy. Fitting sub-surfaces within defined internal boundaries may lead to greater overall surface accuracy.

This model refinement stage improves the accuracy of surface models at areas of high curvature, such as boundaries between differing surface types, as well as offering a computationally effective means of obtaining smaller data files.

Improvements to surface accuracy can occur by the use of bi-directional scan lines. This would more accurately define both 2D and 3D boundaries. The data collection stage can be further enhanced by implementing methods of using a 3D boundary, bounding the object to be measured, rather than the usual 2D quadrilateral boundary. This external 3D boundary can then be used in the modelling stage.

5 ACKNOWLEDGEMENTS

6 REFERENCES

1 Smith, G., Hill, T., Rockliffe, S., and Harris, J., 1994, 'Geometric Assessment of Sculptured Features', *Proceedings of the Tenth National Conference on Manufacturing Research*, pp. 663-667.
2 Aronson, R., 1996, 'Forward Thinkers take to RE', *Man Engineer*, Nov ed., pp. 34-44.
3 Bardell, R., Balendran, V., and Sivayoganathan, K., 1997, 'Representing Surfaces from CMM Data,' *Proceedings of the Thirteen National Conference on Manufacturing Research*, pp.22-26.
4 Sarraga, R., 1990, 'Computer Modelling of Surfaces with Arbitrary Shapes', *IEEE Computer Graphics & Applications*, vol. 10, no. 2, pp. 67-77.
5 Balendran, V., Sivayoganathan, K., and Howarth, M., 1992, 'Sensor Aided Fettling', *Proceedings of the Eighth National Conference on Manufacturing Research*, pp.132-136.
6 Besl, P., and Jain, R., 1988, *'Range Image Segmentation'*, Algorithms, Architectures and Systems, ed. H. Freeman, Academic Press.

Accuracy Analysis of 3D Data Collection and Free-Form Modelling Methods.

R.Bardell, V. Balendran and K. Sivayoganathan.

Department of Mechanical and Manufacturing Engineering, Nottingham Trent University, Burton Street, Nottingham, UK.

In industrial applications such as the automotive industry, it is often necessary to design and manufacture surfaces to a desired smoothness. Without a mathematical model of the surface, it is difficult to confirm that a manufactured surface conforms to the desired specifications. Inspection of the part is necessary for this verification, but this can also succumb to inaccuracies.

This paper offers a method of automating the verification of an acceptable free-form surface, using the Coordinate Measuring Machine (CMM) as a means of collecting data from the surface in question.

1. INTRODUCTION

It has always been difficult to ascertain when a physical surface has the required 'property' of smoothness. This can be dependant on the function of the part in question, or for aesthetic properties [1]. Reflection lines have been used in the past to analyse a surfaces curvature [2], but this relies largely on the designers judgement. Inspection of the part can verify this surface, however all data collection and inspection devices, including the CMM, can be prone to inaccuracies. This can alter the resulting shape or 'feel' of the part.

Analysing the collected data using 3D modelling software, can allow discrepancies in data collection to be highlighted. This can also determine if the original free-form surface is at fault. If this is the case, a method of surface smoothness improvement, based on a Reverse Engineering (RE) machining stage is essential.

2. DATA COLLECTION

Data collection can be achieved using a number of devices; in this study the Coordinate Measuring Machine (CMM) is used. The CMM is a Cartesian robot which has a contact trigger probe in place of a gripper, and is used for the accurate 3D data collection and inspection of physical parts. Despite the need for direct contact with the surface, which can be time consuming, the CMM records data to higher degrees of accuracy than other inspection methods, such as optical scanners and CCD cameras [1].

The fastest method of CMM contact measurement is uni-directional scanning, where the probe 'pecks' the surface in a continuous manner, resulting in scan lines. This is the

method employed throughout this paper, where the overall accuracy depends on the continuity of the original surface and the density of the collected data.

The length and direction of each scan line, as well as the number of scan lines is defined. The CMM is then initialised and data collection can commence on the surface. In the case of an off-line system, the 3D co-ordinate points are saved to a data file. Surface generation is based directly on fitting a surface through these collected data points.

3. AUTOMATED FREE-FORM SURFACE MODELLING

Various Computer Aided Design (CAD) surface modelling methods are available for this process [2],[3]. The method used here involves Gregory patch formation as the basis of surface model creation [4]. Automated surface model generation results in a smooth, continuous surface model which is a 'best fit' of the data points, irrespective of the original surface continuity properties. This is seen as a disadvantage in general cases where the measured surface can be of a complex nature i.e. having a mixture of different surface types, as defined in [5]. However, this automated method of surface fitting can be used to ascertain the accuracy of 3D data where smooth surfaces are required. Figure 1 demonstrates a typical free-form surface model.
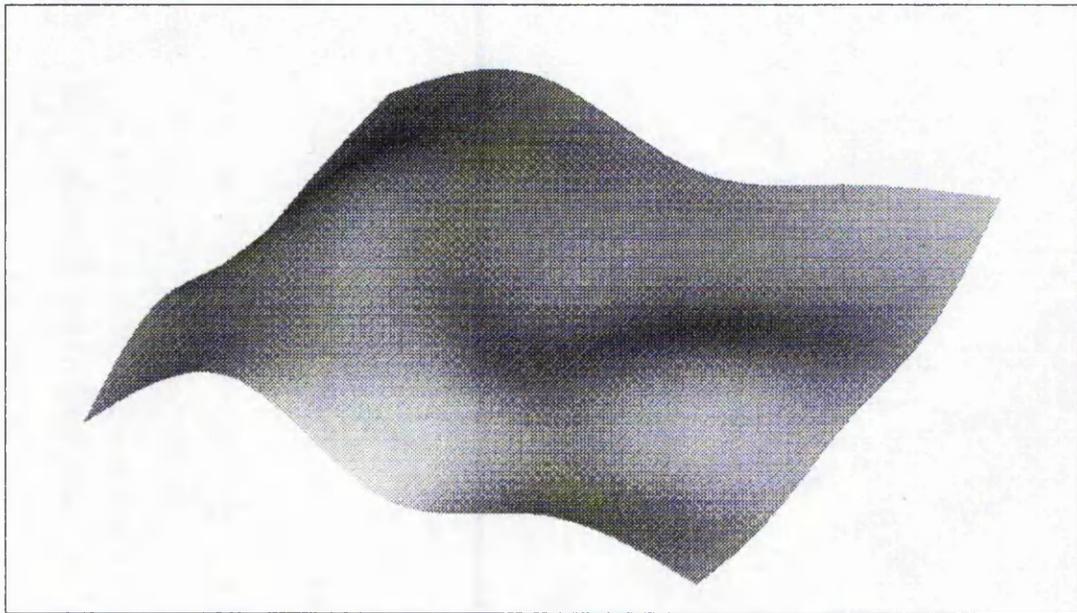

Figure 1. Free-form model from CMM Data.

Judgement could be used here to view the CAD surface and arbitrarily comment on the acceptability of a surfaces smoothness. Inaccuracies from data collection can sometimes be seen, but due to the nature of free-form surfaces these are often missed. What is needed is a method of comparing the generated surface with the original CMM data points, thus assessing the accuracy of the free-form surface.

4. ACCURACY ASSESSMENT

There is a paradox with collected data assessment involving the method of assessment. This is due to the collected data having no point of reference for comparison. The only method is to take multiple data sets of the same object and then compare them. If the variance between these are within acceptable tolerances, then the data is deemed accurate and representative of the original surface. Due to the time consuming nature of CMM contact data collection, it is advantageous to be able to ascertain the accuracy of a single data set. There are two methods employed here to assess free-form surface accuracy: Deviation Analysis, and Reverse Engineering.

4.1. Deviation Analysis

Comparing the deviation between data points and the closest corresponding point on the CAD surface is a method of assessing the accuracy of 3D data of free-form surfaces [6]. Where a surface is assumed to be free-form, there should be a direct correlation between the data points, and points on the CAD surface.

Within the scope of this work, surfaces are assumed to be free-form, thus any points where high variance occur can correspond to discontinuities in the original surface, or from data collection errors. Once errors have been pin-pointed, the data set can be edited, or further data collection can take place to verify the source of the error. An alternative is to use the 'best-fit' CAD surface to reproduce a second physical surface. This would be appropriate where the original surface has been found to contain unwanted discontinuities. This method involves the process of Reverse Engineering.

4.2. Reverse Engineering (RE)

RE is concerned with reproducing a physical prototype, by means of data collection and CAD modelling. This CAD model is then used to obtain surface information for the reproduction machining stage.

The 'best-fit' CAD surface is used to generate point information and cutter paths to control Computer Numerically Controlled (CNC) machines to accurately reproduce the surface. This secondary physical surface can then be inspected using the CMM. The data set for this is used to generate a Reverse Engineered Surface (RES), using the same Gregory patch technique.

A second deviation analysis stage based on the RES, now compares the second CMM data set with the RES. This results in a very low variance between collected data and the surface model, thus showing an improvement in surface smoothness. Any errors which occurred in the first stage of data collection are now compensated for, as the RES is based on the 'best fit' smoothed CAD surface. This can be confirmed by an additional surface comparison stage.

4.3. Surface comparison

This stage highlights the differences between the original surface model and the RES. This involves defining reference points on each surface model, and direct comparison of the CAD models. Variance between these two CAD models highlight where data collection has been inaccurate, or where the original physical surface had flaws.

5. CONCLUSION

Data collection is obviously the only method of obtaining information on a physical object. With correct calibration, data collection tools are assumed to be accurate, although problems may occur which cannot be detected. In the case of free-form data collection, the desired need for smoothness is evident, and this can be used to assess both data collection accuracy, and physical part continuity.

This study allows the accuracy of CMM data to be confirmed on surface models where slight discrepancies would be very hard to detect. These inaccuracies may arise from the manufacture of the part, or from the inspection of the part. In both cases, confirmation that the manufactured surface is continuously smooth, and passes through defined points within defined thresholds, is a useful aid to quality assessment. Deviation analysis allows model verification, whilst RE is a useful tool for surface continuity improvement, as free-form modelling CMM data can improve the overall surface continuity. Surface comparison is a final stage which shows this improvement graphically.

REFERENCES

1   Smith, G., Hill, T., Rockliffe, S., and Harris, J., 1994, 'Geometric Assessment of Sculptured Features', *Proceedings of the Tenth National Conference on Manufacturing Research,* pp. 663-667.

2   Farin, G., 1990, *'Curves and Surfaces for Computer Aided Geometric Design, A Practical Guide, '.* 2nd. Ed., Academic Press.

3   Bezier, P., 1972, *Numerical Control - Mathematics and Applications,* (Translated by Forrest, A., and Pankhurst, A.) Wiley & Sons Ltd.

4   Gregory, J, 1986, *'N-Sided Surface Patches',* The Mathematics of Surfaces, ed. J. A. Gregory.

5   Besl, P., and Jain, R., 1988, 'Range Image Segmentation', *Algorithms, Architectures and Systems,* ed. H. Freeman, Academic Press.

6   Bardell, R, Balendran, V. and Sivayoganathan, K., 1998, 'Optimising Surface Modelling Techniques', *Proceedings of the Mechanics in Design International Conference,* pp. 771-779.

Accuracy Analysis of 3D Data Collection and Free-Form Modelling Methods

R.Bardell, V.Balendran, and K.Sivayoganathan
Department of Mechanical and Manufacturing Engineering, Nottingham Trent University, Burton Street, Nottingham, NG1 4BU,
United Kingdom*
e-mail: rayman.bardell@ntu.ac.uk

Abstract

In industrial applications such as the automotive industry, it is often necessary to design and manufacture surfaces to a desired smoothness. This can be achieved by Computer Aided Design (CAD) methods, or from the creation of a physical prototype. To gain an adequate feel for the part to be manufactured, physical prototype models are often made by the designer.

In the case of free-form surfaces, it can be difficult to judge the overall smoothness of the surface. The optimum smoothness, or continuity, relies on there being no continuity deviations. Without a mathematical model of the surface, it is difficult to confirm that a manufactured surface conforms to the desired specifications. The only method is by way of a designer's judgment and experience.

Thus, to accurately assess a physical surface it is necessary to inspect the part. This is with the aim of collecting accurate 3D data, allowing a 3D CAD surface to be generated. This forms a quality assessment stage. However this method of verification can also succumb to inaccuracies.

This paper offers a method of automating the verification of an acceptable free-form surface, using the Coordinate Measuring Machine (CMM) as a means of collecting data from the surface in question. Methods are proposed to analyse the surface for optimum continuity, using Computer Aided Geometric Design (CAGD), as well as assess the CMM data accuracy. This surface can be improved, if desired, using Reverse Engineering (RE) methods.

Keywords: CAD, Free-Form Surface, CMM, Quality Assessment, Continuity, CAGD, RE.

1. INTRODUCTION

The manufacture of free-form surfaces is an important part of most design-to-build applications. The criteria for objects possessing free-form surfaces can be difficult to specify, especially in cases where a physical prototype is present. A free-form surface is a surface which has a continuous, smooth surface, with no distinguishable features, or deviations in the continuity.

The smoothness of this physical surface is difficult to ascertain as this 'property' could be dependent on the function of the part, or for aesthetic reasons [1]. Where a mathematical model is absent, in the case of an initial physical prototype, the designer's judgment is often relied upon. An example of this is surface analysis using reflection lines, where the surface's curvature is analysed by visual methods [2].

Free-form surface design applications have two major problems, which are highlighted below:

- at the physical prototype stage, where a visually pleasing optimum smoothness is desired, the aesthetic properties of free-form surfaces can be difficult to ascertain.
- at the Computer Aided Design (CAD) stage, the judgment of the designer is relied upon, where model improvements usually involve manipulation of the surface's control points.

This paper concentrates on the assessment of physical prototype models, with the aim of verifying an optimum continuity.

Thus, a Quality Assessment stage is highly desired, in particular with physical objects. This is based on the generation of a CAD model, which is used to analyse the continuity of the surface. This forms a Part-to-CAD Reverse Engineering (RE) module.

The initial stage towards this goal is inspection, where sufficient data is collected from the part. Analysing the collected data using 3D modelling methods, allows discrepancies to be highlighted. These can originate from either the data collection process, or from the actual physical surface, thus determining if the original free-form surface is at fault. If this is the case, a method of surface smoothness improvement, based on a RE machining stage is essential.

2. DATA COLLECTION

Data collection can be achieved using a number of devices, such as optical scanners or CCD cameras. For the work reported here, a Co-ordinate Measuring Machine (CMM) is used. The CMM is a Cartesian robot, which has a contact trigger probe in place of a

---

* In conjunction with LK Ltd, U.K.

gripper. CMMs are Computer Numerically Controlled (CNC) machines used for the faster, flexible, and repeatable measurement of physical parts. Figure 1 outlines the typical touch-trigger probe components.
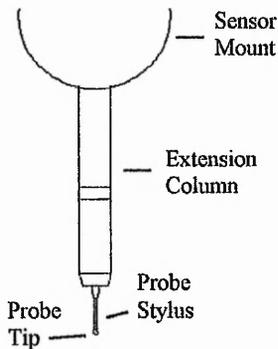

Figure 1 Touch-trigger probe components.

The major system components are the 3-axes mechanical set-up, the probe head, control unit and PC. The CMM used here is an LK horizontal arm CMM, using a Renishaw PH9 sensor mount with a touch-trigger probe.

CMMs have become very powerful pieces of measuring equipment, where practically all accessible dimensional information can be found. They are used in surface and boundary continuous probing, or scanning of parts, as well as the extraction of geometric feature information from data points. Scanning methods result in either uni-directional or bi-directional scan lines, of a set step distance apart. The data is collected along a scan line at arbitrary intervals at a high density. The use of scan lines is a more recent development which allows data to be collected much faster than the previous point-to-point method of data collection, using a 'pecking' action.

Data collection can be accomplished in both manual and automatic modes. In manual mode, one joystick controls the x and y direction and another joystick controls the z direction. Before a point can be taken, the user must use the terminal to input a command for the collection of point data. This is very tedious but is well suited to the data collection of a few specific points. To automate this process, where there is a need to take many data points, the CMM can be programmed, where part programs are generated. By generating part programs, the process is faster, and more repeatable. The CMM will take a pre-defined number of scan lines of a pre-defined step distance apart, defined in the program.

In this work, the CMM is primarily used to measure spatial or planar curves in 2D and non-prismatic 3D features. This results in a data file containing relevant information, such as Cartesian co-ordinates of a recorded position, the diameter of a pre-defined circular hole, or the distance between two edges. Work has been done to improve the CMM accuracy and speed [3], but in most cases the reduced speed vs. increased accuracy issue is unavoidable and thus accepted. This involves the density of data causing the data collection process to take longer. However dense, accurate surface information is desired, so the time taken is justified.

Despite the need for direct contact with the surface, which can be time consuming, the CMM records data to higher degrees of accuracy than other inspection methods, previously mentioned [1]. The CMM is used in surface assessment, thus the method of data collection employed here involves direct contact with the surface.

A number of scan lines are defined along the surface of the part, and the probe pecks the surface in either uni-directional or zigzag lines. The length and direction of each scan line, as well as the number of scan lines is defined. The CMM is then initialised and data collection can commence on the surface. The overall accuracy depends on the continuity of the original surface and the density of the collected data. The faster the data collection, the less dense the data on each scan line.

2.1 Probe Compensation

Despite the fact that the probe touches the surface at a particular point on its spherical circumference, the recorded point is given as the centre of the probe. Thus, the measured surface will differ from the part surface due to the radius of the CMM contact probe. In this way, the co-ordinate of a contact point must be calculated by offsetting the probe radius from the probe centre. This is essential for the later sections of surface modelling and RE. In CAGD it is preferred to compensate for probe radius after the surface modelling stage, as prior to this, the probe radius compensation direction is unknown. This is normal to the surface and can only be found once a surface is fitted through the data points.

2.2 Inspection Errors

Inspection of the part allows surface verification to take place. However, all data collection and inspection devices, including the CMM, can be prone to inaccuracies. There are many external factors that affect the accuracy of a CMM. The main ones are temperature, vibration and humidity. These conditions cannot be easily controlled in most industrial situations, but sensible use of surrounding machinery can minimise errors in data collection by trying to achieve a stable environment for inspection.

Errors can be induced if contact with the surface has not been achieved in a direction normal to the surface. This is often the case with free-form surfaces with steep gradients. These errors can be difficult to detect.

Surface generation is based directly on fitting a surface through these collected data points, and then compensating for the probe radius by offsetting the generated surface. Obviously, the denser the collected data, the closer a representative to the original surface the CAD model will be. The free-form modelling method used here can highlight potential data collection errors.

3. AUTOMATED FREE-FORM SURFACE MODELLING

After obtaining a suitable data set, automatic free-form modelling commences. There are various CAGD surface modelling methods available for this process [2], [4]. The method used here involves Gregory patch formation as the basis of surface model creation [5][6].

Parametric modelling methods involve mapping a 2D domain (u,v parameter space) to 3D space (xyz object space), where for a surface, S:

$$x = x(u,v)$$
$$y = y(u,v)$$
$$z = z(u,v)$$

where:

$0 \le u \le 1$

$0 \le v \le 1$

For curves the parameter is t, and is represented by:

$x = x(t)$

$y = y(t)$

$z = z(t)$

where:

$0 \le t \le 1$

3.1 B-Spline Interpolation

Continuity constraints are essential for the modelling of interpolating B-splines. There are different levels of continuity, given by C^n, where n refers to the nth derivative of the underlying equations. Both the magnitude and direction of the nth derivative are continuous.

- C^0 continuity is where the *zero*th derivatives are the same at their intersection.

- C^1 continuity: the first derivatives, or tangents are identical.

- C^2 continuity: the second derivatives agree.

The first stage in the modelling process is the interpolation of the scan points, forming cubic B-splines, displaying C^1 continuity conditions. This level of continuity is adequate for this work.

B-spline polygons define a B-spline curve, but B-spline curves can be generated as an interpolating spline curve. Knot vectors allow the control points to be interpolated or approximated, where nodes control the curve, but are not on the curve. This can be given as:

$$B_i(u) = \sum_{k=-1}^{2} b_k p_{i+k} \qquad (1)$$

where:

$$b_{-1} = \frac{(1-u)^3}{6}$$

$$b_0 = \frac{u^3}{2} - u^2 + \frac{2}{3}$$

$$b_1 = \frac{u^3}{2} + \frac{u^2}{2} + \frac{u}{2} + \frac{1}{6}$$

$$b_2 = \frac{u^3}{6}$$

In the cubic case, the coefficient, b_k, is a basis weighting factor and is constant from point to point, for a set of four points. This weighted sum creates a B-spline curve. Approximation through four points P_0, P_1, P_2, P_3 only creates a B-spline in the region of the inner two points. Where start and end segments are needed, they are formed by using sets of P_0, P_0, P_0, P_1 and P_{n-1}, P_n, P_n, P_n, respectively, in the cubic case. This allows B-splines to have start and end knot multiplicity, where the degree of the curve determines the number of knot points at the start and end of the curve. Thus, continuity of a curve involves 'marching' along a curve at one point at a time, discarding the first point. This forms a new set of four points. The equations for the weighting factors allow 1st and 2nd degree continuity. Figure 2 demonstrates this procedure, resulting in B-spline interpolation.
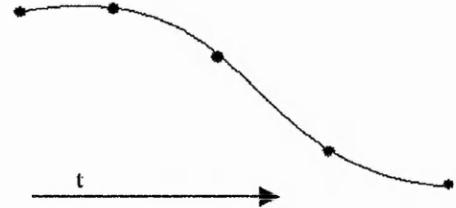

Figure 2. Parametric interpolating spline.

In Figure 2, data points are represented, and a B-spline is passed through each point in turn. These splines are continuous, and pass precisely through each point, interpolating, rather than approximating. This is achieved in the direction of the scan line, and perpendicular to the scan lines, creating a network of interpolating cubic B-splines with at least C^1 continuity. This network is used to form the boundary curves for adjoining surface patches. C^0 continuity is achieved where positional information is continuous. C^1 continuity allows an inter-patch tangent continuity at patch corners. These can be in the form of Gregory/Charrot patches [5].

3.2 Patch fitting

Gregory patches are used to generate a C^1 continuous surface. These use a blending function interpolant to define a boundary curve and cross-boundary tangent vectors. This boundary can be in a Bezier form, but in this work the boundaries are interpolating B-splines. Gregory patches can be N-sided, hence are a very useful patch type. In the realms of this paper, four sided patches are maintained. Two blending functions are used, namely Brown-Little and Gregory/Charrot methods [5]. These methods interpolate the data by calculating the radial direction at each edge from the given boundary data. The Gregory/Charrot method creates interpolants in the V_i and U_i directions, which correspond to interpolants along the radial directions, but differ in parameterisation. In this way, a surface patch is generated using boundary edge data and tangent derivatives at the start and end of each boundary edge. A typical single patch is shown by Figure 3.
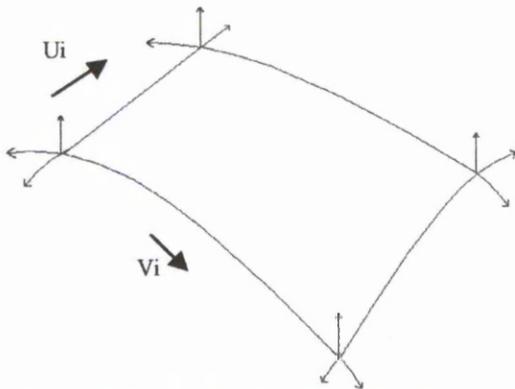
Figure 3. Four-sided Gregory/Charrot patch, showing tangent directions.

Patches of this nature are connected over the underlying spline network, resulting in a C^1 continuous B-spline surface model. The resolution of the surface is an important issue.

3.3 Surface Resolution

The number of Gregory patches in U and V directions in parameter space are pre-defined. If an inadequate number is used, the surface resolution is low, and modelling deviations occur. It is important to calibrate a surface model with the CMM data, to allow an adequate resolution of patches to accurately represent the data points.

3.4 Surface model generation

Automated surface model generation results in a smooth, C^1 continuous surface model. It is a best-fitted surface, approximating all the data points. The approximation tolerance can be relaxed or tightened, allowing a degree of surface smoothness manipulation. It is usually preferred to use a fit tolerance of zero, giving an interpolating surface. These system constraints force the total surface to be continuous. This generates a better overall smoothness.

This 'best-fit' of the data points, irrespective of the original surface continuity properties, is seen as a disadvantage in general cases where the measured surface can be of a complex nature. For example, where there is a mixture of defined features, based on surface types, as defined by Besl and Jain [7]. However, this automated method of surface fitting can be used to ascertain the accuracy of 3D data where smooth surfaces are required. Figure 4 demonstrates a typical free-form B-spline surface model, built up from these Gregory patches. This is purposely a surface with a high degree of oscillating curvature over the whole surface. This CAD model can then be used to assess both the smoothness of the original object, and the accuracy of the CMM data.

Judgement could be used here to view the CAD surface and arbitrarily comment on the acceptability of a surface smoothness. Inaccuracies from data collection can sometimes be seen, but due to the nature of free-form surfaces these are often missed. What is needed is a method of comparing the generated surface with the original CMM data points, thus assessing the smoothness of the free-form surface, as well as the accuracy of the CMM data.

4. ACCURACY ASSESSMENT

A large area which CAD systems lack is a surface analysis and comparison stage. Accuracy is paramount, as surfaces are created based on accurate CMM point data, or from curves fitted through this point data. Accuracy analysis allows a comparison of the point on the fitted model with the corresponding CMM point.

The correlation between original data points and points on a generated surface must be maintained, within defined tolerances. Using an optimum smoothness of output surface, the CMM error, or continuity deviation is highlighted. If these deviations are high, an alternative is to use the 'best-fit' CAD surface to reproduce a second physical surface. This would be appropriate where the original surface has been found to contain unwanted discontinuities. This method involves the process of Reverse Engineering.

4.1 Data set assessment

There is a paradox with methods of collected data assessment, due to the collected data having no direct reference for comparison. The only method is to take multiple data sets of the same object and then compare them. If the variance between these are within acceptable tolerances, then the data is deemed accurate and representative of the original surface. Due to the time consuming nature of CMM contact data collection, it is advantageous to be able to ascertain the accuracy of a single data set. This is partly due to the length of time necessary for data collection, and is possible as the optimum smoothness of the surface in question is desired.
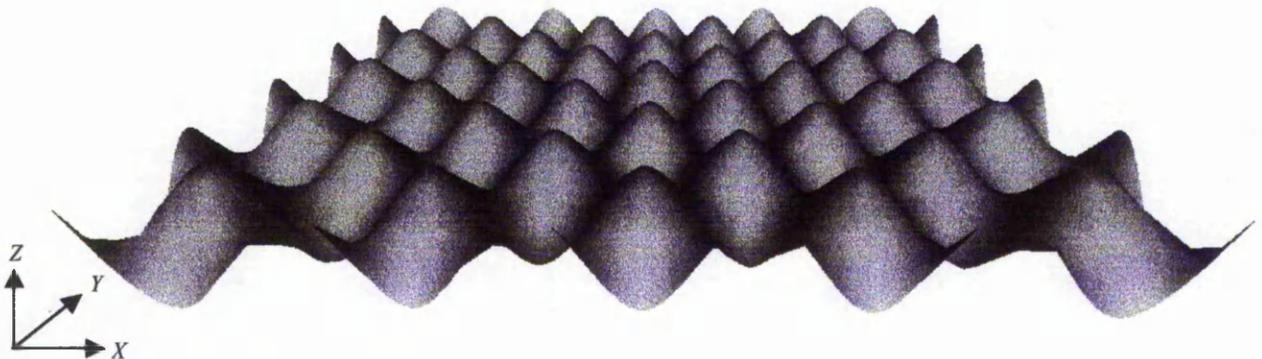

Figure 4. Free-form surface model.

This is the case where the goal is to verify the CMM data from one data set, to check for continuity deviation. There are a number of steps towards the assessment of free-form surface accuracy, outlined below.

4.2 Manual Analysis

Manual analysis is the simple initial stage involving a visually pleasing curve or surface. A fair amount of qualitative information can be attained from this stage. In particular, continuity conditions can be seen with degrees of smoothness, but as mentioned previously, this mainly relies on the judgement of the designer or user.

4.3 Numerical Analysis

Numerical analysis involves positional and tangency continuity constraints. Interpolation or approximation of a spline of known degree through fixed points allows an accuracy tolerance to be maintained. This involves both inter-point continuity, and inter-patch continuity, where quantitative data can be found. The nature of creating B-spline curves from scan data, and the generation of a B-spline surface from Gregory patch methods, maintain C^1 continuity conditions.

4.4 Deviation Analysis

Deviation analysis can determine how well a surface approximates the original data points, by looking at the original CMM data and the resulting generated surface. In this way, deviations show:

- modelling errors due to a low resolution of patches.
- at a high resolution of patches, the CMM error, or original surface discontinuities.

Comparing the deviation between data points and the closest corresponding point on the CAD surface is a method of assessing the accuracy of 3D data of free-form surfaces [8]. Where a surface is assumed to be free-form, there should be a direct correlation between the data points, and points on the CAD surface. This is

with the aim of estimating the surface model deviation error, as seen below.

$$\text{Deviation}_i = F_i(U,V) - C_i(U,V) \qquad (2)$$

Where:
  $F_i(U,V)$ is the ith fitted point
  $C_i(U,V)$ is the ith CMM point

When an acceptable modelling resolution is present, the deviation analysis represents an *improvement* i.e. the model represents a free-form B-spline surface with C^1 continuity *better* than the underlying CMM points.

The close correlation between the CMM data and the generated surface can be shown by the deviation analysis stage. The error graph in Figure 5 shows the deviation between the data points and the surface model (x10), where the base-line shows a deviation of zero. The best-fit surface deviates from the CMM data by an average of +/- 0.04 mm.

This highlights areas where, either the CMM data is in doubt, or the original surface was not as smooth as once believed. What would normally be seen as modelling errors, in fact show areas where compensation for optimum smoothness has occurred. Due to this, deviations occur between the CMM data and the surface model.

A best-fitted B-spline surface, by the nature of the free-form modelling, equally smoothes out the overall surface. This is highly dependent on the resolution of the surface model. By this we mean the number of patches in U and V. The less patches, the worse a fit the surface will be. As the continuity is under observation, flexibility in the best-fit is essential, thus the less patches, the more of an approximation of the CMM points the surface model will be.

Table 1 demonstrates this, results showing the deviations between CMM data and the B-spline surface, at different patch resolution. At 20x20 patches, the error is at a low enough deviation to be representative of a smooth surface. This forms a model calibration stage.
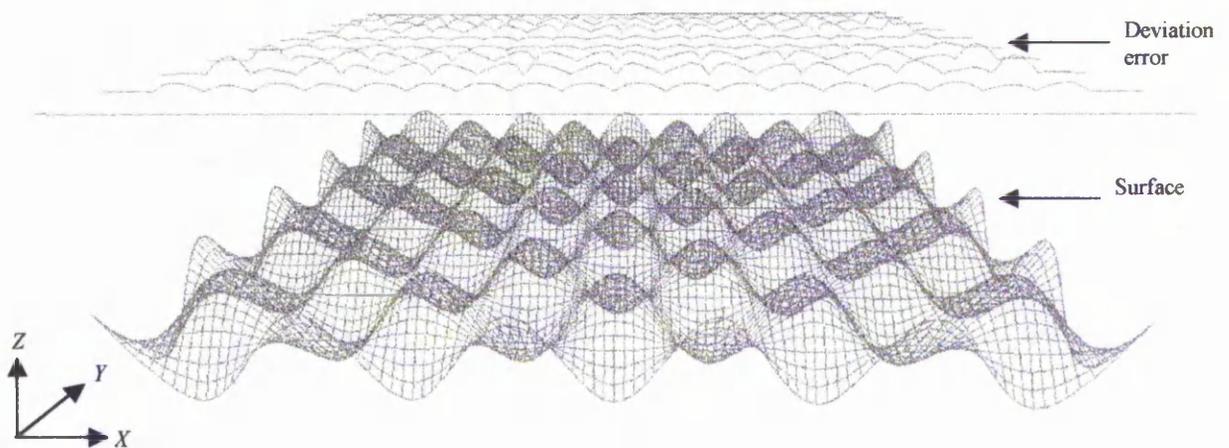

Figure 5. Deviation analysis results, between the CMM data and the generated surface model (at 20x20-patch resolution).

Table 1. Patch resolution and corresponding deviations.

Number of patches (U x V)	Average Deviation (mm)	Maximum Deviation (mm)
8x8	1.53	6.68
10x10	0.20	1.63
14x14	0.17	1.09
20x20	0.04	0.21

4.5. Reverse Engineering (RE)

Conventional engineering involves the stages of concept design, using CAD, and results in the creation of a physical part. This allows the creation of a machining part program, utilising CNC machining. RE is the reverse process, where a CAD model is obtained from a physical part, via data collection using a CMM, or other forms of data digitisation. This pre-cursor to the modelling stage results in the input point data. Reverse Engineering can be defined as: 'Systematic evaluation of a product with the purpose of replication. This involves either direct copies or adding improvements to existing design' [9].

RE is necessary when working from a physical prototype, rather than starting from a CAD concept model. Reproducing this prototype can only be done accurately using RE methods. This is particularly useful where CAD was not used in the original design, and a part must be replicated. RE can also be used where documentation is unavailable on the original design specifications. RE involves the integration of measurement, modelling and machining, in line with Simultaneous Engineering (or Concurrent Engineering) methods of manufacture and inspection. Weir et al. [10] divide the RE process into these stages:

- Surface data collection
- Data segmentation
- Surface fitting

These divisions of the process fits closely to the methods proposed here in Part-to-CAD RE. However, there is no real model refinement and no analysis stage. RE can also form three slightly broader phases, including manufacture, which are outlined here.

- Measurement: This stage involves 3D data collection. This first stage forms the start of the pipeline of information from one stage to the next. The collected data is in the form of 3D point co-ordinates.
- Modelling: The Computer Aided Geometric Design (CAGD) stage uses ACIS® functionality to create models from point data. The second stage forms the major part of this paper, concentrating on surface model analysis.
- Machining: CAD surface information can be used to create part programs for CNC machines, causing the original measured part to be reverse engineered. This stage also forms a part of surface accuracy analysis.

Figure 6 shows this RE process.
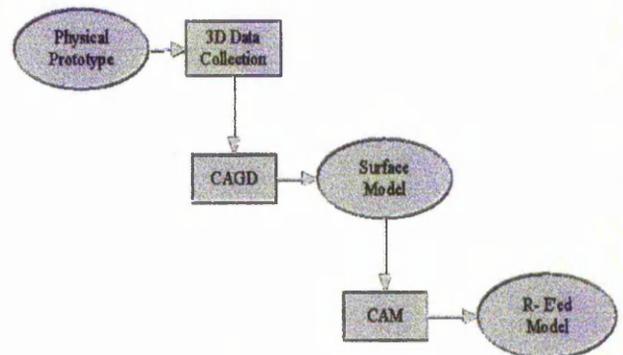
Figure 6. The Reverse Engineering process.

In this case, when a model deviation has been analysed, and it has been concluded that continuity improvement is necessary, RE aims to improve continuity of the desired surface. This is achieved by taking into account the properties of automated free-form modelling. Again, it is important to compensate this surface by the tool offset radius. This CAD model is then used to obtain surface information for the reproduction machining stage.

In order to improve this original surface's smoothness, a post-processing stage creates CNC cutter paths from the best-fit surface model. This minimises any CMM error which may have occurred by allowing a reverse engineered part to be manufactured, which possesses improved continuity.

The 'best-fit' CAD surface is used to generate point information and cutter paths to accurately reproduce the surface. To assess the improvement in continuity of this reverse engineered part, the CMM is used again to collect data. In a similar way deviation analysis is performed. The data set for this is used to generate a Reverse Engineered Surface (RES), using the same Gregory patch technique.

A second deviation analysis stage based on the RES, now compares the second CMM data set with the RES. This results in a very low variance between collected data and the surface model, thus showing an improvement in surface smoothness.

Any errors which occurred in the first stage of data collection are now compensated for, as the RES is based on the 'best-fit' smoothed CAD surface.

This pipeline starts from the original physical prototype and results in a reverse engineered reproduction part. This process can be seen in Figure 7.

From the RES, cutter paths are created. Deviation analysis of these points and the surface will be zero. Any very small errors are purely modelling errors. This can be simulated and shown in Figure 8. To physically manufacture this part, tool offsets are calculated. With these correctly optimised, the new RES will display improved C^1 continuity.

This can be confirmed by an additional surface comparison stage, where these two surfaces are compared, and improvements highlighted.
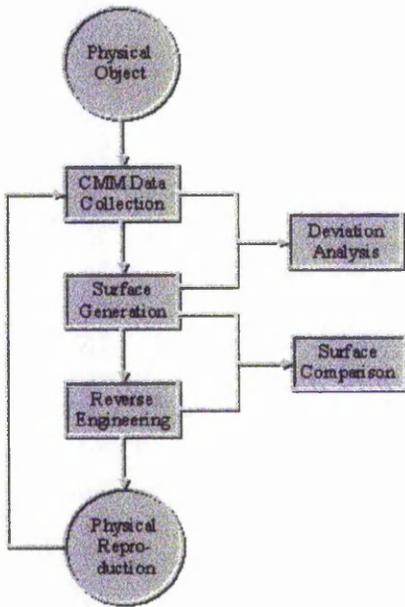
Figure 7. Outline of total process.

4.6. Surface comparison

This stage highlights the differences between the original surface model and the RES. This involves defining reference points on each surface model, and direct comparison of the CAD models. Variance between these two CAD models highlight where data collection has been inaccurate, or where the original physical surface had flaws.

It can be seen, despite the potential of CMM error, the correlation between the CMM data and the best-fit model of the second reverse engineered surface is much closer than in Figure 5.

In this case the surface deviations are compared. Similar results would be found if the actual surfaces were compared.

5. CONCLUSIONS

1.   Within the scope of this work, surfaces are assumed to be free-form, thus any points where high variance occur can correspond to discontinuities in the original surface, or from data collection errors. Once errors have been pinpointed, the data set can be edited, or further data collection can take place to verify the source of the error. Data collection is obviously the only method of obtaining information on a physical object. With correct calibration, data collection tools are assumed to be accurate, although problems may occur which cannot be detected. The conventional way to check for the accuracy of a data collection tool is repeatable results, within tolerance.

2.   In the case of free-form data collection, the desired need for smoothness is evident, and this can be used to assess both data collection accuracy, and physical part continuity.

3.   This study allows the accuracy of CMM data to be confirmed on surface models where slight discrepancies would be very hard to detect. These inaccuracies may arise from the manufacture of the part, or from the inspection of the part. In both cases, confirmation that the manufactured surface is continuously smooth, and passes through defined points within defined thresholds, is a useful aid to quality assessment.

4.   Deviation analysis allows model verification, highlighting potential inaccuracies. RE is a useful tool allowing the manufacture of a surface with improved overall continuity. Deviation analysis of this new RES shows the model continuity improvement. Surface comparison is a final stage, which shows this improvement graphically.

5.   In the case of free-form surfaces, a single data set can be verified, based on its best-fit surface. If the results from deviation analysis show a poor correlation, an improved reverse engineered surface can be manufactured.

6.   In this way, smooth surface data can be used to highlight and reduce possible CMM data inaccuracies, as well as improve the original surface's continuity.
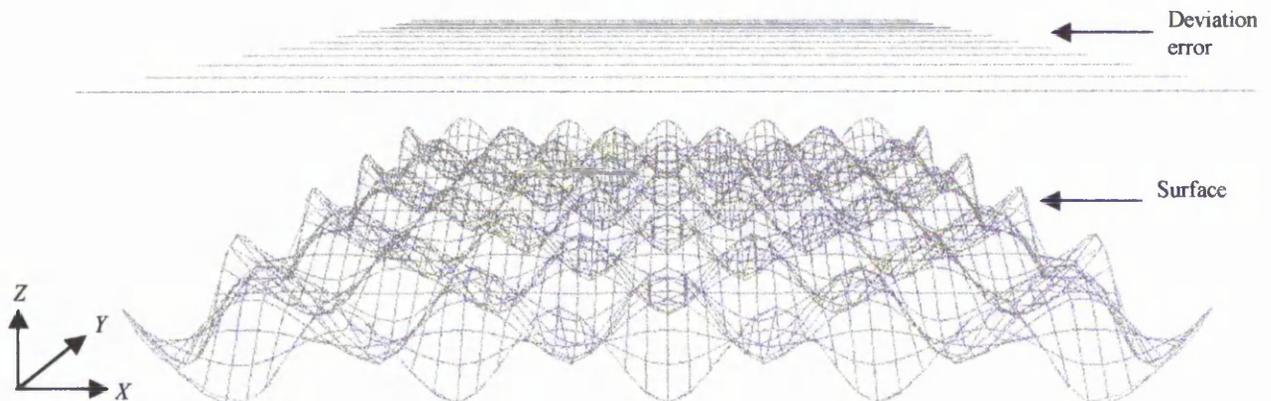

Figure 8. Improved deviation between surface model and CMM data.

REFERENCES

[1] Smith, G., Hill, T., Rockliffe, S., and Harris, J., 1994, 'Geometric Assessment of Sculptured Features', *Proceedings of the Tenth National Conference on Manufacturing Research*, pp. 663-667.

[2] Farin, G., 1990, *'Curves and Surfaces for Computer Aided Geometric Design, A Practical Guide, '.* 2nd. Ed., Academic Press.

[3] Katebi, M., Lee, T., and Grimble, M., 1994, 'Total Control of Fast Co-ordinate Measuring Machines', *IEE Proc. Control Thery Appl.*, vol. 141, no. 6, pp. 373-384.

[4] Bezier, P., 1972, *'Numerical Control - Mathematics and Applications'*, (Translated by Forrest, A., and Pankhurst, A.) Wiley & Sons Ltd.

[5] Gregory, J, 1986, 'N-Sided Surface Patches', *The Mathematics of Surfaces*, ed. J. A. Gregory.

[6] ACIS®, 1998, *Toolkit Development Manual*.

[7] Besl, P., and Jain, R., 1988, 'Range Image Segmentation', *Algorithms, Architectures and Systems,* ed. H. Freeman, Academic Press.

[8] Bardell, R, Balendran, V. and Sivayoganathan, K., 1998, 'Optimising Surface Modelling Techniques', *Proceedings of the Mechanics in Design International Conference*, pp. 771-779.

[9] Aronson, R., 1996, 'Forward Thinkers take to RE', *Man Engineer,* Nov ed., pp. 34-44.

[10] Weir, D., Milroy, M., Bradley, C., and Vickers, G., 1996, 'Reverse engineering physical models employing wrap-around B-Spline surfaces and quadratics'*, Proc. Instn. Mech. Engrs, Part B. Journal of Engineering Manufacture*, vol. 210, pp. 147-157.